The Dissertation Committee for Joseph Gamal Nessim Costandy certifies that this is the approved version of the following dissertation:

Decision-Making Frameworks for Practical Industrial Applications in Optimal Process Design and Control

Committee:

Michael Baldea, Co-Supervisor

Thomas F. Edgar, Co-Supervisor

Roger Bonnecaze

Gary Rochelle

Joseph Beaman

Decision-Making Frameworks for Practical Industrial Applications in Optimal Process Design and Control

by

Joseph Gamal Nessim Costandy

DISSERTATION

Presented to the Faculty of the Graduate School of

The University of Texas at Austin

in Partial Fulfillment

of the Requirements

for the Degree of

DOCTOR OF PHILOSOPHY

THE UNIVERSITY OF TEXAS AT AUSTIN

August 2021

Dedicated to my wife Catherine, my parents Gamal and Titi, and my siblings John and Erini.

Acknowledgments

I cannot express how deeply grateful I am to my advisors and mentors, Professors Michael Baldea and Thomas Edgar. Thank you for your unwavering support for me professionally and personally in my best and worst times, and your generosity in sharing your time, experience, and intellect to guide me towards becoming a better researcher, critical thinker, and person. I cherish all our conversations, and fully intend to maintain the close relationship that I built with you in my time at the University of Texas for as long as God grants me life.

I would also like to thank my committee members: Professors Roger Bonnecaze, Gary Rochelle, and Joseph Beaman for your astute suggestions and invaluable input from the early stages of my research projects that strongly influenced the path I took to advance my research plan.

I consider myself extremely fortunate to have crossed paths with the outstanding students in the groups of Professors Baldea and Edgar. I want to thank the senior lab members: Ankur Kumar, Richard Pattison, Corey James, Abby Ondeck, Ray Wang, Melissa Donahue, Hari Ganesh, and Calvin Tsay for easing my transition into the lab and to Austin, and immersing me into research and graduate school life at UT. I especially wish to thank my dear friends and colleagues Jodie Simkoff, Joannah Otashu, Morgan Kelley, and

Lingqing Yan who have been a tremendous support both academically and personally throughout my time at UT. I am also very grateful to all the younger group members: Omar Santander, Fernando Lejarza, Giannis Gianokopolous, Alkis Skouteris, Jun Seo, and Xin Tang, whose invaluable addition to the lab gives me confidence in its success for many years to come. I especially express my gratitude to my office mates Omar and Jun for the wonderful atmosphere they created when they joined; an atmosphere that I truly missed during the Covid pandemic in the final year of my PhD.

I was granted a wonderful opportunity to join the Data Science team at Sanofi for a co-op program during my final PhD semester. There, I worked with and learned from the incredible team members to whom I am very grateful: Christian Airiau, Steve Benner, Amos Lu, Edouard Duquesne, Kripa Avlani, and Marc-Antoine Fabre. I am especially indebted to Steve for giving me the trust and freedom to explore my ideas while providing the technical support I needed in order to make the project successful.

My PhD career began at Texas A & M University under the supervision of the late Professor Christodoulos Floudas, whom I owe an immense amount of gratitude. In addition to giving me a solid foundation in optimization theory that carried me through to the end of the PhD program at UT (and will stay with me forever), Professor Floudas's mentorship had a profound impact on my personality. His love and care for his students gave me a true appreciation for the humanity of those I work with, a lesson that I hope to remember and live by for the rest of my life. His passing away, while extremely

heartbreaking, revealed the goodness of many people that I must express my sincerest gratitude towards. I wish to thank Professor Efstratios Pistikopoulos for his determination to make sure that all of Professor Floudas's students find a new home, and for his endless support as we navigated through the difficult time. Together with Professors Baldea's and Edgar's gracious acceptance of me into their groups, Professor Pistikopoulos's actions during that difficult time were the beacon of hope that I needed to start on a path towards recovery from the trauma of losing Professor Floudas, and I am eternally grateful to him. I also wish to thank all the professors and students at Texas A & M who I was fortunate to have worked with during my time there: Professors Faruque Hasan, Phanourios Tamamis, Arul Jayaraman, Costas Kravaris, Chris Kieslich, Fani Boukouvala, Maria Papathanasiou, Styliani Avraamidou, Burcu Beykal, and Yuhe Tian, and Drs. Richard Oberdieck, Onur Onel, Alexander Niziolek, Nikolaos Diangelakis, Ioana Nascu, Logan Matthews, Melis Onel, William Tso, Doga Demirhan, Pritishma Lakhe, Emre Demirel, Justin Katz, Baris Burnak, and Utkarsh Shah.

To my mentors and friends from Texas A & M at Qatar: the bonds I developed in Qatar are akin to my relationships with my own family. While I cannot list everyone, I especially owe the following people a huge debt of gratitude for always being behind me at every step of the way: Professors Ioannis Economou, Mohamed Nounou, and Othon Moultos, Drs. Ziyan Sheriff, Sally El Meragawi, Noura Dowass, Vasileios Michalis, and Ioannis Tsimpanogiannis, and my dear friends Nour El Ghazal, Raid Hassiba, Mohammed El Shammasi,

and Talel Zakhama.

Moving to Austin allowed me to partake of the immense blessing of becoming a member of the Holy Cross Coptic Orthodox Church, and every single member of the church's congregation has had a significant impact on my experience throughout my PhD While I can't list each one by name, I wish to particularly thank Fr. Benjamin Abouelkheir and Missy Abouelkheir for their immense support throughout my studies. In addition, I wish to thank all members of the Orthodox Christian Campus Ministries (OCCM) branch at UT, who each have had a profound and positive impact on my experience at the university. Specifically, I would like to thank Sephra Thomas and Root Bahlbi for continuously holding me accountable to my writing tasks and deadlines.

Most of all, I wish now to thank those who worked endlessly behind the scenes to shape me into everything that I am today. I wish to thank the beneficent God, who has given me far more than I deserve, and indeed far more than I ever asked for. To my beautiful wife Catherine, your love, kindness, and care for me throughout my PhD despite my shortcomings have been the fuel by which I persisted to the end. I can only hope to give you a fraction of the joy and peace that you have given me throughout my PhD To my parents Gamal and Titi, my bother John, and my sister Erini, your countless sacrifices are the only reason that I have made it this far. This PhD is as much your achievement as it is mine. I am extremely grateful to Emil, Isis, and Mary Ghali for giving me a home away from home and becoming a second family for me in the United States. To my dear in-laws George and

Mary Masoud, Remon, Therese, Joy and Gabriella Bestawros, I wish to thank you for your belief in me and unwavering support and prayers for my success. I also wish to sincerely thank Hani, Venis, and Amir Rashed, Ramsis, Aiden, Connor, Stephen, and James Dawoud, Nabeel, Georgette, Mary, and Nardin Costandy, Hani, Hanaa, Suzy, and Nancy Fahim, Naim, Wafaa, Michel, and Amir Khalil, and all the rest of my extended family for your continuous well wishes and lovingkindness despite being halfway across the world. Finally, I have made a few friends in my PhD career that I have opted to list among family: Joseph Riad, Mina, Erini and Emily Shaker, and Morcos Murad. I truly appreciate your presence and the positive influence it has had on my PhD experience, and look forward to many more years of close friendship with each of you.

Decision-Making Frameworks for Practical Industrial Applications in Optimal Process Design and Control

Joseph Gamal Nessim Costandy, Ph.D.
The University of Texas at Austin, 2021

Supervisors: Michael Baldea and Thomas F. Edgar

While economics are the driving force behind many of the decisions made by industrial stakeholders, the methodologies employed to make high-level decisions often utilize heuristics that may not be quantitatively optimal. In this dissertation, I develop optimization-based frameworks that enable quantitatively driven high-level decision-making for two problems of practical industrial significance.

In the first part of the dissertation, I address the problem of deciding the operating mode (batch or continuous-flow) of a chemical process, while taking into account the fundamental differences in the natures of the two operating modes (such as the batch advantage of utilizing reactors for the manufacture of multiple products, or the batch disadvantage of reactor cleanup between campaigns), the size and cost of the respective reactor units, and the potential

use of reactor networks to optimize performance. I develop a first-principles-based non-dimensionalization algorithm that unifies the model for all reactor types and chemical systems from the two operating modes which enables direct performance comparisons between reactors of the two operating modes. In addition, I introduce a novel discretization method, the orthogonal collocation on finite elements for reactors (OCFERE), that allows the consideration of networks of reactors of either of the two operating modes, and I unify the description of the economics of the two operating modes. This results in a framework that encompasses the solution of a single optimization problem to make the decision about operating mode and find the optimal reactor network design.

In the second part of the dissertation, I address the problem of quantifying the monetary value of improvements in process control. While methods have been developed for quantifying the value of control in the case of predominantly steady-state processes, there has been no attempt to quantify the monetary value of control for predominantly transient processes. I first review the problem, and highlight the relationship between optimal scheduling and process control for transient processes. Then, I utilize the general framework of integrated scheduling and control to develop novel performance functions that enable the quantification of the monetary value of control from a scheduling perspective for a predominantly transient process. I posit that the transition time between one product and the next in a production sequence can be used as a performance metric over which the value of control can be quantified.

Table of Contents

Acknowledgments **v**

Abstract **x**

List of Tables **xvi**

List of Figures **xviii**

Part I A Unified Framework for Optimal Batch and Continuous Reactor Network Design **xxii**

Chapter 1. Batch to Continuous: Preliminaries **1**

1.1 The Batch to Continuous Problem 1

1.2 Batch to Continuous Feasibility Studies 4

1.3 Scope 7

Chapter 2. Batch to Continuous: Performance-Based Optimization For Single Reactor Transitions **9**

2.1 Problem Statement 9

2.2 Reactor Modeling 10

2.3 Motivating Example 13

2.4 Reactive System Characterization 19

2.5 Performance Metrics 23

2.5.1 Maximum Product Concentrations 28

2.6 Nondimensional Transport Equations 31

2.7 Optimization Problems 33

2.7.1 Optimization Problem 1 34

2.7.1.1 Objective Function 34

2.7.1.2 Constraints 36
2.7.2 Optimization Problem 2 41
2.7.2.1 Objective Function 41
2.7.2.2 Constraints 42
2.8 Case Studies 43
2.8.1 Case Study 1: Single, first-order reaction 43
2.8.1.1 Case Study 1, Optimization Problem 1 44
2.8.1.2 Case Study 1, Optimization Problem 2 47
2.8.2 Case Study 2: Parallel Exothermic Reactive System . . 49
2.8.2.1 Case Study 2, Optimization Problem 1 50
2.8.2.2 Case Study 2, Optimization Problem 2 54
2.9 Summary 58
2.10 Nomenclature 59

Chapter 3. Batch to Continuous: Economics-Based Optimization For Reactor Networks 62

3.1 Introduction 62
3.1.1 Extensions to the Batch/Continuous Reactor Optimization Framework 62
3.1.2 A Brief Overview of Reactor Network Synthesis 64
3.1.3 Goals and Outline 65
3.2 Problem Statement 67
3.3 Unified Batch/Continuous Superstructure Representation for Single Reactor Module 69
3.3.1 Continuous-Flow Single Reactor Module 73
3.3.2 Batch Single Reactor Module 76
3.3.3 Nondimensional Representation of Reactors 78
3.3.4 Review of Orthogonal Collocation on Finite Elements . 81
3.4 Unified Batch/Continuous Superstructure for Reactor Networks 88
3.5 Logical Constraints 95
3.5.1 Differences in the Nature of the Operating Modes 96
3.5.2 Artificial Solution Elimination 98
3.5.3 Identifying the Operating Mode and Determining Reactor Utilization 100

3.5.3.1 Operating Mode Selection 100
3.5.3.2 Reactor Utilization 101
3.5.4 Reactor Type Identification 104
3.5.4.1 Identifying CSTRs 104
3.5.4.2 Identifying PFRs and BRs 107
3.5.4.3 Identifying SBRs 107
3.5.5 Reactor Volumes 109
3.5.5.1 BR and SBR Volume 110
3.5.5.2 PFR Volume 111
3.5.5.3 CSTR Volume 113
3.5.6 Storage Tanks 114
3.5.7 Timing Constraints 115
3.5.8 Operating Mode-Dependent Variable Definitions 117
3.6 A Unified Representation of Batch/Continuous Economics . . 122
3.6.1 Revenue Calculation 122
3.6.2 Cost Calculation 125
3.6.2.1 Investment Costs 125
3.6.2.2 Operating Costs 127
3.7 Case Study: van de Vusse Reaction 131
3.7.1 Optimal Yield: Continuous-Flow Reactor Network . . . 134
3.7.2 Optimal Yield: Batch Reactor Network 136
3.7.3 Optimal Annual Profit 139
3.7.3.1 Results with Nominal Parameter Values 139
3.7.3.2 Sensitivity Analyses 144
3.8 Summary and Future Directions 150
3.9 Nomenclature 154

Part II An Optimization-Based Framework for the Evaluation of the Monetary Value of Improvements in Process Control 166

Chapter 4. Economic Value of Process Control: Preliminaries 167
4.1 Introduction and Literature Review 167

4.2 Motivating Example: Cyclical Scheduling of a CSTR 173
4.3 The Optimal Scheduling Problem 179
4.4 Motivating Example (cont'd): CSTR Production Schedule . . 183
4.4.1 Optimization of Production Schedule 183
4.4.2 Simulation of Production Schedule 186

Chapter 5. Economic Value of Process Control: Novel Performance Metrics 189

5.1 Monetary Performance Metrics 189
5.1.1 Performance Metric 1: Total Transition Time 191
5.1.2 Performance Metric 2: Individual Transition Times . . . 193
5.2 Motvating Example (cont'd): Value of Control for CSTR Operation 195
5.2.1 Performance Metric 1: Total Transition Time 195
5.2.2 Performance Metric 2: Individual Transition Times . . . 197
5.3 Summary and Future Directions 204

Bibliography 206

List of Tables

2.1 Parameters to generate the plots of Figure 2.1. 14

2.2 Typical ranges for the design variables of CFRs [153]. 17

2.3 Pathways From Raw Materials to Final Product L from Figure 2.3. 30

2.4 Calculation of $C_L^{\max}$ for desirable product L in the chemical scheme of Figure 2.3 given values of initial concentrations. From the given values, $C_L^{\max} = 1.01$ mol/m^3, the maximum value in the last column. 31

2.5 Definitions of reference values for all variables. 33

2.6 Transport properties of water at 300 K, used in Case Studies 1 and 2 [104]. 44

2.7 Parameters and optimal variable values for the three runs of case study 1, optimization problem 1. 45

2.8 Optimal variable values obtained by solution of Optimization Problem 2 for Case Study 1. 48

2.9 Parameters for the reaction rate expressions of Case Study 2. . 49

2.10 Parameters and optimal variable values for case study 2, optimization problem 1. 51

2.11 Parameters and optimal variable values for case study 2, optimization problem 2. 55

3.1 Notation followed in the model description 67

3.2 Overall and component balances for the continuous-flow and batch operating modes 77

3.3 Volume and residence time bounds for the different reactor types implemented in this work, as well as the volume bounds on the storage tanks. 133

3.4 Reaction rate coefficients for the two Cases studied in this work, optimal yields reported by previous authors, and optimal yields obtained in this work when operating mode is fixed ($\mathbf{y}_{\mathbf{M}_m} = 1$ to specify operating mode to mode m). 135

3.5 Parameters Used for the Calculation of the Economics as well as the Equation Numbers Where Each Parameter Appears . . 140
3.6 Optimal Profit, Revenues, Costs, Yield, and Reactor Network Configuration for the Nominal Parameters and after Fixing the Operating Modes. 141

4.1 CSTR Model Parameters (adapted from Davis and Thomson [51]) 175
4.2 Product concentrations, and required reactor and coolant temperatures for making each of the P_i products. 175
4.3 Transition time [h] for reactor to switch from making product $P_{i'}$ to product P_i. 178
4.4 Product properties. 184
4.5 Total hourly profit and profit breakdown of four simulations of the fixed production schedule. 188

5.1 Value of control for the four simulations with a fixed production schedule using total transition time as the performance metric. 197

List of Figures

2.1 Time and spatial evolution of reactant concentration for reaction $A \rightarrow B$ in batch and continuous reactors with activation energies (a) $E_A = 88{,}540$ J/mol, and (b) $E_A = 107{,}691$ J/mol. Note that Batch 1 overlaps Continuous 2, and Batch 2 overlaps Continuous 5. 15

2.2 Venn diagram illustrating the subsets of the component superset I. 20

2.3 (a) Fictitious chemical reaction scheme to illustrate component subset memberships. Members of I_R are placed inside point-corner square boxes, members of I_{P_D} are placed inside rounded-corner bold-edged square boxes, and members of I_{P_U} are placed inside circles. (b) Venn diagram illustrating the component subsets for the chemical reaction scheme in (a). 24

2.4 Methodology to calculate maximum product concentration, $C_i^{\max}$. 28

2.5 Non-dimensional (left) and dimensional (right) concentration profiles for the given BR and CFR found by solution of Optimization Problem 1 for Case Study 1. The non-dimensional profiles for all runs, as well as the dimensional profiles for run 1 for batch and CFR overlap. 46

2.6 Non-dimensional (left) and dimensional (right) concentration profiles for the optimal BR and optimal CFR found by solution of Optimization Problem 2 for Case Study 1. The non-dimensional profiles for batch and CFR overlap. 48

2.7 Given batch concentration (black, left ordinate) and temperature (blue, right ordinate) evolution through time for case study 2. 51

2.8 Non-dimensional (top) and dimensional (bottom) time and spatial concentration profiles for the given batch and equivalent CFR found by solution of Optimization Problem 1 for Case Study 2. 52

2.9 Non-dimensional (left) and dimensional (right) time and spatial temperature profiles for the given batch and equivalent CFR found by solution of Optimization Problem 1 for Case Study 2. 53

2.10 Non-dimensional (top) and dimensional (bottom) time and spatial concentration profiles for the optimal batch and optimal CFR found by solution of Optimization Problem 2 for Case Study 2. 56

2.11 Non-dimensional (left) and dimensional (right) time and spatial temperature profiles for the optimal BR and optimal CFR found by solution of Optimization Problem 2 for Case Study 2. . . . 57

3.1 Reactor types considered in this work. 70

3.2 Single reactor used to represent all reactor types in all operating modes. 71

3.3 CFR mass balance on reactor differential element. 75

3.4 Mapped time scales for the OC (a) and OCFE methods. . . . 84

3.5 Reactor superstructure showing connection of N_R individual reactor elements (of those shown in Figure 3.2). 89

3.6 Mapped time subdomains for the OCFERE method. 91

3.7 Optimal concentration profiles after fixing operating mode to continuous-flow ($\mathbf{y}_{\mathbf{M}_{m_C}} = 1$) for the van de Vusse chemical system with parameters of (a) case 1 and (b) case 2. Different reactors are shown by different line colors and separated by a vertical dashed line, diamond-shaped markers and triangles indicate CSTRs and PFRs, respectively, and the solid and dotted line styles indicate reactant A and product B concentrations, respectively. 134

3.8 Optimal concentration profiles after fixing operating mode to batch ($\mathbf{y}_{\mathbf{M}_{m_B}} = 1$) for the van de Vusse chemical system with parameters of (a) case 1 and (b) case 2. Inverted triangles and circles indicate SBRs and BRs, respectively, and the solid and dotted line styles indicate reactant A and product B concentrations, respectively. 137

3.9 Optimal dimensionless (a) volumetric flowrate (continuous-flow) or (b) volume (batch) profiles for the van de Vusse chemical system with parameters of case 1. The line colors and marker shapes have the same meaning as Figures 3.7 and 3.8, and solid, dotted, and dashed lines indicate the values in the reactor, "IN" stream, and "OUT" stream, respectively. 138

3.10 Concentration profiles after maximizing annual profits and fixing operating modes to (a) continuous-flow, or (b) batch, and volume profiles after maximizing annual profits and fixing operating modes to (c) continuous-flow, or (d) batch, for the van de Vusse chemical system with parameters of case 1. The line colors and marker shapes have the same meanings as Figures 3.7 - 3.8. 142

3.11 Sensitivity of profit $\mathbf{\Pi}$ to product sale price ζ_B^{sale} with product demands δ_B ranging from (a) 1000 kmol/yr to (f) 250,000 kmol/yr. 146

3.12 Sensitivity of $\mathbf{\Pi}$ to product demand δ_B with product sale prices ranging from (a) \$300/kmol to (f) \$800/kmol. 147

3.13 Sensitivity of $\mathbf{\Pi}$ to product demand δ_B with finer steps in demand and product sale price of \$400/kmol. 149

3.14 Cross-over points between batch and continuous-flow as ζ_B^{sale} and δ_B are varied. 150

4.1 Impact of reduction in variability on average process value . . 169

4.2 Impact of reduction in transition time on production schedule where a step change is made from one process operating point to another 173

4.3 Setpoint tracking for all possible transitions between products P_1 ($C_{A,sp}$ = 0.2 mol/L), P_2 ($C_{A,sp}$ = 0.15 mol/L), and P_3 ($C_{A,sp}$ = 0.06 mol/L) using the cascaded PI and linearizing control structures, based on the results reported in reference [21]. 177

4.4 Gantt chart of optimal schedule for (a) the cascaded PI controller and (b) the input/output linearizing controller 185

5.1 Total profit as a function of transition time $\tau_{3,1}$ (top abscissa), or change in transition time $\Delta\tau_{3,1}$ (bottom abscissa) for the cascaded PI controller. 198

5.2 Total profit and derivative of profit with respect to transition time as a function of change in individual transition times for the cascaded PI controller. Solid lines indicate that the transition is active in the schedule, while dashed lines indicate the transition is inactive. Line color represents the particular transition. The optimal schedule is indicated by the marker type: $\triangle$ is $P_3 \to P_2 \to P_1$, $\boxdot$ is $P_3 \to P_1 \to P_2$, $\bigcirc$ is $P_1 \to P_3 \to P_2$, $\diamond$ is $P_2 \to P_1 \to P_3$, and $\bigtriangledown$ is $P_1 \to P_2 \to P_3$. 200

5.3 Total profit and derivative of profit with respect to transition time as a function of change in individual transition times for the input/output linearizing controller. Visual representations of active vs. inactive transitions, particular transitions, and optimal schedule are the same as Fig. 5.2. 201

Part I

A Unified Framework for Optimal Batch and Continuous Reactor Network Design

Chapter 1

Batch to Continuous: Preliminaries

In this chapter[1], a literature review of the batch to continuous problem is first provided, then the scope of the work conducted and reported in this dissertation is described.

1.1 The Batch to Continuous Problem

Batch processing remains the production method of choice in the manufacturing of specialty chemicals and pharmaceuticals [152]. The reasons for batch dominance can be summarized into two categories: (1) perception, and (2) flexibility of the batch operation.

The first category of reasons related to perception includes the historical prevalence of batch operations and an inertia to change the already established regulatory framework for quality control of products, the (incorrect) perception that accurate control over continuously operated devices is difficult to achieve,

[1]The contents of this chapter are partially based on the following two publications: [44] J G Costandy, T F Edgar, and M Baldea. Switching from Batch to Continuous Reactors Is a Trajectory Optimization Problem. *Industrial & Engineering Chemistry Research*, 58(30):13718–13736, 2019. [46] Joseph G. Costandy, Thomas F. Edgar, and Michael Baldea. A Unified Reactor Network Synthesis Framework for Simultaneous Consideration of Batch and Continuous-Flow Reactor Alternatives. *Industrial and Engineering Chemistry Research*, 60:7232–7256, 2021. J. C. is the primary author of both manuscripts.

and a lack of motivation to make changes to operating practices because of the minimal cost of production relative to the high profit margins expected in these industries [132].

The second category is the fact that batch processes offer the advantage of flexible, multipurpose units. This difference in the nature of the operation of a batch plant has been recognized by process systems engineers, who have, in turn, offered a wealth of literature on the design and optimal operation of such flexible batch plants. This includes work on the optimal operation of a single batch unit [17, 48, 151, 161] as well as the optimal design and scheduling of multipurpose units [27, 28, 29, 37, 39, 55, 68, 106, 129, 167]. These studies have shown that the effect of flexibility on the overall process economics may be considerable. For example, Gorsek *et al.* [72, 73, 74] used a case study from the specialty chemicals industry to demonstrate that, while the continuous operating mode is superior to the batch operating mode for all plant capacities if single-purpose equipment is considered, the batch operating mode becomes more profitable at low product demands when multipurpose equipment is considered. Therefore, in the problem of determining the best operating mode for the manufacture of a particular chemical species, a fair assessment must not only account for the optimal performance of individual units but must also account for the difference in the nature of the operating modes.

Nevertheless, due to several emerging challenges, particularly in the pharmaceutical industry, there has been a shift in the last two decades towards

the design and operation of continuous production facilities for chemicals that have traditionally been produced in batches. These challenges include an increase in costs of research and development of new drugs due to the failure of more compounds to pass through all the phases of clinical testing [11], expiry of "blockbuster" drug patents at a faster rate than new drugs can be developed [11, 12], and changing revenue and price constraints from third-parties such as insurance companies [8, 120]. The need for increasing profits prompted pharmaceutical companies to streamline their manufacturing practices, giving rise to the quality by design (QbD) paradigm, wherein the process is designed with the end product quality in mind [177]. At this point, the deficiencies inherent to batch manufacturing processes surfaced as top targets for potential cost savings. These deficiences include complexities in scale-up [78, 105] and control [56], losses due to equipment clean up between production campaigns, increased costs of labor, and discarding of entire batches if the product is off-spec.

On the other hand, continuous processes are simpler to operate, require minimal human supervision, the problems associated with scale-up of laboratory experiments are greatly reduced, processes have a smaller throughput per unit time making them safer to operate and reducing their physical footprints, and with appropriate feedback control, we can expect that only a small amount of off-spec product will be made, leading to significant savings in resource consumption [159, 164]. The fact that continuous operation reduces the amount of material being processed per unit time, along with the decreased

mass and heat transfer limitations of continuous flow reactors (CFRs), is why the transition from batch to continuous processing is considered a prime example of process intensification. Not only does the transition allow us to perform existing batch operations more efficiently, but it has also unlocked the potential to exploit novel process windows [22, 82, 83, 89, 176]. With the onset of the process intensification paradigm, a plethora of novel processing options have necessitated more rigorous feasibility studies of the transition between the operating modes [20, 155].

1.2 Batch to Continuous Feasibility Studies

Making the switch from batch to continuous flow has been the subject of much research in the last two decades. The main research questions are whether making the switch is economically and technically feasible, and if so, what are the potential savings that can be made. Significant efforts were invested in developing new technologies to achieve the switch. The wealth of technologies developed for this purpose has been reviewed in references [25, 155, 165]. In addition, experimental feasibility studies of the switch are very common. Some look at individual reactions of interest, and typically involve synthesizing the desired chemical(s) in both batch reactors and CFRs, then comparing the reactor performances (see, for example, references [69, 90, 107, 109, 114, 116, 140, 148]). A literature review of reactions carried out in CFRs is provided by Anderson [10]. Other works focus on defining the best methodology to follow when conducting the feasibility studies. Valera *et*

al. [162] studied the factors that affect the decision to run a laboratory scale reaction in a flask or in a CFR. Hertrampf *et al.* [81] compare the products made using a batch process to those made using a continuous process via Raman spectroscopy, laser diffraction, X-ray powder diffraction and scanning electron microscopy.

In addition to studies that focus exclusively on the reactor, full laboratory-scale production processes have been developed to compare the two production regimes. This includes both "hybrid" (involving both batch and continuous sections) [40, 105, 171] and fully continuous [6, 30, 150] processes. At a larger scale, continuous pharmaceutical pilot plants have been built successfully [43, 149, 178].

The high costs of performing experimental studies fueled the need for alternative screening methods to determine whether a specific batch process would benefit from making the switch to continuous flow. Several qualitative methods have been proposed. Roberge *et al.* [139] related batch unit operations to appropriate continuous counterparts. Calabrese and Pissavini [38] introduced a list of screening criteria to determine the feasibility of switching from batch to continuous based on the particular reaction scheme being considered. The inferences are based on an understanding of the areas where CFRs excel compared to their batch counterparts. Plouffe *et al.* [131] developed a qualitative toolbox that can be used to recommend the type of CFR that would be appropriate for a particular combination of reaction kinetics, the phases present, and the type of reaction network. Brandt and Schembecker

[36] introduced key performance indicators that combine product yield, purity performance, variable manufacturing costs, and production rate into one objective that may be used for the systematic design of batch or continuous-flow downstream processes. Jolliffe and Gerogiorgis [91] tackled the problem of continuous process flowsheeting by first surveying the literature to find active pharmaceutical ingredients (APIs) for which continuous flow processes have been developed, evaluating each candidate for suitability of large-scale process flowsheeting by giving them scores in each of a set of ten broad criteria, such as process complexity or level of product demand, then identified ibuprofen for further analysis. Teoh *et al.* [154] proposed a high-level qualitative screening approach that utilizes existing knowledge about batch processes to determine the feasibility of the switch.

Quantitative feasibility studies have also been developed. Goršek and Glavič [72, 73, 74] introduced a general methodology to analyze the factors that influence the decision on the operating mode of a full chemical plant. Specifically, they developed an approach to estimate the way plant capacity, material recycle, and energy integration affect the decision to design a batch or continuous process when considering plants with single and muli-purpose (batch) equipment. The methodology involved postulating a process flowsheet for a particular process, simulating it for a continuous flow process, replacing each unit with a batch counterpart, simulating the batch process, and comparing the net present value of the two processes. More recent works adopt a similar procedure, where data-driven modeling of novel contin-

uous flow equipment [33, 158] is conducted, followed by plantwide simulations [26, 35, 31, 77, 92, 93, 142, 144, 147, 175], and optimization [32, 34]. The aforementioned studies rely on modeling batch and continuous processes independently, then determining whether the switch is economically attractive. Other studies relied on the modeling of processes using first-principles models [134, 146].

1.3 Scope

In all the aforementioned feasibility studies, the batch and Continuous Flow Reactors (CFRs) are considered independently of one another. The fact that the chemistry being conducted within the two reactors is identical is not exploited in any of the modeling techniques that are offered in the literature. While the existing knowledge of the original batch processes has been used to *qualitatively* guide the design of a potential equivalent CFR, a *quantitative* utilization of batch experimental data has scarcely been used to that end. In chapter 2, I develop an optimization based framework that utilizes existing batch reactor data to determine whether a CFR can be designed that obeys reactor-specific constraints while delivering an equivalent performance to the batch reactor. To illustrate the utility of the methodology in attaining feasible designs for vastly differing reactor types, I focus my attention for the continuous-flow operating mode on the development of a microreactor that performs equivalently to a batch counterpart.

The approach presented in Chapter 2 is effective for the design of a sin-

gle reactor using product yield as the key performance indicator. The methodology is extended to offer a more complete analysis in Chapter 3, where the potential use of reactor networks is accounted for, and process economics is used as the key performance indicator, where the models used for calculating process economics accommodate the differences in the natures of the two operating modes (e.g. multi-purpose batch equipment).

Chapter 2

Batch to Continuous: Performance-Based Optimization For Single Reactor Transitions

In this chapter[1], I present a novel framework for addressing the batch to continuous feasibility problem for a single reactor. I begin by defining the specific research questions I address, and presenting the reactor models I employ along with the modeling assumptions. I then present a motivating example that will lay the groundwork for the rest of the chapter.

2.1 Problem Statement

Given a batch reactor (BR) that processes a set of $I = \{i : i_1, \ldots, i_{N_I}\}$ components undergoing a set $J = \{j : j_1, \ldots, j_{N_J}\}$ of reactions, for which reaction kinetics are known, I seek to develop an optimization-based framework to address the following broad questions:

1. Can an ideal continuous-flow reactor (CFR) that performs "equivalently" to the BR be designed? If so, what are the design parameters of the

[1]The contents of this chapter are largely based on the following publication: [44] J G Costandy, T F Edgar, and M Baldea. Switching from Batch to Continuous Reactors Is a Trajectory Optimization Problem. *Industrial & Engineering Chemistry Research*, 58(30):13718–13736, 2019. J. C. is the primary author of the manuscript.

reactor?

2. From a reactor performance point-of-view, is it beneficial to switch from batch to continuous, or to consider making operational changes to improve the BR performance? Can one quantify this difference?

2.2 Reactor Modeling

To illustrate the utility of the methodology in determining equivalence between vastly differing reactor designs, in this chapter I elected to determine the feasibility of switching from a large-scale autoclave BR to a microreactor in the continuous-flow operating mode. The problem of how to model microreactors using first-principles models received much attention. First-principles models offer the advantage of capturing the wealth of knowledge about the phenomena occurring within the reaction mixture. Roberge [137, 138] classified reactions based on kinetics and the number of phases present. Kockmann [97, 98] performed a detailed analysis of the fluid dynamics in microstructured CFRs, independent of the batch counterparts, and showed that the integration of reaction kinetics into fluid dynamics and transport phenomena is essential for successful application of microstructured devices for continuous pharmaceutical and fine chemicals production. The design concepts were demonstrated on a pilot-scale plant. Nagy *et al.* [118] demonstrated that flow in microreactors may deviate significantly from ideality, and introduced metrics to determine when consideration of mixing and/or dispersion may be essential. Witt *et al.* [170] modeled the flow in mesoscale reactors using 1-D

and 2-D dispersion models, as well as a full 3-D CFD model to determine the importance of including detailed dispersion effects.

In this chapter, I begin with idealized reactor assumptions. Later, I make use of the published literature on microreactor modeling to ensure that the attained designs are feasible. In addition to the ideal batch and CFR assumptions, I make the following assumptions:

1. Cylindrical reactor geometry.
2. Homogeneous, incompressible liquid phase systems.
3. Negligible pressure drop and gravitational acceleration.
4. Negligible dispersion effects.
5. perfect mixing.
6. Constant solvent properties (specific heat capacity, diffusion coefficient, viscosity, thermal conductivity).

The modeling of solids-based processes has many associated challenges, and research on modeling such processes is vast [141]. For this reason, I have elected to deal only with liquids in this work. The assumption of homogeneous liquid phase systems covers the majority of reactive systems that are currently carried out in BRs. With that assumption, assuming incompressible flow becomes reasonable. While it has been reported that dispersion and mixing effects may hamper the predictive ability of the model, I will later introduce

constraints in the optimization framework that ensure the effects are negligible and can be ignored. Nevertheless, expanding the framework to account for cases where these assumptions may not hold is an interesting topic, and can be the subject of a future work.

With these assumptions, the mass and energy balances of any reactive system are given in eqs 2.1 and 2.2, respectively, where C_i is the molar concentration of species i [mol/m^3], v is the flow velocity $[m/s]$, R_i is the sum of rates of generation and consumption of species i [mol/m$^3 s$], ρ is the mixture mass density [kg/m^3], C_p is the specific heat capacity of the mixture [J/kg K], T is the temperature [K], $\triangle H_j$ is the enthalpy change of reaction j [J/mol], r_j is the reaction rate expression for reaction j [mol/m^{3}s], U is the overall heat transfer coefficient [J/m^2 K s], d is the reactor internal diameter [m], and T_s is the temperature of the heating/cooling agent [K].

$$\frac{\partial C_i}{\partial t} = -v\frac{\partial C_i}{\partial z} + R_i \tag{2.1}$$

$$(\rho C_p)\,\frac{\partial T}{\partial t} = -\,(\rho C_p)\,v\frac{\partial T}{\partial z} + \sum_j (-\triangle H_j)\,r_j + \frac{4U}{d}\,(T_s - T) \tag{2.2}$$

I will assume that the reaction kinetics are known, and that a rate expression of the form given in eq 2.3 has been obtained, where k_j is the pre-exponential factor, E_{Aj} is the activation energy, R is the universal gas constant, and g_{ij} is the reaction order of component i in reaction j. Then, the

overall rate of generation of component i, R_i, is given by eq 2.4, where η_{ij} is the stoichiometric coefficient of component i in reaction j. As is the convention, η_{ij} is positive if component i is a product in reaction j, and negative if it is a reactant.

$$r_j\left(T, C_i\right) = k_j \exp\left(-E_{Aj}/RT\right) \prod_i C_i^{g_{ij}} \tag{2.3}$$

$$R_i = \sum_j \eta_{ij} r_j = \sum_j \left\{ \eta_{ij} k_j \exp\left(-E_{Aj}/RT\right) \prod_{i'} C_{i'}^{g_{ij'}} \right\} \tag{2.4}$$

2.3 Motivating Example

Consider an isothermal reactor carrying out a single, first-order reaction $A \rightarrow B$, and has the rate expression $R_i = \eta_j K C_A$, where $K[s^{-1}]$ has the Arrhenius form $K(T) = k_0 e^{-\frac{E_A}{RT}}$. Using eq 2.1, the evolution of reactant concentration with time or position for an ideal, well-mixed BR or, respectively, steady-state plug-flow reactor (PFR) are given by eqs 2.5 and 2.6,

$$\frac{dC_A}{dt} = -KC_A,\ C_A(t=0) = C_{A_{t0}} \quad \Rightarrow C_A(t) = C_{A_{t0}} e^{-Kt} \tag{2.5}$$

$$\frac{dC_A}{dz} = -\frac{1}{v} KC_A,\ C_A(z=0) = C_{A_{z0}} \quad \Rightarrow C_A(z) = C_{A_{z0}} e^{-\frac{1}{v}Kz} \tag{2.6}$$

where $C_{A_{t0}}$ and $C_{A_{z0}}$ are the initial reactant concentrations (at the start of the reaction for the BR, and the inlet for the PFR, respectively). Figure 2.1(a) shows the time and spatial evolution of reactant concentration for the parameter values given in Table 2.1.

Table 2.1: Parameters to generate the plots of Figure 2.1.

Parameter	**Batch 1**	**Continuous 1**	**Continuous 2**	**Continuous 3**	**Batch 2**	**Continuous 4**	**Continuous 5**
$k\ [s^{-1}]$	10^{14}						
$T\ [K]$	300						328.7
$E_A\ [J/mol]$	88,540				107,691		
$t_B\ [s]$	60	-			129600	-	
$X(t_B)$	0.90	-			0.90	-	
$L\ [m]$	-	60			-	3	
$v\ [m/s]$	-	0.75	1.00	1.25	-	0.001	
$X(L)$	-	0.95	0.90	0.84	-	0.052	0.90

A comparison of the time and spatial evolution equations reveals that for the same temperature and initial reactant concentration, the two equations would evaluate to the same numerical values if $t_B = L/v$, where t_B and L are the total batch time and PFR length, respectively. This is seen by the overlapping evolution curves for Batch 1 and Continuous 2 in Figure 2.1(a). Therefore, if the batch process is designed to give the concentration evolution of Batch 1, the design of a CFR to achieve the same total conversion would be straightforward. In addition, for a fixed continuous reactor length, the flow velocity v can be adjusted to obtain a higher (Continuous 1) or lower (Continuous 3) total conversion.

Since t_B and L are the markers of the end of the reaction in batch and CFRs, respectively, L is considered the continuous-flow analogue of t_B in the batch process. If initial concentrations and total batch time are fixed, the only

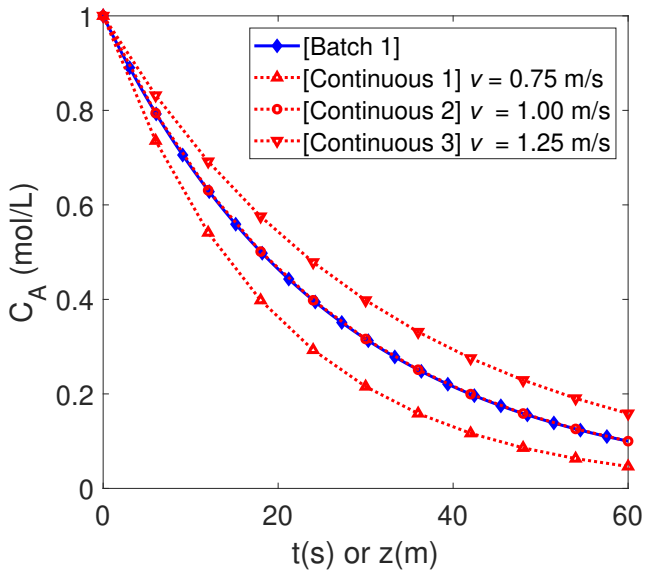

(a) $E_A = 88,540\ J/mol$

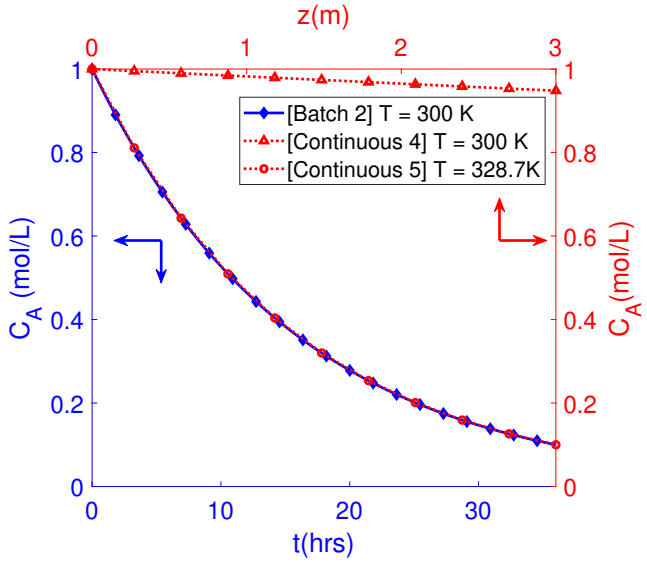

(b) $E_A = 107,691\ J/mol$

Figure 2.1: Time and spatial evolution of reactant concentration for reaction $A \rightarrow B$ in batch and continuous reactors with activation energies (a) E_A = 88,540 J/mol, and (b) E_A = 107,691 J/mol. Note that Batch 1 overlaps Continuous 2, and Batch 2 overlaps Continuous 5.

remaining degree of freedom in the batch process for process control purposes is the reaction temperature. Conversely, in the continuous process with fixed initial concentrations and reactor length, we may change both temperature and flow velocity to control the process. Hence, in establishing an equivalence between the two reaction modes, it quickly becomes clear that continuous operation offers an additional degree of freedom that may be useful from a process control point of view.

One may conclude for the simple example discussed above that the switch from batch to continuous design and operation is trivial, and that the advantage of additional control degrees of freedom makes the switch desirable. Indeed, the switch may be desirable from a control point of view, but in practice may not be attainable. In this example, note that the CFR has a length $L = 60\ m$. Table 2.2 shows the typical ranges for the design variables of continuous-flow microreactors [153]. A reactor length of 60 m far exceeds the reactor lengths typically reported in the literature; in practice, such a reactor is likely to suffer significant pressure losses, or be heat/mass-transfer limited like its batch counterpart. Similarly, the batch process has a total batch time of 60 s to achieve the same 90% conversion. This is much faster than most batch processes in the chemical industry, which typically have a duration that is in the order of several minutes, hours or days.

Consider the concentration evolution for the same reaction ($A \rightarrow B$) with the activation energy increased to a value of $107,691\ J/mol$, such that the same conversion (90 %) requires 36 hours of operation rather than 1 minute

Table 2.2: Typical ranges for the design variables of CFRs [153].

	Design Variable
Reactor Length, L	0.1 m $\leq L \leq$ 3 m
Reactor Diameter, d	0.1 mm $\leq d \leq$ 5 mm
Volumetric Flow Rate, Q	0.01 mL/min $\leq Q \leq$ 10 ml/min
Residence Time, t_R	1 s $\leq t_R \leq$ 3000 s
Lateral Flow Velocity, v (if not available, estimated using $v = L/t_R$ or $v = 4Q/\pi d^2$)	0.001 m/s $\leq v \leq$ 1.00 m/s

in the BR, a more typical batch duration. The concentration evolution for this BR (Batch 2) is shown in Figure 2.1(b). If one was to set $t_B = L/v$ and operate at the same temperature, the length of the reactor would need to be even longer than the 60 m length used before, even if the flow velocity was dropped to unreasonably low values. For example, reducing the flow velocity to the lower limit of 0.001 m/s would still require a 130 m long reactor to achieve the same conversion. Setting reactor length to $L = 3\ m$ (Continuous 4 in Figure 2.1(b)), the total conversion drops to only 5.2 %, making this a poor design. Therefore, in practice, achieving the same conversion as the reference batch system in a CFR with tailored length and flow velocity is not quite as simple due to design limitations.

The aforementioned findings do not imply that a CFR cannot be designed to achieve the same conversion as the batch system. However, they do mean that, from a practical point of view, we must consider the specific design constraints, as well as alternative operating conditions such as different temperatures and flow velocities. For this problem, where the integration of the design equations can be carried out analytically as was shown in eqs 2.5

and 2.6, the temperature at which a 90 % conversion could be achieved in the CFR at the design limits $L = 3\ m$ and $v = 0.001\ m/s$, can be easily computed by setting $C_A(L) = 0.1C_{A_{z0}}$ which leads to a new temperature value of 328.7 K. The reactant concentration spatial evolution along the CFR with these dimensions at this temperature is shown as Continuous 5 in Figure 2.1(b). As can be seen from the figure, the same conversion of 90 % that was achieved by Batch 2 is replicated by Continuous 5.

This example illustrates the concept of batch and continuous equivalence (with regards to reactor performance). While the only mathematical difference between the design equations for batch and continuous reactor design is the independent variable (t for batch, z for continuous), accounting for the different nature of the two processing modes requires further consideration. In this example, I presented a simple case study where the integration of the design equations was performed analytically, and was able to obtain simple closed-form expressions for the evolution of concentration for the single reactant. However, most practical problems are difficult to solve analytically, and numerical solution methods are needed. In addition, in this case, I assigned values to the reactor length and flow velocity of the CFR. No checks were provided to determine the validity of the modeling assumptions made, or to calculate whether the volumetric flow velocity or the reactor diameter are within their typical design ranges. If I was to consider all these aspects, the complexity of the problem increases significantly. Therefore, this problem naturally lends itself to an optimization-based framework.

In this chapter, I aim to develop a framework that is readily applicable to the design of a single chemical reactor handling any reactive system. To this end, I begin by introducing a general characterization algorithm for reaction networks (section 2.4). Then, I define performance metrics that will enable a direct comparison between the designed CFR and the reference BR (section 2.5). I then non-dimensionalize the transport equations (section 2.6). Finally, I present the generalized optimization problems that will be used to address the research questions defined in the problem statement (section 2.7), and demonstrate their use on the case study given in this section, as well as on a second case study (section 2.8).

2.4 Reactive System Characterization

The goal of this work is to offer a framework that may be applied to any reaction network. The method I employ is to develop non-dimensional reactor performance metrics in terms of the concentrations of the chemical species within the reactive system. Then, two optimization problems are constructed. The first minimizes the difference between the performance metrics of the CFR and BR. The second maximizes the sum of the values of the performance metrics for the two reactors. Using those, a clear picture of the potential benefits of making the switch from batch to continuous-flow for the particular reaction scheme under consideration can be formulated. In this section, I describe the generalized method used to define the reactive system in the framework.

The problem of deriving a generalized protocol for characterizing all the species within a reactive system has scarcely been tackled in the literature, and has focused mainly on classifying chemical routes (with the ultimate goal of defining ideality of chemical routes), such that alternative chemical routes to synthesize a desired final product can be quantitatively compared [70, 79]. This characterization is useful when the chemical reaction route is not known *a priori*, and potential alternative routes are to be compared. In this work, the chemical reaction route is assumed to have already been studied and identified, so such detail is not necessary. Instead, I will introduce component subsets of the superset of chemical species $I = \{i : i_1, \ldots, i_{N_I}\}$. I begin by defining subsets $I_R \subset I$ of reactants, and $I_P \subset I$ of products. I further define subsets $I_{P_D} \subseteq I_P$ of desirable products, and $I_{P_U} \subset I_P$ of undesirable products and intermediates. The split between the components is shown in Figure 2.2.

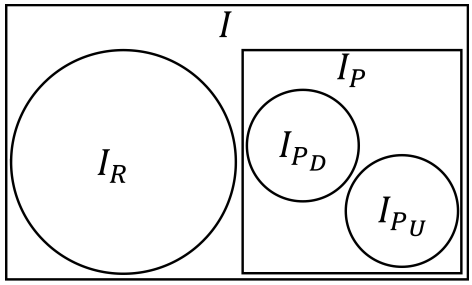

Figure 2.2: Venn diagram illustrating the subsets of the component superset I.

Reactants (belonging to subset I_R) are defined as the components that must be present in the reactor inlet (or loaded into the BR at the start of the batch) for the desirable products to be made. In other words, these are

the components whose inlet (initial) concentrations cannot be zero. Note that this definition does not include all components that act as reactants in the chemical system. For example, for the following system of reactions:

1. $A + B \xrightarrow{k_1} C$
2. $B \underset{k_3}{\overset{k_2}{\rightleftharpoons}} D + E$

where the desirable product is component C, A and B must be present at the inlet of the reactor (or the start of the batch) for the desirable product C to be made. Therefore, $J_R = \{A,\ B\}$. Note that while the addition of components A, D and E would also be sufficient to make C, we have made the decision that for this process, we will supply A and B because those were the available raw materials. Therefore, components D and E do not belong to the reactants subset I_R since their presence is not necessary for the production of the desirable product C if pure component B is being supplied. Here, I indicate that while this framework is general in that it accepts any number of components and reaction scheme, the supplied raw materials must be defined *a priori*.

Products (belonging to set I_P) are all other components within the system, since every component that does not belong to I_R must be the product of at least one reaction within the full chemical network.

Desirable products (belonging to I_{P_D}) are defined as all the components that must be present at the outlet of the continuous reactor or respectively

at the end of the batch. In other words, these are the components for the production of which the reactor was designed. In the reaction system above, this would mean $I_{P_D} = \{C\}$. Note that these may not necessarily be the desirable final products of the entire process. For example, if reaction 1 in the above example had an additional product F, which was to be separated from the desirable product C downstream of the reactor, then component F would still belong to the subset I_{P_D}, along with product C. While there is no restriction on the concentration of components belonging to this subset at the inlet (initially), it is the objective of the reactor that the amount of these components at the outlet (at the end of the batch) be maximized. Like the components in I_R, the components belonging to this subset must be defined *a priori*.

Undesirable products (belonging to I_{P_U}) are all the components that do not belong to either I_R or I_{P_D}. This may include all the products of undesirable side reactions, as well as intermediates. For the above system of reactions, $I_{P_U} = \{D,\ E\}$. The selection of the components in I_R and I_{P_D} determines the membership of I_{P_U}.

With these definitions of the subsets, $I_R \cup I_P = I$, $I_{P_D} \cup I_{P_U} = I_P$, and $I_R \cap I_P = I_{P_D} \cap I_{P_U} = \emptyset$. That is, each component i in the system belongs to one, and only one of the subsets I_R, I_{P_D}, and I_{P_U}. This is illustrated in Figure 2.2.

To further illustrate the set definitions above, I utilize the fictitious, but not unrealistic chemical scheme of Figure 2.3(a). The chemical scheme

is of a reactive system in a process that aims to manufacture component M. I use such a scheme to illustrate that this methodology for set definition encompasses even the most complex of schemes. In the figure, members of I_R, I_{P_D} and I_{P_U} are placed inside point-corner square boxes, rounded-corner (bold-edged) square boxes, and circles, respectively. The set membership is further illustrated in the Venn diagram of Figure 2.3(b). The scheme involves a total of 12 reactions (placed in round brackets under each reaction). Therefore, $J = \{j_1, j_2, \ldots j_{12}\}$. The membership of the reactants set is $I_R = \{A, B, E, G, H, I, J\}$, since these are all the components that would only be present if they are added at the reactor inlet. The membership of the desirable products set is $I_{P_D} = \{L, M\}$. Note that while the aim from the process is the manufacture of product M, the product cannot be manufactured without making product L (through reactions 6 and 9), so both components belong to the desirable products set. Finally, the membership of the undesirable products set is $I_{P_U} = \{C, D, F, K, N\}$, all the other components within the system.

2.5 Performance Metrics

As was shown in the motivating example, one cannot expect that all variables in the two reactors be the same. The comparison between the two reaction modes necessitates the definition of a set of universal performance metrics. All feasibility studies utilize some form of performance metric to evaluate the utility of the newly designed reactor or process. Experimental

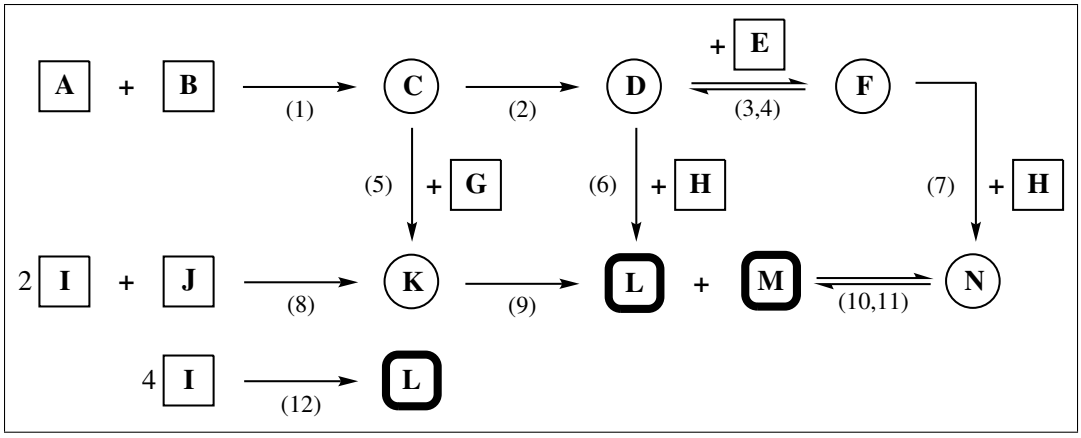

(a)

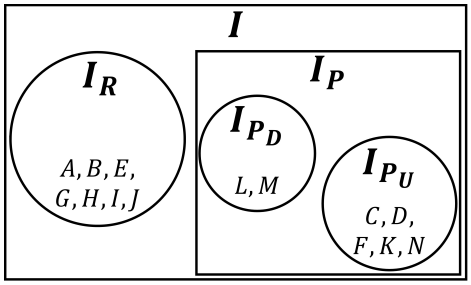

(b)

Figure 2.3: (a) Fictitious chemical reaction scheme to illustrate component subset memberships. Members of I_R are placed inside point-corner square boxes, members of I_{P_D} are placed inside rounded-corner bold-edged square boxes, and members of I_{P_U} are placed inside circles. (b) Venn diagram illustrating the component subsets for the chemical reaction scheme in (a).

feasibility studies typically involve the synthesis of a product using batch and CFRs, then utilizing Process Analytical Technology (PAT) [81] to compare physical and chemical attributes of the products. Some examples of performance metrics that have been used include level of impurities [26] and Envi-

ronmental factors (E-factor) [92, 93]. Winkelnkemper and Schembecker [169] introduced the separation cost indicator (SCI) that combines yield, purity, and variable manufacturing costs into a single metric to assess the performance of a production stage. This was later extended to consider production rate in the modified separation performance indicator (SPI) metric [36].

At the plant scale, performance metrics often come from empirical considerations, and involve several factors that have been observed to have the most pronounced effects on the full process performance. For example, van Aken *et al.* [163] introduce the "EcoScale" tool, which compares processing routes by assigning a perfect route a score of 100, then penalizing every route based on its performance as quantified in the overall yield, cost, safety, operating conditions, and the ease of purification. Dach *et al.* [49] extend the approach by using a modified version of the EcoScale as one of eight criteria to evaluate a full chemical process, including material cost, atom economy, yield, volume-time-output, environmental factor, quality service level, and the process excellence index. This approach allows direct comparisons between processing routes, but the criteria account only for batch processes, and their direct applicability for a continuous-flow system is not straightforward. For the specific problem of retrofitting an existing batch process with a continuous-flow counterpart, Dencic *et al.* [52] identify the following four factors as the most relevant indicators for process improvement: (1) operation time, (2) operating costs, (3) waste production, and (4) resource usage.

Both the laboratory and plant scale studies place an emphasis on the

following four criteria:

1. Maximizing resource (raw material) usage.
2. Maximizing yield of desirable products.
3. Minimizing yield of undesirable products (waste).
4. Minimizing operating costs.

In this chapter, I will focus on quantifying the performance with respect to the first three criteria. An equitable comparison of operating costs (criterion (4)) would entail consideration of different aspects of the manufacturing process, such as differences in labor costs and downtime between batch and CFRs. Since these differences significantly add to the complexity of the problem, they are addressed in detail in Chapter 3. At this stage, I aim to build a framework that compares the performance of the individual reactor while considering the difference in individual reactor design between the two operating modes. Nevertheless, criteria (1)-(3) directly affect operating costs, in that they reduce raw material costs, downstream separation costs, and profit from the sale of product.

Having created appropriate subsets of the components in the previous section for reactants (I_R), desirable products (I_{P_D}), and undesirable products (I_{P_U}), I will introduce separate performance metrics for each of the component subsets that will assure that the CFR can meet the same performance of the batch counterpart with regards to criteria (1) - (3) above.

In order to maximize resource usage, we aim to maximize the conversion of raw materials ($X_{i \in I_R}$), making this the appropriate performance metric. The definition of conversion and the performance metric for reactants is shown in eq 2.7, where C_{i0} is the concentration of reactant i at the reactor inlet (for the CFR), or at the start of the batch (for the BR), $C_{i,F}$ is the concentration of component i at the reactor outlet or at the end of the batch for the CFR or BR, respectively, and P_i is the performance metric for component i.

$$P_i = X_i = 1 - \frac{C_{i,F}}{C_{i0}} \qquad \forall i \in I_R \tag{2.7}$$

The performance metric for desirable products is maximizing the yield ($y_{i \in I_{P_D}}$), where yield is the ratio of the actual concentration of product to the maximum possible concentration ($C_i^{\max}$). The definition of yield and the performance metric for desirable products is shown in eq 2.8. The determination of $C_i^{\max}$ will be discussed in detail in section 2.5.1.

$$P_i = y_i = \frac{C_{i,F}}{C_i^{\max}} \quad \forall i \in I_{P_D} \tag{2.8}$$

Conversely, minimizing waste is equivalent to minimizing the yield of undesirable products ($y_{i \in I_{P_U}(i)}$), or to maximize its negative. Therefore, the performance metric for undesirable products is shown in eq 2.9, with yield y_i defined as in eq 2.8.

$$P_i = -y_i \quad \forall i \in I_{P_U}(i) \tag{2.9}$$

2.5.1 Maximum Product Concentrations

I now define a general methodology to obtain the maximum product concentration $C_{i\in I_P}^{\max}$, which is needed to define the yield. The methodology is summarized in Figure 2.4. In the following discussion, I will refer to the component $i \in I_P$ for which we are calculating $C_{i\in I_P(i)}^{\max}$ as i'_p. In order to facilitate the explanation, I will use desirable product $i'_p = L$ in Figure 2.3(a) to demonstrate each step, but the reader should note that the same method will be used to define maximum concentration for all the members of I_P.

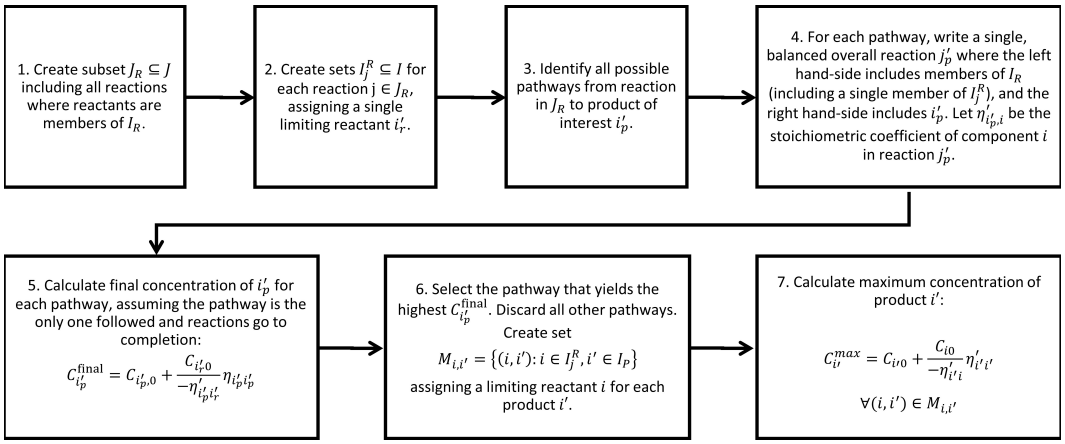

Figure 2.4: Methodology to calculate maximum product concentration, $C_i^{\max}$.

Step 1: List all the reactions where all reactants are members of I_R, since we know that at least one of these reactions must be the first step in a sequence of reactions to reach the product i'_p. The subset of reactions that fit this description are listed in subset $J_R \subset J(j)$. For the scheme of Figure 2.3(a), these reactions are:

1. Reaction 1: $A + B \rightarrow C$

2. Reaction 8: $2I + J \rightarrow K$

3. Reaction 12: $4I \rightarrow L$

Step 2: Select a limiting reactant i'_r for each initial reaction $j \in J_R$. Given a BR design that carries out the chemical reaction scheme, the limiting reactant can be inferred from the initial concentrations of each of the reactants in the identified initial reactions and the reaction stoichiometry. An important assumption is that the limiting reactant for the equivalent CFR is the same as that of the BR, and that the limiting reactant does not change at any point along the length of the reactor (or the batch time). The limiting reactant could be the least available raw material or the most expensive. The set of limiting reactants i'_r for each reaction in $J_R(j)$ is $I_j^R = \{i | j \in J_R\}$.

Step 3: List all possible pathways leading from each initial reaction $j \in J_R$ to $i'_p \in I_P$. These are listed for the scheme of Figure 2.3(a) and $i'_p = L$ in Table 2.3.

Step 4: For each pathway, write a single, balanced overall reaction j'_p that neglects all intermediates and relates the product of interest to the limiting reactant of the pathway. These are shown in the final column of Table 2.3.

Step 5: If any individual pathway was followed, the maximum possible concentration of the product can be related to the initial concentration of the limiting reactant for the pathway. Therefore, we need to identify the pathway that, if followed, will give the maximum concentration of the product. Given

Table 2.3: Pathways From Raw Materials to Final Product L from Figure 2.3.

Initial Reaction		**Pathway**		**Overall Reaction**
1	$A + B \rightarrow C$	(1)	$A + B \rightarrow C \rightarrow D \xrightarrow{+H} L + M$	$A + B \rightarrow L + M$
		(2)	$A + B \rightarrow C \rightarrow D \xrightarrow{+E} F \xrightarrow{+H} N \rightarrow L + M$	
		(3)	$A + B \rightarrow C \xrightarrow{+G} K \rightarrow L + M$	
8	$2I + J \rightarrow K$	(1)	$2I + J \rightarrow K \rightarrow L + M$	$2I + J \rightarrow L + M$
12	$4I \rightarrow L$	(1)	$4I \rightarrow L$	$4I \rightarrow L$

the initial concentration of the limiting reactant of the pathway $C_{i'_r 0}$ and that of the current product of interest $C_{i'_p 0}$, then the outlet (or final) concentration of the product i'_p would not exceed the ratio $C_{i'_p 0} + (C_{i_r 0}/(-\eta'_{i'_p i'_r}))\eta'_{i'_p i'_p}$, where $\eta'_{i'_p i'_r}$ and $\eta'_{i'_p i'_p}$ are the stoichiometric coefficients of the limiting reagent and the product of interest in the overall reaction of that particular pathway. These initial concentrations may be variables to optimize, or they may be fixed. If we are given the values for the reference batch system, then we can use those directly. Otherwise, we must estimate approximate values for the initial concentrations. After evaluating this function for all possible pathways, we can find the pathway that will be used to calculate $C^{\max}_{i'_p}$ by choosing the maximum one. If multiple pathways give the same value, then intuition should be used to select the most likely pathway. The evaluation of this function for each of the possible pathways to make L of Figure 2.3, for given values of the initial concentrations of the limiting reagents is shown in Table 2.4. From the given values, the three pathways corresponding to initial reaction 1 give the maximum value. I will select the first of these pathways as the most likely pathway.

Step 6: Construct set $M_{i,i'}$ assigning a limiting reactant i to each

Table 2.4: Calculation of $C_L^{\max}$ for desirable product L in the chemical scheme of Figure 2.3 given values of initial concentrations. From the given values, $C_L^{\max} = 1.01$ mol/m^3, the maximum value in the last column.

$\mathbf{i'_p}$	$\mathbf{C_{i'_p 0}}$ [mol/m^3]	$\mathbf{i'_r}$	$\mathbf{C_{i'_r 0}}$ [mol/m^3]	$\eta_{\mathbf{i'_p i'_r}}$	**Pathway**	$\eta_{\mathbf{i'_p i'_p}}$	$\mathbf{C_{i'_p}^{final}}$ [mol/m^3]
L	0.01	B	1.0	-1	1	1	1.010
					2	1	1.010
					3	1	1.010
		I	0.3	-2	1	1	0.160
		I	0.3	-4	1	1	0.085

product i':

$$M_{i,i'} = \left\{(i, i') : i \in I_j^R, i' \in I_P\right\} \tag{2.10}$$

Step 7: The maximum concentration $C_{i'}^{\max}$ can be defined as shown in eq 2.11.

$$C_{i'}^{\max} = C_{i'0} + \frac{(C_{i0})}{-\eta'_{i'i}}\eta_{i'i'} \quad \forall (i, i') \in M_{i,i'} \tag{2.11}$$

For the pathway of Figure 2.3(a), the set $M_{i,L} = (B, L)$, and $C_L^{\max} = C_{L0} + \frac{(C_{B0})}{1}(1) = C_{L0} + C_{B0}$.

2.6 Nondimensional Transport Equations

Since the governing equations for temperature and concentration evolution for the PFR and BR have the same functional form, but with different independent variables, I will present the analysis for both reactors using a single equation for temperature and a single equation for concentration. The

independent variable will be represented by x_r, where x_r can be time t or position z for the BR or PFR, respectively. Subscripts t and z will also be added to all dependent variables to indicate whether I am referring to the BR or the PFR, respectively.

From eq 2.1, the evolution of reactant concentration in either operating mode can be represented using eq 2.12,

$$\frac{dC_{i_r}}{dx_r} = \frac{1}{\gamma_r} \sum_j \eta_{ij} k_j \exp\left(-\frac{E_{A_j}}{RT_r}\right) \prod_{i'} C_{i'_r}^{g_{ij'}} \tag{2.12}$$

where γ_r is equal to 1 for the BR ($\gamma_r = \gamma_t = 1$) and v for the CFR ($\gamma_r = \gamma_z = v$). Similarly, the energy conservation eq 2.2 can be rewritten as eq 2.13,

$$\frac{dT_r}{dx_r} = \frac{1}{\rho C_p \gamma_r} \sum_j (- \triangle H_j) k_j \exp\left(-\frac{E_{A_j}}{RT_r}\right) \prod_i C_{i_r}^{g_{ij}} + \frac{4U_r}{\rho C_p \gamma_r d_r} (T_{s,r} - T_r) \tag{2.13}$$

In order to make the equations for the two reactors directly comparable, I non-dimensionalize all variables using the following definitions:

$$\hat{x}_r = \frac{x_r}{x_{\text{ref}_r}}, \quad \hat{C}_{i_r} = \frac{C_{i_r}}{C_{i,\text{ref}_r}}, \quad \hat{T}_r = \frac{T_r}{T_{\text{ref}_r}}, \quad \hat{T}_s = \frac{T_{s,r}}{T_{\text{ref}_r}} \tag{2.14}$$

where subscript "ref" indicates a reference value for the variable on which the subscript appears. The definitions of the constants used as reference values for each of the variables is summarized in Table 2.5.

Table 2.5: Definitions of reference values for all variables.

	Batch		CFR	
Variable	Reference Parameter Symbol	**Definition**	Reference Parameter Symbol	**Definition**
x_r	t_{ref_t}	t_B, batch duration	z_{ref_z}	L, reactor length
C_{i_r}	C_{i,ref_t}	C_{it0}, $\forall i \in I_R$ initial concentration of i	C_{i,ref_z}	C_{iz0}, $\forall i \in I_R$ inlet concentration of i
		$C_{i_t}^{\max}$, $\forall i \in I_P$ maximum possible concentration of i		$C_{i_z}^{\max}$, $\forall i \in I_P$ maximum possible concentration of i
T_r	T_{ref_t}	T_{t0}, initial temperature	T_{ref_z}	T_{z0}, inlet temperature

Rewriting eqs 2.12 and 2.13 in terms of the non-dimensional variables yields eqs 2.15 and 2.16,

$$\frac{d\hat{C}_{i_r}}{d\hat{x}_r} = \frac{x_{\text{ref}_r}}{\gamma_r C_{i,\text{ref}_r}} \sum_j \eta_{ij} k_j \exp\left(-\frac{E_{A_j}}{RT_{\text{ref}_r}\hat{T}_r}\right) \prod_{i'} C_{i',\text{ref}_r}^{g_{ij'}} \prod_{i'} \hat{C}_{i'_r}^{g_{ij'}} \tag{2.15}$$

$$\frac{d\hat{T}_r}{d\hat{x}_r} = \frac{x_{\text{ref}_r}}{\rho C_p \gamma_r T_{\text{ref}_r}} \sum_j (-\triangle H_j) k_j \exp\left(-\frac{E_{A_j}}{RT_{\text{ref}_r}\hat{T}_r}\right) \prod_i C_{i,\text{ref}_r}^{g_{ij}} \prod_i \hat{C}_{i_r}^{g_{ij}} + \frac{4U_r x_{\text{ref}_r}}{\rho C_p \gamma_r d_r}\left(\hat{T}_{s,r} - \hat{T}_r\right) \tag{2.16}$$

2.7 Optimization Problems

Having defined appropriate performance metrics and introduced appropriate non-dimensionalization reference values that allow direct comparisons between the two reactor types, the two optimization problems that will be solved in order to answer the questions raised in the problem statement (section 2.1) may now be introduced. The first question is addressed in optimization problem 1; namely, whether switching from batch to continuous is

feasible. The second question is addressed in optimization problem 2; namely, whether switching from batch to continuous is desirable. Both problems take on the form of trajectory optimization (or optimal control) problems, where the control inputs are the (time-invariant) reactor design variables (dimensions, initial or inlet concentrations and temperature, etc.), and the states are the non-dimensional concentration and temperature trajectories.

To describe each problem in the following two sections, I begin by presenting the relevant objective function, followed by the applicable constraints. It should be noted that some of the variables may be assigned fixed values for the particular case studies, so as to reduce the complexity of the problem. However, I present the problems in as general a manner as possible, and the framework is flexible to accept any reactive system under its specific design constraints.

2.7.1 Optimization Problem 1

2.7.1.1 Objective Function

The first question I address is whether an ideal PFR can be designed that performs "equivalently" to a given BR, and if so, what are the design parameters for the reactor? Having defined performance metrics (eqs 2.7 - 2.9), reactor equivalence can be defined as having two reactors with the same values of the non-dimensional performance metrics. Therefore, I minimize the difference in the value of the performance metrics in reactants, desirable and undesirable products between the two reactors, as is shown in eq 2.17,

$$\min \quad \left[\sum_{i \in I_R} (X_{i_z} - X_{i_t})^2 + \sum_{i \in I_{P_D}} (y_{i_z} - y_{i_t})^2 + \sum_{i \in I_{P_U}} (-y_{i_z} + y_{i_t})^2 \right] \tag{2.17}$$

or equivalently,

$$\min \quad \left[\sum_{i} (P_{i_z} - P_{i_t})^2 \right] \tag{2.18}$$

Combining the performance metric definitions (eqs 2.7 - 2.9), the non-dimensionalized concentration definition (eq 2.14) with objective function (2.18) gives objective function (2.19).

$$\min \quad \left[\sum_{i} \left(\hat{C}_{i_z}(\hat{z} = 1) - \hat{C}_{i_t}(\hat{t} = 1) \right)^2 \right] \tag{2.19}$$

Here, I make two comments: First, this objective function does not assume equal numerical values for all design parameters. It allows for different combinations of reference values for the two reactor modes. However, it still ensures that raw material usage and yield of products from the two reactors are equal, meaning that the reactors are "equivalent". Second, in the given form, an equal weight is assigned to each component towards the total reactor performance. This may not be a suitable assumption for a particular reactive system being considered. For example, a manufacturer may prioritize one desirable (or more valuable) product, or there may be systems with large differences between the number of reactants, desirable, and undesirable products. In such situations, each component can be assigned a different weight.

2.7.1.2 Constraints

For this problem, I assume that the concentration and temperature trajectories for the BR are given. Therefore, the only constraints are those which govern the CFR. The constraints I consider for the CFR are the trajectory constraints, constraints that ensure reactor design parameters are reasonable, and constraints to check the validity of the assumptions made in the model. These are described below.

Trajectory Constraints

The mass and energy balances govern the trajectories of concentration and temperature. Therefore, eqs 2.15 and 2.16 written for the case of the CFR are the trajectory governing constraints, as shown in eqs 2.20 and 2.21. The initial conditions are given in eq 2.22.

$$\frac{d\hat{C}_{i_z}}{d\hat{z}} = \frac{L}{vC_{i,\mathrm{ref}_z}} \sum_j \eta_{ij} k_j \exp\left(-\frac{E_{A_j}}{RT_{z0}\hat{T}_z}\right) \prod_{i'} C_{i',\mathrm{ref}_z}^{g_{ij'}} \prod_{i'} \hat{C}_{i'_z}^{g_{ij'}} \tag{2.20}$$

$$\frac{d\hat{T}_z}{d\hat{z}} = \frac{L}{\rho C_p v T_{z0}} \sum_j (-\triangle H_j) k_j \exp\left(-\frac{E_{A_j}}{RT_{z0}\hat{T}_z}\right) \prod_i C_{i,\mathrm{ref}_z}^{g_{ij}} \prod_i \hat{C}_{i_z}^{g_{ij}} + \frac{4U_z L}{\rho C_p v d_z}\left(\hat{T}_{s,z} - \hat{T}_z\right) \tag{2.21}$$

$$\hat{C}_{i\in I_R}\Big|_{\hat{z}=0} = 1, \qquad \hat{C}_{i\in I_P}\Big|_{\hat{z}=0} = \frac{C_{iz0}}{C_{i_z}^{\max}}, \qquad \hat{T}\Big|_{\hat{z}=0} = 1 \tag{2.22}$$

Finally, eqs 2.23 and 2.24 give the definitions of the reference concentrations for the reactants and products, respectively, and eq 2.25 introduces bounds on the non-dimensional concentration.

$$C_{i,\mathrm{ref}_z} = C_{iz0} \quad \forall i \in I_R \tag{2.23}$$

$$C_{i'}^{\max} = C_{i'0} + \frac{(C_{i0})}{-\eta'_{i'i}} \eta_{i'i'} \quad \forall (i,i') \in M_{i,i'} \tag{2.24}$$

$$0 \leq \hat{C}_{iz} \leq 1 \tag{2.25}$$

Design Constraints

The typical ranges for the microreactor dimensions, flowrates, and residence time were presented in Table 2.2. Therefore, these ranges will be used in all problems as bounds for each of the design variables. Several combinatorial constraints of these variables will appear later as assumption validity checks.

Appropriate constraints on the temperature will depend on the particular reactions taking place; whether they are endothermic or exothermic. Therefore, temperature bounds for the utilities ($T_{s,z}$) and the temperature (T) will be assigned as appropriate for every problem. However, I offer a general restriction on the change of temperature along the length of the reactor, constraint 2.26, where $\triangle T_{\max_z}$ is the maximum temperature deviation from the inlet temperature. This is included to avoid large temperature fluctuations

that would be difficult to control. In addition, this constraint is necessary to avoid the formation of hotspots, a common problem for reactions that have a high heat production potential [168].

$$T_{z0} - \triangle T_{\max_z} \leq T \leq T_{z0} + \triangle T_{\max_z} \Rightarrow 1 - \frac{\triangle T_{\max_z}}{T_{z0}} \leq \hat{T}_z \leq 1 + \frac{\triangle T_{\max_z}}{T_{z0}} \quad (2.26)$$

Second, I will assume isoperibolic operation; that is, the available cooling and heating utilities are kept at a constant temperature, $T_{s,z}$.

Finally, in order to calculate the overall heat transfer coefficient U_z, note that Renken *et al.* [136] have shown that the Nusselt number, Nu, of a circular pipe with typical microreactor dimensions is roughly constant. Rearranging the correlation given in eq 2.27 gives U_z as a function of the thermal conductivity $\lambda[J\,/\,m\,K\,s]$, a parameter that is tabulated for many solvents, and the internal diameter of the reactor d_z.

$$Nu = \frac{U_z d_z}{\lambda} = 3.66 \Rightarrow U_z = \frac{3.66\lambda}{d_z} \quad (2.27)$$

These constraints are generally applicable. However, additional constraints may be included on a case-by-case basis to address specific considerations for the problem at hand.

Assumption Validity Constraints

The model makes several assumptions that may not always be valid. For this reason, I ensure that the solutions obtained using the framework are

valid by introducing constraints to verify that the modeling assumptions made are justified.

First, I assumed there is no turbulence or recirculation eddies. In addition, radial diffusion was neglected. This assumption is not always valid, and was discussed in detail by other authors [76, 118]. The Damkohler number (Da), a non-dimensional number describing the ratio between reaction rate and diffusion rate, was identified as an indicator of the significance of diffusion. For the effect of diffusion to be negligible compared to reaction (i.e. for the process to be reaction rate limited), Da < 1. While the number is difficult to obtain with complete accuracy, Nagy *et al.* provided a theoretically derived expression (eq 2.28) that may be used to provide estimates for CFR systems [118]. In the expression, F_o is the Fourier number, a non-dimensional number describing the ratio of residence time to transverse diffusion time, and D is the diffusion coefficient $[m^2/s]$. The parameter χ was introduced to account for the effect of the chemical reactions. The authors introduced analytical expressions relating χ to the reactant conversion. However, they stated that in the majority of their calculations, $2 \leq \chi \leq 19$. Therefore, where an analytical expression is not available, I have used $\chi = 2$.

$$\mathrm{Da} = \frac{\chi}{F_o} = \frac{\chi d_z^2 v}{4LD} \tag{2.28}$$

Second, since turbulence was not accounted for, I have implicitly assumed the flow is laminar. Therefore, I introduce a constraint ensuring the

Reynold's number, Re, is within the laminar region. This is shown in eq 2.29, where μ is the viscosity [kg / m s].

$$\mathrm{Re} = \frac{d_z v_z \rho}{\mu} < 1000 \tag{2.29}$$

Third, the assumption of laminar flow implies a parabolic velocity profile across the diameter of the reactor. However, I have assumed plug flow, which ignores the radial variation. Nagy *et al.* [118] showed that these two assumptions can be reconciled when the Bodenstein number, a non-dimensional number measuring the ratio of convection to dispersion, is high. Therefore, the constraint given by eq 2.30 was added, where β is a parameter that depends on the channel geometry, and is 48 for cylindrical tubes.

$$\mathrm{B_o} = F_o \beta = \frac{192 D L}{d_z^2 v} > 100 \tag{2.30}$$

Finally, in the definition of the maximum concentration for each of the products in the set I_P, I made the assumption that a certain reactant was limiting for the pathway resulting in the maximum possible concentration of the product. I ensure this assumption remains true by introducing constraint 2.31 which ensures the concentrations of all reactants i'' in the overall reaction of the pathway are always above the stoichiometric minimum they need to be for i' to maintain its limiting status. In the equation, $\eta'_{i,i''}$ is the stoichiometric coefficient of all reactants in the overall reaction of the limiting pathway except that of the limiting reactant i'.

$$-\eta'_{i,i'}\hat{C}_{i'z}C_{i',\mathrm{ref}_z} \leq -\eta'_{i,i''}\hat{C}_{i''z}C_{i'',\mathrm{ref}_z} \quad \forall (i,i') \in M_{i,i'},\, \eta'_{i,i''} < 0,\, i'' \neq i' \quad (2.31)$$

2.7.2 Optimization Problem 2

2.7.2.1 Objective Function

The second question I address concerns providing a quantitative estimate of the maximum possible benefit from making the switch from batch to continuous-flow, compared to the possibility of changing the operational conditions of the original BR. The framework allows answering this question in a straightforward manner by obtaining the maximum possible performance from the two reactors, and since the performance metrics are non-dimensional, I can perform direct comparisons. To this end, I maximize objective functions 2.32 and 2.33 for the CFR and BR, respectively.

$$\max \quad \sum_i P_{i,z} = \sum_{i \in I_R} \left(1 - \hat{C}_{i_z}\right)\Big|_{\hat{z}=1} + \sum_{i \in I_{P_D}} \hat{C}_{i_z}\Big|_{\hat{z}=1} - \sum_{i \in I_{P_U}} \hat{C}_{i_z}\Big|_{\hat{z}=1} \quad (2.32)$$

$$\max \quad \sum_i P_{i,t} = \sum_{i \in I_R} \left(1 - \hat{C}_{i_t}\right)\Big|_{\hat{t}=1} + \sum_{i \in I_{P_D}} \hat{C}_{i_t}\Big|_{\hat{t}=1} - \sum_{i \in I_{P_U}} \hat{C}_{i_t}\Big|_{\hat{t}=1} \quad (2.33)$$

The maximum possible value for any of the component performance metrics P_i is 1. Since the aim is to maximize conversion and yield of desirable products, the maximum possible value for the sum of the species performance metrics is the sum of the cardinalities of sets I_R and I_{P_D}. Therefore, the value

of the sum after the optimization can be used as a score for the reactor, and the scores of the two reactors can be directly compared. To make a direct comparison, I introduce the percent species benefit, B_P, as the scoring metric for the reactor. The metric is defined in eq 2.34. The asterisks in the equation indicate the optimal values for the variables.

$$B_P = \frac{\sum_{i \in I_R} \left(1 - \hat{C}^*_{i_r}\right)\Big|_{\hat{x}_r=1} + \sum_{i \in I_{P_D}} \hat{C}^*_{i_r}\Big|_{\hat{x}_r=1} - \sum_{i \in I_{P_U}} \hat{C}^*_{i_r}\Big|_{\hat{x}_r=1}}{|I_R| + |I_{P_D}|} \times 100\% \tag{2.34}$$

A perfect reactor has a B_P score of 100%, indicating that all reactants are fully converted to desirable products. Therefore, a higher B_P value indicates closer performance to ideality.

2.7.2.2 Constraints

For the CFR, objective function 2.32 is maximized such that constraints 2.20 - 2.31 are satisfied. As was the case in optimization problem 1, all design variables are allowed to vary within their bounds to achieve the maximum percentage species benefit, B_P.

For the BR, reactor dimensions are fixed. In addition, the overall heat transfer coefficient is assumed constant with changing temperature. All other variables (temperature, concentration, and batch time) are allowed to vary. Therefore, optimization problem (2.33) is maximized such that trajectory constraints 2.20 - 2.25, temperature fluctuation constraint 2.26, and limiting re-

actant constraint 2.31, all written for the BR, are satisfied.

2.8 Case Studies

In this section, I present two case studies to illustrate the use of the framework. In both examples, I have assumed solvent properties (viscosity, diffusion coefficient, thermal conductivity, and specific heat capacity) of water at 300 K, given in Table 2.6. The differential variables (non-dimensional concentrations and temperature) were discretized using a finite-difference approach on a grid consisting of 1000 nodes, and integrated using the forward Euler method. In addition to the differential variables, the problems involved $2 \times |I_R| + 2$ scalar variables ($C_{i \in I_R,\text{ref}}$, $C_{i_0 \in I_R}$, d, L or t_B). The CFR optimization includes v as an additional scalar variable. For the two case studies presented in this chapter, the initial concentrations of all products ($i \in I_P$) were set to zero. Note that due to the non-convex nature of the problem and to the strong nonlinearities imposed by the reaction rate expressions, the solutions obtained were very sensitive to the initial guesses. Nevertheless, modern NLP solvers are readily capable of handling relatively large problems, as demonstrated in Case Study 2.

2.8.1 Case Study 1: Single, first-order reaction

In this section, I solve the problem presented in section 2.3 ($A \rightarrow B$) using the framework. The parameters for the reaction rate expression are as given in Table 2.1 ($E_A = 107,691$ J/mol, $k = 10^{14}$ s^{-1}). Nagy *et*

Table 2.6: Transport properties of water at 300 K, used in Case Studies 1 and 2 [104].

Property	**Value**
Density, ρ [kg/m^3]	996.5
Viscosity, μ [Pa s]	8.5367×10^{-4}
Thermal conductivity, λ [W / $m\,K$]	0.61032
Specific heat capacity, C_p [J / kg K]	4182
Diffusion coefficient, D [m^2 / s]	2.3×10^{-9}

al. [118] examined this particular system, and gave a theoretically-derived approximate value of $\chi = 3$. For this problem, $I_R = \{A\}$, $I_P = I_{P_D} = \{B\}$. I begin by answering the question of finding an equivalent CFR to the given BR (optimization problem 1), then proceed by comparing the optimal CFR with the BR after optimizing the operational conditions (optimization problem 2).

2.8.1.1 Case Study 1, Optimization Problem 1

I perform three runs of optimization problem 1, and present the main results in Table 2.7. Figure 2.5 shows the non-dimensional (left) and dimensional (right) concentration profiles along the non-dimensional and dimensional length and time of the CFR and BR, respectively. In run 1, the initial concentration for both reactors is fixed at 1 mol/L, as was done in section 2.3. The obtained non-dimensional profile is identical for both the CFR and the BR. The selected temperature (330 K) is close to that which was obtained in section 2.3, and the only difference is caused by the selection of a different total reactor length (2.97 m, instead of 3.00 m in the motivating example). The dimensional profiles along length and time in the CFR and BR are also

identical to those which were given in Figure 2.1(b) of section 2.3. This result validates the framework and verifies that the non-dimensional representation of the framework is equivalent to the original, dimensional problem.

Table 2.7: Parameters and optimal variable values for the three runs of case study 1, optimization problem 1.

	Run 1	**Run 2**	**Run 3**
$\mathbf{C_{A_{z0}}}$ [mol/L]	1.0	2.0	2.0
$\mathbf{T_z^{min}}$ [K]	280	280	390
$\mathbf{T_z^{max}}$ [K]	350	350	450
$\mathbf{T_z}^*$ [K]	330	330	397.4
$\mathbf{L}^*$ [m]	2.97	2.97	0.1
$\mathbf{v}^*$ [mm/s]	1.2	1.2	30.3
$\mathbf{d_z}^*$ [mm]	2.8	2.8	0.1

In run 2, the initial concentration of the CFR was changed to 2 mol/L while using the same reference BR. As can be seen in Figure 2.5, The non-dimensional profile of the CFR is identical to that of the reference BR. However, the dimensional profiles of the two reactors are different. This result shows that in the framework developed herein, two "equivalent" profiles do not necessitate equal numerical values, but the numerical values obey those imposed by the specific constraints that are relevant to the CFR. Nevertheless, the non-dimensional performance metrics (reactant conversion and desired product yield) are equal for the two reactors rendering them equivalent.

This fact is reinforced by run 3, where the allowable temperature range for the CFR is changed to higher values (see Table 2.7). As can be seen in Figure 2.5, the non-dimensional profiles of the batch and CFRs for run 3 remain

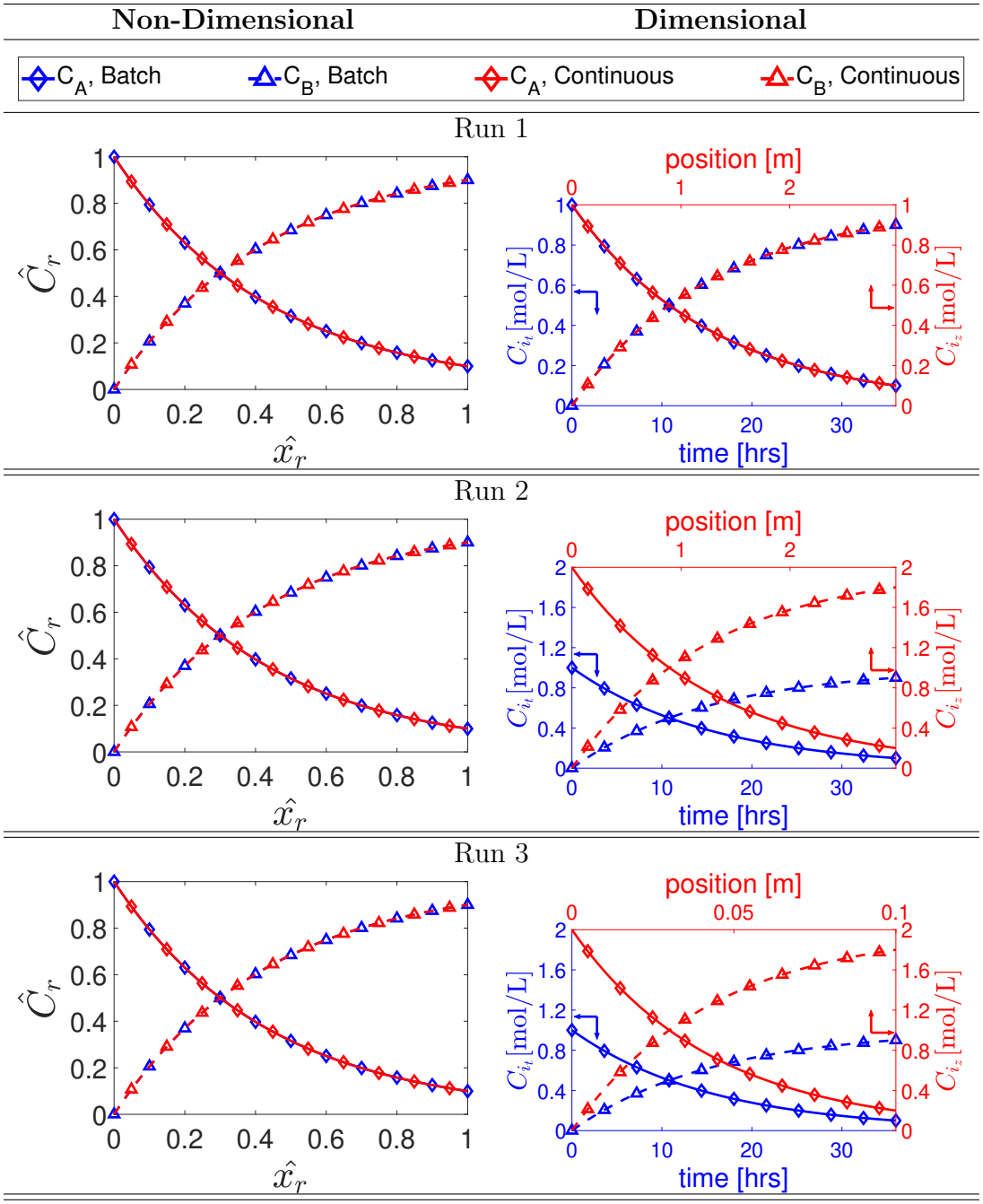

Figure 2.5: Non-dimensional (left) and dimensional (right) concentration profiles for the given BR and CFR found by solution of Optimization Problem 1 for Case Study 1. The non-dimensional profiles for all runs, as well as the dimensional profiles for run 1 for batch and CFR overlap.

identical, and the equivalence is achieved by selecting a different operating temperature, flow velocity, total reactor length and reactor diameter. All the values are within their allowable limits, and the reasonable design, assumption validity, and stability constraints are all met. Note that the reaction enthalpy, $\triangle H$, for this problem was assumed to be zero. As a result, the initial concentration of reactant A in this problem does not affect the temperature, and in turn the non-dimensional profiles of reactant and product.

2.8.1.2 Case Study 1, Optimization Problem 2

Optimization problem 2 was solved for both the BR and CFR, and I present optimal variable values and concentration profiles in Table 2.8 and Figure 2.6. Multiple global minima exist for both problems, and the presented solutions constitute one such minimum. The results presented indicate that by making modifications to the batch duration and operating temperature, 100% conversion of reactant A to product B can be achieved. Similarly, solutions exist that would allow complete conversion of the reactant to the product in the CFR. As such, both reactors obtain a percent species benefit of $B_P = 100\%$. Therefore, for this problem, the results indicate that improved operations can be achieved for both reactor types, and the operators should consider both modifying the conditions of the existing batch process or investing in the development of a novel, continuously operated process. A deeper economic analysis of the alternatives is therefore necessary.

Table 2.8: Optimal variable values obtained by solution of Optimization Problem 2 for Case Study 1.

BR		**CFR**	
$C_{A_{t0}}$ [mol/L]	1.0	$C_{A_{z0}}$ [mol/L]	2.0
t_B^* [hrs]	47.2	L^* [m]	0.1
T_t^* [K]	305.8	T_z^* [K]	371.0
$\hat{C}_A^*\left(\hat{t}=1\right)$	1.0	v^* [mm/s]	1.0
B_{P_t} [%]	100	d_z^* [mm]	0.5
		$\hat{C}_A^*\left(\hat{z}=1\right)$	1.0
		B_{P_z} [%]	100

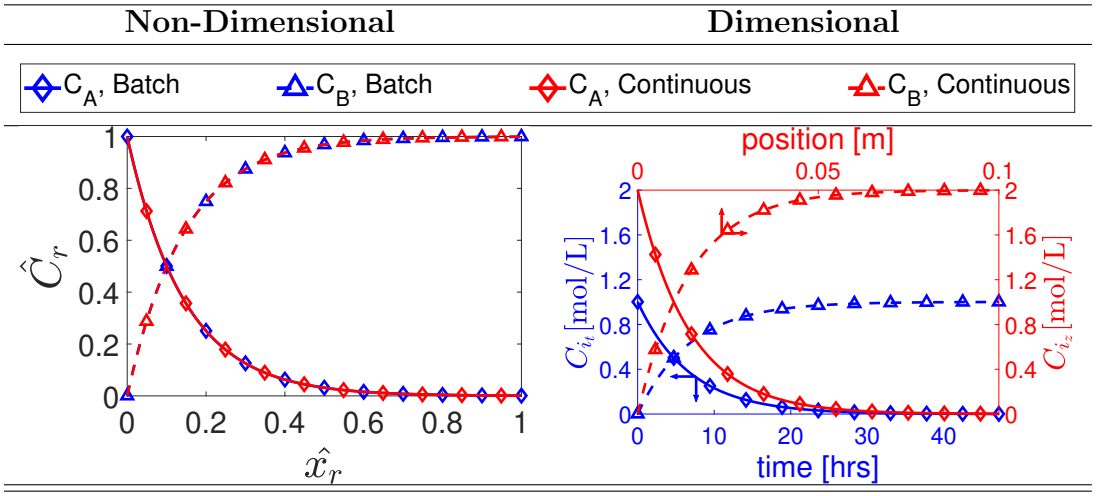

Figure 2.6: Non-dimensional (left) and dimensional (right) concentration profiles for the optimal BR and optimal CFR found by solution of Optimization Problem 2 for Case Study 1. The non-dimensional profiles for batch and CFR overlap.

2.8.2 Case Study 2: Parallel Exothermic Reactive System

Consider the system of three parallel reactions:

1. $A + B \rightarrow C$
2. $C \rightarrow 2E$
3. $2A \rightarrow D$

where product C is desirable. The parameters for the reaction rate expressions are given in Table 2.9. This problem is more complex in that it involves more chemical species, and because the reaction is highly exothermic. Contrary to case study 1, the magnitude of the concentration of reactant species will affect the evolution of both the concentration and temperature of the system, and maintaining a controllable temperature fluctuation within the reactor becomes more difficult.

Table 2.9: Parameters for the reaction rate expressions of Case Study 2.

	k_i	E_{A_i} [kJ/mol]	$\triangle H_i$ [kJ/mol]
Reaction 1	$6.493 \times 10^9 \ \ m^3 \, \text{mol}^{-1} \, s^{-1}$	66.275	-500
Reaction 2	$2.109 \times 10^4 \ \ s^{-1}$	33.137	0
Reaction 3	$1.631 \times 10^{14} \ \ m^3 \, \text{mol}^{-1} \, s^{-1}$	99.412	0

Following the system characterization procedure presented in section 2.4, $J_R = \{A, B\}$, $J_{P_D} = \{C\}$, and $J_{P_U} = \{D, E\}$. I assume that the concentration and temperature profiles of a BR are known, and are as shown in Figure 2.7. The exothermic reaction (reaction 1) is the only active reaction at

the start of the batch. This causes an initial rapid increase in temperature. However, after the concentrations of A and B are depleted, and due to the presence of a cold surrounding fluid at $T_{s_t} = 300$ K, the temperature reaches a maximum at $T_t = 343$ K then decreases to the starting temperature. A total heat transfer coefficient $U_t = 150$ W / $m^2\,K$ is assumed.

From the concentration profiles, it can be seen that reactant B has a lower initial concentration than A. This makes reactant B the limiting reactant for products C and E. Reactant A is the limiting reactant for product D. Therefore, the same limiting reactants are assigned for the CFR in both optimization problems 1 and 2.

2.8.2.1 Case Study 2, Optimization Problem 1

Optimization problem 1 is solved minimizing the total performance difference between the two reactors, allowing all design variables of the CFR to vary. The resulting non-dimensional and dimensional concentration and temperature profiles for both reactors are shown in Figs. 2.8 and 2.9, respectively. The parameters of the reference BR and the obtained equivalent CFR are summarized in Table 2.10. As can be seen from the non-dimensional concentration profiles, a comparison of the batch and CFRs reveals that the final reactant conversion and product yields for all species are within 5% of each other. This is despite the fact that the magnitudes of the concentration of all species are different, as can be seen from the dimensional concentration profiles. In addition, all constraints on the CFR dimensions are satisfied. This result validates

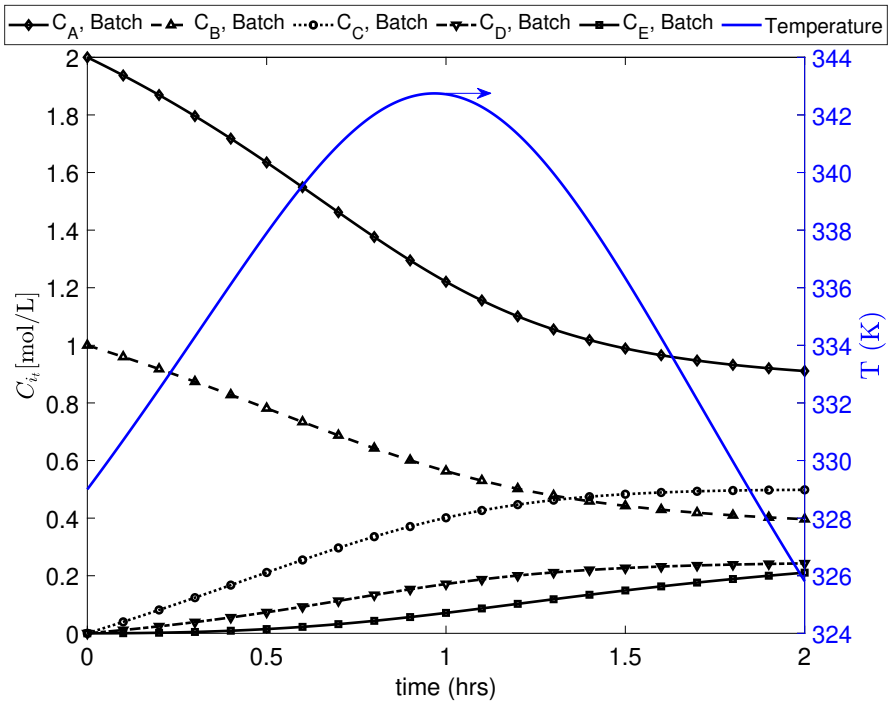

Figure 2.7: Given batch concentration (black, left ordinate) and temperature (blue, right ordinate) evolution through time for case study 2.

the utility of this approach in determining the feasibility of making a batch to continuous switch, even for complex reactive systems.

Table 2.10: Parameters and optimal variable values for case study 2, optimization problem 1.

	Batch				**Continuous**			
	$C_{i_{t0}}$ [mol/L]	$C_i(t=t_B)$ [mol/L]	C_{i,ref_t} [mol/L]	P_{i_t}	$C_{i_{z0}}$ [mol/L]	$C_i(z=L)$ [mol/L]	C_{i,ref_z} [mol/L]	P_{i_z}
A	2.000	0.911	2.000	0.544	3.229	1.456	3.229	0.549
B	1.000	0.396	1.000	0.604	1.632	0.692	1.632	0.576
C	0.000	0.498	1.000	0.498	0.000	0.855	1.632	0.524
D	0.000	0.243	1.000	-0.243	0.000	0.416	1.615	-0.258
E	0.000	0.211	2.000	-0.105	0.000	0.172	3.265	-0.0528
B_P [%]	43.267				44.606			
d [mm]	500.000				3.640			
t_B [hrs]	2.000				-			
L [m]	-				3.000			
v [mm/s]	-				1.000			

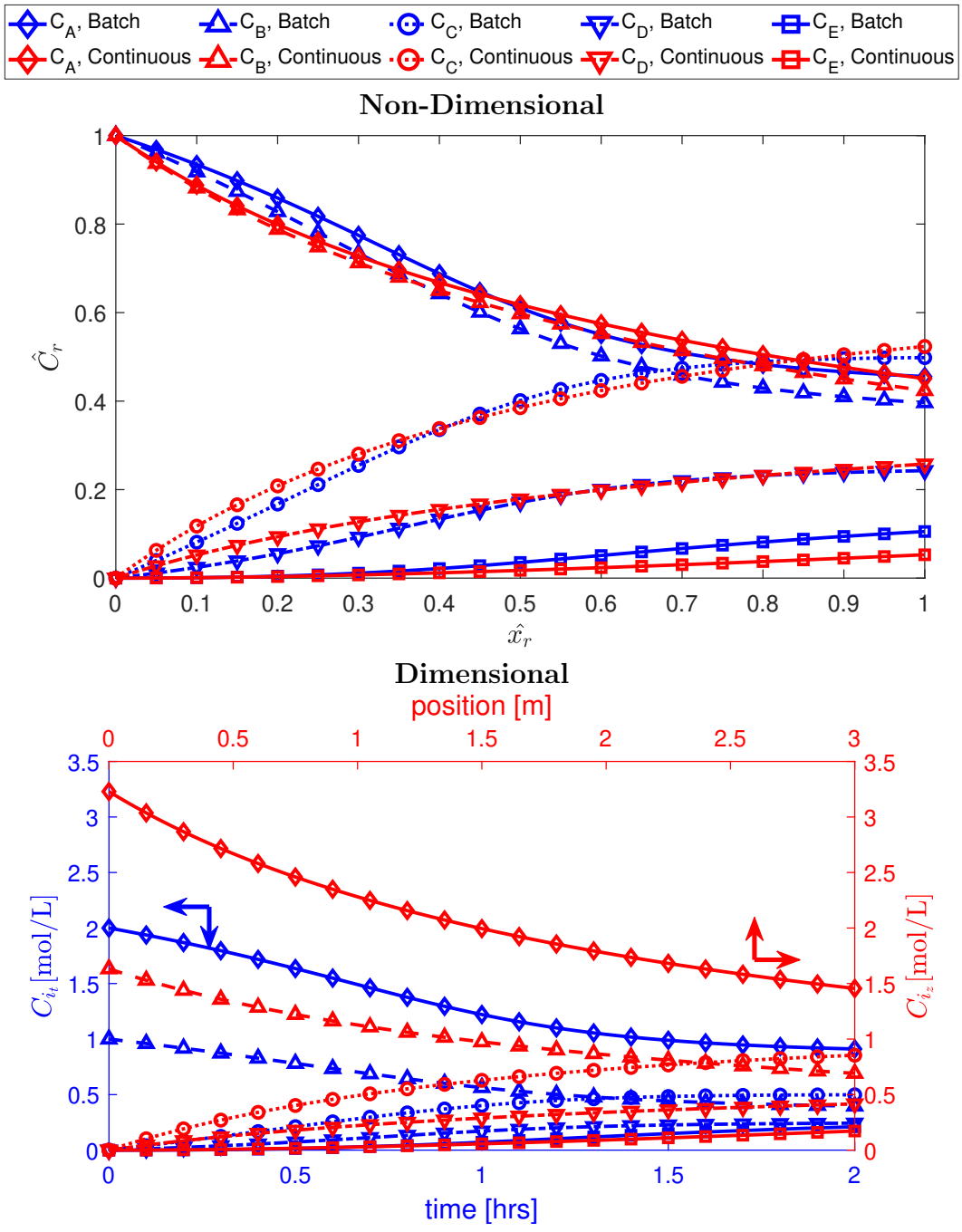

Figure 2.8: Non-dimensional (top) and dimensional (bottom) time and spatial concentration profiles for the given batch and equivalent CFR found by solution of Optimization Problem 1 for Case Study 2.

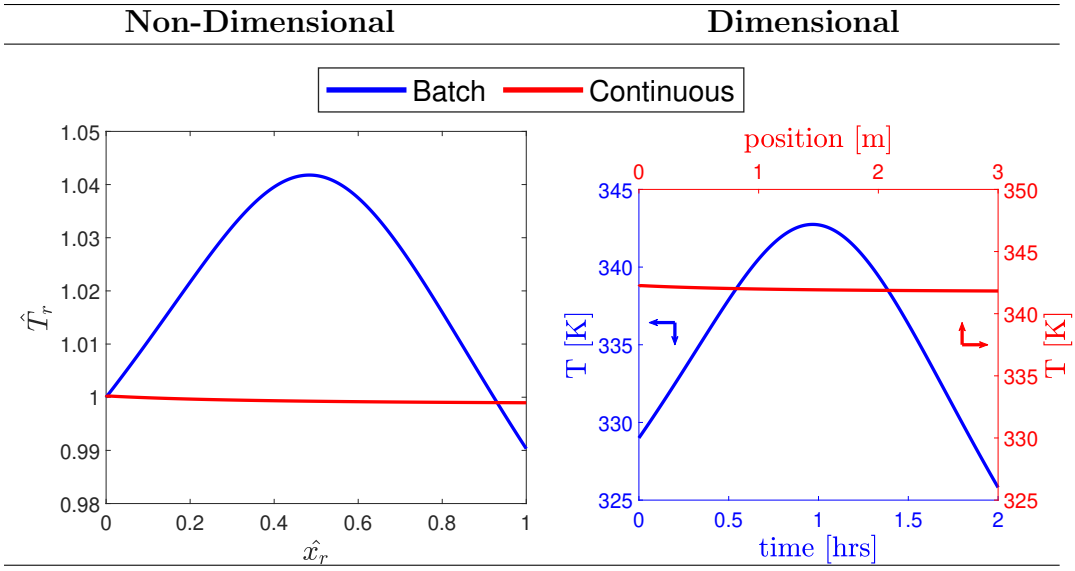

Figure 2.9: Non-dimensional (left) and dimensional (right) time and spatial temperature profiles for the given batch and equivalent CFR found by solution of Optimization Problem 1 for Case Study 2.

The temperature profiles (Figure 2.9) of the BR and CFR are vastly different, and are both respectively representative of their reactor class. The excellent heat dissipation of microreactors ensures that the reaction heat does not accumulate within the reactor, resulting in an almost constant temperature along the reactor length. The numbering up (instead of scaling up) concept that is used for scaling out microreactors to meet industrial demands means that this statement is true for all scales.

On the contrary, conventional BRs are expected to have much slower heat transfer rates, as reflected in the lower heat transfer coefficient. Therefore, the temperature variation is much higher. It should be noted that the constant wall temperature assumption is scarcely representative of industrial scale

BRs, the size of which hinders tight control over wall temperatures. In addition, making the well-mixed assumption and neglecting position-dependent temperature variation within the reactor is a less reasonable assumption for the large batch vessels compared to the intensified CFRs.

Furthermore, the excellent heat management within the CFR enables the use of a more concentrated reactant mixture of A and B than the reference BR. The higher concentration further promotes lower reactor volumes or the higher throughput of the continuous-flow regime, and will therefore contribute towards reducing both capital and operating investments. The difference in operating costs associated with labor and reactor clean-up for the BR was also neglected in the work presented in this chapter. Including this difference would have further weakened the BR position.

Considering all the aforementioned points, the proposed framework is optimistic for the BR, and rather conservative for the CFR, despite its simplicity. The framework becomes more optimistic for the BR with increasing scale, since the modeling assumptions are less accurate for "scaling up" (batch) than "scaling out" (CFR). This is true of all problems assessed using our framework.

2.8.2.2 Case Study 2, Optimization Problem 2

Optimization problem 2 was solved for this case study, and the results are presented in Table 2.11 and Figs. 2.10-2.11. Maximizing the total performance of the BR allowing the temperature, batch time, and initial reactant concentration to vary resulted in an increase in performance (as quantified

by B_{P_t}) by 8.5%. This is achieved by increasing the initial concentration of reactant A to its upper bound in order to maximize the rate of the desired reaction. This increase is accompanied by a necessary decrease in the initial concentration of reactant B so that the maximum temperature attained is less than the upper bound on the temperature fluctuation, $\triangle T_{\max_t}$, that was imposed in the problem. An increase in $\triangle T_{\max_t}$ would directly correlate with a further increase in total BR performance. However, the improvement comes at a cost of a less controllable system due to the larger temperature fluctuation.

Table 2.11: Parameters and optimal variable values for case study 2, optimization problem 2.

	Batch				**Continuous**			
	C_{it0} [mol/L]	$C_i(t=t_B)$ [mol/L]	C_{i,ref_t} [mol/L]	P_{i_t}	C_{iz0} [mol/L]	$C_i(z=L)$ [mol/L]	C_{i,ref_z} [mol/L]	P_{i_z}
A	10.000	6.238	10.000	0.376	10.000	1.220	10.000	0.878
B	1.000	0.177	1.000	0.823	6.381	1.220	6.383	0.809
C	0.000	0.735	1.000	0.735	0.000	4.506	6.383	0.706
D	0.000	1.469	5.000	-0.294	0.000	1.808	5.000	-0.362
E	0.000	0.176	2.000	-0.088	0.000	1.316	12.766	-0.103
B_P [%]	51.738				64.268			
d [mm]	500.000				4.607			
t_B [hrs]	2.201				-			
L [m]	-				3.000			
v [mm/s]	-				1.000			

Solving optimization problem 2 for the CFR results in an increase of 19.7% in total reactor performance. The better heat dissipation of the CFR means that the initial concentrations of reactants A and B take on their maximum allowable values without fear of hot spot formation or an uncontrollable temperature. The maximum concentration of reactant B is dictated by the decision to assign reactant B the limiting reactant status for reaction 1. Since a portion of reactant A goes towards forming the undesirable product D, the

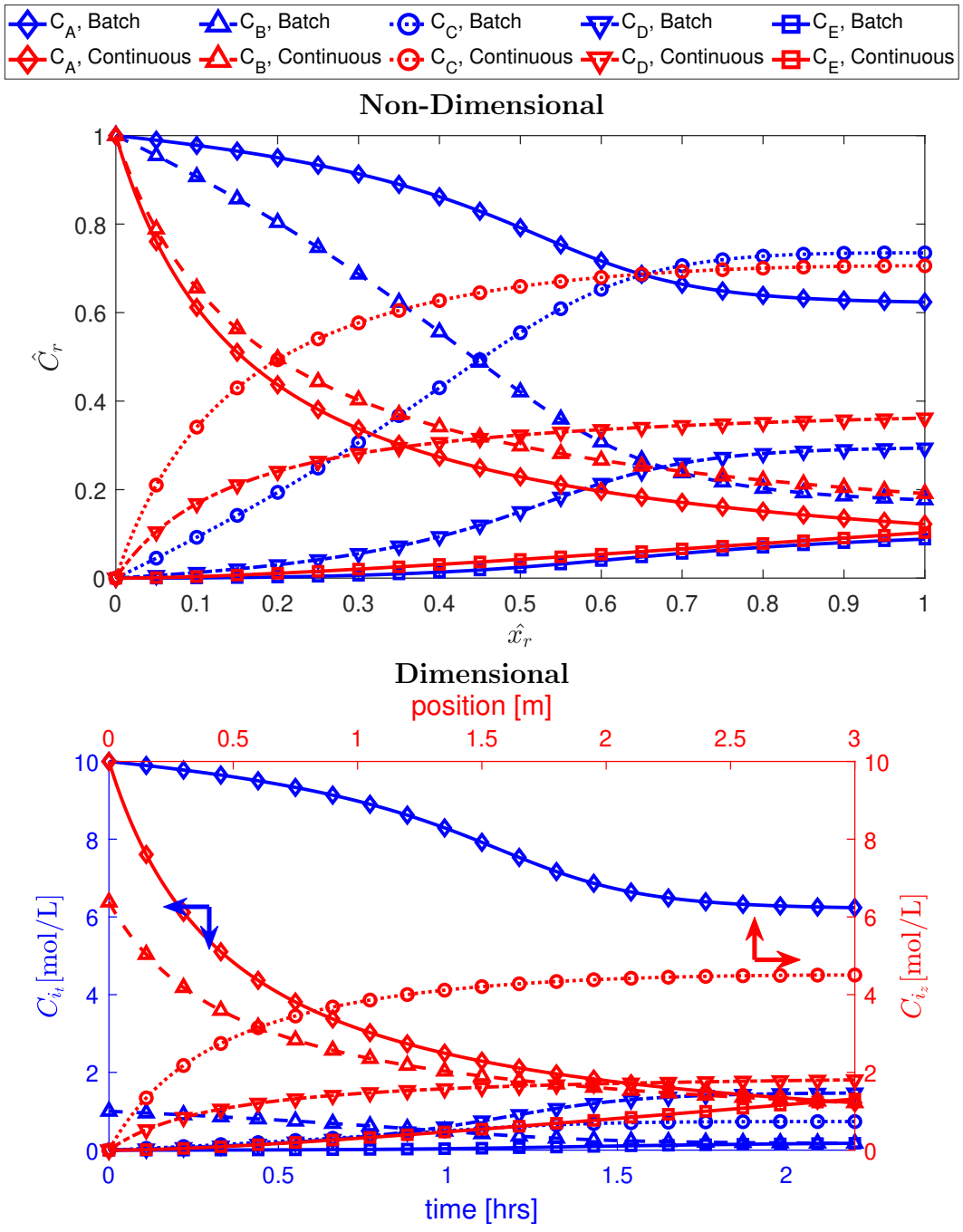

Figure 2.10: Non-dimensional (top) and dimensional (bottom) time and spatial concentration profiles for the optimal batch and optimal CFR found by solution of Optimization Problem 2 for Case Study 2.

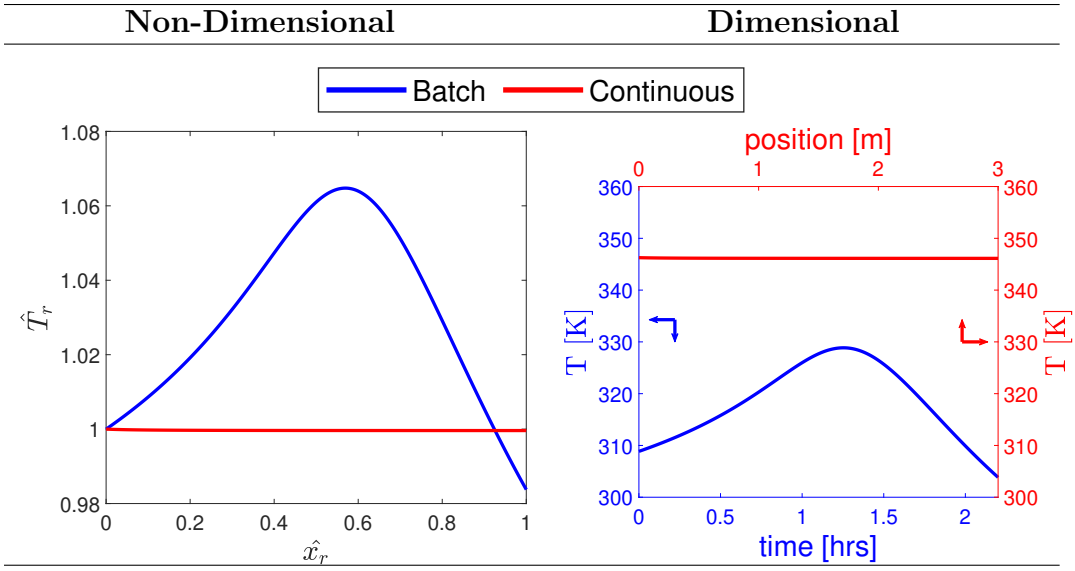

Figure 2.11: Non-dimensional (left) and dimensional (right) time and spatial temperature profiles for the optimal BR and optimal CFR found by solution of Optimization Problem 2 for Case Study 2.

maximum allowable initial concentration of B is bounded by the extent of reaction 3. This, in turn, means that the maximum reactor performance is bounded by the extent of reaction 3, and the upper bound on reactant concentrations. Changing the initial concentrations of the reactants to achieve a better performance is a much easier task than designing better control algorithms. This example therefore clearly highlights the utility of the framework in quantifying the value of the well known superior heat management advantage of microreactors compared to conventional BR vessels.

2.9 Summary

In this chapter, I have introduced a general framework that facilitates the comparison between the performance of an existing BR to a potential CFR, and can serve to guide the business decision of whether to invest in a transition between the two reactors or to consider the optimization of an existing batch unit. The methodology involves (1) characterizing the chemical species within the reaction mixture, and assigning roles to each species (reactant, desirable product, or undesirable product); (2) Defining a species-based, non-dimensional performance metric to quantify the ability of the reactor to deliver a system where each species achieves its chemical role (i.e. the ability of a reactant to fully react, a desired product to form, or an undesired product to not form); (3) writing non-dimensional energy and mass balances to model the evolution of the reactive system through time or space; (4) constructing and solving an optimization problem to answer the question of the feasibility of the switch by finding out whether there exists a feasible CFR that may deliver equivalent performance to an existing BR while satisfying all the design constraints that are specific to CFRs; (5) constructing and solving an optimization problem to quantify the potential benefit that may be gained from designing a new CFR compared to optimizing the operational conditions of an existing BR. The framework was successfully demonstrated using two case studies.

As anticipated, using the framework on a non-exothermic, simple case study such as case study 1 shows that there is no clear benefit in making

the batch to continuous switch. However, applying the framework on the more realistic, highly exothermic case study 2 with multiple parallel reactions showed that the switch from batch to continuous can yield a 12% improvement in total reactor performance score. This is an agreement with literature studies that conclude that for highly exothermic reactions, CFRs can provide major advantages. Case study 2 also highlights the generality of the framework in admitting relatively complex reaction schemes without the need to perform detailed modeling and simulations.

2.10 Nomenclature

Sets

$I = \{i : i_1, \ldots, i_{N_I}\}$ Set of chemical species.

$I_P(i)$ Subset of chemical species that are products.

$I_{P_D}(i)$ Subset of chemical species that are desirable products.

$I_{P_U}(i)$ Subset of chemical species that are undesirable products.

$I_R(i)$ Subset of chemical species that are reactants.

$I_j^R(i)$ Limiting reactant for reaction j, where $j \in J_R$.

$J = \{j : j_1, \ldots, j_{N_J}\}$ Set of chemical reactions.

$J_R(j)$ Subset of chemical reactions where all reactants are members of I_R.

Parameters

C_p Specific heat capacity of the mixture [J/kg K].

D Solvent diffusion coefficient $[m^2/s]$.

E_{Aj} Activation energy for reaction j.

R Universal gas constant.

g_{ij} Reaction order of component i in reaction j.

k_j Pre-exponential factor for reaction j.

$\triangle H_j$ Enthalpy change of reaction j [J/mol].

γ_r Parameter to indicate whether equation is written for batch ($\gamma_t = 1$) or continuous flow ($\gamma_z = v$) operating mode.

λ Thermal conductivity of solvent $[J \,/\, m\, K\, s]$.

μ Solvent viscosity [kg / m s].

η_{ij} Stoichiometric coefficient of component i in reaction j.

ρ Mixture mass density [kg/m^3].

χ Parameter introduced to account for the effect of chemical reactions on Damkohler number.

Continuous Variables

C_i Molar concentration of species i [mol/m^3].

$C_{i,F}$ concentration of component i at the reactor outlet or at the end of the batch for the flow reactor or batch reactor, respectively [mol/m$^3 s$].

$C_i^{\max}$ Maximum possible concentration of product $i \in I_P$ [mol/m$^3 s$].

d Reactor internal diameter [m].

Da Damkohler number.

P_i Performance metric for chemical species i.

r_j Reaction rate expression for reaction j [mol/m^{3}s].

R_i Sum of rates of generation and consumption of species i [mol/m$^3 s$].

T Temperature [K].

T_s Temperature of the heating/cooling agent [K].

U Overall heat transfer coefficient [J/m^2 K s].

v Flow velocity $[m/s]$.

X_i Conversion of reactant $i \in I_R(i)$.

y_i Yield of product $i \in I_P(i)$.

Chapter 3

Batch to Continuous: Economics-Based Optimization For Reactor Networks

3.1 Introduction

In this chapter[1], I extend the framework presented in the previous chapter to offer a more complete framework that combines the problems of batch and continuous optimal reactor design with the problems of optimizing process economics, and optimal reactor network synthesis.

3.1.1 Extensions to the Batch/Continuous Reactor Optimization Framework

The strength of the approach presented in Chapter 2 was illustrated in its ability to make quick comparisons between the performances of the optimal reactors of the two operating modes due to the generalized, dimensionless performance metrics used in the objective functions. To the author's knowledge, the approach presented in the previous chapter was the first to generalize the batch to continuous reactor feasibility problem and to give a systematic

[1]The contents of this chapter are largely based on the following publication: [46] Joseph G. Costandy, Thomas F. Edgar, and Michael Baldea. A Unified Reactor Network Synthesis Framework for Simultaneous Consideration of Batch and Continuous-Flow Reactor Alternatives. *Industrial and Engineering Chemistry Research*, 60:7232–7256, 2021. J. C. is the primary author of the manuscript.

procedure for determining whether the switch is feasible and desirable for any chemical system (i.e., not specific to a particular set of chemical species) [44].

Nevertheless, there were several limitations to the methodology presented in Chapter 2, which are addressed in this chapter:

1. The methodology employed in Chapter 2 necessitated the solution of *two* optimization problems: one for the batch reactor (BR) and one for the continuous-flow reactor (CFR). Ultimately, I aim to arrive at a framework that utilizes a *single* optimization problem to simultaneously provide answers to the questions of optimal operating mode as well as optimal reactor design. This is provided in this chapter.

2. The methodology employed in Chapter 2 only considered the plug-flow reactor (PFR) for the continuous-flow operating mode and the BR for the batch operating mode. In this chapter, the continuously stirred tank reactor (CSTR) and the semi-batch reactor (SBR) are included in addition to the PFR and BR for the continuous-flow and batch operating modes, respectively, completing the set of all possible ideal reactors for the two operating modes.

3. The methodology employed in Chapter 2 defined performance metrics in terms of product yield and reactant conversion only, without explicitly accounting for economics. As was discussed in Chapter 1.1, the evaluation of economics must account for the difference in the nature of

the operations between the two operating modes (e.g., batch time includes time for loading and unloading the reactor and clean-up between batches, the use of the batch reactors for the manufacture of other products after demand for the product of interest has been met, etc.). These considerations are included in this chapter.

4. The methodology employed in Chapter 2 only considered the use of a single reactor for each operating mode. In many cases, networks of interconnected reactors substantially increase the overall performance. For example, Fonseca *et al.* illustrated that, for the transesterification of vegetable oils, many CSTRs in series are necessary to achieve the same performance of a single BR [66]. Therefore, in this chapter, a more complete framework is presented that not only selects the optimal operating mode but also optimizes the number and type of reactors within the selected operating mode.

3.1.2 A Brief Overview of Reactor Network Synthesis

The problem of reactor network synthesis has received much attention, and many frameworks exist to address the problem. The majority of the work in the literature, however, addresses only the problem of continuous-flow reactor networks. After selecting the continuous-flow operating mode, the attainable region method [2, 7, 53, 61, 62, 71, 84, 85, 86, 87, 96, 133], superstructure optimization [3, 4, 5, 15, 16, 42, 59, 99, 100, 101, 102, 143, 145, 156], stochastic optimization [110, 111], and dynamic optimization [18,

19, 58, 67, 80, 88, 94, 95, 121, 122, 123, 124, 125, 126, 127, 172, 173, 174] have been used to arrive at the optimal reactor network and/or the optimal process. Note that some of the referenced literature merges several of the aforementioned categories and may focus only on the reactor or on the full process synthesis problem. Dedicated literature reviews on reactor network and process synthesis are available in the recent literature [41, 64, 155, 157].

Unlike the previously referenced works that focus on the continuous-flow operating mode, there are few works that introduce strategies for batch reactor network optimization. The methodologies exploit the similarity between the BR and the PFR and apply design approaches that were previously developed for the continuous-flow operating mode to design networks of PFRs and CSTRs and then interpret the flow profiles in the context of a BR or a SBR [14, 115, 166, 179]. These works provide the tool for addressing the reactor network design problem for batch *or* continuous-flow. A framework that simultaneously considers the two operating modes in a single optimization problem has not, to my knowledge, been reported prior to this work.

3.1.3 Goals and Outline

The product of this chapter is a framework that consists of a single optimization problem (given in eq 3.1), the solution of which provides the optimal operating mode (batch/continuous), optimal reactor network configuration (number and type of each reactor within a network), and the optimal design (reactor volume) of each reactor for the manufacture of a given product,

where optimality is defined based on an economic metric, and the impacts of the differences in the nature of the operating modes are accounted for.

$$\begin{aligned} \max \quad & \text{Profit} \\ \text{s.t.} \quad & \text{Reactor profiles (sections } 3.3 - 3.4) \\ & \text{Logical conditions (section } 3.5) \\ & \text{Process economics (section } 3.6) \end{aligned} \tag{3.1}$$

After stating the problem (section 3.2), I begin by describing a single reactor module and illustrating how this reactor module may be used to represent the different reactor types within the two operating modes (section 3.3). Next, I show how the single reactor module may be considered a unit within a wider network of reactors in series. To this end, I introduce orthogonal collocation on finite elements on reactor elements (OCFERE) as an extension of the orthogonal collocation on finite elements (OCFE) method where reactors in series naturally appear as an added layer of elements (section 3.4). Next, I introduce a series of logical constraints that allow the automatic consideration of the differences in the operations of the two operating modes and the considered reactor types (section 3.5). Next, I introduce the equations used to calculate the economic performance of the reactor network, taking into account the differences in the economics between the operating modes (section 3.6). Finally, I illustrate the utility of the framework on a case study for the van de Vusse reaction system (section 3.7). The notation used in the chapter is summarized in Table 3.1.

Table 3.1: Notation followed in the model description

Notation	Type	Example
Sets		
upper-case Latin letters	set names	P
lower-case Latin letters	set indices	p_0
superscripts (on variables)	time-related set indices	$\mathbf{x}^{p_0}$
subscripts (on variables)	superstructure-related set indices	$\mathbf{x}_{j_1}$
Parameters		
Greek letters	model parameters	α
overbars and underbars on Latin letters	non-zero upper and lower bounds	$\underline{X}$, $\overline{X}$
Variables		
boldface, lower-case Latin letter $\mathbf{y}$	binary variables	$\mathbf{y}^r_{\mathbf{U}}$
boldface, upper-case Greek letter $\mathbf{\Lambda}$	integer variables	$\mathbf{\Lambda_B}$
boldface, lower-case Latin letters	time-varying variables (within reactor)	$\mathbf{x}^{p,q,r}$
boldface, upper-case Latin letters	reactor-varying variables (between reactors)	$\mathbf{X}^r$
boldface, upper-case Greek letters	global variables	$\mathbf{\Psi}$

3.2 Problem Statement

Given:

1. A system of chemical reactions $J = \{j : j_1, \ldots, j_{N_J}\}$ involving a set of chemical species $I = \{i : i_1, \ldots, i_{N_I}\}$.

   - Each reaction j has a known reaction rate expression $\mathbf{r}_j(t) = \mathbf{g}_j\left(\mathbf{c}_i(t)\right)$ where $\mathbf{g_j}$ is a known function of chemical species concentrations $\mathbf{c}_i(t)$.

- Each chemical species i belongs to one of three sets: $I_R(i)$ of reactants, $I_{P_D}(i)$ of desirable products, or $I_{P_U}(i)$ of undesirable products. A mixed stream containing the members of $I_R(i)$ at concentrations C_i^{feed} is available and can be purchased at cost ζ_i^{raw} [\$/kmol]. Species that belong to $I_{P_D}(i)$ are the process products and are sold at ζ_i^{sale} [\$/kmol]. Impurities in the product stream (members of $I_R(i)$ or $I_{P_U}(i)$) are subjected to a product treatment that costs ζ_i^{treat} [\$/kmol].
- There is a maximum demand of δ_i [kmol/yr] of species $i \in I_{P_D}$.
- Note that the energy balance and the effect of temperature may also be included but has been neglected in this chapter for simplicity.

2. A set of operating modes $M = \{m : m_B, m_C\}$ denoting the two operating modes, batch (m_B) and continuous-flow (m_C).

    - Each operating mode has an appropriate model for calculating the annual revenues, $\mathbf{\Theta}_m$, and annualized costs, $\mathbf{\Xi}_m$. These models account for the differences in the nature of the operations of the two operating modes (e.g., reactor clean-up between batches) and are discussed in detail in section 3.6.

3. A set of reactor types $T = \{t : t_{PFR}, t_{CSTR}, t_{BR}, t_{SBR}\}$, where PFRs, CSTRs, BRs, and SBRs are the four types I consider in this work. The flow diagrams of the options considered are shown in Figure 3.1.

- Each reactor type t may have a volume that lies within the interval $\left[\underline{V_t}, \overline{V_t}\right]$ [m^3] and a residence time that lies within the interval $\left[\underline{W_t}, \overline{W_t}\right]$ [hrs].
- Storage tanks are available if needed for operating a SBR (see Figure 3.1) and have a volume that lies within the interval $\left[\underline{V_{\text{st}}}, \overline{V_{\text{st}}}\right]$.

4. A map of reactor type to operating mode $M_T(m,t) = \{(m_C, t_{PFR}), (m_C, t_{CSTR}), (m_B, t_{BR}), (m_B, t_{SBR})\}$, where the existence of the member (m,t) means that reactor type t belongs to operating mode m.

Determine:

1. The optimal operating mode, where optimality is achieved by maximizing annual net profits.
2. The optimal reactor network configuration, including the number and types of all reactors connected in series that will be employed in a single plant.
3. The volume and residence time of each of the reactors that will be employed, as well as the optimal concentration profiles.

3.3 Unified Batch/Continuous Superstructure Representation for Single Reactor Module

In order to develop a reactor network superstructure that encompasses both the batch and the continuous-flow operating modes, I begin in this sec-

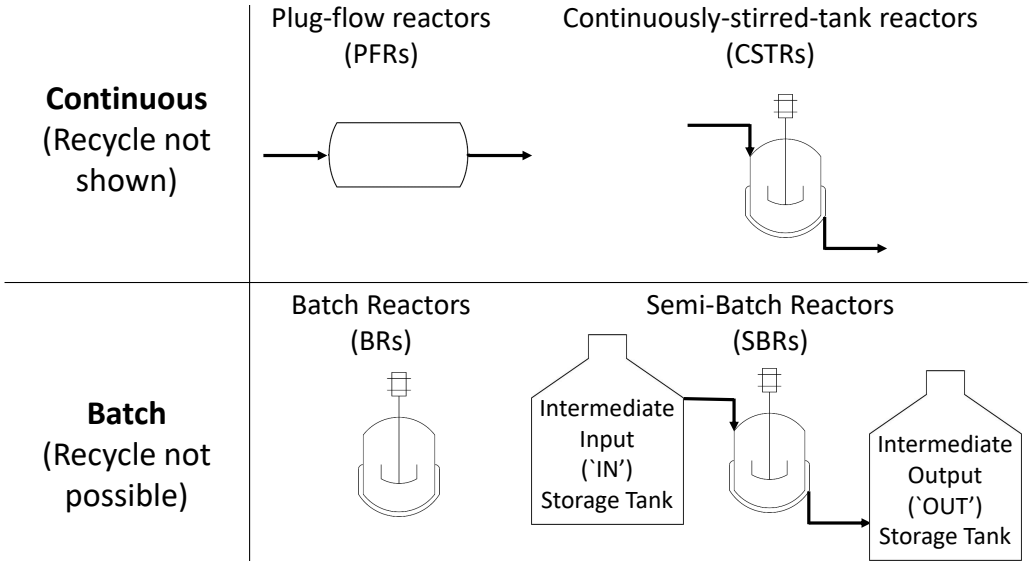

Figure 3.1: Reactor types considered in this work.

tion by focusing on a single reactor module. The goal of this section is to demonstrate the utility of the chosen reactor module in representing all the considered reactor types within the two operating modes. The representation of a reactor network will be achieved by connecting multiple single reactor modules in series and will be discussed in section 3.4.

The superstructure of units used to represent a single reactor is shown in Figure 3.2. The single reactor module involves a set $U = \{u : u_f, u_{s_1}, u_{s_2}, u_{s_3}, u_{m_1}, u_{m_2}, u_{m_3}, u_r, u_e\}$ of units. These units are connected, and the map of unit-unit connections is $U_u(u, u') = \{ (u_f, u_{s_1}),\ [(u, u'), (u \in U_s, u' \in U_m)], (u_{m_1}, u_r),\ (u_{m_2}, u_r),\ (u_r, u_{s_2}),\ (u_r, u_{s_3}),\ (u_{m_3}, u_e) \}$. The units u_f and u_e are the feed and the effluent units of the reactor. Between the two, there is a network involving stream splitters $U_s(u) = \{u_{s_1}, u_{s_2}, u_{s_3}\}$, mixers $U_m(u) =$

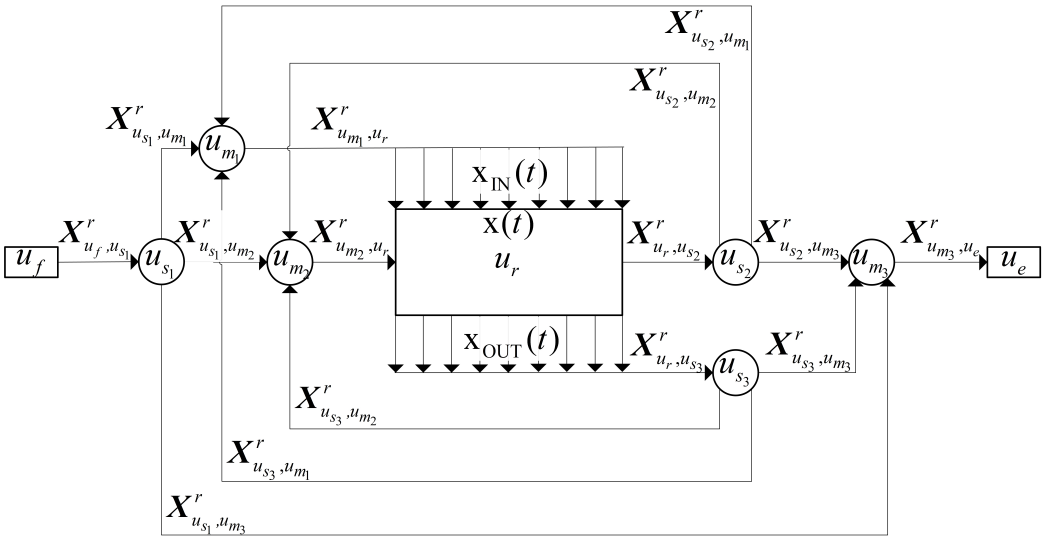

Figure 3.2: Single reactor used to represent all reactor types in all operating modes.

$\{u_{m_1}, u_{m_2}, u_{m_3}\}$, and the reactor $U_r = \{u_r\}$. The reactor takes on the "differential sidestream reactor" (DSR) configuration, which is defined by the availability of the option to admit or expel material as the reaction progresses into the parallel streams labeled "IN" and "OUT", respectively.

Within a single reactor module, there are two types of variables. The first, denoted by $x(t)$ in Figure 3.2, are variables that vary with time within the reactor. The second, denoted $\mathbf{X}^r_{u,u'}$ in Figure 3.2, are variables that take on a single value for the reactor module. The actual variable identities depend on the operating mode. For example, whereas volumetric flow rate can be used to describe material transport from one unit to the next in the case of the continuous-flow operating mode, absolute volume is the appropriate metric for the batch operating mode. This fact will be demonstrated in the following

two subsections (3.3.1 and 3.3.2), where the material balances for each of the two operating modes will be derived. In section 3.3.3, I show how variables are normalized in order to achieve a system of equations that describes a reactor of either operating mode.

Several modeling assumptions are made for the derivation of the equations for both operating modes:

- Cylindrical reactor geometry
- Homogeneous, incompressible liquid-phase systems
- Negligible pressure drop and no effect of gravitational acceleration
- Negligible dispersion effects
- Perfect mixing
- Constant solvent properties (specific heat capacity, diffusion coefficient, viscosity, and thermal conductivity)
- Isothermal operation
- Ideal splitters and mixers

The aforementioned assumptions are made to simplify the presentation of the framework. Nevertheless, the framework can be extended to accommodate systems where the assumptions must be relaxed, and any reactor, splitter, and mixer models may be employed instead of those I present herein

to accommodate the specific chemical reaction scheme of interest in any case study.

3.3.1 Continuous-Flow Single Reactor Module

In the continuous-flow operating mode, constant transport of material from one unit to the next is occurring. For steady-state operation, this means that a constant molar flowrate is present between any two adjacent units. Therefore, after applying the constant density assumption, the overall mass balance for the splitter, mixer, and reactor units reduces to eq 3.2, where $\mathbf{F}_{u,u'} \in \left[\underline{F}, \overline{F}\right]$ is the volumetric flowrate of the stream connecting units u and u' [m^3/hr].

$$\sum_{u \in U_u} \mathbf{F}_{u,u'} = \sum_{u'' \in U_u} \mathbf{F}_{u',u''} \qquad u' \in (U_s \cup U_m \cup U_r) \tag{3.2}$$

The component balances for the ideal splitters and mixers are given by eqs 3.3 and 3.4, respectively, where $\mathbf{C}_{i,u,u'} \in \left[0, \overline{C_i}\right]$ is the molar concentration of species i in the stream connecting units u and u' [kmol/m^3], and an upper bound on concentration is obtained using the known reaction stoichiometry (see section 2.5.1 for the detailed algorithm used to calculate $\overline{C_i}$).

$$\mathbf{C}_{i,u,u'} = \mathbf{C}_{i,u',u''} \qquad u' \in U_s,\ (u,u') \in U_u,\ (u',u'') \in U_u,\ \forall i \in I \tag{3.3}$$

$$\sum_{u \in U_u} \mathbf{F}_{u,u'} \cdot \mathbf{C}_{i,u,u'} = \sum_{u'' \in U_u} \mathbf{F}_{u',u''} \cdot \mathbf{C}_{i,u',u''} \qquad u' \in U_m,\ \forall i \in I \qquad (3.4)$$

To model the reactor unit, overall and component material balances on a differential element of the reactor are performed as shown in Figure 3.3. The independent variables over which the element is defined may be position (as was the case in the analysis presented in Chapter 2), volume or time (τ), and the three can be related using the volumetric flowrate and/or the cross-sectional area of the reactor. For consistency with the batch case, time is used as the independent variable for the differential element in this chapter, but note that the three variables are interchangeable, and several works have used volume or position as the independent variable for writing the material balance for a DSR (see, for example, Schweiger and Floudas [145]). The variables whose values may change with residence time are the volumetric flowrate within the reactor, $\mathbf{f}(\tau) \in \left[\underline{F}, \overline{F}\right]$, the concentration of species i inside the reactor, $\mathbf{c}_i(\tau) \in \left[0, \overline{C_i}\right]$, the volumetric flowrate in the "IN" and "OUT" streams that flow parallel to the reactor, $\mathbf{f_{IN}}(\tau) \in \left[\underline{F}, \overline{F}\right]$ and $\mathbf{f_{OUT}}(\tau) \in \left[\underline{F}, \overline{F}\right]$, and the concentration of species i in the "OUT" stream, $\mathbf{c_{OUT},}_i(\tau) \in \left[0, \overline{C_i}\right]$. Additionally, the concentration of species i in the "IN" stream can be allowed to vary with time for added design flexibility but has been considered constant along the reactor length, $\mathbf{C_{IN},}_i \in \left[0, \overline{C_i}\right]$, for this work.

The overall material balances yield eqs 3.5 - 3.7 for the differential

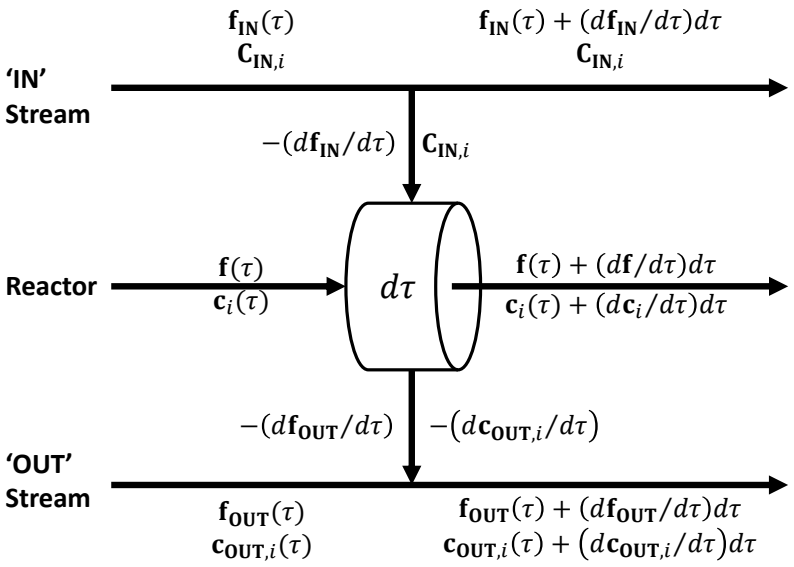

Figure 3.3: CFR mass balance on reactor differential element.

change in $\mathbf{f}$, $\mathbf{f_{IN}}$ and $\mathbf{f_{OUT}}$. The differential change in flowrate in the "IN" and "OUT" streams ($\dot{\mathbf{f}}_{\mathbf{IN}}$ and $\dot{\mathbf{f}}_{\mathbf{OUT}}$) are design variables whose values depend on the chosen reactor type. The component material balances yield eqs 3.8 and 3.9 for the differential change in $\mathbf{c}_i$ and $\mathbf{c_{OUT,}}_i$. The initial and final conditions for each of the differential variables are given by eqs 3.10 and 3.11, respectively, where $\boldsymbol{\Omega}$ is the total residence time of the reactor.

$$\left(\frac{\mathbf{df}}{\mathbf{d}\tau}\right) = -\dot{\mathbf{f}}_{\mathbf{IN}} - \dot{\mathbf{f}}_{\mathbf{OUT}} \tag{3.5}$$

$$\left(\frac{\mathbf{df_{IN}}}{\mathbf{d}\tau}\right) = \dot{\mathbf{f}}_{\mathbf{IN}} \tag{3.6}$$

$$\left(\frac{\mathbf{df_{OUT}}}{\mathbf{d}\tau}\right) = \dot{\mathbf{f}}_{\mathbf{OUT}} \tag{3.7}$$

$$\left(\frac{\mathbf{dc_i}}{\mathbf{d}\tau}\right) = \frac{\dot{\mathbf{f}}_{\mathbf{IN}}}{\mathbf{f}}\left(\mathbf{c}_i - \mathbf{C}_{\mathbf{IN},i}\right) + \sum_{j}^{j_{N_J}} \eta_{i,j} \cdot \mathbf{r}_j \quad \forall i \in I \tag{3.8}$$

$$\left(\frac{\mathbf{dc_{OUT,i}}}{\mathbf{d}\tau}\right) = \frac{\dot{\mathbf{f}}_{\mathbf{OUT}}}{\mathbf{f}_{\mathbf{OUT}}}\left(\mathbf{c}_i - \mathbf{c}_{\mathbf{OUT},i}\right) \quad \forall i \in I \tag{3.9}$$

$$\begin{aligned} &\mathbf{f}(\tau = 0) = \mathbf{F}_{u_{m_2},u_r}, \qquad \mathbf{f}_{\mathbf{IN}}(\tau = 0) = \mathbf{F}_{u_{m_1},u_r}, \quad \mathbf{f}_{\mathbf{OUT}}(\tau = 0) = 0, \\ &\mathbf{c}_i(\tau = 0) = \mathbf{C}_{i,u_{m_2},u_r}, \quad \mathbf{c}_{\mathbf{OUT},i}(\tau = 0) = \mathbf{C}_{i,u_{m_2},u_r}, \quad \mathbf{C}_{\mathbf{IN},i} = \mathbf{C}_{i,u_{m_1},u_r} \ \forall i \in I \end{aligned} \tag{3.10}$$

$$\begin{aligned} &\mathbf{f}(\tau = \mathbf{\Omega}) = \mathbf{F}_{u_r,u_{s_2}}, \qquad \mathbf{f}_{\mathbf{IN}}(\tau = \mathbf{\Omega}) = 0, \qquad \mathbf{f}_{\mathbf{OUT}}(\tau = \mathbf{\Omega}) = \mathbf{F}_{u_r,u_{s_3}}, \\ &\mathbf{c}_i(\tau = \mathbf{\Omega}) = \mathbf{C}_{i,u_r,u_{s_2}}, \quad \mathbf{c}_{\mathbf{OUT},i}(\tau = \mathbf{\Omega}) = \mathbf{C}_{i,u_r,u_{s_3}} \qquad \forall i \in I \end{aligned} \tag{3.11}$$

3.3.2 Batch Single Reactor Module

In the batch operating mode, material is loaded into the reactor, brought to the reaction conditions, the reaction proceeds, and finally the material is unloaded. The independent variable is now real-time (t), as opposed to residence-time (τ) as in the continuous-flow case. Nevertheless, the overall and component material balances on a differential element in real-time (dt instead of $d\tau$ in Figure 3.3) for a well-mixed batch reactor yield an identical

system of equations to that for the continuous-flow case (eqs 3.5 - 3.11), with volume ($\mathbf{V}$ or $\mathbf{v}$) replacing volumetric flowrate ($\mathbf{F}$ or $\mathbf{f}$). The material balances for the two operating modes are summarized in Table 3.2.

Table 3.2: Overall and component balances for the continuous-flow and batch operating modes

	Continuous-Flow	Batch	Sets
Overall material balance on units	$\sum_{u \in U_u} \mathbf{F}_{u,u'} = \sum_{u'' \in U_u} \mathbf{F}_{u',u''}$, (eq 3.2)	$\sum_{u \in U_u} \mathbf{V}_{u,u'} = \sum_{u'' \in U_u} \mathbf{V}_{u',u''}$	$u' \in (U_s \cup U_m \cup U_r)$
Component balance on splitters	$\mathbf{C}_{i,u,u'} = \mathbf{C}_{i,u',u''}$, (eq 3.3)	$\mathbf{C}_{i,u,u'} = \mathbf{C}_{i,u',u''}$	$u' \in U_s$, $(u,u') \in U_u$, $(u',u'') \in U_u$, $\forall i \in I$
Component balance on mixers	$\sum_{u \in U_u} \mathbf{F}^r_{u,u'} \cdot \mathbf{C}_{i,u,u'} = \sum_{u'' \in U_u} \mathbf{F}_{u',u''} \cdot \mathbf{C}_{i,u',u''}$, (eq 3.4)	$\sum_{u \in U_u} \mathbf{V}^r_{u,u'} \cdot \mathbf{C}_{i,u,u'} = \sum_{u'' \in U_u} \mathbf{V}_{u',u''} \cdot \mathbf{C}_{i,u',u''}$	$u' \in U_m$, $\forall i \in I$
ODE describing reactor volume variation	$\left(\frac{\mathbf{df}}{\mathbf{d}\tau}\right) = -\dot{\mathbf{f}}_{\mathbf{IN}} - \dot{\mathbf{f}}_{\mathbf{OUT}}$, (eq 3.5)	$\left(\frac{\mathbf{dv}}{\mathbf{dt}}\right) = -\dot{\mathbf{v}}_{\mathbf{IN}} - \dot{\mathbf{v}}_{\mathbf{OUT}}$	
ODE describing "IN" stream volume variation	$\left(\frac{\mathbf{df_{IN}}}{\mathbf{d}\tau}\right) = \dot{\mathbf{f}}_{\mathbf{IN}}$, (eq 3.6)	$\left(\frac{\mathbf{dv_{IN}}}{\mathbf{dt}}\right) = \dot{\mathbf{v}}_{\mathbf{IN}}$	
ODE describing "OUT" stream volume variation	$\left(\frac{\mathbf{df_{OUT}}}{\mathbf{d}\tau}\right) = \dot{\mathbf{f}}_{\mathbf{OUT}}$, (eq 3.7)	$\left(\frac{\mathbf{dv_{OUT}}}{\mathbf{dt}}\right) = \dot{\mathbf{v}}_{\mathbf{OUT}}$	
ODE describing reactor concentration variation	$\left(\frac{\mathbf{dc_i}}{\mathbf{d}\tau}\right) = \frac{\dot{\mathbf{f}}_{\mathbf{IN}}}{\mathbf{f}}(\mathbf{c}_i - \mathbf{C}_{\mathbf{IN},i}) + \sum_{j}^{j_{N_J}} \eta_{i,j} \cdot \mathbf{r}_j$, (eq 3.8)	$\left(\frac{\mathbf{dc_i}}{\mathbf{dt}}\right) = \frac{\dot{\mathbf{v}}_{\mathbf{IN}}}{\mathbf{v}}(\mathbf{c}_i - \mathbf{C}_{\mathbf{IN},i}) + \sum_{j}^{j_{N_J}} \eta_{i,j} \cdot \mathbf{r}_j$	$\forall i \in I$
ODE describing "OUT" stream concentration variation	$\left(\frac{\mathbf{dc_{OUT,i}}}{\mathbf{d}\tau}\right) = \frac{\dot{\mathbf{f}}_{\mathbf{OUT}}}{\mathbf{f}_{\mathbf{OUT}}}(\mathbf{c}_i - \mathbf{c}_{\mathbf{OUT},i})$, (eq 3.9)	$\left(\frac{\mathbf{dc_{OUT,i}}}{\mathbf{dt}}\right) = \frac{\dot{\mathbf{v}}_{\mathbf{OUT}}}{\mathbf{v}_{\mathbf{OUT}}}(\mathbf{c}_i - \mathbf{c}_{\mathbf{OUT},i})$	$\forall i \in I$

While the system of equations for the two operating modes is identical, there are differences in the nature of the operating modes that must be accounted for in order to achieve an accurate assessment of the performance of the reactor (e.g., time for batch operations, the potential need for additional storage units in the batch operating mode, the different bounds on reactor volumes for the two operating modes, the physical meaning of the recycle stream in the two operating modes, the potential for use of the batch plant infrastructure for the manufacture of multiple products, and the differences in the economic parameters associated with the two operating modes such as the need for more labor in the batch operating mode). The detailed discussion

of these differences and the methodologies I employed to account for these differences is provided in sections 3.5 and 3.6.

3.3.3 Nondimensional Representation of Reactors

In this section, the systems of ODEs shown in Table 3.2 are merged into a single system of equations that can be used as constraints in an optimization problem, the solution of which provides the optimal operating mode and reactor design. To achieve this, the system of equations for the CFR (left-hand side of Table 3.2) are non-dimensionalized using definitions (eq 3.12), where $\mathbf{\Omega}$ is the (variable) total residence time of the reactor and $\hat{\mathbf{x}}$ is the new dimensionless variable:

$$\hat{\tau} = \frac{\tau}{\mathbf{\Omega}},$$

$$\hat{\mathbf{F}}_{u,u'} = \frac{\mathbf{F}_{u,u'}}{\overline{F}}, \qquad \hat{\mathbf{v}} = \frac{\mathbf{f}}{\overline{\overline{F}}}, \qquad \hat{\mathbf{v}}_{\mathbf{IN}} = \frac{\mathbf{f}_{\mathbf{IN}}}{\overline{\overline{F}}}, \qquad \hat{\mathbf{v}}_{\mathbf{OUT}} = \frac{\mathbf{f}_{\mathbf{OUT}}}{\overline{\overline{F}}},$$

$$\hat{\mathbf{w}}_{\mathbf{IN}} = \left(\frac{\mathbf{\Omega}}{\overline{\overline{F}}}\right)\dot{\mathbf{f}}_{\mathbf{IN}}, \quad \hat{\mathbf{w}}_{\mathbf{OUT}} = \left(\frac{\mathbf{\Omega}}{\overline{\overline{F}}}\right)\dot{\mathbf{f}}_{\mathbf{OUT}},$$

$$\hat{\mathbf{C}}_{i,u,u'} = \frac{\mathbf{C}_{i,u,u'}}{\overline{C_i}}, \qquad \hat{\mathbf{c}}_i = \frac{\mathbf{c}_i}{\overline{\overline{C_i}}}, \qquad \hat{\mathbf{C}}_{\mathbf{IN},i} = \frac{\mathbf{C}_{\mathbf{IN},i}}{\overline{C_i}}, \qquad \hat{\mathbf{c}}_{\mathbf{OUT},i} = \frac{\mathbf{c}_{\mathbf{OUT},i}}{\overline{C_i}} \tag{3.12}$$

Similarly, the system of equations for the batch reactor (right-hand side of Table 3.2) are non-dimensionalized using definitions (eq 3.13), where $\mathbf{\Omega}$ is

the (variable) total batch time for the reactor, and the same dimensionless variable notations $\hat{\mathbf{x}}$ as were used for the CFR above are used:

$$\hat{\tau} = \frac{t}{\boldsymbol{\Omega}},$$

$$\hat{\mathbf{F}}_{u,u'} = \frac{\mathbf{V}_{u,u'}}{\overline{V}}, \qquad \hat{\mathbf{v}} = \frac{\mathbf{v}}{\overline{V}}, \qquad \hat{\mathbf{v}}_{\mathbf{IN}} = \frac{\mathbf{v}_{\mathbf{IN}}}{\overline{V}}, \qquad \hat{\mathbf{v}}_{\mathbf{OUT}} = \frac{\mathbf{v}_{\mathbf{OUT}}}{\overline{V}},$$

$$\hat{\mathbf{w}}_{\mathbf{IN}} = \left(\frac{\boldsymbol{\Omega}}{\overline{V}}\right)\dot{\mathbf{v}}_{\mathbf{IN}}, \quad \hat{\mathbf{w}}_{\mathbf{OUT}} = \left(\frac{\boldsymbol{\Omega}}{\overline{V}}\right)\dot{\mathbf{v}}_{\mathbf{OUT}},$$

$$\hat{\mathbf{C}}_{i,u,u'} = \frac{\mathbf{C}_{i,u,u'}}{\overline{C_i}}, \qquad \hat{\mathbf{c}}_i = \frac{\mathbf{c}_i}{\overline{C_i}}, \qquad \hat{\mathbf{C}}_{\mathbf{IN},i} = \frac{\mathbf{C}_{\mathbf{IN},i}}{\overline{C_i}}, \qquad \hat{\mathbf{c}}_{\mathbf{OUT},i} = \frac{\mathbf{c}_{\mathbf{OUT},i}}{\overline{C_i}} \tag{3.13}$$

The goal of eliminating dimensions from the equations is that the bounds on all variables can lie between 0 and 1, regardless of the operating mode. Note that the value of the upper bound on volume, $\overline{V}$ [m^3], used to non-dimensionalize the batch equations may differ from the CFR case. In addition, the volume bounds of the different reactor types may be different (i.e., each reactor type t has appropriate bounds, $\left[\underline{V_t}, \overline{V_t}\right]$). In order to preserve the bounds on all variables, regardless of operating mode, between 0 and 1, the upper bound on reactor volume is set to be the maximum allowed volume of reactor or storage tank (i.e., $\overline{V} = \max\left[\max_t\left(\overline{V_t}\right), \overline{V_{\text{st}}}\right]$. Applying the definitions (eqs 3.12 and 3.13) to the systems shown in Table 3.2 yields the following, unified system of equations (eqs 3.14 - 3.21), with initial and final

conditions given by (eqs 3.22 and 3.23):

$$\sum_{u \in U_u} \hat{\mathbf{F}}_{u,u'} = \sum_{u'' \in U_u} \hat{\mathbf{F}}_{u',u''} \qquad u' \in (U_s \cup U_m \cup U_r) \tag{3.14}$$

$$\sum_{u \in U_u} \hat{\mathbf{F}}_{u,u'} \cdot \hat{\mathbf{C}}^r_{i,u,u'} = \sum_{u'' \in U_u} \hat{\mathbf{F}}_{u',u''} \cdot \hat{\mathbf{C}}_{i,u',u''} \qquad u' \in U_m,\ \forall i \in I \tag{3.15}$$

$$\hat{\mathbf{C}}_{i,u,u'} = \hat{\mathbf{C}}_{i,u',u''} \qquad u' \in U_s,\ (u,u') \in U_u,\ (u',u'') \in U_u,\ \forall i \in I \tag{3.16}$$

$$\left(\frac{\mathbf{d}\hat{\mathbf{v}}}{\mathbf{d}\hat{\tau}}\right) = -\hat{\mathbf{w}}_{\mathbf{IN}} - \hat{\mathbf{w}}_{\mathbf{OUT}} \tag{3.17}$$

$$\left(\frac{\mathbf{d}\hat{\mathbf{v}}_{\mathbf{IN}}}{\mathbf{d}\hat{\tau}}\right) = \hat{\mathbf{w}}_{\mathbf{IN}} \tag{3.18}$$

$$\left(\frac{\mathbf{d}\hat{\mathbf{v}}_{\mathbf{OUT}}}{\mathbf{d}\hat{\tau}}\right) = \hat{\mathbf{w}}_{\mathbf{OUT}} \tag{3.19}$$

$$\left(\frac{\mathbf{d}\hat{\mathbf{c}}}{\mathbf{d}\hat{\tau}}\right)_i = \frac{\hat{\mathbf{w}}_{\mathbf{IN}}}{\hat{\mathbf{v}}} \left(\hat{\mathbf{c}}_i - \hat{\mathbf{C}}_{\mathbf{IN},i}\right) + \frac{\boldsymbol{\Omega}}{\overline{C_i}} \sum_{j}^{j_{N_J}} \eta_{i,j} \cdot \mathbf{r}_j \qquad \forall i \in I \tag{3.20}$$

$$\left(\frac{\mathbf{d}\hat{\mathbf{c}}_{\mathbf{OUT},\mathrm{i}}}{\mathbf{d}\hat{\tau}}\right) = \frac{\hat{\mathbf{w}}_{\mathbf{OUT}}}{\hat{v}_{\mathbf{OUT}}} \left(\hat{\mathbf{c}}_i - \hat{\mathbf{c}}_{\mathbf{OUT},i}\right) \qquad \forall i \in I \tag{3.21}$$

$$\hat{\mathbf{v}}(\hat{\tau}=0)=\hat{\mathbf{F}}_{u_{m_2},u_r},\qquad \hat{\mathbf{v}}_{\mathbf{IN}}(\hat{\tau}=0)=\hat{\mathbf{F}}_{u_{m_1},u_r},\qquad \hat{\mathbf{v}}_{\mathbf{OUT}}(\hat{\tau}=0)=0,$$
$$\hat{\mathbf{c}}_i(\hat{\tau}=0)=\hat{\mathbf{C}}_{i,u_{m_2},u_r},\quad \hat{\mathbf{c}}_{\mathbf{OUT},i}(\hat{\tau}=0)=\hat{\mathbf{C}}_{i,u_{m_2},u_r},\qquad \hat{\mathbf{C}}_{\mathbf{IN},i}=\hat{\mathbf{C}}_{i,u_{m_1},u_r}\qquad \forall i\in I \tag{3.22}$$

$$\hat{\mathbf{v}}(\hat{\tau}=1)=\hat{\mathbf{F}}_{u_r,u_{s_2}},\qquad \hat{\mathbf{v}}_{\mathbf{IN}}(\hat{\tau}=1)=0,\qquad \hat{\mathbf{v}}_{\mathbf{OUT}}(\hat{\tau}=1)=\hat{\mathbf{F}}_{u_r,u_{s_3}},$$
$$\hat{\mathbf{c}}_i(\hat{\tau}=1)=\hat{\mathbf{C}}_{i,u_r,u_{s_2}},\quad \hat{\mathbf{c}}_{\mathbf{OUT},i}(\hat{\tau}=1)=\hat{\mathbf{C}}_{i,u_r,u_{s_3}}\qquad \forall i\in I \tag{3.23}$$

3.3.4 Review of Orthogonal Collocation on Finite Elements

An optimization problem subject to the system of ODEs given by eqs 3.17 - 3.21 is an infinite dimensional optimal control problem. To make the solution of this problem possible, one method is the conversion of the infinite dimensional problem to a finite dimensional problem that may be solved with standard NLP solvers. The conversion is typically performed using finite difference methods or may be performed using the orthogonal collocation on finite elements (OCFE) approach. The latter is the approach used in this work, and a derivation of the methodology that points out key features that allow it to be an ideal approach for the problem addressed in this work is provided in this section. For a more in-depth discussion of the method, the reader is directed to the work of Bhatia and Biegler [27].

Let $z=[\hat{\mathbf{v}},\ \hat{\mathbf{v}}_{\mathbf{IN}},\ \hat{\mathbf{v}}_{\mathbf{OUT}},\ \hat{\mathbf{c}}_i,\ \hat{\mathbf{c}}_{\mathbf{OUT},i}]$, and $u=[\hat{\mathbf{w}}_{\mathbf{IN}},\ \hat{\mathbf{w}}_{\mathbf{OUT}}]$. Then, eqs 3.17 - 3.23 give an ODE system of the form given in eq 3.24:

$$\dot{z}\left(t\right) = \Phi(z\left(t\right), u(t), t) \qquad z\left(t = t^0\right) = z^0 \tag{3.24}$$

where $z \in \mathbb{R}^{n=3+2N_I}$ is a vector of states, and $u \in \mathbb{R}^{m=2}$ is a vector of time-varying inputs. To approximate the integral of eq 3.24, assume that the state vector can be approximated as a weighted sum of shifted Lagrange polynomials $\phi^p(t)$:

$$\tilde{z}(t) = \sum_{p_0}^{N_P} z^p \phi^p(t) \text{ where } \phi^p(t) = \prod_{p'=p_0,p}^{N_P} \frac{(t - \alpha^{p'})}{\alpha^p - \alpha^{p'}} \tag{3.25}$$

where $\tilde{z}(t)$ is the approximate solution of the ODE, $P = \{p : p_0, \ldots, p_{N_P}\}$ is a set of collocation points along the domain t of $z(t)$, α^p denotes the location of collocation point p on the domain that we have selected, with $\alpha^{p_0} = t^0$, N_P is the number of collocation points (not including α^{p_0}), and the notation $p' = p_0, p$ denotes p' starting from p_0 and $p \neq p'$.

Similarly, approximate $u(t)$ as a sum of weighted Lagrange polynomials:

$$\tilde{u}(t) = \sum_{p_1}^{N_P} u^p \psi^p(t) \text{ where } \psi^p(t) = \prod_{p'=p_1,p}^{N_P} \frac{(t - \alpha^{p'})}{\alpha^p - \alpha^{p'}} \tag{3.26}$$

The use of shifted Lagrange polynomials guarantees that the coefficient z^p of the polynomial $\phi^p(\alpha^p)$ is exactly equal to $z(\alpha^p)$. Therefore, the approximation is exact at the collocation points and the residual of the differential equation at the collocation points is exactly equal to zero:

$$R(\alpha^p) = \sum_{p'=p_0}^{N_P} z^{p'} \dot{\phi}^{p'}(\alpha^p) - \Phi(z^p, u^p, \alpha^p) = 0 \qquad p = p_1, \cdots, p_{N_P} \tag{3.27}$$

Equation 3.27 gives $n \times N_P$ equations in $N_P(n+m)$ unknowns ($z^p \in \mathbb{R}^{n \times N_P}$ and $u^p \in \mathbb{R}^{m \times N_P}$). Note that z^0 may or may not be given in the problem as an initial condition, potentially adding n unknowns if it is considered variable. Therefore, if eq 3.24 was a constraint to an infinite-dimensional optimal control problem, the problem can be converted to a finite NLP by replacing eq 3.24 with eq 3.27 and solving the problem using standard NLP solvers.

A key point is that the orthogonal properties obtained are preserved only when the domain of the ODE is $[0, 1]$. Therefore, a prerequisite to the use of this method is that the original domain of the problem is mapped to a new time domain $\hat{t} \in [0, 1]$, where $\hat{t}$ represents the normalized time. The two time domains for a domain of real-time $t \in [t^0, t^F]$ and two collocation points ($N_P = 2$) are shown in Figure 3.4a. Real time can be obtained from the normalized time using:

$$t = t^0 + \hat{t}\left(t^F - t^0\right) \tag{3.28}$$

In order to make the solution of eq 3.24 more accurate, more collocation points may be used, or the domain may be further discretized into finite elements and orthogonal collocation applied within each element. The second

(a) Time mapping for orthogonal collocation.

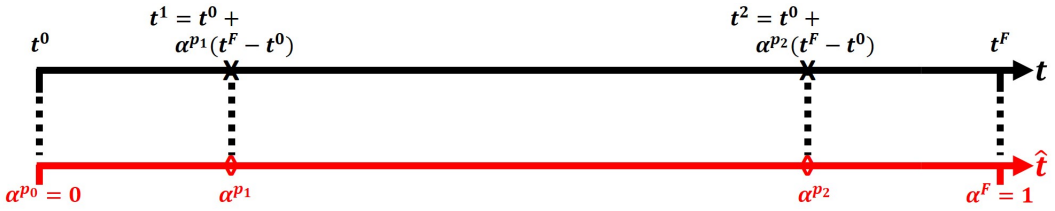

(b) Time mapping for orthogonal collocation on finite elements.

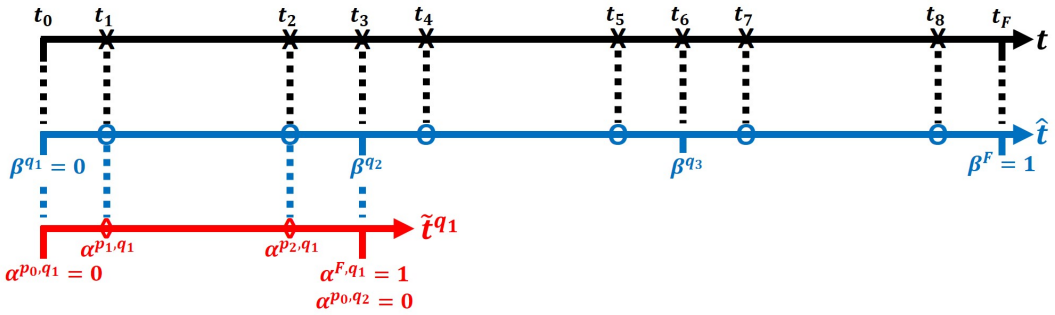

Figure 3.4: Mapped time scales for the OC (a) and OCFE methods.

method offers the advantage of dealing with poorly behaved systems and is therefore more commonly used.

To apply the orthogonal collocation method to finite elements, the set $Q = \{q : q_1, \ldots, q_{N_Q}\}$ of finite elements is introduced, and the normalized domain $\hat{t}$ is discretized into N_Q finite elements q, with each finite element beginning at normalized time $\hat{t} = \beta^q$, ending at $\hat{t} = \beta^{q+1}$, and with $\beta^{q_1} = 0$. The values of β^q are parameters, and elements of equal length $1/N_Q$ are used in this work.

As was mentioned above, the orthogonal properties that allow the use of the residual equations of eq 3.27 are only valid for the domain $[0, 1]$. Since

the goal is to fit a polynomial within each element, a new time domain $\tilde{t}^q$ is introduced within each element q such that the domain of the finite element becomes $\tilde{t}^q \in [0,1]$. The two subdomains for a domain of real-time $t \in [t^0, t^F]$ with three finite elements, and two internal collocation points are shown in Figure 3.4b. To simplify the figure, only the subdomain for the first finite element $\tilde{t}^{q_1}$ is shown, but the reader should infer that two remaining subdomains $\tilde{t}^{q_2}$ and $\tilde{t}^{q_3}$ also exist.

The normalized time $\hat{t}$ can be obtained from the time along the subdomain $\tilde{t}^q$ using eq 3.29. Of particular interest is the time of each of the collocation points, since those are the times for which the remainder equation (eq 3.27) is written. There is a total of $(N_P+1) \times N_Q$ collocation points. Since the collocation point locations are measured relative to the subdomains $\tilde{t}^q$, the position of each collocation point values of $\alpha^{p,q}$ are the same for all the subdomains (i.e. $\alpha^{p,q} = \alpha^p,\ p = p_0, \cdots, p_{N_P},\ q = q_1, \cdots, q_{N_Q}$). Denoting each point in order starting from t^0 to $t^{(N_Q-1)(N_P+1)+N_P}$, as shown on the main domain t of Figure 3.4b, the normalized time at each collocation point can be found using eq 3.30, where α^p is the time along the subdomain of finite element q, $\tilde{t}^q$, of collocation point p, and β^q is the time along the normalized domain $\hat{t}$ of the beginning of finite element q. For example, the first collocation point (p_1) in the third finite element (q_3) will be at $\hat{t}^7 = \beta^{q_3} + \alpha^{p_1}(\beta^{q_4} - \beta^{q_3})$, which can be seen in Figure 3.4b. Then, the corresponding real-time t along the main domain can be found using eq 3.31.

$$\hat{t} = \beta^q + \tilde{t}^q \left(\beta^{q+1} - \beta^q\right) \tag{3.29}$$

$$\hat{t}^{(q-1)(N_P+1)+p} = \beta^q + \alpha^p \left(\beta^{q+1} - \beta^q\right) \qquad \forall q \in Q,\ \forall p \in P \tag{3.30}$$

$$t^{(q-1)(N_P+1)+p} = t^0 + \hat{t}^{(q-1)(N_P+1)+p} \left(t^F - t^0\right) \qquad \forall q \in Q,\ \forall p \in P \tag{3.31}$$

Denoting the value of state z at collocation point p of element q as $z^{p,q}$, the solution of the ODE system can be approximated by extending the orthogonal collocation method (eq 3.25) to the case of finite elements using eq 3.32. The residual may then be calculated at each collocation point p inside each finite element q using eq 3.33.

$$\begin{aligned} \tilde{z}^q(\hat{t}) &= \sum_{p_0}^{N_P} z^{p,q} \phi^{p,q}(\hat{t}) \\ \text{where} \qquad \phi^{p,q}(\hat{t}) &= \prod_{p'=p_0,p}^{N_P} \frac{(\hat{t} - \hat{t}^{p',q})}{(\hat{t}^{p,q} - \hat{t}^{p',q})} \end{aligned} \tag{3.32}$$

$$\sum_{p'=p_0}^{N_P} z^{p',q} \dot{\phi}^{p',q}(\hat{t}^{p,q}) - \Phi(z^{p,q}, u^{p,q}, \hat{t}^{p,q}) = 0 \qquad \forall q \in Q,\ p = p_1, \cdots, p_{N_P} \tag{3.33}$$

Combining eq 3.29 with the definition of $\phi^{p,q}$ from eq 3.32, the derivative $d\phi^{p',q}(\hat{t})/d\hat{t}$ can be given as a function of the derivative with respect to the normalized time domain $\tilde{t}^q$ by the chain rule:

$$\frac{d\phi^{p',q}(\hat{t})}{d\hat{t}} = \frac{1}{\beta^{q+1} - \beta^q} \frac{d\phi^{p'}(\tilde{t}^q)}{d\tilde{t}^q} \qquad \forall q \in Q, p' = p_1, \cdots, p_{N_P}, p = p_1, \cdots, p_{N_P} \tag{3.34}$$

where tabulated values of the derivatives for the orthogonal collocation method can be directly applied. Noting that the point $\hat{t}^{p,q}$ coincides with the point $\tilde{t}^q = \alpha^p$, eq 3.33 can be modified as follows:

$$\sum_{p'=p_0}^{N_P} \frac{z^{p',q}}{\beta^{q+1} - \beta^q} \dot{\phi}^{p'}(\tilde{t}^q = \alpha^p) - \Phi(z^{p,q}, u^{p,q}, \hat{t}^{p,q}) = 0 \qquad \forall q \in Q, p = p_1, \cdots, p_{N_P} \tag{3.35}$$

To ensure continuity of the states $z(\hat{t})$ at the boundaries of the finite elements, additional conditions can be added equating the solutions at the end of each finite element (q) with the initial value of the subsequent element $(q+1)$ yielding $N_Q - 1$ additional equations:

$$z^{p_0,q} = \sum_{p_0}^{N_P} z^{p,(q-1)} \phi^p(\tilde{t}^{(q-1)} = 1) \qquad q = q_2, \cdots, q_{N_Q} \tag{3.36}$$

Equations 3.35 and 3.36 may be written for the concentration and volume profiles of a single batch reactor or CFR, with $\Phi(z^{p,q}, u^{p,q}, \hat{t}^{p,q})$ given in eqs 3.17 - 3.21, and initial condition z^0 given by eq 3.22. The final conditions

of the reactor (eq 3.23) can be obtained by writing eq 3.36 for $q = q_{N_Q+1}$, and equating the resulting expression for $z^{p_0,q_{(N_Q+1)}}$ to the states at $\hat{t} = 1$ in eq 3.23. The remaining variables to optimize are the flowrates and concentrations of each stream in the outer superstructure, $\hat{\mathbf{F}}_{u,u'}$ and $\hat{\mathbf{C}}^r_{i,u,u'}$, which are related to each other and to the reactor through eqs 3.14 - 3.16.

This concludes the derivation of the system to solve for obtaining the profiles along a single reactor using the OCFE method. While the additional time subdomains for finite element discretization enabled the solution of the differential equation system more accurately, it offered a secondary advantage in that it created a natural separation along the time domain between different portions of the overall time horizon. The full time horizon could then be solved simultaneously, but each finite element had its own polynomial fit that was only connected to the preceding and following time subdomains at the boundary. This fact is exploited in section 3.4 for the extension of the approach to accommodate multiple reactors in series.

3.4 Unified Batch/Continuous Superstructure for Reactor Networks

Figure 3.5 shows the series connection of N_R individual reactor modules (of the type shown in Figure 3.2). Let $R = \{r : r_1, \ldots, r_{N_R}\}$ be the set of reactor modules.

Connectivity between the reactors is enforced using constraints (eqs 3.37 and 3.38), where superscript r denotes the values of the variable in the

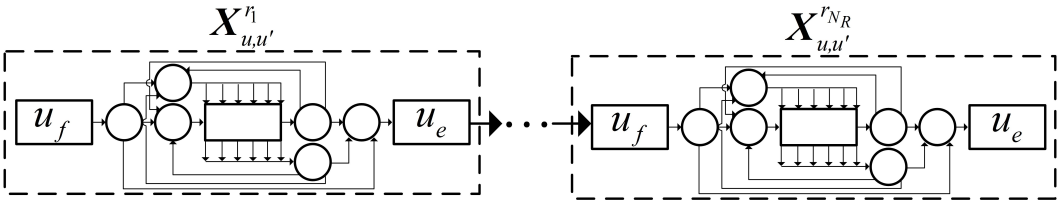

Figure 3.5: Reactor superstructure showing connection of N_R individual reactor elements (of those shown in Figure 3.2).

rth reactor:

$$\hat{\mathbf{F}}^{r}_{u_f,u_{s_1}} = \hat{\mathbf{F}}^{r-1}_{u_{m_3},u_e} \qquad r = r_2, \ldots, r_{N_R} \tag{3.37}$$

$$\hat{\mathbf{C}}^{r}_{i,u_f,u_{s_1}} = \hat{\mathbf{C}}^{r-1}_{i,u_{m_3},u_e} \qquad \forall i \in I,\ r = r_2, \ldots, r_{N_R} \tag{3.38}$$

The overall material balances on the splitter and mixer units (eqs 3.14 - 3.16) are extended to the network case using eqs 3.39 - 3.41:

$$\sum_{u \in U_u} \hat{\mathbf{F}}^{r}_{u,u'} = \sum_{u'' \in U_u} \hat{\mathbf{F}}^{r}_{u',u''} \qquad u' \in (U_s \cup U_m \cup \{u_r\}),\ \forall r \in R \tag{3.39}$$

$$\sum_{u \in U_u} \hat{\mathbf{F}}^{r}_{u,u'} \cdot \hat{\mathbf{C}}^{r}_{i,u,u'} = \sum_{u'' \in U_u} \hat{\mathbf{F}}^{r}_{u',u''} \cdot \hat{\mathbf{C}}^{r}_{i,u',u''} \qquad u' \in U_m,\ \forall i \in I,\ \forall r \in R \tag{3.40}$$

$$\hat{\mathbf{C}}^{r}_{i,u,u'} = \hat{\mathbf{C}}^{r}_{i,u',u''} \qquad u' \in U_s,\ (u,u') \in U_u,\ (u',u'') \in U_u,\ \forall i \in I,\ \forall r \in R \tag{3.41}$$

Note that a reactor may be bypassed by utilizing stream (u_{s_1}, u_e). Therefore, the existence of N_R modules gives the choice of utilizing *up to* N_R reactors in the final solution but does not necessitate using that exact number of reactors.

In order to compute the time evolution of the differential variables within each of the reactors in the reactor network, I extend the OCFE method to accommodate the discretization of multiple reactors. As outlined in section 3.3.4, the OCFE approach for integrating the ODE system for a single reactor necessitates the mapping of the time horizon of one reactor onto a normalized domain $\hat{t}$ (such that the inlet of the reactor occurs at $\hat{t} = 0$ and the effluent occurs at $\hat{t} = 1$). This normalized domain is further split into N_Q finite elements of equal length, and a normalized subdomain $\tilde{t}^q$ is defined for each finite element q (see Figure 3.4).

To adapt the methodology for the problem of a network of reactors in series, I first introduce a third set of normalized time subdomains $\bar{t}$ to the existing normalized global time domain $\hat{t}$ and the set of connected time subdomains $\tilde{t}$. The time domain mapping for a network of two reactors with a domain of real-time $t \in [t^0, t^F]$ with three finite elements and two internal collocation points is shown in Figure 3.6. To simplify the figure, only the first subdomain within each layer is shown, but the reader should infer that a second subdomain $\tilde{t}$ and five additional subdomains $\bar{t}$ exist and are not shown in the figure.

As can be seen in the figure, the overall time horizon is mapped onto the domain $\hat{t}$, where $\hat{t} = 0$ and $\hat{t} = 1$ correspond to the starting and ending

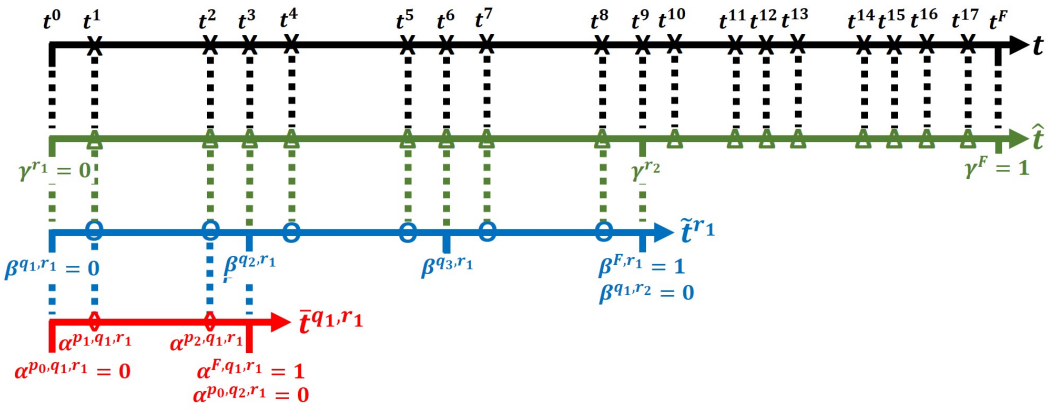

Figure 3.6: Mapped time subdomains for the OCFERE method.

points of the full time horizon, respectively. This overall horizon is split into N_R elements of variable lengths ($N_R = 2$ in Figure 3.6). The beginning of segment r is at time γ^r along the $\hat{t}$ time domain, with $\gamma^{r_1} = 0$ and $\gamma^{r_{(N_R+1)}} = 1$. I will refer to these segments as "reactor elements" to distinguish them from the finite elements introduced in the previous section.

I discretize each of the N_R segments into N_Q finite elements ($N_Q = 3$ in Figure 3.6), each of equal length for a single reactor, and introduce the time subdomains $\tilde{t}^r$ to mark the starting and ending positions of each of the N_Q segments along the rth time subdomain. Each of the $\tilde{t}^r$ time subdomains begins at $\tilde{t}^r = 0$ and ends at $\tilde{t}^r = 1$. Finite element q spans the overall normalized times $\hat{t}^{p_0,q,r}$ and $\hat{t}^{p_0,q+1,r}$, which coincides with the region of subdomain $\tilde{t}^r$ between points β^q and β^{q+1}. Note that, even though reactor elements have variable lengths ($\gamma^{r+1} - \gamma^r$), the fact that each reactor element is partitioned into N_Q equal finite elements means that the values of the location of the partitions relative to the subdomains $\tilde{t}^r$ are the same in all reactor elements (i.e.,

$\beta^{q,r} = \beta^q,\ q = q_1, \cdots, q_{N_Q},\ r = r_1, \cdots r_{N_R}$).

Finally, each finite element q is further mapped onto a time subdomain $\overline{t}^{q,r}$, where the point $\overline{t}^{q,r} = 0$ coincides with the beginning of finite element q in reactor element r ($\tilde{t}^r = \beta^q$ and $\hat{t} = \hat{t}^{p_0,q,r}$), and the point $\overline{t}^{q,r} = 1$ coincides with the end of that same finite element ($\tilde{t}^r = \beta^{q+1}$ and $\hat{t} = \hat{t}^{p_0,q+1,r}$). N_P collocation points are added along the subdomain $\overline{t}^{q,r}$ with collocation point p at the point α^p relative to subdomain $\overline{t}^{q,r}$ ($N_P = 2$ in Figure 3.6). As with the layer above, since the positions of the collocation points are measured relative to the subdomains $\overline{t}^{q,r}$, the values of the positions are the same across all reactors and finite elements (i.e., $\alpha^{p,q,r} = \alpha^p,\ p = p_0, \cdots, p_{N_P},\ q = q_1, \cdots, q_{N_Q},\ r = r_1, \cdots r_{N_R}$).

With the new time subdomain, the overall normalized time $\hat{t}$ can be calculated as a function of the time in the subdomains using eq 3.42, and the exact time of collocation point $\hat{t}^{p,q,r}$ can therefore be obtained by eq 3.43:

$$\begin{aligned} \hat{t} &= \gamma^r + \tilde{t}^r \left(\gamma^{r+1} - \gamma^r\right) \\ &= \gamma^r + \left(\gamma^{r+1} - \gamma^r\right) \left[\beta^q + \overline{t}^{q,r} \left(\beta^{q+1} - \beta^q\right)\right] \end{aligned} \tag{3.42}$$

$$\hat{t}^{(r-1)N_Q(N_P+1)+(q-1)(N_P+1)+p} = \gamma^r + \left(\gamma^{r+1} - \gamma^r\right) \left[\beta^q + \alpha^p \left(\beta^{q+1} - \beta^q\right)\right], \quad \forall r \in R,\ \forall q \in Q,\ p = p_1, \cdots, p_{N_P} \tag{3.43}$$

For example, from Figure 3.6, the reader may verify that the second collocation

point (p_2) in the third finite element (q_3) of the second reactor element (r_2), $\hat{t}^{p_2,q_3,r_2}$, is located at $\hat{t}^{17}$.

The solution for any differential variable z in finite element q of reactor element r can be approximated as a polynomial (extension of eq 3.32) as follows:

$$\begin{aligned} \tilde{z}^{q,r}(\hat{t}) &= \sum_{p_0}^{N_P} z^{p,q,r}\phi^{p,q,r}(\hat{t}) \\ \text{where} \qquad \phi^{p,q,r}(\hat{t}) &= \prod_{p'=p_0,p}^{N_P} \frac{(\hat{t}-\hat{t}^{p',q,r})}{\hat{t}^{p,q,r}-\hat{t}^{p',q,r}} \end{aligned} \tag{3.44}$$

The residual may then be calculated at each collocation point p inside each finite element q of reactor element r using

$$\sum_{p'=p_0}^{N_P} z^{p',q,r}\dot{\phi}^{p',q,r}(\hat{t}^{p,q,r}) - \Phi(z^{p,q,r}, u^{p,q,r}, \hat{t}^{p,q,r}) = 0 \qquad \forall r \in R, \forall q \in Q, p = p_1, \cdots, p_{N_P} \tag{3.45}$$

Combining eq 3.42 with the definition of $\phi^{p,q,r}$ from eq 3.44, the derivative $d\phi^{p',q,r}(\hat{t})/d\hat{t}$ can be given as a function of the derivative with respect to the $\bar{t}^{q,r}$ time domain by the chain rule:

$$\begin{aligned} \frac{d\phi^{p',q,r}(\hat{t}^{p,q,r})}{d\hat{t}} &= \frac{1}{(\beta^{q+1}-\beta^q)(\gamma^{r+1}-\gamma^r)} \frac{d\phi^{p'}(\bar{t}^{q,r})}{d\bar{t}^{q,r}} \\ &\forall r \in R,\ \forall q \in Q,\ p' = p_1, \cdots, p_{N_P},\ p = p_1, \cdots, p_{N_P} \end{aligned} \tag{3.46}$$

where tabulated values of the derivatives for the global orthogonal collocation method can be directly applied. Equation 3.45 can now be modified as follows:

$$\sum_{p'=p_0}^{N_P} \frac{z^{p',q,r}}{(\beta^{q+1}-\beta^q)(\gamma^{r+1}-\gamma^r)} \dot{\phi}^{p'}(\bar{t}^{q,r}=\alpha^p) - \Phi(z^{p,q,r}, u^{p,q,r}, \hat{t}^{p,q,r}) = 0$$
$$\forall r \in R,\ \forall q \in Q,\ p = p_1, \cdots, p_{N_P} \quad (3.47)$$

To ensure continuity of the states at the boundaries of the finite elements $z(\tilde{t}^r)$, additional conditions can be added equating the solutions at the end of each finite element (q) with the initial value of the subsequent element $(q+1)$:

$$z^{p_0,q,r} = \sum_{p'=p_0}^{N_P} z^{p',(q-1),r}\phi^{p'}(\bar{t}^{(q-1),r}=1) \qquad \forall r \in R,\ q = q_2, \cdots, q_{N_Q} \quad (3.48)$$

Finally, the initial and final conditions for each reactor element r can be enforced by noting that the start and end of the reactor element are at the points $\hat{t}^{p_0,q_1,r}$ and $\hat{t}^{p_0,q_{(N_Q+1)},r}$, respectively. Therefore, initial conditions may be included by introducing bounds on the value of $z^{p_0,q_1,r}$, and final conditions may be included by introducing bounds on the value of $z^{p_0,q_{(N_Q+1)},r}$, as well as eq 3.48 written for $q = q_{(N_Q+1)}$.

To implement this on the reactor network synthesis problem, let $z^{p,q,r} = [\hat{\mathbf{v}}^{p,q,r},\ \hat{\mathbf{v}}^{p,q,r}_{\mathbf{IN}},\ \hat{\mathbf{v}}^{p,q,r}_{\mathbf{OUT}},\ \hat{\mathbf{c}}^{p,q,r}_i,\ \hat{\mathbf{c}}^{p,q,r}_{\mathbf{OUT},i}]$ and $u^{p,q,r} = [\hat{\mathbf{w}}^{p,q,r}_{\mathbf{IN}},\ \hat{\mathbf{w}}^{p,q,r}_{\mathbf{OUT}}]$ where $\hat{\mathbf{x}}^{p,q,r}$ is

the value of state $\hat{\mathbf{x}}$ at collocation point p of finite element q in reactor element r, write eqs 3.47 and 3.48, with $\Phi(z^{p,q,r}, u^{p,q,r}, \tau^{p,q,r})$ given by the right-hand side of eqs 3.17 - 3.21, initial conditions for each reactor $z^{p_0,q_1,r}$ given by the right-hand side of eq 3.22, and final conditions for each reactor $z^{p_0,q_{(N_Q+1)},r}$ given by eq 3.23. This gives a system of equations that may be solved for the unknown profiles $z^{p,q,r}$ by varying $u^{p,q,r}$ along with the outer superstructure flowrates and concentrations, where an impact on reactor operation is reflected in the material balances of eqs 3.39 - 3.41.

Note that, in performing the non-dimensionalization of the variables (section 3.3.3), a dimensionless time domain $\hat{\tau}$ that varies from $\hat{\tau} = 0$ to $\hat{\tau} = 1$ has already been derived. Therefore, the relationship provided for the normalized time domain $\hat{t}$ in this section (eq 3.42) may be directly utilized for calculation of normalized time within the reactor network $\hat{\tau}$.

3.5 Logical Constraints

So far, I have developed a device that allows the computation of the concentration and volume profiles of a reactor from any of the operating modes considered, and that is general enough to be applicable to any reactor type. In this section, I first discuss the differences in the nature of the two operating modes that are accounted for in the framework (section 3.5.1). Then, I introduce logical constraints that eliminate artificial solutions (section 3.5.2), select operating mode and identify the utilized (i.e. not bypassed) reactors (section 3.5.3), identify the types of the utilized reactors (section 3.5.4), se-

lect and implement the correct volume expressions to calculate total reactor volume (section 3.5.5), determine whether storage tanks are needed, and if so, calculate their volumes (section 3.5.6), calculate timing-related variables (section 3.5.7) and compute the values of operating-mode dependent variables that will be required for the economics calculations (section 3.5.8). The full economic model is presented in section 3.6.

3.5.1 Differences in the Nature of the Operating Modes

First, a major difference between the continuous-flow and batch operating modes is that when operating in the batch mode, additional time is required for the loading/unloading, conditioning, and cleaning of the reactor. Since the system of ODEs is written over an independent variable of real-time with a domain that begins at the onset of the reaction and ends when the reaction is terminated, the true time allotted to a batch must be greater than the time over which the model ODEs are integrated. This is not the case for the continuous-flow mode, where the system of ODEs is written over an independent variable of residence time with a domain that begins at the reactor inlet and ends at the reactor outlet, meaning that the time over which the ODEs are integrated correctly represents the reactor's physical dimensions.

Second, in the batch operating mode, the differential variables $\mathbf{v}(t)$, $\mathbf{v_{IN}}(t)$, and $\mathbf{v_{OUT}}(t)$ represent the actual volume of material within the reactor, and the volume of material within the "IN" and "OUT" storage tanks that may be needed if the semi-batch reactor type is selected (see Figure 3.1). This

is not the case for the continuous-flow operating mode, where calculating the volume of material inside the reactor at residence-time τ may necessitate an additional ODE, eq 3.49, where $\mathbf{v_C}$ is the volume of the CFR [m^3]. However, since only PFRs and CSTRs are considered for the continuous-flow operating mode in this work, which both feature a constant volumetric flowrate inside the reactor, the additional equation is not necessary. Nevertheless, the methodology employed to calculate the reactor volume for the two operating modes must account for the difference in the definitions of the volume differential variable.

$$\left(\frac{\mathbf{dv_C}}{\mathbf{d}\tau}\right) = \mathbf{f} \tag{3.49}$$

In addition, appropriate bounds on the volume must account for the reactor type. Batch, semi-batch, and the CSTR reactor types take the form of an autoclave tank of fixed total volume, while the PFR reactor type assumes the tubular form. This means that the methodology for calculating the reactor volume must accommodate the use of different equations for calculating the total volume in the two operating modes as well as reactor type-dependent bounds on the total reactor volume $\left[\underline{V_t}, \overline{V_t}\right]$.

Third, for the continuous-flow operating mode, recycle streams $(u, u) \in U_{rec} = \{(u_{s_2}, u_{m_1}),\ \ (u_{s_2}, u_{m_2}), (u_{s_3}, u_{m_1}), (u_{s_3}, u_{m_2})\}$ serve the purpose of removing material downstream of the reactor (at high τ) and re-introducing the material upstream (at low τ). In the batch operating mode, since real-time

is the independent variable, recycle streams transporting material from future (at larger values of t) to the past (at lower values of t) cannot be allowed. Therefore, referring to Figure 3.2, recycle streams cannot be active if the batch operating mode is chosen.

Finally, an equitable economic comparison between the operating modes must take into account the often-cited advantages and disadvantages of the two modes. On the one hand, the batch operating mode offers the potential of utilizing the infrastructure for the manufacture of multiple products. Therefore, in addition to the inclusion of the individual reactor performance in the overall economic model, adjustments must be made to acknowledge this advantage of the batch operating mode when estimating total costs and profits. On the other hand, the batch operating mode has several economic disadvantages. Of note are the increased amount of labor that is necessary to operate the batch plant and the larger waste incurred in the event of a batch failure. Therefore, the economic models employed will also account for these differences between the operating modes.

3.5.2 Artificial Solution Elimination

On close examination of the ODE system of eqs 3.17 - 3.23, and specifically the evolution of concentration in the "OUT" stream (eq 3.21), it can be seen that artificial solutions that maximize yield are possible for the semi-batch reactor by setting $\hat{\mathbf{v}}_{\mathbf{OUT}}^{p,q,r}$ to 0, then artificially varying $\left(\frac{\mathbf{d}\hat{\mathbf{c}}_{\mathbf{OUT}}}{\mathbf{d}\hat{\tau}}\right)_i^{p,q,r}$, and hence $\hat{\mathbf{c}}_{\mathbf{OUT},i}^{p,q,r}$, at a time after the initial time ($\hat{\tau}^{p,q,r} > \hat{\tau}^{p_0,q_1,r}$). Then, a solution

may include a flow $\hat{\mathbf{v}}_{\mathbf{OUT}}^{p,q,r}$ by increasing $\hat{\mathbf{w}}_{\mathbf{OUT}}^{p,q,r}$, gaining artificial advantages in species concentration that directly translate to higher values of the objective function.

In order to avoid this, I include constraint 3.50:

$$-\left(\frac{1}{\underline{\hat{v}_{\mathrm{OUT}}}}\right)\hat{\mathbf{v}}_{\mathbf{OUT}}^{p,q,r} \leq \hat{\mathbf{c}}_i^{p,q,r} - \hat{\mathbf{c}}_{\mathbf{OUT},i}^{p,q,r} \leq \left(\frac{1}{\underline{\hat{v}_{\mathrm{OUT}}}}\right)\hat{\mathbf{v}}_{\mathbf{OUT}}^{p,q,r} \qquad \forall r \in R, \forall q \in Q, \forall p \in P \tag{3.50}$$

where $\underline{\hat{v}_{\mathrm{OUT}}}$ is the lower bound on $\hat{\mathbf{v}}_{\mathbf{OUT}}$. This constraint sets the lower and upper bounds of $\hat{\mathbf{c}}_i^{p,q,r} - \hat{\mathbf{c}}_{\mathbf{OUT},i}^{p,q,r}$ to zero if $\hat{\mathbf{v}}_{\mathbf{OUT}}{}^{p,q,r} = 0$, or to values that are below -1 and 1 if $\hat{\mathbf{v}}_{\mathbf{OUT}}{}^{p,q,r} > 0$. Since the bounds on both variables $\hat{\mathbf{c}}_i^{p,q,r}$ and $\hat{\mathbf{c}}_{\mathbf{OUT},i}^{p,q,r}$ are [0,1], the tightest bound on $\hat{\mathbf{c}}_i^{p,q,r} - \hat{\mathbf{c}}_{\mathbf{OUT},i}^{p,q,r}$ is the interval [-1,1]. Therefore, this constraint is superfluous in the presence of a positive value for $\hat{\mathbf{v}}_{\mathbf{OUT}}$.

This constraint ensures that if the volume of the "OUT" storage tank is zero at any time $\hat{\tau}$, the concentration of any species i in the "OUT" stream, $\hat{\mathbf{c}}_{\mathbf{OUT},i}$, is set equal to its concentration inside the reactor, $\hat{\mathbf{c}}_i$. At the time point $\hat{\tau}'$ where the solution involves increasing the volume of the storage tank, $\hat{\mathbf{w}}_{\mathbf{OUT}}$ is set to some positive value, while keeping the value of the volume of the storage tank at zero. Therefore, the concentration in the "OUT" stream is set to the concentration within the reactor at that point using constraint 3.50. However, at the next time point $\hat{\tau}' + \delta\tau$, $\hat{\mathbf{v}}_{\mathbf{OUT}}$ will take on a positive value after integrating the ODE, rendering constraint 3.50 superfluous (since both

$\hat{\mathbf{c}}_i^{p,q,r}$ and $\hat{\mathbf{c}}_{\mathbf{OUT},i}^{p,q,r}$ are $\in [0,1]$ from the non-dimensionalization procedure), and allowing the initial value for integrating the material balance for the "OUT" stream at that point (eq 3.21) to be the concentration of material in the reactor at the previous time point $\hat{\tau}'$, as required.

3.5.3 Identifying the Operating Mode and Determining Reactor Utilization

In this section, I define several binary variables $y \in \{0,1\}$ to allow the identification of the optimal operating mode and the number and type of utilized reactors.

3.5.3.1 Operating Mode Selection

First, I define $\mathbf{y}_{\mathbf{M}_m}$ as:

$$\mathbf{y}_{\mathbf{M}_m} = \begin{cases} 1, & \text{if operating mode } m \text{ is chosen} \\ 0, & \text{otherwise} \end{cases} \tag{3.51}$$

I enforce the choice of a single operating mode using eq 3.52, where m_B and m_C are the indices for batch and continuous-flow operating modes, respectively.

$$\mathbf{y}_{\mathbf{M}_{m_B}} + \mathbf{y}_{\mathbf{M}_{m_C}} = 1 \tag{3.52}$$

While the selection of operating mode will depend on the types of reactors used and their associated economics, one straightforward difference that can immediately be introduced at this point is the infeasibility of a recycle

stream for the batch case (as explained in section 3.5.1). This can be implemented by defining the set of recycle streams $U_{rec} = \{(u_{s_2}, u_{m_1}),\ (u_{s_2}, u_{m_2}),\ (u_{s_3}, u_{m_1}), (u_{s_3}, u_{m_2})\}$, and implementing eq 3.53, which forces dimensionless volumes in those streams to 0 when the batch mode is selected, but maintains an upper bound of 1 on flowrates within those streams when the continuous-flow operating mode is selected.

$$\hat{\mathbf{F}}^r_{u,u'} \leq \left(1 - \mathbf{y}_{\mathbf{M}_{m_B}}\right) \qquad (u, u') \in U_{rec},\ \forall r \in R \tag{3.53}$$

3.5.3.2 Reactor Utilization

Similarly, I define $\mathbf{y}^r_{\mathbf{U}}$ as:

$$\mathbf{y}^r_{\mathbf{U}} = \begin{cases} 1, & \text{if reactor } r \text{ is utilized} \\ 0, & \text{otherwise} \end{cases} \tag{3.54}$$

Before directly enforcing this definition, I note that the choice of whether a reactor is utilized and the operating mode are directly linked. In other words, for a reactor to be utilized, the reactor type must be one that has a good performance in maximizing the overall objective, and that reactor type belongs to only one operating mode. Therefore, I also introduce $\mathbf{y}^r_{\mathbf{UM}_m}$ as:

$$\mathbf{y}^r_{\mathbf{UM}_m} = \begin{cases} 1, & \text{if } \mathbf{y}_{\mathbf{M}_m} = 1 \wedge \mathbf{y}^r_{\mathbf{U}} = 1 \\ 0, & \text{otherwise} \end{cases} \tag{3.55}$$

To implement the condition that $\mathbf{y}_{\mathbf{M}_m} = 1 \wedge \mathbf{y}^r_{\mathbf{U}} = 1$ implies that $\mathbf{y}^r_{\mathbf{UM}_m} = 1$, I use eq 3.56. To implement the opposite condition ($\mathbf{y}^r_{\mathbf{UM}_m} = 1$

implies that $\mathbf{y}_{\mathbf{M}_m} = 1 \wedge \mathbf{y}^r_{\mathbf{U}} = 1$), I use eqs 3.57 and 3.58.

$$\mathbf{y}_{\mathbf{M}_m} + \mathbf{y}^r_{\mathbf{U}} \leq 1 + \mathbf{y}^r_{\mathbf{UM}_m} \qquad \forall m \in M,\, \forall r \in R \tag{3.56}$$

$$\mathbf{y}^r_{\mathbf{UM}_m} \leq \mathbf{y}_{\mathbf{M}_m} \qquad \forall m \in M,\, \forall r \in R \tag{3.57}$$

$$\mathbf{y}^r_{\mathbf{UM}_m} \leq \mathbf{y}^r_{\mathbf{U}} \qquad \forall m \in M,\, \forall r \in R \tag{3.58}$$

Now, I enforce definition 3.54 for $\mathbf{y}^r_{\mathbf{U}}$ by imposing constraints on $\mathbf{y}^r_{\mathbf{UM}_m}$ when differences occur between the operating modes, or directly on $\mathbf{y}^r_{\mathbf{U}}$ if the two operating modes are identical.

Recall that the bypass streams are available to circumvent reactors. Therefore, there are always flows in the outer streams that belong to the mapping set $U_e(u, u') = \{(u_f, u_{s_1}), (u_{s_1}, u_{m_3}),\ \ (u_{m_3}, u_e)\}$. If a reactor is not utilized, these are the only streams that should include flows. If a reactor is utilized, then flows may or may not exist in the other streams that belong to the set $U_i(u, u') = U_u \backslash U_e$. This is enforced using eq 3.59, where $\underline{\hat{F}}_m$ is the lower bound on $\hat{\mathbf{F}}^r_{u,u'}$ for operating mode m (equal to non-dimensional volumetric flowrate for continuous-flow, or non-dimensional volume for batch):

$$\sum_m \underline{\hat{F}}_m \cdot \mathbf{y}^r_{\mathbf{UM}_m} \geq \hat{\mathbf{F}}^r_{u,u'} \qquad (u, u') \in U_i,\, \forall r \in R \tag{3.59}$$

If a reactor is utilized, constraints are included to ensure:

1. that every utilitized reactor admits material from the inlet to the reactor module (u_f, u_{s_1}) and produces material that gets recovered at the outlet of the reactor module (u_{m_3}, u_e). In other words, to avoid either generating artificial flows, or infinite recycles of products within a reactor module. This is implemented in eq 3.60.

$$\underline{\hat{F}}_m \cdot \mathbf{y}^r_{\mathbf{UM}_m} \leq \hat{\mathbf{F}}^r_{u,u'} + \hat{\mathbf{F}}^r_{u'',u'''}$$
$$(u, u', u'', u''') \in \{(u_{s_1}, u_{m_1}, u_{s_1}, u_{m_2}), (u_{s_2}, u_{m_3}, u_{s_3}, u_{m_3})\}, \forall m \in M, \forall r \in R \tag{3.60}$$

2. that material is present at the start time for the reactor $\hat{\tau}^{p_0,q_1,r}$ (eq 3.61), throughout the reaction time (eq 3.62), and at the final time for the reactor $\hat{\tau}^{r,q_{N_Q+1},p_0}$ (eq 3.63). This is necessary to avoid an incorrect determination of the total residence (or batch) time by including time when the reactors were empty.

$$\sum_m \underline{\hat{F}}_m \cdot \mathbf{y}^r_{\mathbf{UM}_m} \leq \hat{\mathbf{F}}^r_{u_{m_2},u_r} \qquad \forall r \in R \tag{3.61}$$

$$\sum_m \underline{\hat{F}}_m \cdot \mathbf{y}^r_{\mathbf{UM}_m} \leq \hat{\mathbf{v}}^{p,q,r} \qquad \forall r \in R,\ \forall q \in Q,\ \forall p \in P \tag{3.62}$$

$$\sum_m \underline{\hat{F}}_m \cdot \mathbf{y}^r_{\mathbf{UM}_m} \leq \hat{\mathbf{F}}^r_{u_r,u_{s_2}} \qquad \forall r \in R \tag{3.63}$$

3.5.4 Reactor Type Identification

Defining $\mathbf{y}^r_{\mathbf{T}_t}$ as:

$$\mathbf{y}^r_{\mathbf{T}_t} = \begin{cases} 1, & \text{if reactor } r \text{ is of type } t \\ 0, & \text{otherwise} \end{cases} \tag{3.64}$$

First, I deal with relating this binary variable to whether a reactor is utilized. If reactor r is not utilized, all $\mathbf{y}^r_{\mathbf{T}_t}$ must be equal to 0. If it is utilized and is of type t that belongs to $M_T(m,t)$ (the map of reactor types to operating mode), $\mathbf{y}^r_{\mathbf{UM}_m} = 1$. These are implemented using:

$$\mathbf{y}^r_{\mathbf{T}_t} \leq \mathbf{y}^r_{\mathbf{UM}_m} \qquad (m,t) \in M_T,\ \forall r \in R \tag{3.65}$$

Also, if reactor r is utilized, exactly one $\mathbf{y}^r_{\mathbf{T}_t}$ is active, and the reactor type chosen must belong to the available reactor types of operating mode m (i.e. $(m,t) \in M_T$). This is implemented using:

$$\mathbf{y}^r_{\mathbf{UM}_m} \leq \sum_{t \in M_T} \mathbf{y}^r_{\mathbf{T}_t} \leq 1 \qquad \forall m \in M,\ \forall r \in R \tag{3.66}$$

Next, I deal with identifying the specific reactor types that are considered in this work.

3.5.4.1 Identifying CSTRs

The general DSR module (Figure 3.2) becomes a CSTR operating at steady state when there is a constant flow into and out of the DSR at all time

points along the time axis of the reactor. In addition, a well-mixed CSTR has a constant concentration at all time points. Therefore, I introduce a series of equations to ensure that these conditions are met when $\mathbf{y}^r_{\mathbf{T}_{t_{CSTR}}} = 1$.

To enforce the condition that the concentration of species i is constant throughout the CSTR, I add eq 3.67, which sets the change in concentration $\left(\frac{\mathbf{d}\hat{\mathbf{c}}}{\mathbf{d}\hat{\tau}}\right)_i^{p,q,r} = 0$ if reactor r is a CSTR.

$$\underline{\left(\frac{d\hat{c}}{d\hat{\tau}}\right)_i}\left(1 - \mathbf{y}^r_{\mathbf{T}_{t_{CSTR}}}\right) \leq \left(\frac{\mathbf{d}\hat{\mathbf{c}}}{\mathbf{d}\hat{\tau}}\right)_i^{p,q,r} \leq \overline{\left(\frac{d\hat{c}}{d\hat{\tau}}\right)_i}\left(1 - \mathbf{y}^r_{\mathbf{T}_{t_{CSTR}}}\right)$$
$$\forall i \in I,\ \forall r \in R,\ \forall q \in Q,\ p = p_1, \ldots, p_{N_P} \quad (3.67)$$

Care must be taken in enforcing the constraint for constant flowrate throughout the reactor. The goal of constant flowrate inside the reactor may be erroneously achieved by maintaining equal rates of material addition and removal at each point throughout the reactor axis ($\hat{\mathbf{w}}^{p,q,r}_{\mathbf{IN}} = \hat{\mathbf{w}}^{p,q,r}_{\mathbf{OUT}}$) but changing the value of the rates of change at different points along the axis ($\hat{\mathbf{w}}^{p,q,r}_{\mathbf{IN}} \neq \hat{\mathbf{w}}^{p',q',r}_{\mathbf{IN}}$). While this may give a correct CSTR profile, it may not be achievable in practice for a well-mixed CSTR that operates at steady state because it necessitates dynamic operation of the unit and grants an unfair advantage to the continuous-flow case. Therefore, in order to ensure a constant rate of material addition and removal throughout the residence time axis, I introduce the variable $\hat{\mathbf{F}}^r_{\text{CSTR}}$, and implement eqs 3.68 - 3.71, where $\mathbf{s}_{\hat{\mathbf{v}}^+_{\mathbf{CSTR}}}$ and $\mathbf{s}_{\hat{\mathbf{v}}^-_{\mathbf{CSTR}}}$ are positive slack variables:

$$\hat{\mathbf{w}}^{p,q,r}_{\mathbf{IN}} + \hat{\mathbf{F}}^{r}_{\mathrm{CSTR}} + \mathbf{s}^{p,q,r}_{\hat{\mathbf{v}}^{+}_{\mathbf{CSTR}}} = 0 \qquad \forall r \in R,\, \forall q \in Q,\, p = p_1, \ldots, p_{N_P} \quad (3.68)$$

$$\hat{\mathbf{w}}^{p,q,r}_{\mathbf{OUT}} - \hat{\mathbf{F}}^{r}_{\mathrm{CSTR}} - \mathbf{s}^{p,q,r}_{\hat{\mathbf{v}}^{-}_{\mathbf{CSTR}}} = 0 \qquad \forall r \in R,\, \forall q \in Q,\, p = p_1, \ldots, p_{N_P} \quad (3.69)$$

$$0 \leq \hat{\mathbf{F}}^{r}_{\mathrm{CSTR}} \leq \overline{\hat{w}_{\mathrm{OUT}}} \mathbf{y}^{r}_{\mathbf{T}_{t_{CSTR}}} \qquad \forall r \in R \quad (3.70)$$

$$0 \leq \mathbf{s}^{p,q,r}_{\hat{\mathbf{v}}^{+}_{\mathbf{CSTR}}} + \mathbf{s}^{p,q,r}_{\hat{\mathbf{v}}^{-}_{\mathbf{CSTR}}} \leq 2\overline{\hat{w}_{\mathrm{OUT}}} \left(1 - \mathbf{y}^{r}_{\mathbf{T}_{t_{CSTR}}}\right) \qquad \forall r \in R, \forall q \in Q, p = p_1, \ldots, p_{N_P} \quad (3.71)$$

Equations 3.68 - 3.71 ensure that the flowrate entering and exiting the reactor at all points is constant. In order to ensure that the constant flowrate within the reactor ($\hat{\mathbf{F}}^{r}_{u_{m_2},u_r}$) is equal to the total flowrate that enters and exits the reactor from the "IN" and "OUT" streams, a fact that is necessary for the accurate calculation of the reactor volume, I impose eqs 3.72 and 3.73, where $\mathbf{S}^{r}_{\hat{\mathbf{V}}^{+}_{\mathbf{CSTR}}}$ and $\mathbf{S}^{r}_{\hat{\mathbf{V}}^{-}_{\mathbf{CSTR}}}$ are positive slack variables.

$$\hat{\mathbf{F}}^{r}_{u_{m_2},u_r} - \hat{\mathbf{F}}^{r}_{u_{m_1},u_r} + \mathbf{S}^{r}_{\hat{\mathbf{V}}^{+}_{\mathbf{CSTR}}} - \mathbf{S}^{r}_{\hat{\mathbf{V}}^{-}_{\mathbf{CSTR}}} = 0 \qquad \forall r \in R \quad (3.72)$$

$$0 \leq \mathbf{S}^{r}_{\hat{\mathbf{V}}^{+}_{\mathbf{CSTR}}} + \mathbf{S}^{r}_{\hat{\mathbf{V}}^{-}_{\mathbf{CSTR}}} \leq 2\left(1 - \mathbf{y}^{r}_{\mathbf{T}_{t_{CSTR}}}\right) \qquad \forall r \in R \quad (3.73)$$

3.5.4.2 Identifying PFRs and BRs

There is no flow into or out of PFRs or BRs except at the main reactor feed and reactor outlet. This is implemented using eq 3.74:

$$\hat{\mathbf{F}}^r_{u,u'} \leq 1 - \mathbf{y}^r_{\mathbf{T}_t} \qquad t \in \{t_{PFR}, t_{BR}\}, (u,u') \in \{(u_{m_1}, u_r), (u_r, u_{s_3})\}, \forall r \in R \tag{3.74}$$

3.5.4.3 Identifying SBRs

For semi-batch operation, a storage tank is necessary if there is an "IN" stream or "OUT" stream. To account for its existence, I first need to identify if it is needed. I define binaries $\mathbf{y}^r_{\mathbf{IN}}$ and $\mathbf{y}^r_{\mathbf{OUT}}$ as:

$$\mathbf{y}^r_{\mathbf{IN}} = \begin{cases} 1, & \text{if "IN" stream exists in reactor } r \\ 0, & \text{otherwise} \end{cases} \tag{3.75}$$

$$\mathbf{y}^r_{\mathbf{OUT}} = \begin{cases} 1, & \text{if "OUT" stream exists in reactor } r \\ 0, & \text{otherwise} \end{cases} \tag{3.76}$$

To implement these definitions, I use eqs 3.77 and 3.78, where $\underline{\hat{F}}$ is a positive lower bound on $\hat{\mathbf{F}}_{u_{m_1},u_r}$:

$$\underline{\hat{F}} \cdot \mathbf{y}^r_{\mathbf{IN}} \leq \hat{\mathbf{F}}^r_{u_{m_1},u_r} \leq \mathbf{y}^r_{\mathbf{IN}} \qquad \forall r \in R \tag{3.77}$$

$$\underline{\hat{F}} \cdot \mathbf{y}^r_{\mathbf{OUT}} \leq \hat{\mathbf{F}}^r_{u_r,u_{s_3}} \leq \mathbf{y}^r_{\mathbf{OUT}} \qquad \forall r \in R \tag{3.78}$$

Further, I define binaries $\mathbf{y^r_{IN,B}}$ and $\mathbf{y^r_{OUT,B}}$ as:

$$\mathbf{y^r_{IN,B}} = \begin{cases} 1, & \text{if } \mathbf{y_{M_{m_B}}} = 1 \wedge \mathbf{y^r_{IN}} = 1 \\ 0, & \text{otherwise} \end{cases} \tag{3.79}$$

$$\mathbf{y^r_{OUT,B}} = \begin{cases} 1, & \text{if } \mathbf{y_{M_{m_B}}} = 1 \wedge \mathbf{y^r_{OUT}} = 1 \\ 0, & \text{otherwise} \end{cases} \tag{3.80}$$

To implement the logical conditions that $\mathbf{y_{M_{m_B}}} = 1 \wedge \mathbf{y^r_{IN}} = 1$ imply that $\mathbf{y^r_{IN,B}} = 1$, and $\mathbf{y_{M_{m_B}}} = 1 \wedge \mathbf{y^r_{OUT}} = 1$ imply that $\mathbf{y^r_{OUT,B}} = 1$, I use eqs 3.81 and 3.82.

$$\mathbf{y_{M_{m_B}}} + \mathbf{y^r_{IN}} \leq 1 + \mathbf{y^r_{IN,B}} \qquad \forall r \in R \tag{3.81}$$

$$\mathbf{y_{M_{m_B}}} + \mathbf{y^r_{OUT}} \leq 1 + \mathbf{y^r_{OUT,B}} \qquad \forall r \in R \tag{3.82}$$

To implement the reverse logic, ensuring that $\mathbf{y^r_{IN,B}} = 1$ implies that $\mathbf{y_{M_{m_B}}} = 1 \wedge \mathbf{y^r_{IN}} = 1$, and $\mathbf{y^r_{OUT,B}} = 1$ implies that $\mathbf{y_{M_{m_B}}} = 1 \wedge \mathbf{y^r_{OUT}} = 1$, I use eqs 3.83 - 3.86:

$$\mathbf{y^r_{IN,B}} \leq \mathbf{y_{M_{m_B}}} \qquad \forall r \in R \tag{3.83}$$

$$\mathbf{y^r_{IN,B}} \leq \mathbf{y^r_{IN}} \qquad \forall r \in R \tag{3.84}$$

$$\mathbf{y}^r_{\mathbf{OUT,B}} \leq \mathbf{y}_{\mathbf{M}_{m_B}} \qquad \forall r \in R \tag{3.85}$$

$$\mathbf{y}^r_{\mathbf{OUT,B}} \leq \mathbf{y}^r_{\mathbf{OUT}} \qquad \forall r \in R \tag{3.86}$$

Finally, I introduce the condition that if $\mathbf{y}^r_{\mathbf{IN,B}} = 1 \vee \mathbf{y}^r_{\mathbf{OUT,B}} = 1$ (i.e. the batch operating mode is chosen and an "IN" and/or "OUT" stream is present), $\mathbf{y}^r_{\mathbf{T}_{t_{SBR}}} = 1$ (i.e. SBR is the reactor type for reactor r), and $\mathbf{y}^r_{\mathbf{IN,B}} = 0$ otherwise, using eqs 3.87 - 3.89:

$$\mathbf{y}^r_{\mathbf{IN,B}} + \mathbf{y}^r_{\mathbf{OUT,B}} \geq \mathbf{y}^r_{\mathbf{T}_{t_{SBR}}} \qquad \forall r \in R \tag{3.87}$$

$$\mathbf{y}^r_{\mathbf{IN,B}} \leq \mathbf{y}^r_{\mathbf{T}_{t_{SBR}}} \qquad \forall r \in R \tag{3.88}$$

$$\mathbf{y}^r_{\mathbf{OUT,B}} \leq \mathbf{y}^r_{\mathbf{T}_{t_{SBR}}} \qquad \forall r \in R \tag{3.89}$$

3.5.5 Reactor Volumes

In this section, I explain how the normalized total volume of a reactor r is calculated. I first introduce the variable $\hat{\mathbf{V}}^r_{\mathbf{T},t}$, which is the volume of reactor r if r is of type t. This is enforced using eq 3.90:

$$\left(\frac{V_t}{\overline{\overline{V}}}\right) \mathbf{y}^r_{\mathbf{T}_t} \leq \hat{\mathbf{V}}^r_{\mathbf{T},t} \leq \left(\frac{\overline{V_t}}{\overline{\overline{V}}}\right) \mathbf{y}^r_{\mathbf{T}_t} \qquad \forall t \in T,\ \forall r \in R \tag{3.90}$$

Thus, since only one reactor type is allowed for any reactor r (see eq 3.66), the volume bounds $\left(\underline{V_t}/\overline{V}\right) \leq \hat{\mathbf{V}}^r_{\mathbf{T},t} \leq \left(\overline{V_t}/\overline{V}\right)$ apply only when reactor r is of type t. The calculation of the reactor volumes of each reactor type will now be discussed.

3.5.5.1 BR and SBR Volume

Equations 3.91 and 3.92 define the maximum volume attained in the reactor throughout the reaction time, $\hat{\mathbf{V}}^r_{\mathbf{max},t}$, where $\mathbf{s}^{p,q,r}_{\hat{\mathbf{V}}_{\mathbf{T_t}}}$ and $\mathbf{S}^r_{\hat{\mathbf{V}}_{\mathbf{T_t}}}$ are positive slack variables that are forced by eqs 3.93 and 3.94 to equal 0 if reactor r is of type t.

$$\hat{\mathbf{V}}^r_{\mathbf{max},t} - \hat{\mathbf{v}}^{p,q,r} + \mathbf{s}^{p,q,r}_{\hat{\mathbf{V}}_{\mathbf{T_t}}} \geq 0 \qquad t \in \{t_{\mathrm{BR}}, t_{\mathrm{SBR}}\},\ \forall r \in R,\ \forall q \in Q,\ \forall p \in P \tag{3.91}$$

$$\hat{\mathbf{V}}^r_{\mathbf{max},t} - \hat{\mathbf{F}}^r_{u_r,u_{s_2}} + \mathbf{S}^r_{\hat{\mathbf{V}}_{\mathbf{T_t}}} \geq 0 \qquad t \in \{t_{\mathrm{BR}}, t_{\mathrm{SBR}}\},\ \forall r \in R \tag{3.92}$$

$$0 \leq \mathbf{s}^{p,q,r}_{\hat{\mathbf{V}}_{\mathbf{T_t}}} \leq 1 - \mathbf{y}^r_{\mathbf{T}_t} \qquad t \in \{t_{\mathrm{BR}}, t_{\mathrm{SBR}}\},\ \forall r \in R,\ \forall q \in Q,\ \forall p \in P \tag{3.93}$$

$$0 \leq \mathbf{S}^r_{\hat{\mathbf{V}}_{\mathbf{T_t}}} \leq 1 - \mathbf{y}^r_{\mathbf{T}_t} \qquad t \in \{t_{\mathrm{BR}}, t_{\mathrm{SBR}}\},\ \forall r \in R \tag{3.94}$$

To calculate the actual reactor volume, note that for safety purposes, the purchased tank volume, $\hat{\mathbf{V}}^r_{\mathrm{T},t}$, must be greater than the maximum fluid

volume throughout the duration of the batch, and I impose a safety factor Υ to relate the maximum volume attained to the actual reactor volume, where $\Upsilon > 1$. A value of $\Upsilon = 1.1$ was used in this work, but can be easily changed. Then, the bounds on the maximum volume, $\hat{\mathbf{V}}^r_{\mathbf{max},t}$ are given by eq 3.95.

$$0 \leq \Upsilon \cdot \hat{\mathbf{V}}^r_{\mathbf{max},t} \leq \left(\frac{\overline{V_t}}{\overline{V}}\right) \mathbf{y}^r_{\mathbf{T}_t} \qquad t \in \{t_{\mathrm{BR}}, t_{\mathrm{SBR}}\},\ \forall r \in R \tag{3.95}$$

Finally, I add constraint (3.96) to impose that the reactor volume must be greater than the maximum volume multiplied by the safety factor. This constraint, coupled with the lower bound on $\hat{\mathbf{V}}^r_{\mathrm{T},t}$ (eq 3.90) and the fact that the optimal solution is one that minimizes reactor volume (and hence capital investment), state that $\hat{\mathbf{V}}^r_{\mathrm{T},t} = \max\left(\underline{V_t}/\overline{V}, \Upsilon \cdot \hat{\mathbf{V}}^r_{\mathbf{max},t}\right) \forall r \in R,\ t \in \{t_{\mathrm{BR}}, t_{\mathrm{SBR}}\}$.

$$\hat{\mathbf{V}}^r_{\mathrm{T},t} - \Upsilon \cdot \hat{\mathbf{V}}^r_{\mathbf{max},t} \geq 0 \qquad t \in \{t_{\mathrm{BR}}, t_{\mathrm{SBR}}\},\ \forall r \in R \tag{3.96}$$

3.5.5.2 PFR Volume

As was mentioned in section 3.5.1, for the general DSR where flowrate inside the reactor is allowed to vary with location along the time axis, the reactor volume would require an additional ODE (given in eq 3.49, page 97). Letting $\hat{\mathbf{v}}_{\mathbf{C}} = \mathbf{v}_{\mathbf{C}}/\overline{V}$ be the non-dimensional variable for the volume of the DSR in the continuous-flow operating mode, eq 3.49 becomes eq 3.97 after non-dimensionalization.

$$\left(\frac{\mathbf{d}\hat{\mathbf{v}}_{\mathbf{C}}}{\mathbf{d}\hat{\tau}}\right) = \left(\frac{\overline{F}}{\overline{\overline{V}}}\right)\boldsymbol{\Omega}\cdot\hat{\mathbf{f}} \tag{3.97}$$

In this work, the two reactor types considered for the continuous-flow operating mode are the PFR and CSTR, both of which (under the constant density assumption) exhibit constant volumetric flowrate throughout the reactor axis that is equal to the inlet volumetric flowrate, $\hat{\mathbf{F}}^{r}_{u_{m_2},u_r}$. Therefore, letting the total volume at the end of the reactor be $\hat{\mathbf{V}}^{r}_{\mathbf{C}}$, eq 3.97 can be integrated with reactor inlet boundary condition $\hat{\mathbf{v}}_{\mathbf{C}}\left(\hat{\tau}=\gamma^{r}\right)=0$ (recall from section 3.4 that reactor element r starts at $\hat{\tau}=\gamma^{r}$), and outlet boundary condition $\hat{\mathbf{v}}_{\mathbf{C}}\left(\hat{\tau}=\gamma^{r+1}\right)=\hat{\mathbf{V}}^{r}_{\mathbf{C}}$ (recall from section 3.4 that reactor element r ends at $\hat{\tau}=\gamma^{r+1}$), to give the reactor volume expression of eq 3.98.

$$\hat{\mathbf{V}}^{r}_{\mathbf{C}} = \left(\frac{\overline{F}}{\overline{\overline{V}}}\right)\boldsymbol{\Omega}\cdot\hat{\mathbf{F}}^{r}_{u_{m_2},u_r}\cdot\left(\gamma^{r+1}-\gamma^{r}\right) \tag{3.98}$$

Let the residence time of reactor r be $\mathbf{W}^{r}_{\mathbf{reac}}$ [hrs]. The difference between the dimensionless time at the inlet and outlet of reactor r, $\gamma^{r+1}-\gamma^{r}$, is equal to $\mathbf{W}^{r}_{\mathbf{reac}}/\boldsymbol{\Omega}$. Inserting this relationship into eq 3.98, and writing it for all reactors, gives eq 3.99, which is the final equation for calculating $\hat{\mathbf{V}}^{r}_{\mathbf{C}}$ that is implemented in the model.

$$\hat{\mathbf{V}}^{r}_{\mathbf{C}} = \left(\frac{\overline{F}}{\overline{\overline{V}}}\right)\cdot\hat{\mathbf{F}}^{r}_{u_{m_2},u_r}\cdot\mathbf{W}^{r}_{\mathbf{reac}} \qquad \forall r\in R \tag{3.99}$$

Finally, to obtain the volume of the reactor if the PFR reactor type is chosen, eqs 3.100 and 3.101 are added, where $\mathbf{S}^{r}_{\hat{\mathbf{V}}_{\mathbf{T}_{\mathbf{t}_{\mathrm{PFR}}}}}$ is a positive slack

variable, and $\overline{W_{\mathbf{reac}}}$ is the maximum possible residence/batch time for a single reactor ($\overline{W_{\mathbf{reac}}} = \max_t\left(\overline{W_t}\right)$). These state that if $\mathbf{y}^r_{\mathbf{T}_{t_{\mathrm{PFR}}}} = 1$, the total reactor volume $\hat{\mathbf{V}}^r_{\mathbf{T},t_{\mathrm{PFR}}}$ is equal to $\hat{\mathbf{V}}^r_{\mathbf{C}}$. Otherwise, $\hat{\mathbf{V}}^r_{\mathbf{T},t_{\mathrm{PFR}}} = 0$ by eq 3.90, and the slack variable $\mathbf{S}^r_{\hat{\mathbf{V}}_{\mathbf{T}_{\mathrm{PFR}}}}$ is allowed by eq 3.101 to take on any value below the upper bound of $\hat{\mathbf{V}}^r_{\mathbf{C}}$ (equal to $\left(\overline{F}/\overline{V}\right)\cdot\overline{W_{\mathbf{reac}}}$) to satisfy the equality of eq 3.100.

$$\hat{\mathbf{V}}^r_{\mathbf{T},t_{\mathrm{PFR}}} - \hat{\mathbf{V}}^r_{\mathbf{C}} + \mathbf{S}^r_{\hat{\mathbf{V}}_{\mathbf{T}_{\mathbf{t}_{\mathrm{PFR}}}}} = 0 \qquad \forall r \in R \tag{3.100}$$

$$0 \leq \mathbf{S}^r_{\hat{\mathbf{V}}_{\mathbf{T}_{\mathbf{t}_{\mathrm{PFR}}}}} \leq \left(\frac{\overline{F}}{\overline{V}}\right)\cdot\overline{W_{\mathbf{reac}}}\left(1 - \mathbf{y}^r_{\mathbf{T}_{t_{\mathrm{PFR}}}}\right) \qquad \forall r \in R \tag{3.101}$$

3.5.5.3 CSTR Volume

In general, the volume of fluid inside a CSTR is given by the volumetric flowrate of material entering and exiting the reactor multiplied by the residence time. The total volumetric flowrate entering the CSTR when represented by the DSR configuration of this work is equal to the total volumetric flowrate in the "IN" or "OUT" streams, $\hat{\mathbf{F}}^r_{u_{m_1},u_r}$. This amount is set equal to the volumetric flowrate within the reactor, $\hat{\mathbf{F}}^r_{u_{m_2},u_r}$, by eqs 3.72 and 3.73 (page 106). Then, the volume of fluid inside the reactor is accurately represented by $\hat{\mathbf{V}}^r_{\mathbf{C}}$, calculated by eq 3.99.

Therefore, the volume of the CSTR, $\hat{\mathbf{V}}^r_{\mathbf{T},t_{\mathrm{CSTR}}}$, can be calculated in the same manner as the PFR, as is shown in eqs 3.102 and 3.103. One minor difference, however, is that the CSTR takes on the autoclave geometry, so a

safety factor Υ is added for the CSTR case to ensure that the actual vessel volume is greater than the fluid holdup (as was the case for the BR and SBR).

$$\hat{\mathbf{V}}^r_{\mathbf{T},t_{\mathrm{CSTR}}} - \Upsilon \cdot \hat{\mathbf{V}}^r_{\mathbf{C}} + \mathbf{S}^r_{\hat{\mathbf{V}}_{\mathbf{T}_{\mathbf{t}_{\mathrm{CSTR}}}}} = 0 \qquad \forall r \in R \tag{3.102}$$

$$0 \leq \mathbf{S}^r_{\hat{\mathbf{V}}_{\mathbf{T}_{\mathbf{t}_{\mathrm{CSTR}}}}} \leq \Upsilon \left(\frac{\overline{F}}{\overline{V}}\right) \cdot \overline{W_{\mathbf{reac}}} \left(1 - \mathbf{y}^r_{\mathbf{T}_{t_{\mathrm{CSTR}}}}\right) \qquad \forall r \in R \tag{3.103}$$

3.5.6 Storage Tanks

The need for an "IN" or "OUT" storage tank in reactor r had been designated the binary variables $\mathbf{y}^r_{\mathbf{IN,B}}$ and $\mathbf{y}^r_{\mathbf{OUT,B}}$, respectively, and those variables were defined in section 3.5.4.3 (page 107). To calculate the volumes of the storage tanks, $\hat{\mathbf{V}}^r_{\mathbf{T,st,IN}}$ or $\hat{\mathbf{V}}^r_{\mathbf{T,st,OUT}}$, eqs 3.104 - 3.109 are added, where $\underline{\hat{V}_{\mathrm{st}}} = \left(\underline{V_{\mathrm{st}}}/\overline{V}\right)$ and $\overline{\hat{V}_{\mathrm{st}}} = \left(\overline{V_{\mathrm{st}}}/\overline{V}\right)$ are the lower and upper bounds on the non-dimensionalized storage tank volumes, and $\mathbf{S}^r_{\hat{\mathbf{V}}_{\mathbf{T,st,IN}}}$ and $\mathbf{S}^r_{\hat{\mathbf{V}}_{\mathbf{T,st,OUT}}}$ are positive slack variables.

$$\Upsilon \cdot \hat{\mathbf{F}}^r_{u_{m_1},u_r} - \hat{\mathbf{V}}^r_{\mathbf{T,st,IN}} - \mathbf{S}^r_{\hat{\mathbf{V}}_{\mathbf{T,st,IN}}} \leq 0 \qquad \forall r \in R \tag{3.104}$$

$$\Upsilon \cdot \hat{\mathbf{F}}^r_{u_r,u_{s_3}} - \hat{\mathbf{V}}^r_{\mathbf{T,st,OUT}} - \mathbf{S}^r_{\hat{\mathbf{V}}_{\mathbf{T,st,OUT}}} \leq 0 \qquad \forall r \in R \tag{3.105}$$

$$\underline{\hat{V}_{\text{st}}} \cdot \mathbf{y}^r_{\mathbf{IN,B}} \leq \hat{\mathbf{V}}^r_{\mathbf{T,st,IN}} \leq \overline{\hat{V}_{\text{st}}} \cdot \mathbf{y}^r_{\mathbf{IN,B}} \qquad \forall r \in R \qquad (3.106)$$

$$\underline{\hat{V}_{\text{st}}} \cdot \mathbf{y}^r_{\mathbf{OUT,B}} \leq \hat{\mathbf{V}}^r_{\mathbf{T,st,OUT}} \leq \overline{\hat{V}_{\text{st}}} \cdot \mathbf{y}^r_{\mathbf{OUT,B}} \qquad \forall r \in R \qquad (3.107)$$

$$0 \leq \mathbf{S}^r_{\hat{\mathbf{V}}_{\mathbf{T,st,IN}}} \leq \Upsilon \left(1 - \mathbf{y}^r_{\mathbf{IN,B}}\right) \qquad \forall r \in R \qquad (3.108)$$

$$0 \leq \mathbf{S}^r_{\hat{\mathbf{V}}_{\mathbf{T,st,OUT}}} \leq \Upsilon \left(1 - \mathbf{y}^r_{\mathbf{OUT,B}}\right) \qquad \forall r \in R \qquad (3.109)$$

If a storage tank is deemed necessary for reactor element r (i.e. if $\mathbf{y}^r_{\mathbf{IN,B}} = 1$ or $\mathbf{y}^r_{\mathbf{OUT,B}} = 1$), the slack variables are forced to equal 0 by eqs 3.108 and 3.109. Then, eqs 3.104 and 3.105 state that $\hat{\mathbf{V}}^r_{\mathbf{T,st,IN}} = \max\left(\underline{\hat{V}_{\text{st}}}, \Upsilon \cdot \hat{\mathbf{F}}^r_{u_{m_1},u_r}\right)$, and $\hat{\mathbf{V}}^r_{\mathbf{T,st,OUT}} = \max\left(\underline{\hat{V}_{\text{st}}}, \Upsilon \cdot \hat{\mathbf{F}}^r_{u_r,u_{s_3}}\right)$. If a storage tank is unnecessary (i.e. if $\mathbf{y}^r_{\mathbf{IN,B}} = 0$ or $\mathbf{y}^r_{\mathbf{OUT,B}} = 0$), the storage tank volume is set equal to 0 by eqs 3.106 and 3.107, and the slack variable is allowed by eqs 3.108 and 3.109 to take any value to satisfy the constraints of eqs 3.104 and 3.105.

3.5.7 Timing Constraints

Let the residence time of reactor r, if reactor r is of type t, be $\mathbf{W}^r_{\mathbf{t}}$. The choice of reactor type determines the bounds on the residence time. This is implemented using eq 3.110. Then, the residence time of reactor r, $\mathbf{W}^r_{\mathbf{reac}}$, is

given by eq 3.111. The total residence time, $\mathbf{\Omega}$ [hrs], of the reactor network is given by eq 3.112.

$$\underline{W_{\mathrm{t}}} \cdot \mathbf{y}^r_{\mathbf{T}_t} \leq \mathbf{W}^r_{\mathbf{t}} \leq \overline{W_{\mathrm{t}}} \cdot \mathbf{y}^r_{\mathbf{T}_t} \qquad \forall t \in T,\, \forall r \in R \tag{3.110}$$

$$\mathbf{W}^r_{\mathbf{reac}} = \sum_t \mathbf{W}^r_{\mathbf{t}} \qquad \forall r \in R \tag{3.111}$$

$$\mathbf{\Omega} = \sum_r \mathbf{W}^r_{\mathbf{reac}} \tag{3.112}$$

For any problem, at least reactor r_1 must be utilized. Therefore, $\mathbf{y}^{r_1}_{\mathbf{U}} = 1$. Furthermore, reactors upstream must all be used before a downstream reactor is used. This is implemented using eq 3.113.

$$\mathbf{y}^r_{\mathbf{U}} \leq \mathbf{y}^{r-1}_{\mathbf{U}} \qquad r = r_2, \ldots, r_{N_R} \tag{3.113}$$

If a reactor downstream of reactor r_1 is utilized, the normalized time γ^{r+1} of the endpoint of reactor r along the global domain must be between 0 and 1. If it is not utilized (and therefore all further downstream reactors are not utilized), then it must have reached 1. This is implemented using eq 3.114.

$$1 - \mathbf{y}^r_{\mathbf{U}} \leq \gamma^r \leq 1 \qquad r = r_2, \ldots, r_{N_R} \tag{3.114}$$

The relationship between the global normalized time at the boundary and the residence time of each individual reactor is given by eq 3.115.

$$\gamma^r = \frac{\sum_{r'=1}^{r'=r-1} \mathbf{W}_{\mathbf{reac}}^{r'}}{\mathbf{\Omega}} \qquad r = r_2, \ldots, r_{N_R+1} \tag{3.115}$$

As was derived in section 3.4, the normalized time of collocation point p in finite element q of reactor r is given by eq 3.116.

$$\hat{\tau}^{p,q,r} = \gamma^r + \left(\gamma^{r+1} - \gamma^r\right)\left(\beta^q + \alpha^p\left[\beta^{q+1} - \beta^q\right]\right) \qquad \forall r \in R,\, \forall q \in Q,\, \forall p \in P \tag{3.116}$$

3.5.8 Operating Mode-Dependent Variable Definitions

There are some variables that are relevant only to the batch operating mode. Here, I describe how these variables are set.

First, the time for additional operations (charging, conditioning, discharging, cleaning), $\mathbf{W}_{\mathbf{op}}^r$, must be added to the time spent for reaction, $\mathbf{W}_{\mathbf{reac}}^r$, to calculate the actual duration of each reactor unit, $\mathbf{T}_{\mathbf{a}}^r$.

$$\mathbf{T}_{\mathbf{a}}^r = \mathbf{W}_{\mathbf{reac}}^r + \mathbf{W}_{\mathbf{op}}^r \qquad \forall r \in R \tag{3.117}$$

Previous works on batch reactor modeling often adopt a simplistic approach of assuming a value between $\underline{W_{\text{op}}} = 2.5$ hr and $\overline{W_{\text{op}}} = 7.5$ hrs [65, 60]. In this work, since an explicit calculation of the batch reactor volumes is

included, I assume that the time for cleaning, conditioning, loading, and unloading the reactors is directly proportional to the reactor volume, and that this relationship is linear. This is reflected in eq 3.118.

$$\mathbf{W}^r_{\mathbf{op}} = \underline{W_{\mathrm{op}}} \cdot \mathbf{y}^r_{\mathbf{UM}_{m_B}} + \sum_{t \in M_T(m_B,t)} \frac{\overline{W_{\mathrm{op}}} - \underline{W_{\mathrm{op}}}}{\left(\frac{\overline{V_t}}{\overline{\overline{V}}}\right) - \left(\frac{\underline{V_t}}{\underline{\underline{V}}}\right)} \left(\hat{\mathbf{V}}^r_{\mathbf{T},t} - \underline{\hat{V}_{\mathrm{T},t}} \cdot \mathbf{y}^r_{\mathbf{T}_t}\right) \qquad \forall r \in R \tag{3.118}$$

The total batch time for the batch reactor network, $\mathbf{\Psi}$, is needed within the revenues and costs expressions only when the batch operating mode is selected. For the continuous-flow operating mode, the value of the total batch time should equal to 1 to give the correct numerical values of the costs (see discussion for eq 3.131 in section 3.6.1 for explanation of why this is so). Equations 3.119 - 3.120 are used to enforce this, where $\overline{\Psi_B} = N_R \times \left[\max\left(\overline{W_{t_{SBR}}}, \overline{W_{t_{BR}}}\right) + \overline{W_{\mathrm{op}}}\right]$ is the upper bound on the total batch time, and $\overline{\Omega_C} = N_R \times \max\left(\overline{W_{t_{PFR}}}, \overline{W_{t_{CSTR}}}\right)$ is the upper bound on the total residence time if the continuous-flow operating mode is chosen.

$$-\mathbf{y}_{\mathbf{M}_{m_B}} \leq \mathbf{\Psi} - 1 \leq \left(\overline{\Psi_B} - 1\right) \mathbf{y}_{\mathbf{M}_{m_B}} \tag{3.119}$$

$$-\left(\overline{\Omega_C} - 1\right) \mathbf{y}_{\mathbf{M}_{m_C}} \leq \mathbf{\Psi} - \sum_r \mathbf{T}^r_{\mathbf{a}} \leq \mathbf{y}_{\mathbf{M}_{m_C}} \tag{3.120}$$

Another variable that is needed in the cost equations is the reference value used to non-dimensionalize the volume variables. As was discussed in

section 3.3.3, the batch operating mode uses the upper bound on volume, $\overline{V}$, to non-dimensionalize the volume equations (see eq 3.13 on page 79), while the continuous-flow operating mode uses the upper bound on volumetric flowrate, $\overline{F}$, to non-dimensionalize the volumetric flowrate ODE. In order to select the correct reference value, I introduce the variable F^{ref}, and use eq 3.121 to assign the variable the correct reference parameter.

$$F^{\text{ref}} - \overline{F} = (\overline{V} - \overline{F})\mathbf{y}_{\mathbf{M}_{m_B}} \tag{3.121}$$

Also, the amount of useful product made must be scaled by a factor μ_B (where $\mu_B > 0$) to account for the fact that some batches are off-spec. This factor is zero if the continuous-flow operating mode is selected. To enforce this, a variable $\mathbf{\Gamma}_B$ is introduced that equals μ_B for the batch operating mode, and zero otherwise. This is enforced using eq 3.122.

$$\mathbf{\Gamma}_B = \mu_B \cdot \mathbf{y}_{\mathbf{M}_{m_B}} \tag{3.122}$$

Finally, I introduce variables for the accurate calculation of the annual production. I assume that each plant (in either operating mode) operates for a total of ω hours per year (a known parameter). First, I introduce the variable $\mathbf{\Phi}$. For the batch operating mode, this is set equal to the amount of desirable product per batch [kmol/batch]. For the continuous-flow operating mode, this is set equal to the amount of desirable product made per hour of operation [kmol/hr]. This is enforced using eq 3.123.

$$\mathbf{\Phi} = \overline{C}_i \hat{\mathbf{C}}^{r_{N_R}}_{i,u_{m3},u_e} F^{\text{ref}} \hat{\mathbf{F}}^{r_{N_R}}_{u_{m3},u_e} (1 - \mathbf{\Gamma}_B) \qquad i \in I_{P_D} \tag{3.123}$$

Next, I introduce the variable $\mathbf{\Lambda_B}$. For the batch operating mode, this is set equal to the number of batches per year in a single batch plant [batches/yr]. For the continuous-flow operating mode, this is set equal to the number of hours of operation per year ω [hrs/yr]. This is enforced using eq 3.124.

$$\omega \cdot \mathbf{y}_{\mathbf{M}_{m_C}} + \mathbf{y}_{\mathbf{M}_{m_B}} \leq \mathbf{\Lambda_B} \leq \frac{\omega}{\mathbf{\Psi}} \tag{3.124}$$

Then, I introduce the variable $\mathbf{\Delta}$, which is equal to the amount of product made per year in a single plant for both operating modes. This is enforced using eq 3.125, which is applicable for both operating modes since the variables $\mathbf{\Phi}$ and $\mathbf{\Lambda_B}$ have values that depend on the operating mode.

$$\mathbf{\Delta} = \mathbf{\Phi} \cdot \mathbf{\Lambda_B} \tag{3.125}$$

At this point, I have allowed as much production in a single plant of either operating mode as can be accommodated by the volume constraints on the processing units. In order to allow the calculation of economics for any product demand ($\delta_i, i \in I_{P_D}$), I also allow the presence of multiple plants operating in parallel. Let $\mathbf{\Lambda_P}$ be the number of plants operating in parallel. Then, the total production is set equal to the demand of product by eq 3.126.

$$\boldsymbol{\Delta} \cdot \boldsymbol{\Lambda_P} = \delta_i \qquad \forall i \in I_{P_D} \tag{3.126}$$

However, care must be taken in order to ensure that the number of plants in parallel is the minimum number of plants needed to accommodate the product demand. Otherwise, for the batch operating mode, the methodology I use to grant the batch mode the advantage of utilizing the units after the product demand is met (discussed in section 3.6.1) will incentivize making the minimum product possible in a single batch, scaling the economics to a full year from a single batch, then using many plants in parallel to meet the desired product demand.

In order to ensure that the number of plants in parallel is the minimum number needed to meet demand, I impose eq 3.127. This constraint states that for there to be $\boldsymbol{\Lambda_P}$ plants in parallel, the demand of product i, δ_i, must be greater than the maximum amount of product that could be made in $\boldsymbol{\Lambda_P} - 1$ plants, given by the multiplication of the amount of product made in a single batch (or in a single hour for the continuous-flow case), $\boldsymbol{\Phi}$, with the maximum number of batches per year (or the number of hours of operation per year for the continuous-flow case), $\frac{\omega}{\boldsymbol{\Psi}}$.

$$\frac{\omega}{\boldsymbol{\Psi}} \cdot \boldsymbol{\Phi} \left(\boldsymbol{\Lambda_P} - 1 \right) \leq \delta_i \qquad i \in I_{P_D} \tag{3.127}$$

3.6 A Unified Representation of Batch/Continuous Economics

In this section, I present the model used to calculate the annualized profits for either operating mode. The general approach is given in standard chemical engineering economics text books, such as the works of Peters *et al.* [128] and Towler and Sinnott [160]. However, modifications are made to account for the differences in the natures of the two operating modes. It should be noted that all parameters used in the economics models can be easily adjusted for different case studies.

The objective function to maximize is the annual profit, $\mathbf{\Pi}$, defined as the difference between annual revenues, $\mathbf{\Theta}$, and the total annualized cost, $\mathbf{\Xi}$:

$$\mathbf{\Pi} = \mathbf{\Theta} - \mathbf{\Xi} \tag{3.128}$$

3.6.1 Revenue Calculation

The total annual revenues can be calculated by summing the revenues obtained by selling each of the desirable products. For the continuous-flow operating mode, the total annual revenue can be obtained by eq 3.129, where $\mathbf{\Theta_C}$ is the annual revenue if the continuous-flow operating mode is selected, and the units of each term are included for ease of reading. Note that the units for $\mathbf{\Phi}$ are specific to the continuous-flow operating mode, and are different if the batch operating mode was selected, as was discussed in section 3.5.8.

$$\mathbf{\Theta_C}\left[\frac{\$}{\text{yr}}\right] = \sum_{i \in I_{P_D}} \omega \left[\frac{\text{hrs}}{\text{yr} \cdot (\text{Plant})}\right] \cdot \zeta_i^{\text{sale}} \left[\frac{\$}{\text{kmol}}\right] \cdot \mathbf{\Phi} \left[\frac{\text{kmol}}{\text{hr}}\right] \cdot \mathbf{\Lambda_P}\,[\text{plants}] \tag{3.129}$$

For the batch operating mode, the revenues obtained from a single batch are given by eq 3.130, where $\mathbf{\Theta_B}$ are the revenues from a single batch, and the units of the variable $\mathbf{\Phi}$ are again given for the case where the batch operating mode is selected.

$$\mathbf{\Theta_B}\left[\frac{\$}{\text{Batch}}\right] = \sum_{i \in I_{P_D}} \zeta_i^{\text{sale}} \left[\frac{\$}{\text{kmol}}\right] \cdot \mathbf{\Phi} \left[\frac{\text{kmol}}{\text{Batch}}\right] \tag{3.130}$$

If economics were to be calculated only for the desirable products being considered in the problem, the annual revenues for the batch case can be calculated by multiplying the right-hand-side of eq 3.130 by $\mathbf{\Lambda_B}$ [Batches/yr]. However, this approach assumes that the batch plant will only be used for the manufacture of the desirable products in the problem, and would not account for the use of the batch plant for the manufacture of other products throughout the year.

In this work, I propose an alternative approach where batch economics are obtained by assuming the hourly rate of profit for a batch continues to be generated by the plant for the full year, regardless of the annual demand of the specific desirable product. The hourly rate of revenue generation [$/hr] from a single batch can be obtained from the expression given in eq 3.130 by

dividing the right-hand-side by the number of hours per batch, $\mathbf{\Psi}$ [hrs/batch]. Then, assuming the revenue generation is maintained at a constant rate for all ω hours of operation of the plant in the year, the annual revenue for the batch plant can be given by eq 3.131.

$$\mathbf{\Theta}\left[\frac{\$}{\text{yr}}\right] = \frac{\omega\left[\frac{\text{hrs}}{\text{yr}\cdot(\text{Plant})}\right]}{\mathbf{\Psi}\left[\frac{\text{hrs}}{\text{batch}}\right]} \sum_{i\in I_{P_D}} \zeta_i^{\text{sale}}\left[\frac{\$}{\text{kmol}}\right]\cdot\mathbf{\Phi}\left[\frac{\text{kmol}}{\text{Batch}}\right]\cdot\mathbf{\Lambda_P}\,[\text{plants}] \quad (3.131)$$

Essentially, this constraint circumvents the demand constraint for the batch case (eq 3.126), and allows the solver to assume that an unlimited amount of product could be sold to the market. Therefore, one potential solution that can be used to maximize profit for the batch operating mode is to set the number of batches per year per plant to the minimum value of 1 ($\mathbf{\Lambda_B} = 1$), then use many plants in parallel to achieve the demand of the desired product, while scaling the individual economics of each plant to assume that the plant is used for the entire year, potentially generating an extremely high profit compared to the continuous-flow counterpart. To eliminate this solution from the feasible space, a limit was placed on the number of plants in parallel (constraint 3.127 on page 121), and was discussed in section 3.5.8.

Finally, I point out that in its current form, eq 3.131 may be used to describe the annual revenues from the continuous-flow operating mode (eq 3.129) if $\mathbf{\Psi} = 1$. Therefore, in defining the variable $\mathbf{\Psi}$, I used eq 3.119 (page 118) in section 3.5.8 to set $\mathbf{\Psi} = 1$ when $\mathbf{y}_{\mathbf{M}_{m_C}} = 1$ (i.e. when the continuous-

flow operating mode is selected), and I use eq 3.131 in our final model to unify the calculation of the annual revenues obtained from either operating mode.

3.6.2 Cost Calculation

The total annualized cost, $\mathbf{\Xi}$, is the sum of the annualized investment costs, $\mathbf{I_C}$, and the annual operating costs, $\mathbf{O_C}$:

$$\mathbf{\Xi}\left[\frac{\$}{\text{yr}}\right] = \mathbf{I_C}\left[\frac{\$}{\text{yr}}\right] + \mathbf{O_C}\left[\frac{\$}{\text{yr}}\right] \tag{3.132}$$

3.6.2.1 Investment Costs

The total investment cost for $\mathbf{\Lambda_P}$ plants, $\mathbf{I_C}$ [\$/yr], is the sum of the fixed capital investments per plant, $\mathbf{I_{C,F}}$ [\$/plant], and the working capital investment per plant, $\mathbf{I_{C,W}}$ [\$/plant], multiplied by an annualizing factor θ [yr^{-1}], multiplied by the number of plants $\mathbf{\Lambda_P}$. This is shown in eq 3.133. The working capital investment is assumed to be 15% of the total capital investment, and is therefore calculated as a function of the fixed capital investment (85% of the total investment) using eq 3.134.

$$\mathbf{I_C}\left[\frac{\$}{\text{yr}}\right] = \theta\left[\text{yr}^{-1}\right]\left(\mathbf{I_{C,F}}\left[\frac{\$}{\text{plant}}\right] + \mathbf{I_{C,W}}\left[\frac{\$}{\text{plant}}\right]\right)\mathbf{\Lambda_P}\,[\text{plants}] \tag{3.133}$$

$$\mathbf{I_{C,W}}\left[\frac{\$}{\text{plant}}\right] = \frac{0.15}{0.85}\mathbf{I_{C,F}}\left[\frac{\$}{\text{plant}}\right] \tag{3.134}$$

The fixed capital investment per plant is the sum of the direct, $\mathbf{I_{C,F,D}}$ [\$/plant], and indirect, $\mathbf{I_{C,F,I}}$ [\$/plant], capital investments, as is shown in eq 3.135. Those are directly proportional to the purchased equipment cost per plant, $\mathbf{I_{C,P}}$ [\$/plant], and the relationships are shown in eqs 3.136 and 3.137.

$$\mathbf{I_{C,F}}\left[\frac{\$}{\text{plant}}\right] = \mathbf{I_{C,F,D}}\left[\frac{\$}{\text{plant}}\right] + \mathbf{I_{C,F,I}}\left[\frac{\$}{\text{plant}}\right] \tag{3.135}$$

$$\mathbf{I_{C,F,D}}\left[\frac{\$}{\text{plant}}\right] = 3.6\left(\mathbf{I_{C,P}}\left[\frac{\$}{\text{plant}}\right]\right) \tag{3.136}$$

$$\mathbf{I_{C,F,I}} = 1.44(\mathbf{I_{C,P}}\left[\frac{\$}{\text{plant}}\right]) \tag{3.137}$$

The equipment purchase costs is the sum over all reactor elements of the cost of each reactor in a reactor element, $\mathbf{I^r_{C,P,reac}}$ [\$/plant], as well as the cost of the storage units used in the element, $\mathbf{I^r_{C,P,st}}$ [\$/plant], if they are needed. This is shown in eq 3.138.

$$\mathbf{I_{C,P}}\left[\frac{\$}{\text{plant}}\right] = \sum_r \left(\mathbf{I^r_{C,P,reac}}\left[\frac{\$}{\text{plant}}\right] + \mathbf{I^r_{C,P,st}}\left[\frac{\$}{\text{plant}}\right]\right) \tag{3.138}$$

The cost of each reactor depends on the reactor type. Let $\mathbf{I^r_{C,P,reac}}_t$ [\$/plant] be the cost of reactor r if reactor r was of type t. Standard cost correlations may be used to calculate the reactor cost based on the reactor volume, as is shown in eq 3.139, where $\pi^{\text{reac}}_{a_t}$, $\pi^{\text{reac}}_{b_t}$, and $\pi^{\text{reac}}_{c_t}$ are correlation coefficients for

the cost of a reactor of type t. The binary $\mathbf{y}^r_{\mathbf{T}_t}$ is included to set the reactor cost to 0 if the reactor is not of type t. Then, the total reactor cost for a reactor element r is given by eq 3.140.

$$\mathbf{I}^r_{\mathbf{C,P,reac}_t} = \pi^{\text{reac}}_{a_t} \cdot \mathbf{y}^r_{\mathbf{T}_t} + \pi^{\text{reac}}_{b_t} \cdot \left(\overline{V} \cdot \hat{\mathbf{V}}^r_{\mathbf{T},t}\right)^{\pi^{\text{reac}}_{c_t}} \qquad \forall t \in T, \forall r \in R \quad (3.139)$$

$$\mathbf{I}^r_{\mathbf{C,P,reac}} = \sum_t \mathbf{I}^r_{\mathbf{C,P,reac}_t} \qquad \forall r \in R \quad (3.140)$$

Similarly, the cost of storage units for a reactor element r can be related to the volume of the storage units using standard cost correlations for storage tanks, as is shown in eq 3.141.

$$\mathbf{I}^r_{\mathbf{C,P,st}} = \pi^{\text{st}}_a \cdot \mathbf{y}^r_{\mathbf{IN,B}} + \pi^{\text{st}}_b \cdot \left(\overline{V} \cdot \hat{V}^r_{\mathbf{T,st,IN}}\right)^{\pi^{\text{st}}_c} + \pi^{\text{st}}_a \cdot \mathbf{y}^r_{\mathbf{OUT,B}} + \pi^{\text{st}}_b \cdot \left(\overline{V} \cdot \hat{V}^r_{\mathbf{T,st,OUT}}\right)^{\pi^{\text{st}}_c} \qquad \forall r \in R \quad (3.141)$$

3.6.2.2 Operating Costs

The total annual operating cost for $\mathbf{\Lambda_P}$ plants, $\mathbf{O_C}$ [\$/yr] is the sum of the annual variable operating cost per plant, $\mathbf{O_{C,V}}$ [\$/ (yr · plant)], and the annual fixed operating cost per plant, $\mathbf{O_{C,F}}$ [\$/ (yr · plant)], multiplied by the number of plants operating in parallel, $\mathbf{\Lambda_P}$. This is shown in eq 3.142.

$$\mathbf{O_C}\left[\frac{\$}{\text{yr}}\right] = \left(\mathbf{O_{C,V}}\left[\frac{\$}{(\text{yr})(\text{plant})}\right] + \mathbf{O_{C,F}}\left[\frac{\$}{(\text{yr})(\text{plant})}\right]\right)\mathbf{\Lambda_P}\,[\text{plants}] \tag{3.142}$$

The annual variable operating cost is the sum of the costs of purchasing raw materials, $\mathbf{O_{C,V,R}}\,[\$/\,(\text{yr}\cdot\text{plant})]$, and the cost of product treatment $\mathbf{O_{C,V,T}}\,[\$/\,(\text{yr}\cdot\text{plant})]$. This is shown in eq 3.143. The raw material costs for a single plant can be obtained by multiplying the amount of raw material needed per year of operation by the cost of each raw material. This is shown in eq 3.144, where the amount of raw material needed per year has been scaled for the batch plants to assume that the batch plant is used for the entirety of the year, regardless of the desirable product demand, as was done for the revenues. The treatment costs were obtained in the same manner, and the expression used to calculate the annual treatment costs per plant is shown in eq 3.145.

$$\mathbf{O_{C,V}}\left[\frac{\$}{(\text{yr})(\text{plant})}\right] = \mathbf{O_{C,V,R}}\left[\frac{\$}{(\text{yr})(\text{plant})}\right] + \mathbf{O_{C,V,T}}\left[\frac{\$}{(\text{yr})(\text{plant})}\right] \tag{3.143}$$

$$\begin{aligned}\mathbf{O_{C,V,R}}\left[\frac{\$}{(\text{yr})(\text{plant})}\right] =& \frac{\omega\left[\frac{\text{hrs}}{(\text{yr})\cdot(\text{Plant})}\right]}{\mathbf{\Psi}\left[\left(\frac{\text{hrs}}{\text{batch}}\,\text{if batch}\right)\text{or}\ (\text{dimensionless if continuous})\right]} \\ &\times \mathit{F}^{\text{ref}}\hat{\mathbf{F}}^{r_1}_{u_f,u_{s_1}}\left[\left(\frac{\text{m}^3}{\text{batch}}\,\text{if batch}\right)\text{or}\ \left(\frac{\text{m}^3}{\text{hr}}\,\text{if continuous}\right)\right] \\ &\times \sum_{i\in I_R}\zeta_i^{\text{raw}}\left[\frac{\$}{\text{kmol}}\right]\cdot C_i^{\text{feed}}\left[\frac{\text{kmol}}{\text{m}^3}\right]\cdot\end{aligned} \tag{3.144}$$

$$\mathbf{O_{C,V,T}}\left[\frac{\$}{(\text{yr})(\text{plant})}\right] = \frac{\omega\left[\frac{\text{hrs}}{(\text{yr})\cdot(\text{Plant})}\right]}{\boldsymbol{\Psi}\left[\left(\frac{\text{hrs}}{\text{batch}}\text{ if batch}\right)\text{ or }(\text{dimensionless if continuous})\right]} \times F^{\text{ref}}\hat{\mathbf{F}}^{r_{N_R}}_{u_{m_3},u_e}\left[\left(\frac{\text{m}^3}{\text{batch}}\text{ if batch}\right)\text{ or }\left(\frac{\text{m}^3}{\text{hr}}\text{ if continuous}\right)\right] \times \sum_{i\in I_R\cup I_{P_U}} \zeta_i^{\text{treat}}\left[\frac{\$}{\text{kmol}}\right]\cdot\overline{C_i}\hat{\mathbf{C}}^{r_{N_R}}_{i,u_{m_3},u_e}\left[\frac{\text{kmol}}{\text{m}^3}\right] \tag{3.145}$$

The annual fixed operating cost, $\mathbf{O_{C,F}}$ [\$/ (yr · plant)], is the sum of the costs of supervision, $\mathbf{O_{C,F,S}}$, overhead, $\mathbf{O_{C,F,O}}$, maintenance, $\mathbf{O_{C,F,M}}$, taxes, $\mathbf{O_{C,F,T}}$, rent, $\mathbf{O_{C,F,R}}$, insurance, $\mathbf{O_{C,F,I}}$, and labor costs, $\mathbf{O_{C,F,L}}$. This summation is shown in eq 3.146, and the correlations used to relate each of the contributing terms to the investment costs or labor costs are shown in (3.147 - 3.151), where the same units of [\$/ (yr · plant)] have now been dropped from each term.

$$\mathbf{O_{C,F}} = \mathbf{O_{C,F,L}}+\mathbf{O_{C,F,S}}+\mathbf{O_{C,F,O}}+\mathbf{O_{C,F,M}}+\mathbf{O_{C,F,T}}+\mathbf{O_{C,F,R}}+\mathbf{O_{C,F,I}} \tag{3.146}$$

$$\mathbf{O_{C,F,S}} = 0.25\cdot\mathbf{O_{C,F,L}} \tag{3.147}$$

$$\mathbf{O_{C,F,O}} = 0.5(\mathbf{O_{C,F,S}} + \mathbf{O_{C,F,L}}) \tag{3.148}$$

$$\mathbf{O_{C,F,M}} = 0.05\cdot\mathbf{I_{C,F,D}} \tag{3.149}$$

$$\mathbf{O_{C,F,T}} = 0.01 \cdot \mathbf{I_{C,F,D}} \tag{3.150}$$

$$\mathbf{O_{C,F,R}} = \mathbf{O_{C,F,I}} = 0.01 \cdot \mathbf{I_{C,F}} \tag{3.151}$$

Labor costs must include estimates based on the operating mode as well as the number of processing units present. The annual labor cost per plant is equal to the annual salary per operator, a parameter ζ^{op} [\$/ (yr · operator)], multiplied by the number operators needed for the plant, $\mathbf{\Lambda_O}$ [operators], as shown in eq 3.152. To calculate the number of operators needed, I assume that the number of shift positions per reactor (σ_m^{reac}) for the batch operating mode is double that of the continuous-flow operating mode [128], and assume that 3 operators are needed per reactor for the continuous-flow operating mode (i.e. $\sigma_{m_C}^{\text{reac}} = 3$, $\sigma_{m_B}^{\text{reac}} = 6$). In addition, I assume that two additional operators are needed per storage tank (a minimum, since one is needed on the plant while the other is in the control room) for the semi-batch operating mode (i.e. $\sigma^{\text{st}} = 2$). The number of operators per shift position is $\sigma^{\text{op}} = 4.8$. Therefore, the total number of operators needed per plant is given by eq 3.153.

$$\mathbf{O_{C,F,L}} = \zeta^{\text{op}} \cdot \mathbf{\Lambda_O} \tag{3.152}$$

$$\mathbf{\Lambda_O} = \sigma^{\text{op}} \sum_r \left[\left(\sum_m \sigma_m^{\text{reac}} \cdot \mathbf{y}^r_{\mathbf{UM}_m} \right) + \sigma^{\text{st}} \left(\mathbf{y}^r_{\mathbf{IN,B}} + \mathbf{y}^r_{\mathbf{OUT,B}} \right) \right] \tag{3.153}$$

3.7 Case Study: van de Vusse Reaction

In order to illustrate the utility of the framework, I implement the framework on the problem of finding the optimal reactor network for production of product B using the isothermal van de Vusse chemical system:

1. $A \xrightarrow{\kappa_1} B$
2. $B \xrightarrow{\kappa_2} C$
3. $2A \xrightarrow{\kappa_3} D$

The objective is maximizing the yield of B using up to two chemical reactors in series ($N_R = 2$). This chemical system has been used to test reactor network synthesis approaches proposed by numerous groups, who find the optimum continuous-flow reactor network for several different sets of values for the reaction rate constants κ_j. In this work, I first present results for the optimum yield using two of these sets of values considering only the continuous-flow options to make comparisons with the literature. Next, I present results for the optimum yield allowing the batch reactor options to demonstrate the utility of the framework in simultaneously representing the two operating modes. Finally, I present results of the optimization of the total annual profits.

Before presenting the results, I should point out several modifications that have been made to the problem for use in this work. First, I note that the reaction rate constants presented in the literature have units of s^{-1}, s^{-1}, and L/(mol s) for κ_1, κ_2, and κ_3, respectively. These units result in CFR

volumes in the order of 20 L, and residence times below 1 s. These dimensions are appropriate only for laboratory-scale CFRs and the fast reaction speeds eliminate the batch operating mode altogether. Since the strength of the framework presented herein lies in its utility for considering industrial-scale operations in the two operating modes simultaneously, an effort is made to arrive at industrial-scale dimensions for the two operating modes. To this end, I modify the units of the reaction rate constants to hr^{-1}, hr^{-1}, and $\text{m}^3/(\text{kmol hr})$ for κ_1, κ_2, and κ_3, respectively, while using the same numerical values as the cases reported in the literature. In addition, I implement industrially realistic bounds on the reactor volumes and residence times. For PFRs, bounds on the reactor volume are obtained by assuming the reactors take on the form of a U-tube heat exchanger with a diameter of 1 inch [128] and heat exchanger areas that lie between 10 and 1000 m^2 [160]. For CSTRs, BRs, and SBRs, bounds on reactor volume are taken from Coker *et al.* [1]. Finally, bounds on the residence times of the different reactor types were taken from the practical guidelines given by Fogler [65]. The bounds used for the different reactor types are summarized in Table 3.3. In addition, the volume bounds on the storage tanks used in this work are shown in the table.

The second modification that is made to the problem for this work is the target flowrate. In the problem presented in previous papers, the authors specify the feed flowrate ($F^{r_1}_{u_f,u_{s_1}} = 100\,L/s$), while the desirable product flowrate ($\mathbf{F}^{r_{N_R}}_{u_{m_3},u_e} \cdot \mathbf{C}^{r_{N_R}}_{i_B,u_{m_3},u_e}$ [mol/s]) is a variable determined by the overall yield. This formulation does not conform to the typical industrial case where a

Table 3.3: Volume and residence time bounds for the different reactor types implemented in this work, as well as the volume bounds on the storage tanks.

reactor type t	volume bounds [m^3]		residence time bounds [hrs]	
	$\underline{V_t}$	$\overline{V_t}$	$\underline{W_t}$	$\overline{W_t}$
PFR	0.0635	6.35	1×10^{-4}	1.0
CSTR	0.5	76	0.1	4
BR	0.5	76	0.25	20
SBR	0.5	76	0.25	20
storage tank	10	200	-	-

product demand δ is specified, and the plant is designed to meet that demand. This product demand parameter is one that plays a key role in the decision of optimal operating mode, a decision that was made *a priori* in previous works on reactor network synthesis. Therefore, in this work, I adopt the more industrially representative scenario of specifying an annual demand of product and allowing the solution process to calculate the appropriate feed flowrate to meet the demand. This allows me to conduct a sensitivity analysis on this parameter (in section 3.7.3).

Despite the aforementioned modifications, one can expect that the optimization of product yield for the CFR case (section 3.7.1) should yield directly comparable total yields of product. Nevertheless, the total reactor volumes that are found in this work cannot be directly compared to previous works due to the differences in the bounds, and therefore comparisons of the reactor volumes are not included in the discussion.

3.7.1 Optimal Yield: Continuous-Flow Reactor Network

In order to make comparisons with values reported in the literature, the yield of product B is maximized for two cases of reaction rate parameter values after fixing the operating mode to continuous-flow ($\mathbf{y}_{\mathbf{M}_{m_C}} = 1$). The sets of values of the parameters of the two cases studied in this work as well as results for these particular cases from the literature are reported in Table 3.4. Note that the difference between the two cases studied is in the value of the third reaction rate coefficient, κ_3. In addition, the optimal concentration evolution in the reaction coordinate for the two cases is shown in Figure 3.7.

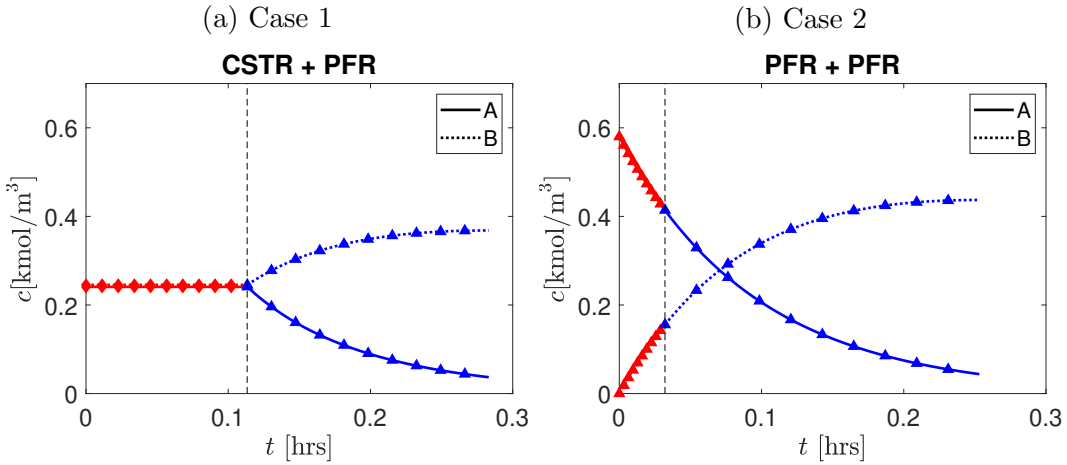

Figure 3.7: Optimal concentration profiles after fixing operating mode to continuous-flow ($\mathbf{y}_{\mathbf{M}_{m_C}} = 1$) for the van de Vusse chemical system with parameters of (a) case 1 and (b) case 2. Different reactors are shown by different line colors and separated by a vertical dashed line, diamond-shaped markers and triangles indicate CSTRs and PFRs, respectively, and the solid and dotted line styles indicate reactant A and product B concentrations, respectively.

The optimal yield for the two cases is the same as the highest reported

Table 3.4: Reaction rate coefficients for the two Cases studied in this work, optimal yields reported by previous authors, and optimal yields obtained in this work when operating mode is fixed ($\mathbf{y}_{\mathbf{M}_m} = 1$ to specify operating mode to mode m).

	case 1	**case 2**
κ_1 [s^{-1} or hr^{-1}]	10	10
κ_2 [s^{-1} or hr^{-1}]	1	1
κ_3 [L/(mol s) or m^3/(kmol hr)]	5	0.5
$C_{i_A}^{\text{feed}}$ [mol/L or kmol/m^3]	0.58	0.58
Previous Author Results		
Chitra and Govind [42]	-	Yield = 0.752, PFR
Achenie and Biegler [4]	-	Yield = 0.753, PFR
Kokossis and Floudas [100]	-	Yield = 0.752, PFR
Schweiger and Floudas [145]	-	Yield = 0.754, PFR
Esposito and Floudas [59]	Yield = 0.635, CSTR + PFR	Yield = 0.754, PFR
Ashley and Linke [13]	-	Yield = 0.746, PFR + PFR + PFR + PFR
Xie and Freund [172]	Yield = 0.635, CSTR + PFR	Yield = 0.754, PFR
This Work		
continuous-flow operating mode	Yield = 0.635, CSTR + PFR	Yield = 0.754, PFR + PFR
batch operating mode	Yield = 0.635, SBR	Yield = 0.754, BR

by other authors in the literature. This validates the discretization approach and the models used for the two reactor types as employed in this work. The necessity of a second PFR in the optimal network of case 2 is attributed to the higher product demand and the difference in the scale of operation of the problem implemented in this work compared to the literature. At the upper bound of 6.35 m^3 for the PFR (see Table 3.3 on page 133), the maximum yield that can be attained in a single PFR for the kinetics of case 2 was found to be 0.751 (calculated by running a separate optimization with fixed binaries $\mathbf{y}_{\mathbf{M}_{m_C}} = 1$, $\mathbf{y}^{r_1}_{\mathbf{T}_{t_{\text{PFR}}}} = 1$, and $\mathbf{y}^{r_2}_{\mathbf{T}_t} = 0 \, \forall t \in T$). Therefore, the solution consists of using two PFRs in series to increase the yield to the reported value of 0.754. Note that, since this problem maximizes yield without minimizing reactor cost, any point along the PFR trajectory shown in Figure 3.7b could have been used as the boundary between the two reactors as long as the two reactors have volumes that lie within their allowable bounds. This may not be the case when monetary profits are optimized, where the increase in yield from one extra reactor must bring about substantial increases in profit, and where the boundary between reactors, if two reactors are used, will be selected to maximize the individual reactor sizes in order to exploit economies of scale.

3.7.2 Optimal Yield: Batch Reactor Network

In this section, I present the results of optimizing yield for the two cases with the batch operating mode enforced by setting $\mathbf{y}_{\mathbf{M}_{m_B}} = 1$. The optimal yield and reactor for each case is reported in Table 3.4, and the optimal

concentration evolution in time is shown in Figure 3.8.

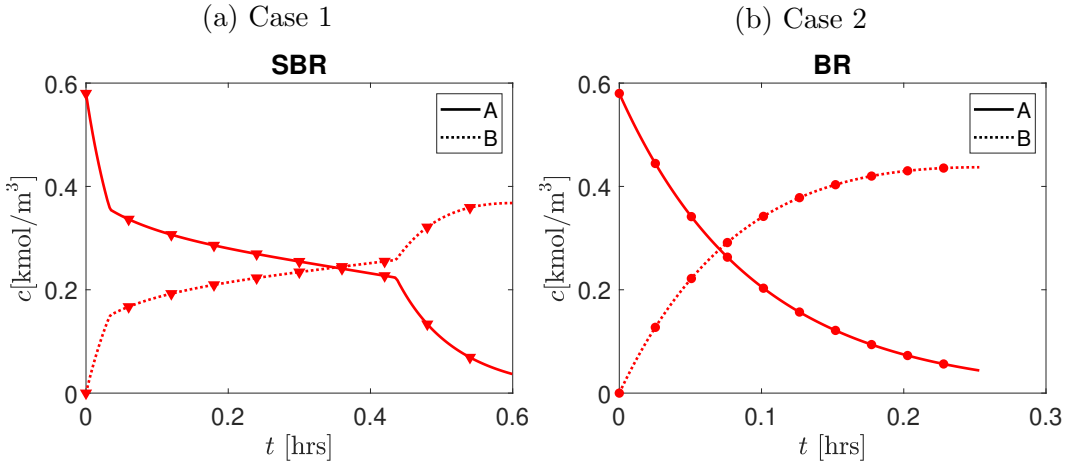

Figure 3.8: Optimal concentration profiles after fixing operating mode to batch ($\mathbf{y}_{\mathbf{M}_{m_B}} = 1$) for the van de Vusse chemical system with parameters of (a) case 1 and (b) case 2. Inverted triangles and circles indicate SBRs and BRs, respectively, and the solid and dotted line styles indicate reactant A and product B concentrations, respectively.

The optimal yield achieved for the two cases is the same as that obtained in the continuous-flow counterpart. However, for the batch operating mode, the optimal yield is achieved in a single reactor for the two cases, with a longer batch time.

Case 1 optimal yield is achieved by making use of a SBR to achieve a similar concentration profile to that achieved in the CSTR + PFR in the continuous-flow case. The manner by which the concentration profile is achieved is different between the two operating modes and can be seen by inspecting the plots of dimensionless volume in the reactor ($\hat{\mathbf{v}}$), "IN" stream ($\hat{\mathbf{v}}_{\text{IN}}$), and "OUT" stream ($\hat{\mathbf{v}}_{\text{OUT}}$) for case 1, shown in Figure 3.9. In the continuous-flow

case, the volumetric flowrate inside the CSTR is kept constant by adding and removing material at the same rate at each point along the reactor axis. In the semi-batch reactor, the feed is mostly sent to the "IN" stream, allowing a small amount of material to enter the reactor at the beginning. This causes a sharp change in concentration at the beginning of the batch. Then, the feed is gradually and increasingly added to the reactor from the "IN" storage tank, maintaining a relatively smooth concentration gradient until the "IN" tank is emptied at 0.42 hrs. Finally, the content of the reactor is allowed to react unhindered for an extra 0.18 hrs, replicating the PFR portion of the continuous-flow operation.

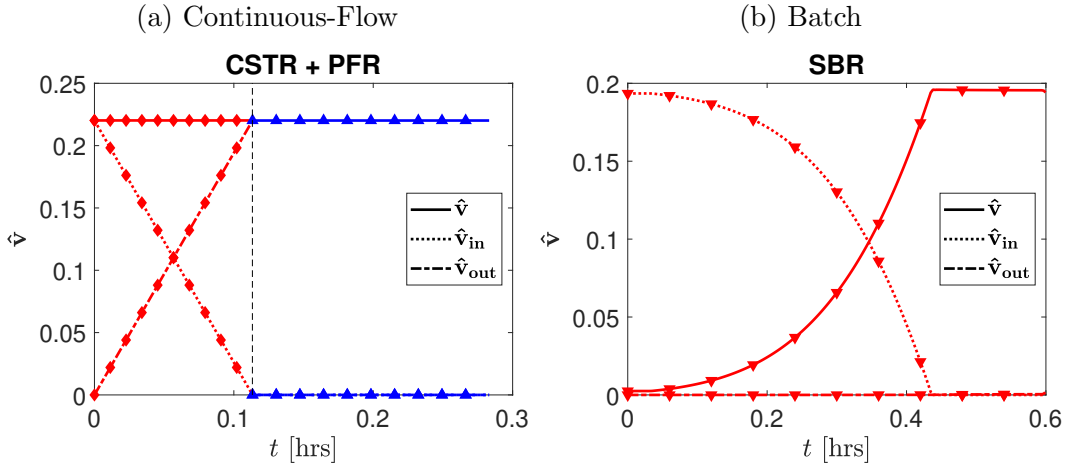

Figure 3.9: Optimal dimensionless (a) volumetric flowrate (continuous-flow) or (b) volume (batch) profiles for the van de Vusse chemical system with parameters of case 1. The line colors and marker shapes have the same meaning as Figures 3.7 and 3.8, and solid, dotted, and dashed lines indicate the values in the reactor, "IN" stream, and "OUT" stream, respectively.

Case 2 for the batch operating mode achieves the same concentration

profile as the continuous-flow case by making use of a simple batch reactor since both reactor types require no addition or removal of material at any point along the reactor length and the total residence and batch times for the two cases coincide with the lower bound on batch time for the batch reactor of 0.25 hrs.

3.7.3 Optimal Annual Profit

In this section, I present the results of maximizing $\mathbf{\Pi}$, the total annual profit [\$/yr] for case 1 of the van de Vusse chemical system. First, I give results using the nominal parameter values shown in Table 3.5. Note that the cost parameters used for all reactor types have been assumed to be equal for this work, but that the framework is flexible to accommodate different cost functions for the different reactor types. The optimal operating mode is selected by the integer variable $\mathbf{y}_{\mathbf{M}_m}$. In addition, runs are performed after fixing the operating mode $\mathbf{y}_{\mathbf{M}_m}$ to batch or continuous in order to observe the effect of operating mode choice on the economics.

3.7.3.1 Results with Nominal Parameter Values

Table 3.6 shows the optimal reactor networks after fixing the operating modes to continuous or batch with the nominal parameter values shown in Table 3.5. These results indicate that, for this case, the batch operating mode is superior to the continuous-flow operating mode, as evidenced by its higher annual profit. Allowing the optimizer to select the operating mode (i.e., freeing

Table 3.5: Parameters Used for the Calculation of the Economics as well as the Equation Numbers Where Each Parameter Appears

Parameter	**Equation Numbers**	**Value**
$\omega \left[\frac{\text{hrs}}{\text{yr}\cdot(\text{Plant})}\right]$	(3.124), (3.127), (3.131), (3.144), (3.145)	8400
$\zeta_A^{\text{raw}} \left[\frac{\$}{\text{kmol}}\right]$	(3.144)	100
$\zeta_B^{\text{sale}} \left[\frac{\$}{\text{kmol}}\right]$	(3.131)	500
$\zeta_i^{\text{treat}} \left[\frac{\$}{\text{kmol}}\right]$, $i \in \{A, C, D\}$	(3.145)	10
$\delta_B \left[\frac{\text{kmol}}{\text{yr}}\right]$	(3.126), (3.127)	100000
$\theta \left[\text{yr}^{-1}\right]$	(3.133)	0.15
$\pi_{a_t}^{\text{reac}} \left[\frac{\$}{\text{plant}}\right]$, $\forall t \in T$	(3.139)	61500
$\pi_{b_t}^{\text{reac}} \left[\frac{\$}{\text{m}^{3\pi_{c_t}^{\text{reac}}}\cdot(\text{plant})}\right]$, $\forall t \in T$	(3.139)	32500
$\pi_{c_t}^{\text{reac}}$, $\forall t \in T$	(3.139)	0.8
$\pi_a^{\text{st}} \left[\frac{\$}{\text{plant}}\right]$	(3.141)	5800
$\pi_b^{\text{st}} \left[\frac{\$}{\text{m}^{3\pi_c^{\text{st}}}\cdot(\text{plant})}\right]$	(3.141)	1600
π_c^{st}	(3.141)	0.7
μ_B	(3.122)	0.1
$\zeta^{\text{op}} \left[\frac{\$}{(\text{yr})(\text{operator})}\right]$	(3.152)	30000

variable $\mathbf{y}_{\mathbf{M}_m}$) results in selecting the batch operating mode as the optimal operating mode, as expected. The concentration and volume profiles for the optimum economics of the two cases are shown in Figure 3.10. Now, I make several comments about these results.

First, the reader may have noticed that while the optimal reactor types and network configuration after optimizing annual profits is the same as that which was obtained when optimizing for product yield (sections 3.7.1 and

Table 3.6: Optimal Profit, Revenues, Costs, Yield, and Reactor Network Configuration for the Nominal Parameters and after Fixing the Operating Modes.

	continuous	**batch**
annual profit, $\mathbf{\Pi}$ [\$/yr]	3.23×10^7	3.47×10^7
annual revenues, $\mathbf{\Theta}$ [\$/yr]	5.00×10^7	7.50×10^7
total annual costs, $\mathbf{\Xi}$ [\$/yr]	1.77×10^7	4.03×10^7
annual investment costs, $\mathbf{I_C}$ [\$/yr]	3.03×10^5	2.95×10^6
annual operating costs, $\mathbf{O_C}$ [\$/yr]	1.74×10^6	3.74×10^7
number of parallel plants, $\mathbf{\Lambda}_P$	1	3
$\mathbf{\Lambda}_B$	8400 hrs/[(yr)(plant)]	717 Batches/[(yr)(plant)]
total reaction time, $\mathbf{\Omega}$ [hrs]	0.277	0.993
$\mathbf{\Psi}$	1	7.810 hrs/batch
yield	0.618	0.537
reactor network configuration	CSTR + PFR	SBR

3.7.2), the optimal yields for both operating modes have dropped from 0.635 to 0.618 in the continuous-flow case, and from 0.634 to 0.537 in the batch case. In the continuous-flow case, the reason for the drop can be seen by observing in Figures 3.7a and 3.10a that, toward the outlet of the PFR, there is a "flattening" region, where additional residence time results in minimal increases in the overall yield. Therefore, the solution recognizes that profits gained by increasing total product yield are not justified by the additional

(a) Continuous-Flow Concentration Profile

(b) Batch Concentration Profile

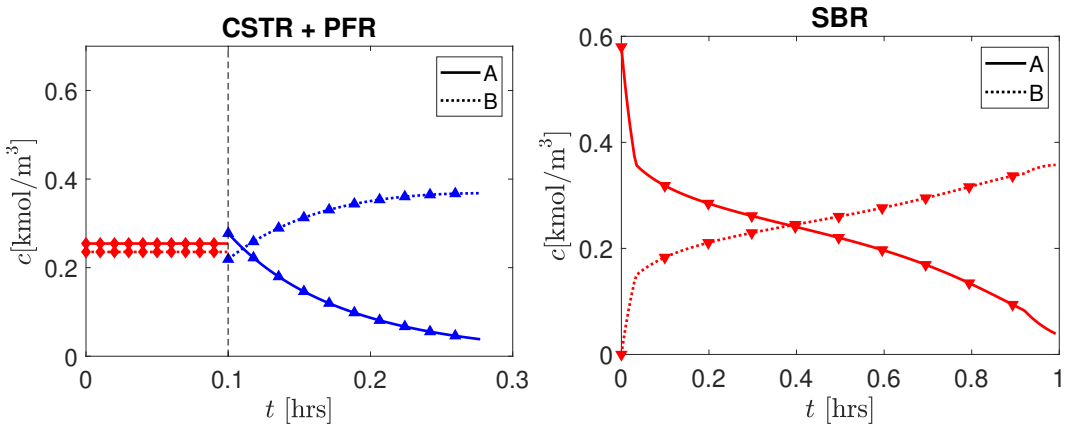

(c) Continuous-Flow Volume Profiles

(d) Batch Volume Profiles

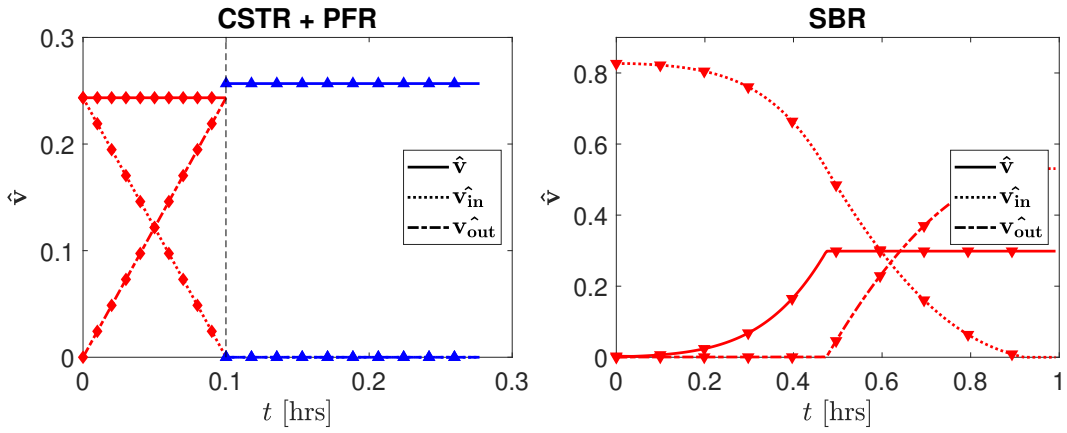

Figure 3.10: Concentration profiles after maximizing annual profits and fixing operating modes to (a) continuous-flow, or (b) batch, and volume profiles after maximizing annual profits and fixing operating modes to (c) continuous-flow, or (d) batch, for the van de Vusse chemical system with parameters of case 1. The line colors and marker shapes have the same meanings as Figures 3.7 - 3.8.

costs incurred by the purchase of a larger reactor.

In the case of the batch operating mode, there is a larger decrease in overall yield for a single batch. The reason for this can be seen by observing the total (dimensionless) volume plots for the SBR. Specifically, by comparing Figure 3.10d with Figure 3.9b, it is immediately apparent that the inclusion of the demand constraint largely influences the solution. The larger demand necessitates a larger feed flow of reactants. The solution reported is one where the large feed to an individual plant is almost entirely sent to the "IN" storage tank. After reacting a portion of the reactants following the same profile that was reported for optimizing the yield, the reactor content is discharged (at a lower concentration) to the "OUT" stream in order to make room for the remainder of the feed to enter the reactor. Eventually, the concentration of the reactor effluent stream (u_r, u_{s_2}) is the same as that which was obtained for the optimization of the yield. However, after mixing the effluent with the material that was discharged to the "OUT" storage tank at a lower concentration, the overall yield drops to 0.537, as reported in the final result in Table 3.6. While including a second SBR downstream may have given a higher yield, the solution indicates that the increase in yield does not justify the additional costs incurred and indicates using three parallel plants to satisfy the total demand. These results especially highlight the need for explicitly accounting for economics when performing plant design and the potential risks of using product yield as a proxy for better economics.

Second, the reader should note that, while the demand of desirable

product is the same for the two operating modes, the economics of the batch process are scaled to assume each batch plant is used for the full duration of the year (ω = 8400 hrs/yr). This is done to grant the batch operating mode the advantage of potentially using the plant for manufacturing multiple products and is discussed earlier and in detail in section 3.6.1. It is therefore expected that the rate of change of profits as parameter values vary will be different between the two operating modes, and the two operating modes will converge as the use of a single batch plant for a single product approaches a full year. This difference in the way profits vary with changing economic parameter values plays a major role in deciding the optimal operating mode and is therefore explicitly explored in the sensitivity analyses presented in the following section.

3.7.3.2 Sensitivity Analyses

Of the parameters used in this work, two of the commonly used parameters to make decisions about the optimal operating mode are the product sale price, $\zeta_i^{\text{sale}} \left[\frac{\$}{\text{kmol}}\right]$, and the annual product demand, $\delta_i \left[\frac{\text{kmol}}{\text{yr}}\right]$. A common practice is to assign the batch operating mode to processes that manufacture high-value products (i.e., high values of ζ_i^{sale}) with low demands. In this work, since the differences between the operating modes are explicitly accounted for within the unified framework, I am able to readily test these conventions numerically. In this section, I present the sensitivity analyses performed using the framework for varying the two variables for the van de Vusse case study.

I varied the product sale price across the range [300, 800] \$/kmol and the annual product demand across the range [1000, 250000] kmol/yr. Figure 3.11 shows the plots of the optimal annual profit for the two operating modes as the product sale price is varied, in addition to the results when the operating mode is a free variable selected by optimization. Figure 3.12 shows the plots of the optimal annual profit for the two operating modes as the annual product demand is varied, in addition to the results when the operating mode is a free variable selected by optimization. It was verified that, in all cases, the free selection of the operating mode $\mathbf{y}_{\mathbf{M}_m}$ results in selecting the same point as the operating mode with higher profit among the two options.

Figure 3.11 shows that the relationship between optimal profit and the product sale price for both operating modes is linear. For a low annual product demand ($\delta_B = 1000$ kmol/yr), the continuous-flow process fails to generate a profit for any of the sale prices within the range tested. When the product demand exceeds 50,000 kmol/yr and the continuous-flow operating mode begins to generate profit, a clear trend emerges that holds for all the values of δ_B tested. At low sale prices, the continuous-flow operating mode always outperforms the batch operating mode. As the sale price increases, the higher slope of the line for the batch operating mode means that there is a cross-over point at which the batch operating mode becomes more lucrative than the continuous-flow operating mode.

Similarly, Figure 3.12 shows that, as expected, the total annual profit increases as the annual demand increases. At low values of the product de-

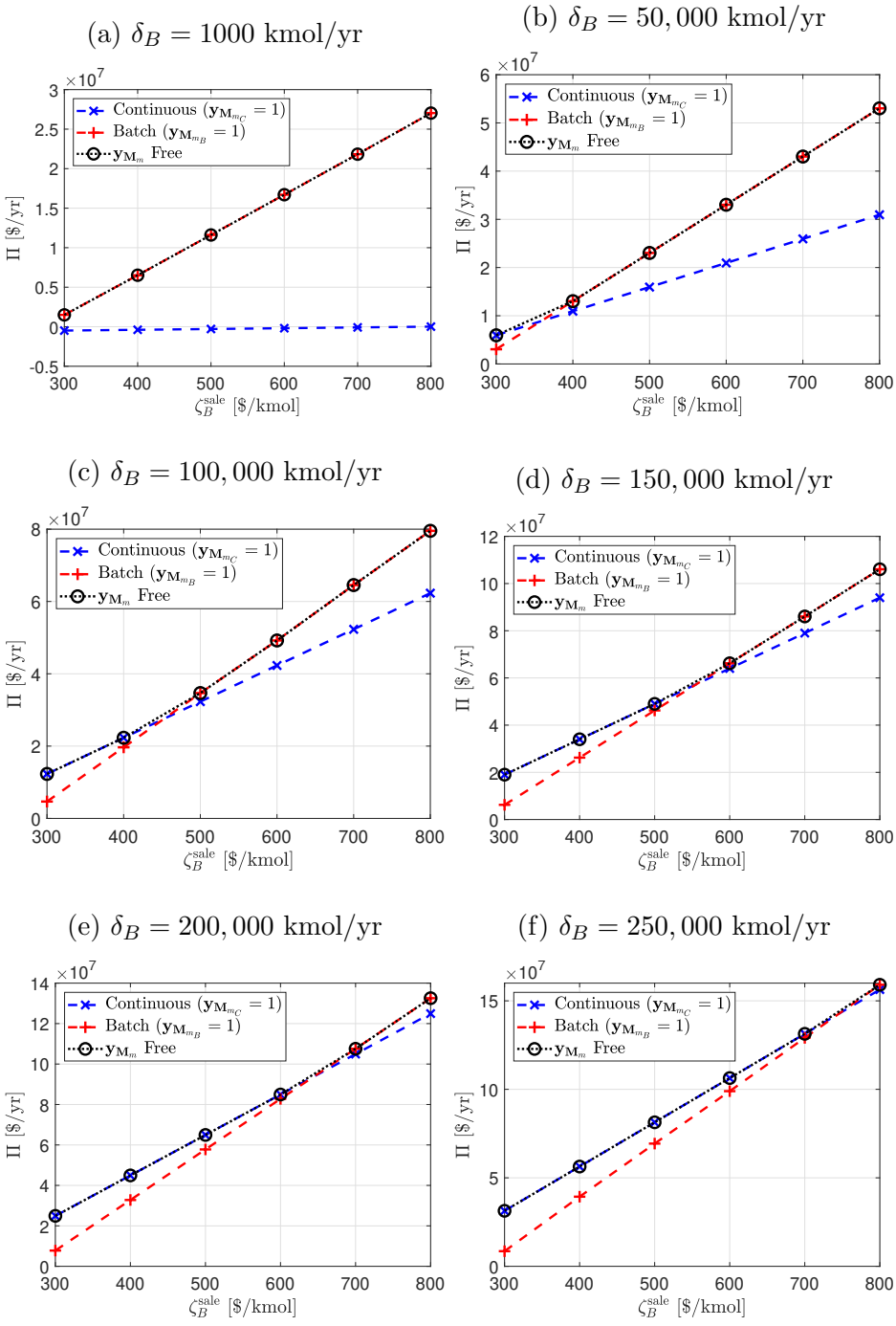

Figure 3.11: Sensitivity of profit $\mathbf{\Pi}$ to product sale price ζ_B^{sale} with product demands δ_B ranging from (a) 1000 kmol/yr to (f) 250,000 kmol/yr.

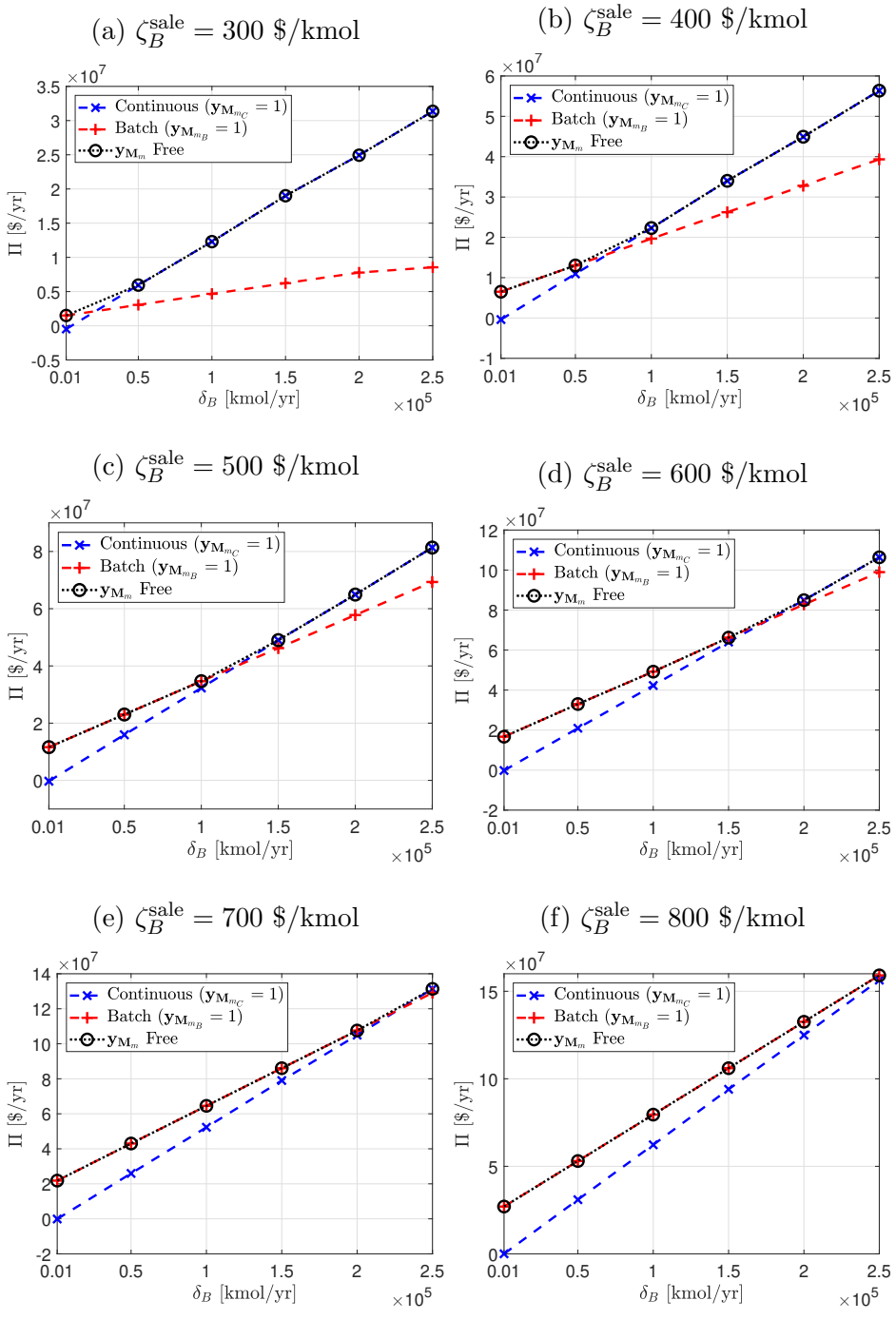

Figure 3.12: Sensitivity of $\mathbf{\Pi}$ to product demand δ_B with product sale prices ranging from (a) \$300/kmol to (f) \$800/kmol.

mand, the batch operating mode outperforms the continuous-flow counterpart. As the product demand increases, the continuous-flow line approaches the batch line, until at some intermediate value, the lines cross over, giving the continuous-flow operating mode the advantage at high values of the annual product demand. This trend holds for all the values of the product sale price tested.

The trends are in direct agreement with the conventional heuristics mentioned earlier for the determination of the appropriate operating mode. The main cause for this agreement is the explicit accounting in our framework of the use of the batch plant for the entirety of the year. The fact that the economics for the batch plant are scaled to assume the rate of profit generation per batch holds constant for the whole year dampens the slope of the optimal profit vs δ_B line, allowing the continuous-flow operating mode to "catch up" at higher product demands. This is more apparent in Figure 3.13, where I have carried out a sensitivity analysis over narrower steps in the product demand for a fixed sale price of \$400/kmol. The figure shows that the total profit for small changes in the overall demand initially results in no improvement in the overall economics for the batch operating mode according to the model employed in this work. It is only when the demand increases enough to warrant the addition of plants in parallel that we see a discrete jump in overall profit.

Of major significance to the stakeholders is the knowledge of the point at which one operating mode becomes more lucrative than the other. The framework developed herein provides a convenient methodology by which this

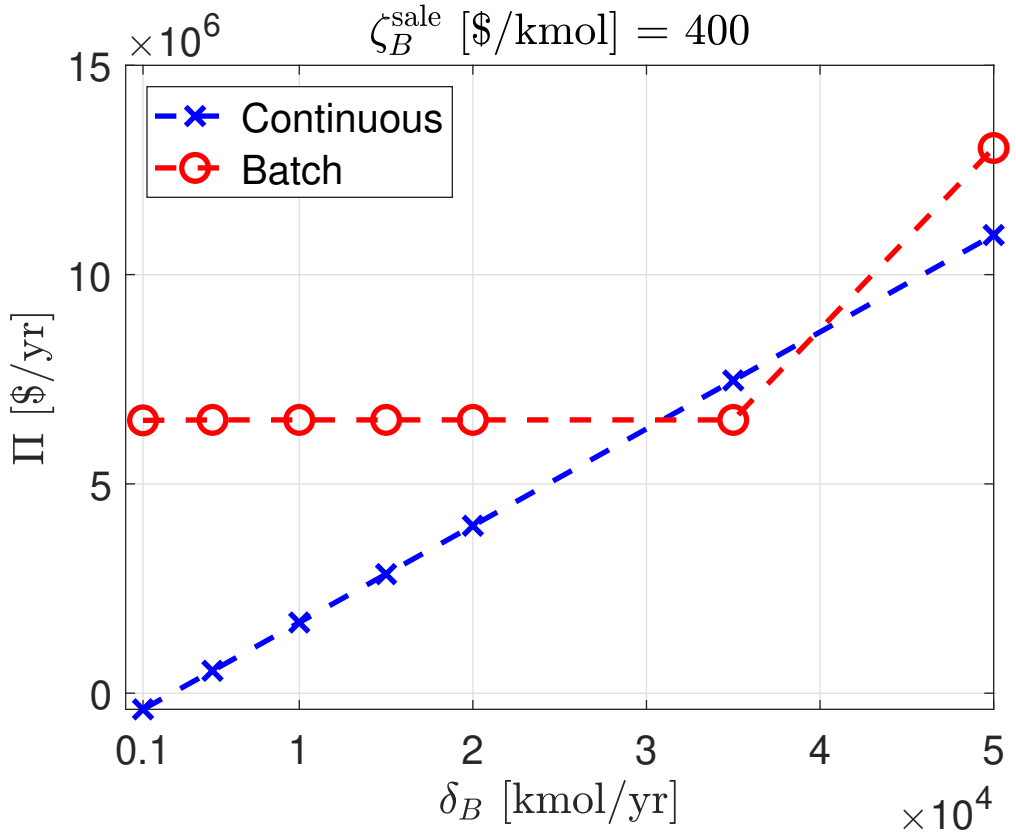

Figure 3.13: Sensitivity of $\mathbf{\Pi}$ to product demand δ_B with finer steps in demand and product sale price of \$400/kmol.

point can be obtained. Namely, by conducting the sensitivity analyses described above, I am able to locate the cross-over points across the entirety of the sets of values used for the two parameters examined. Figure 3.14 shows a map of the points at which cross-overs of the optimal performance being delivered from one operating mode to the other. The line traced by the points separates the economic space into two subspaces, with the lower part of the figure (low product demand, high product sale price) being a region where the

batch operating mode delivers the optimal profits and the upper part of the figure (high product demand, low product prices) being a region where the continuous-flow operating mode delivers the optimal profits.

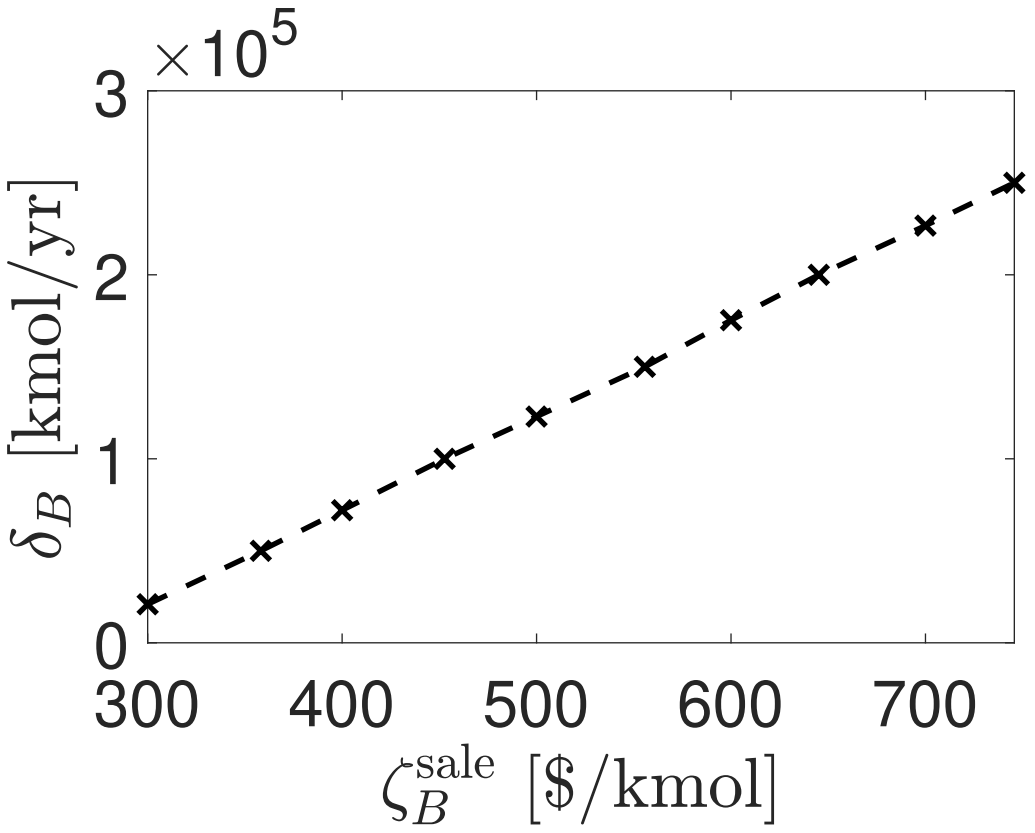

Figure 3.14: Cross-over points between batch and continuous-flow as ζ_B^{sale} and δ_B are varied.

3.8 Summary and Future Directions

In this chapter, I presented a general framework that unifies the problems of operating mode decision-making and reactor network synthesis into a

single optimization problem. The methodology employs an economic model that accounts for the differences between the natures of the operating modes. Specifically, the effects on the overall economics of (1) the fact that the batch plant may be used for the manufacture of multiple products, (2) the additional time needed for batch operations, (3) the fact that batch failures result in the loss of entire, off-spec batches, and (4) the differences in the labor requirements between the two operating modes were accounted for. To achieve this, I presented a general reactor module that adopts the DSR configuration and derived dimensionless material balances of the two operating modes, highlighting the strategy by which the models for the two operating modes converge into a single, dimensionless model. Then, I presented the novel OCFERE discretization approach by which individual reactor modules are connected to allow reactor networks. After this, I presented a series of logical constraints that allow the automatic identification of the optimal operating mode and reactor network configuration. Finally, I provided the economic model that relies on the logical constraints to assign appropriate values to the economic parameters.

The methodology was employed for the van de Vusse case study. After demonstrating the validity of the models employed by replicating literature results for the same case study, I showed that the framework provided herein is able to replicate the known heuristic rules for determining the optimal operating mode, namely, that batch operation is better suited for the manufacture of high-value products at low demands, and continuous-flow operation is more

suited for low-value products at high demand. The unification of the description of the two operating modes meant that the switch between operating modes can be simply achieved by setting the value of a single binary variable in the problem, giving us immense versatility in studying the different operating modes. This was illustrated by presenting sensitivity analyses on two economic parameters for the two operating modes and demonstrating the point at which the optimal operating mode switches from one mode to the other.

Finally, I conclude the first part of the dissertation by describing areas of future work. First, making the assumptions of ideal reactors allowed the simplification of the mass and energy balances such that the two operating modes had governing equations that followed the same mathematical form, allowing for direct comparisons. This does not completely eliminate the use of the framework for other reactor types. For example, in chapter 2 I showed how this framework can be utilized for considering microreactors by the simple introduction of additional constraints that tighten the feasible region to ensure realistic designs.

Nevertheless, the inclusion of other reactors with complex flow attributes that deviate from ideality is an interesting area of research. Analyses that account for flow dispersion, mass and heat transfer limitations for example, would significantly expand the utility of the framework. The detailed derivations provided in this work makes the inclusion of more advanced reactor types a simple procedure of following the steps presented in this work and

including the specific models needed for the additional reactor types. It is my belief that this framework can therefore be employed for the consideration of more complex reactor types and we aim to provide such work in the future.

Second, in its current form, the framework is applicable only for homogeneous liquid reactive systems. Further investigation into how this can be extended to solid or gas phase reactive systems, as well as the phase changes that may occur will open many avenues for further exploiting this idea for a wider range of chemical systems.

Third, pooling operations between reactors has not been considered in this framework. For example, in the continuous flow case, there is currently no mechanism by which material can be recycled from a downstream reactor to an upstream reactor. In the batch case, storage tanks are available to satisfy a single reactor only, and the use of a single storage tank to meet the storage needs of multiple reactors is currently not considered. An even more general framework must account for the capability of pooling operations between reactors, and the mechanism to incorporate this consideration can be explored in a future work.

Last, this work focused on the reactor portion of the chemical plant. The utility of extending the approach presented herein to other operations (e.g. formulation, separation/purification steps) could not be understated. The accurate description of each step in a unified manner for both operating modes will not only allow the exploration of the plantwide optimal operating mode, but will also open the door for a systematic methodology for designing

integrated batch and continuous processes which have thus far been developed on a case-by-case basis.

3.9 Nomenclature

Sets

$I = \{i : i_1, \ldots, i_{N_I}\}$ Set of chemical species.

$I_R(i)$ Subset of chemical species that are reactants.

$J = \{j : j_1, \ldots, j_{N_J}\}$ Set of chemical reactions.

$M = \{m : m_B, m_C\}$ Set of Operating modes where m_B and m_C are the batch and continuous-flow operating modes, respectively.

$M_T \ (m,t) = \{(m_C, t_{PFR}), (m_C, t_{CSTR}), (m_B, t_{BR}), (m_B, t_{SBR})\}$ Mapping of reactor types t to operating modes m.

$P = \{p : p_0, \ldots, p_{N_P}\}$ Set of collocation points.

$I_{P_D}(i)$ Subset of chemical species that are desirable products.

$I_{P_U}(i)$ Subset of chemical species that are undesirable products.

$Q = \left\{q : q_1, \ldots, q_{N_Q}\right\}$ Set of finite elements.

$R = \{r : r_1, \ldots, r_{N_R}\}$ Set of reactor elements.

$T = \{t : t_{PFR}, t_{CSTR}, t_{BR}, t_{SBR}\}$ Set of Reactor types.

$U = \{u : u_f, u_{s_1}, u_{s_2}, u_{s_3}, u_{m_1}, u_{m_2}, u_{m_3}, u_r, u_e\}$ Set of process units.

U_e $(u, u') = \{(u_f, u_{s_1}), (u_{s_1}, u_{m_3}), (u_{m_3}, u_e)\}$ Subset of unit-unit connection map that contains external flows that do not flow through reactor.

U_i $(u, u') = U_u \setminus U_e$ Subset of unit-unit connections map that contains internal flows that, if present, must ultimately lead to a flow inside the reactor.

$U_m(u) = \{u_{m_1}, u_{m_2}, u_{m_3}\}$ Subset of units that are stream mixers.

$U_r(u) = \{u_r\}$ Subset of units that is the reactor.

U_{rec} $(u, u') = \{(u_{s_2}, u_{m_1}), (u_{s_2}, u_{m_2}), (u_{s_3}, u_{m_1}), (u_{s_3}, u_{m_2})\}$ Subset of unit-unit connections map that contains recycle streams.

$U_s(u) = \{u_{s_1}, u_{s_2}, u_{s_3}\}$ Subset of units that are stream splitters.

U_u $(u, u') = \{(u_f, u_{s_1}),\ (u \in U_s, u' \in U_m), (u_{m_1}, u_r), (u_{m_2}, u_r), (u_r, u_{s_2}), (u_r, u_{s_3}),\ (u_{m_3}, u_e)\}$ Mapping of unit-unit connections.

Parameters

$\eta_{i,j}$ Stoichiometric coefficient for species i in reaction j.

κ_j Reaction rate coefficient of reaction j.

$\underline{V_t}$ **and** $\overline{V_t}$ Lower and upper bounds on reactor volume for a reactor of type t [m^3].

$\underline{V_{\mathrm{st}}}$ **and** $\overline{V_{\mathrm{st}}}$ Lower and upper bounds on reactor volume for a reactor of type t [m^3].

ν^{ref} Reference volume [m^3].

$\underline{W_t}$ **and** $\overline{W_t}$ Lower and upper bounds on residence time volume for a reactor of type t [hrs].

$\underline{F}$ **and** $\overline{F}$ Lower and upper bounds on volumetric flowrate [m^3/hr].

ξ^{ref} Reference volumetric flowrate [m^3/hr].

C_i^{feed} **:** $i \in I_R$ Feed concentration of species i [kmol/m^3].

$\overline{C_i}$ Reference concentration for species i [kmol/m^3].

Υ Safety factor for reactor volume.

N_P Number of collocation points per finite element.

N_Q Number of finite elements per reactor element.

N_R Number of reactor elements.

α^p Time of collocation point p along normalized finite element.

β^q Time of finite element q along normalized reactor element.

ω Number of hours of plant operation per year [hrs/yr].

$\dot{\phi}^{p,p'}$ Value of $\dot{\phi}^p$ function at collocation point p'.

ϕ_1^p Value of ϕ^p function at normalized time 1, corresponding to the border between two adjacent finite elements.

δ_i **:** $i \in I_{P_D}$ Annual demand of desirable product i [kmol/yr].

ζ_i^{sale} **:** $i \in I_{P_D}$ Sale price of desirable product per kmol of species$i$ [\$/kmol].

ζ_i^{raw} **:** $i \in I_R$ Cost of purchase of raw material i [\$/kmol].

ζ_i^{treat} **:** $i \in (I_R \cup I_{P_U})$ Cost of product treatment per kmol of species i present in the product stream [\$/kmol].

ζ^{op} Operator annual salary.

σ_m^{reac} Number of shift positions per reactor for operating mode m.

σ^{store} Number of shift positions per storage tank (Integer).

σ^{op} Number of operators per shift position (Integer).

$\pi_{a_t}^{\text{reac}}$ Cost function parameter for reactor type t [\$/plant].

$\pi_{b_t}^{\text{reac}}$ Cost function parameter for reactor type t [\$/[(m$^{3\pi_{c_t}^{\text{reac}}}$) $\cdot$ (plant)]].

$\pi_{c_t}^{\text{reac}}$ Cost function parameter for reactor type t.

π_a^{st} Cost function parameter for storage tank [\$/plant].

π_b^{st} Cost function parameter for storage tank [\$/[(m$^{3\pi_{c_t}^{\text{reac}}}$) $\cdot$ (plant)]].

π_c^{store} Cost function parameter for storage tank.

μ_B Average fraction of batches that fail per year.

θ Annualizing factor for capital investment [1/yr].

Continuous Variables

$\mathbf{F_{u,u'}}$ Volumetric flowrate between units u and u' [m^3/hr].

$\mathbf{C_{i,u,u'}}$ Concentration of species i in stream connecting units u and u' [kmol/m^3].

$\mathbf{f}$ Volumetric flowrate inside reactor at residence time τ [m^3/hr].

$\mathbf{f_{IN}}$ Volumetric flowrate in "IN" stream at residence time τ [m^3/hr].

$\mathbf{f_{OUT}}$ Volumetric flowrate in "OUT" stream at residence time τ [m^3/hr].

$\mathbf{c}_i$ Concentration of species i inside reactor at batch time t or residence time τ [kmol/m^3].

$\mathbf{c_{OUT},}_i$ Concentration of species i in "OUT" stream at batch time t or residence time τ [kmol/m^3].

$\mathbf{C_{IN},}_i$ Concentration of species i in "IN" stream [kmol/m^3].

$\dot{\mathbf{f}}$ Derivative with respect to τ of volumetric flowrate inside reactor [m^3/hr^2].

$\mathbf{\dot{f}_{IN}}$ Derivative with respect to τ of volumetric flowrate in "IN" stream [m^3/hr^2].

$\mathbf{\dot{f}_{OUT}}$ Derivative with respect to τ of volumetric flowrate in "OUT" stream [m^3/hr^2].

$\mathbf{V_{u,u'}}$ Volume of material transported between units u and u' [m^3].

$\mathbf{v}$ Volume inside reactor at batch time t [m^3].

$\mathbf{v_{IN}}$ Volume in "IN" stream at batch time t [m^3].

$\mathbf{v}_{\mathrm{OUT}}$ Volume in "OUT" stream at batch time t [m^3].

$\dot{\mathbf{v}}$ Derivative with respect to t of volume inside reactor [m^3/hr].

$\dot{\mathbf{v}}_{\mathbf{IN}}$ Derivative with respect to t of volume in "IN" stream [m^3/hr].

$\dot{\mathbf{v}}_{\mathbf{OUT}}$ Derivative with respect to t of volume in "OUT" stream [m^3/hr].

$\hat{\mathbf{v}}_{\mathbf{C}}$ Dimensionless volume of the continuous-flow reactor.

$\mathbf{v}_{\mathbf{C}}$ Volume of the continuous-flow reactor [m^3].

$\mathbf{\Omega}$ Total batch/residence time of the network [hrs].

$\hat{\tau}$ Dimensionless time domain of ODE system.

γ^r The dimensionless time $\hat{\tau}$ at which reactor r begins within a network of reactors in series.

$\hat{\mathbf{F}}_{u,u'}$ Dimensionless volumetric flowrate (continuous-flow) or volume (batch) between units u and u'.

$\hat{\mathbf{C}}_{i,u,u'}$ Dimensionless concentration between units u and u'.

$\hat{\mathbf{v}}$ Dimensionless volumetric flowrate (continuous-flow) or volume (batch) inside reactor at dimensionless time $\hat{\tau}$.

$\hat{\mathbf{v}}_{\mathbf{IN}}$ Dimensionless volumetric flowrate (continuous-flow) or volume (batch) in "IN" stream at dimensionless time $\hat{\tau}$.

$\hat{\mathbf{v}}_{\mathbf{OUT}}$ Dimensionless volumetric flowrate (continuous-flow) or volume (batch) in "OUT" stream at dimensionless time $\hat{\tau}$.

$\hat{\mathbf{w}}_{\mathbf{IN}}$ Dimensionless derivative of volumetric flowrate (continuous-flow) or volume (batch) in "IN" stream with respect to dimensionless time $\hat{\tau}$ at $\hat{\tau}$.

$\hat{\mathbf{w}}_{\mathbf{OUT}}$ Dimensionless derivative of volumetric flowrate (continuous-flow) or volume (batch) in "OUT" stream with respect to dimensionless time $\hat{\tau}$ at $\hat{\tau}$.

$\hat{\mathbf{c}}_{\mathrm{i}}$ Dimensionless concentration inside reactor at dimensionless time $\hat{\tau}$.

$\hat{\mathbf{c}}_{\mathbf{OUT},i}$ Dimensionless concentration in "OUT" stream at dimensionless time $\hat{\tau}$.

$\mathbf{C}_{\mathbf{IN},i}$ Dimensionless concentration in "IN" stream.

$\hat{\mathbf{F}}^{r}_{\mathrm{CSTR}}$ Constant dimensionless derivative of flowrate in "IN" and "OUT" streams if reactor type r is a CSTR.

$\mathbf{s}^{p,q,r}_{\hat{\mathbf{v}}^{+}_{\mathbf{CSTR}}}$ Slack variables for satisfying CSTR equations in the case that reactor r is not a CSTR.

$\mathbf{s}^{p,q,r}_{\hat{\mathbf{v}}^{-}_{\mathbf{CSTR}}}$ Slack variables for satisfying CSTR equations in the case that reactor r is not a CSTR.

$\mathbf{S}^{r}_{\hat{\mathbf{V}}^{+}_{\mathbf{CSTR}}}$ Slack variables for satisfying CSTR equations in the case that reactor r is not a CSTR.

$\mathbf{S}^{r}_{\hat{\mathbf{V}}^{-}_{\mathbf{CSTR}}}$ Slack variables for satisfying CSTR equations in the case that reactor r is not a CSTR.

$\hat{\mathbf{V}}^{r}_{\mathbf{T},t}$ Dimensionless volume of reactor r, if r is of type t.

$\hat{\mathbf{V}}^{r}_{\mathbf{max},t}$ Maximum volume of fluid inside reactor r if batch operating mode is selected.

$\mathbf{s}^{p,q,r}_{\hat{\mathbf{V}}_{\mathbf{T_t}}}$ Slack variables for satisfying reactor volume constraints for type t if reactor r is not of type t.

$\mathbf{S}^{r}_{\hat{\mathbf{V}}_{\mathbf{T_t}}}$ Slack variables for satisfying reactor volume constraints for type t if reactor r is not of type t.

$\hat{\mathbf{V}}^{r}_{\mathbf{C}}$ The total dimensionless volume of a reactor if the continuous-flow operating mode is selected.

$\mathbf{W}^{r}_{\mathbf{reac}}$ Residence time of reactor r [hrs].

$\hat{\mathbf{V}}^{r}_{\mathbf{T,st,IN}}$ Dimensionless volume of "IN" storage tank of reactor element r.

$\hat{\mathbf{V}}^{r}_{\mathbf{T,st,OUT}}$ Dimensionless volume of "OUT" storage tank of reactor element r.

$\mathbf{S}^{r}_{\hat{\mathbf{V}}_{\mathbf{T,st,IN}}}$ Positive slack variables to satisfy storage unit volume constraints if storage units are not needed.

$\mathbf{S}^{r}_{\hat{\mathbf{V}}_{\mathbf{T,st,OUT}}}$ Positive slack variables to satisfy storage unit volume constraints if storage units are not needed.

$\mathbf{W}^{r}_{\mathbf{t}}$ Residence time of reactor r if reactor r is of type t [hrs].

$\mathbf{W}_{\mathbf{op}}^{r}$ Time for additional operations needed for batch [hrs].

$\mathbf{T}_{\mathbf{a}}^{r}$ Actual duration of a batch reactor element r after accounting for additional operations [hrs].

$\mathbf{\Psi}$ Operating-mode dependent variable, equal to actual batch network duration (if batch is chosen), or equal to 1 (if continuous is chosen) [hrs/batch (if batch), dimensionless (if continuous)].

F^{ref} Operating-mode dependent variable, equal to $\overline{V}$ if batch, or equal to $\overline{F}$ if continuous [m^3 (if batch), m^3/hr (if continuous)].

$\mathbf{\Gamma}_B$ Operating-mode dependent variable, equal to μ_B if batch, or equal to 0 if continuous.

$\mathbf{\Phi}$ Operating-mode dependent variable, equal to amount desirable product per batch (if batch), or equal to amount desirable product per hour (if continuous) [kmol/batch (if batch), or kmol/hr (if continuous)].

$\mathbf{\Delta}$ Amount of product made per year in a single plant [kmol/[(yr) $\cdot$ (plant)]].

$\mathbf{\Pi}$ Annual profit [$/yr].

$\mathbf{\Theta}$ Annual revenue [$/yr].

$\mathbf{\Xi}$ Annual cost [$/yr].

$\mathbf{I_C}$ Annual investment costs [$/yr].

$\mathbf{O_C}$ Annual operating costs [$/yr].

$\mathbf{I_{C,F}}$ Fixed capital investment per plant [\$/(yr $\cdot$ plant)].

$\mathbf{I_{C,W}}$ Working capital investment per plant [\$/(yr $\cdot$ plant)].

$\mathbf{I_{C,F,D}}$ Direct capital investment per plant [\$/plant].

$\mathbf{I_{C,F,I}}$ Indirect capital investment per plant [\$/plant].

$\mathbf{I_{C,P}}$ Purchased equipment cost per plant [\$/plant].

$\mathbf{I^r_{C,P,reac}}$ Purchased reactor cost per plant for reactor element r [\$/plant].

$\mathbf{I^r_{C,P,st}}$ Purchased storage unit cost per plant for reactor element r [\$/plant].

$\mathbf{I^r_{C,P,reac}}_t$ Purchased reactor cost per plant for reactor element r if reactor is of type t [\$/plant].

$\mathbf{O_{C,V}}$ Annual variable operating cost per plant [\$/(yr $\cdot$ plant)].

$\mathbf{O_{C,F}}$ Annual fixed operating cost per plant [\$/(yr $\cdot$ plant)].

$\mathbf{O_{C,V,R}}$ Annual raw material cost per plant [\$/(yr $\cdot$ plant)].

$\mathbf{O_{C,V,T}}$ Annual treatment cost per plant [\$/(yr $\cdot$ plant)].

$\mathbf{O_{C,F,S}}$ Annual supervision cost per plant [\$/(yr $\cdot$ plant)].

$\mathbf{O_{C,F,O}}$ Annual overhead cost per plant [\$/(yr $\cdot$ plant)].

$\mathbf{O_{C,F,M}}$ Annual maintenance cost per plant [\$/(yr $\cdot$ plant)].

$\mathbf{O_{C,F,T}}$ Annual taxes per plant [\$/(yr $\cdot$ plant)].

$\mathbf{O_{C,F,R}}$ Annual rent per plant [\$/(yr $\cdot$ plant)].

$\mathbf{O_{C,F,I}}$ Annual insurance costs per plant [\$/(yr $\cdot$ plant)].

$\mathbf{O_{C,F,L}}$ Annual labor costs per plant [\$/(yr $\cdot$ plant)].

Binary Variables

$\mathbf{y_{M}}_m$ Binary equal 1 when operating mode m is chosen.

$\mathbf{y^r_U}$ Binary equal 1 if reactor r is utilized.

$\mathbf{y^r_{UM}}_m$ Binary equal 1 if operating mode m is chosen, and reactor r is utilized.

$\mathbf{y^r_T}_t$ Binary equal 1 if reactor r is of type t.

$\mathbf{y^r_{IN}}$ Binary equal 1 if "IN" stream exists in reactor r.

$\mathbf{y^r_{OUT}}$ Binary equal 1 if "OUT" stream exists in reactor r.

$\mathbf{y^r_{IN,B}}$ Binary equal 1 if "IN" stream exists in reactor r and the batch operating mode is chosen.

$\mathbf{y^r_{OUT,B}}$ Binary equal 1 if "OUT" stream exists in reactor r and the batch operating mode is chosen.

Integer Variables

$\mathbf{\Lambda_B}$ Operating-mode dependent variable, equal to number of batches per year per plant if batch, or equal to hours of operation per year per plant if continuous.

$\mathbf{\Lambda_P}$ Number of plants operating in parallel.

$\mathbf{\Lambda_O}$ Number of operators per plant [operators/plant].

Part II

An Optimization-Based Framework for the Evaluation of the Monetary Value of Improvements in Process Control

Chapter 4

Economic Value of Process Control: Preliminaries

In this chapter[1], I first present a literature review of previous work that focuses on the economic evaluation of process control. Next, I present a motivating case study that will be used in the rest of the dissertation to illustrate the utility of the framework developed herein. Next, I present the general formulation of integrated control and scheduling problems, and illustrate the implementation of this formulation in section 4.4.

4.1 Introduction and Literature Review

Advanced process control (APC) strategies such as Model Predictive Control (MPC) have become the standard control technique in the process industries due to their unique capability of dealing with complex interactions, process nonlinearities, and operational constraints. The use of APC offers many advantages, such as an increase in throughput, process stability, yield,

[1]The contents of this chapter are largely based on the following publication: [45] Joseph G Costandy, Thomas F Edgar, and Michael Baldea. A Scheduling Perspective on the Monetary Value of Improving Process Control. *Computers & Chemical Engineering*, 112:121–131, 2018. J. C. is the primary author of the manuscript.

or a reduction in energy consumption, waste, raw material, and costs [135].

However, the implementation of a novel APC technology can be expensive due to the costs of manpower, hardware, software, and production loss due to installation downtime. While there are well-established metrics for the evaluation of the closed-loop performance of a control technology (either in-silico or once implemented on a physical system), a strong case for its implementation can only be established by quantitatively defining the associated monetary benefits. Such analyses are more straightforward to conduct in the context of plant construction and design, where the product of the design activity (the plant itself) has a measurable dollar value that can be quantified through standard metrics, such as Net-Present-Value (NPV) or Return-on-Investment (ROI). Nevertheless, the significance of such metrics for business decision-making makes this a continuously researched field, with ongoing efforts to streamline the metrics [112, 113]. However, in the case of process control, where the product in question (a control system) has the purpose of achieving and maintaining the process controlled variables at their desired set points, the question of how to assess the economic impact of improving a control system is a lot more challenging, despite being a concern of the process systems community since the inception of the field [23, 57].

Thus far, all the results reported in the literature for the economic benefit analysis of control systems have focused on steady-state operation, where the benefit of a control system stems from its ability to reject process disturbances and thus reduce state variability over time. This reduction in

variability allows maintaining the operation of key states closer to their limits, as illustrated in Figure 4.1. Operational limits (e.g. quality, throughput, safety) are normally directly related to the most economically favorable operating points, so the difference between the average operating points before and after variability reduction ($A_2 - A_1$) can be directly related to a monetary value [57].

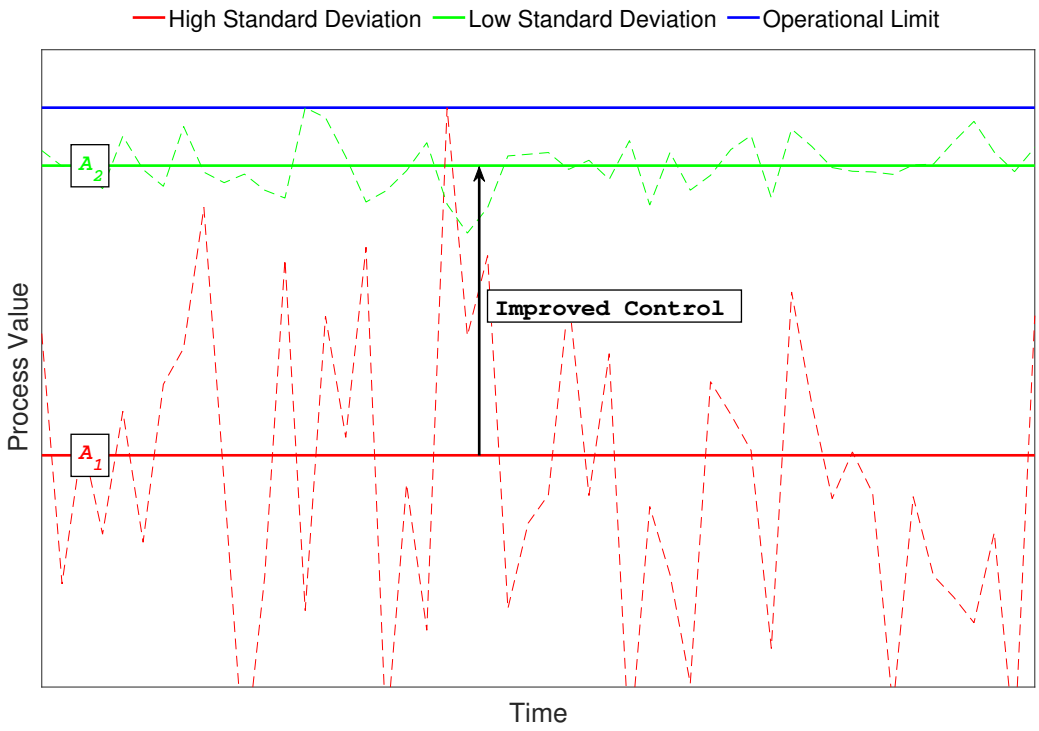

Figure 4.1: Impact of reduction in variability on average process value

Several frameworks have been proposed for the evaluation of the economic driving forces of improving process control [108, 47]. Most of the work reported for the case of predominantly steady-state processes does not take

into account the complex, multivariate nature of most processes, and focuses on the univariate reduction of variance. However, more recent works have adopted a stochastic optimization approach that exploits multivariate effects for identifying the maximum possible monetary value that can be attained by improving process control [180, 181]. The general strategy employed can be summarized as follows:

1. Define a benchmark controller as a basis for economic performance comparison. The most commonly used benchmark is the Minimum Variance Controller (MVC) [117, 181, 24], or more recently the Linear-Quadratic-Gaussian Controller (LQG) [180].

2. Select an appropriate performance function $v(x)$ that defines the relationship between the total profit and the average value A_x of the controlled variable x as its variability approaches that of the benchmark controller. The most common functions used are quadratic, linear, or piecewise linear reflecting saturation such as the so-called CLIFFTENT function [103]. Alternatively, this relationship can be obtained using comprehensive simulations of the specific system being studied under the proposed and benchmark controllers [75, 119].

3. Obtain the probability density function $f(x, \sigma_x, A_x)$ of the controlled variable x with a variability σ_x and average operating value A_x. This is often obtained from industrial data or via simulation. Where an explicit

evaluation of $f(x, \sigma_x, A_x)$ is difficult to conduct, a Gaussian distribution is typically assumed.

4. Finally, the economic driving force of improving process control is obtained as a function $\psi(\sigma_x, A_x) = \int_x v(x) f(x, \sigma_x, A_x) dx$. Profit indices for the three most common performance functions and assuming a Gaussian distribution of the controlled variable x have been derived by Bauer *et al.* [24].

In contrast to the case of predominantly steady-state operation, the monetary benefits of improved control in the case of predominantly transient operation have not been studied. In today's fast-changing markets, transient operation has become ever-more relevant. Fast market dynamics call for the development of better automation algorithms that can rapidly adjust to changing operational objectives, which are typically defined by the solution of a process scheduling optimization problem. The common aim of the two activities (process scheduling and plant-wide control) of locating and tracking optimal state trajectories implies that a tight integration of process scheduling and control activities can yield significant economic benefits. The importance of this topic has been highlighted by the increase in research efforts dedicated towards this integration, as was discussed in several recent review articles [21, 54, 130].

In this dissertation, I posit that the monetary value of a particular control system improvement can be quantified for the case of predominantly transient operation by defining control performance metrics and quantifying

the change in a production scheduling profit objective value as the performance of the controller (as reflected by the performance metric) changes. While a reduction of state variability is an appropriate performance metric for the evaluation of the value of control during steady-state operation, a reduction in transition time between one state and another is the main driving force for economic gains for transient operation, as is illustrated in Figure 4.2. Lower transition times would result in maximizing the overall hourly production rate, minimizing waste of raw materials and off-spec products and reducing storage costs. However, lower transition times require more aggressive control action, which can result in more equipment wear and tear. Nevertheless, the effect of increased maintenance costs may often be negligible compared to the economic benefits resulting from the improved control, so has been ignored in this work. Transition time has therefore been selected as the performance metric over which I assess the value of improved process control. Also, while MVC or LQG controllers were appropriate benchmarks for the case of steady-state operation, a clear benchmark for the case of transient operation is a hypothetical, zero-transition time, "perfect" controller (as shown in Figure 4.2), with the realization that this controller may also have many high ratios of change ("spikes") for the manipulated variables.

My goal is to develop a framework for the assessment of control value for predominantly transient operation by developing appropriate performance functions based on an integrated scheduling and control problem featuring a finite, non-zero number of production transitions.

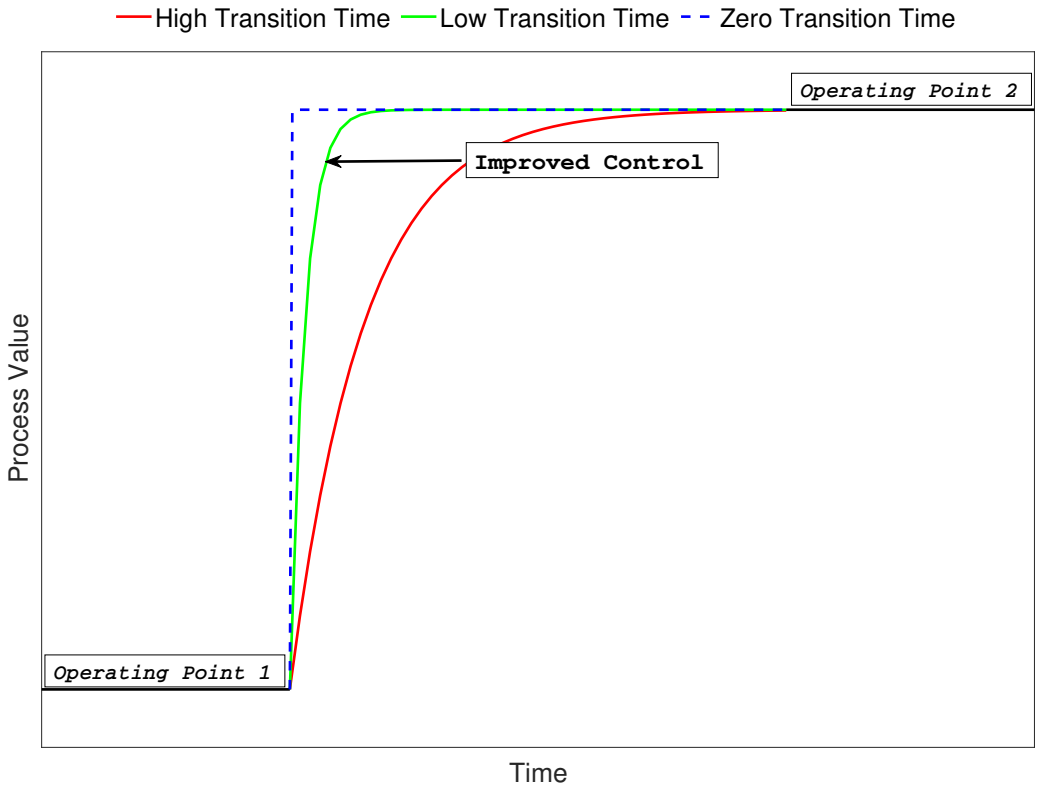

Figure 4.2: Impact of reduction in transition time on production schedule where a step change is made from one process operating point to another

4.2 Motivating Example: Cyclical Scheduling of a CSTR

In this section, I present a problem where transient conditions play an important role, and aim to illustrate that the choice of controller has a direct influence on the performance of the system. This problem will be used in subsequent chapters to illustrate the development of economic metrics for control performance, and as a basis for deriving appropriate performance functions for

the evaluation of the monetary value of process control from the scheduling perspective.

Consider a CSTR that converts a feed stream containing reactant $\boldsymbol{A}$ into one of three products: P_1 (80% feed conversion), P_2 (85% feed conversion), or P_3 (94% feed conversion), by manipulating the reactor temperature. The reactor model was adapted from Davis and Thomson [51], and is given by eq 4.1, where the states are the concentration C_A [mol/L] and temperature T [K], q is the feed flow rate $[m^3/h]$, V is the reactor volume $[m^3]$,k_0 is the pre-exponential factor in the reaction rate expression $[h^{-1}]$, E_A is the activation energy $[J]$, U $[W/m^2K]$ and A $[m^2]$ are the heat transfer coefficient and area, respectively, ρ $[kg/m^3]$ and C_p $[J/kgK]$ are the density and heat capacity of the reaction mixture, respectively, T_c is the coolant temperature [K], ΔH is the enthalpy of reaction $[J/mol]$, and subscript 0 denotes conditions at the reactor inlet. Values of the model parameters are provided in Table 4.1.

$$\begin{bmatrix} \dot{C}_A \\ \dot{T} \end{bmatrix} = \begin{bmatrix} \frac{q}{V}(C_{A0} - C_A) - k_0 e^{-E_A/RT} C_A \\ \frac{q}{V}(T_0 - T) - \frac{1}{\rho C_p} k_0 e^{-E_A/RT} C_A \Delta H - \frac{UA}{\rho V C_p}(T - T_c) \end{bmatrix} \tag{4.1}$$

The conversion of the feed $\boldsymbol{A}$, and therefore the product made by the reactor (P_i), can be controlled by manipulating the temperature of the coolant and allowing the reactor to reach steady-state. The system of ODEs above was solved at steady-state for the reactor and coolant temperatures (T and T_c) that will yield the desired outlet concentrations C_A for the three products. The concentration C_A, and required coolant and reactor temperatures needed

Table 4.1: CSTR Model Parameters (adapted from Davis and Thomson [51])

Parameter	**Value**
$\frac{q}{V}$	1 min^{-1}
$\frac{E_A}{R}$	10^4 K
$\frac{UA}{\rho V C_p}$	1 min^{-1}
k_0	$e^{25}\text{min}^{-1}$
C_{A0}	1 mol/L
T_0	350 K
$-\frac{\Delta H}{\rho C_p}$	-200 K L / mol

for each of the three products is summarized in Table 4.2. At this point, it is necessary to design controllers that are able to achieve the desired reactor conditions, and the transitions between them. Since the scheduling problem has yet to be addressed, the controllers must first be designed such that all possible transitions between the products can be achieved.

Table 4.2: Product concentrations, and required reactor and coolant temperatures for making each of the P_i products.

	$\boldsymbol{i=1}$	$\boldsymbol{i=2}$	$\boldsymbol{i=3}$
Outlet concentration, C_A [mol/L]	0.20	0.15	0.06
Reactor temperature, T [K]	423.6	429.8	449.5
Coolant temperature, T_c [K]	337.0	339.7	360.9

Baldea and Harjunkoski [21] proposed and simulated two control structures for this problem:

1. Two cascaded proportional-integral (PI) controllers, where an inner loop stabilizes the reactor temperature by manipulating the coolant temperature and the outer loop manipulates the setpoint temperature to track the desired composition setpoint.

2. A nonlinear input-output linearizing controller that imposes a second-order closed-loop system behavior [50] .

The choice of controllers is driven by the purpose of this work, that is, to quantify the value of the effort of improving control. Specifically, the cascaded PI controller is easier to design and implement than the linearizing controller since it does not require a full process model. However, the linear closed-loop dynamics that would result from implementing the linearizing controller are expected to yield better performance. This therefore helps address the key question: given a controller design and a production schedule, what is the monetary value of improving process control? In other words, if this production schedule is executed using either controller, what would be the economic value of investing in improving the process controller? Note that I focus here on a situation where the computation of the setpoints (i.e., scheduling) and the control calculations are performed separately; a converse situation – not considered here – is the simultaneous calculation of the optimal setpoints and optimal control moves, as is the case, e.g., in economic MPC [9].

Baldea and Harjunkoski [21] simulated both control structures with all the possible transitions between the three products by imposing composition setpoint changes every 10 hours. The simulation results are reproduced in Figure 4.3. In addition, the authors calculated all possible transition times between the three products, defined as the time taken to reach a value within 0.1% of the new target value after a set-point change. The transition times they calculated are reproduced in Table 4.3.

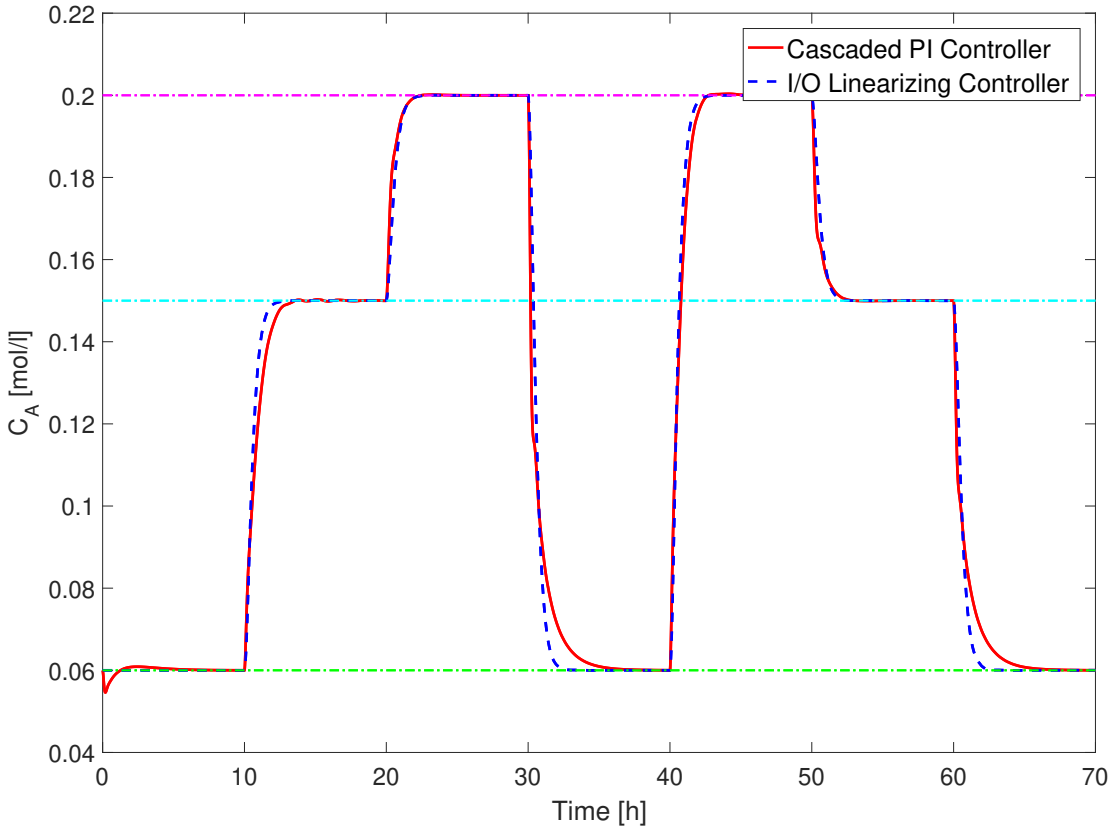

Figure 4.3: Setpoint tracking for all possible transitions between products P_1 ($C_{A,sp} = 0.2$ mol/L), P_2 ($C_{A,sp} = 0.15$ mol/L), and P_3 ($C_{A,sp} = 0.06$ mol/L) using the cascaded PI and linearizing control structures, based on the results reported in reference [21].

The simulation results show that both control structures yield good performance with reasonable transition times between all possible product transitions, and low values of the integral square error (ISE), defined as $\int_0^t (C_{A,sp} - C_A)^2 dt^*$. The ISE for the cascaded PI controller is $\text{ISE}_{PI} = 0.0199$ mol^{2}hr/L^2, and that for the input/output linearizing controller is $\text{ISE}_{\text{IOL}} = 0.0226$ mol^{2}hr/L^2.

Table 4.3: Transition time [h] for reactor to switch from making product $P_{i'}$ to product P_i.

Cascaded PI Controller				**Linearizing Controller**			
$\tau_{i'i}$	P_1	P_2	P_3	$\tau_{i'i}$	P_1	P_2	P_3
P_1	-	2.83	8.36	P_1	-	2.40	3.05
P_2	2.30	-	8.20	P_2	2.30	-	2.90
P_3	4.45	3.50	-	P_3	2.65	2.60	-

Here, I make two observations: First, the simulation shows that transient operation occupies a significant portion of the simulation. While products are only obtained when the system is at steady-state, the transient portion of production campaign cannot be ignored since it will clearly affect the total makespan of any proposed production schedule, with further implications on the amount of time products must spend in storage and associated storage costs (as discussed later). This fact indicates that the evaluation of the monetary benefits of control for any production schedule must take the transient portion of the schedule into account. Second, the chosen controller has a clear and direct impact on the process operation. Owing to the nonlinearity of the closed-loop response of the cascaded PI control structure, I direct the reader's attention to transitions such as $P_1 \rightarrow P_3$ and $P_2 \rightarrow P_3$, which have a much larger duration for the cascaded PI controller compared to the input/output linearizing controller. Such differences can affect the production sequence and total profit drastically.

4.3 The Optimal Scheduling Problem

In this section, I present the general integrated scheduling and control problem framework that was proposed by Flores-Tlacuahac and Grossmann [63], and used by Baldea and Harjunkoski [21] as a basis to perform a systematic investigation into the use of elements of control and scheduling as building blocks for the formulation and solution of the integrated scheduling and control problem. I specifically focus on identifying the role of control on the overall schedule, since defining the monetary value of control from a scheduling perspective requires knowledge of where control plays a role on the overall schedule.

The scheduling problem aims to identify the optimal production sequence that achieves the maximum profit $J[\$/h]$ from supplying a given demand $\delta_i[m^3]$ for each of the N_P products $P_i(i \in 1, ..., N_P)$ in the lowest makespan time $T_m[h]$. The total cycle time for which the schedule is optimized is split into N_s time-slots. The objective function is given by eq 4.2, where ϕ_1 is the total profit generated in one cycle of the production schedule, ϕ_2 is the total cost of raw materials, and ϕ_3 is the cost of storage of products until the end of the cycle.

$$J = \frac{1}{T_m} [\phi_1 - \phi_2 - \phi_3] \tag{4.2}$$

The total profit generated ϕ_1 is given by eq 4.3, where $\omega_i[m^3]$ is the total volume of product P_i made, and $\pi_i[\$/m^3]$ is the price of product P_i.

$$\phi_1 = \sum_{i=1}^{N_P} \pi_i \omega_i \tag{4.3}$$

The cost of raw materials ϕ_2 is given by eq 4.4, where $q_s[m^3/h]$ is the feed flow rate in slot s, $c_{rm}[\$/m^3]$ is the cost per volume of raw material, and the term $(t_s^f - t_s^s)$ is the time occupied by slot s with superscripts s and f denoting start and finish times, respectively. Assuming a constant reactor inlet flow rate q allows reduction of this term to $qc_{rm}T_m$.

$$\phi_2 = \sum_{s=1}^{N_s} q_s c_{rm} (t_s^f - t_s^s) \tag{4.4}$$

The cost of storage of products ϕ_3 is given by eq 4.5, where $c_{\text{storage},i}[\$/m^3 h]$ is the cost of storing 1 m^3 of product P_i for 1 h, the term $(T_m - t_s^f)$ is the time from the end of slot s, t_s^f, to the end of the full cycle T_m, and $z_{i,s}$ is a binary variable defined as:

$$z_{i,s} = \begin{cases} 1, & \text{if product } i \text{ is made in slot } s \\ 0, & \text{otherwise.} \end{cases}$$

It is assumed here that any stored product will remain in storage until the end of the cycle, and will be removed immediately after the cycle ends.

$$\phi_3 = \sum_{i=1}^{N_P} c_{\text{storage},i} \omega_i \sum_{s=1}^{N_s} z_{i,s} (T_m - t_s^f) \tag{4.5}$$

The transition time in any slot s, τ_s, is calculated using eq 4.6, with a known amount of time assigned to the setup of the first slot ($\tau_{s=1}$). The start

(t_s^s) time of each slot is defined using eq 4.7, with the start time of the first slot ($t_{s=1}^s$) fixed at zero. The end (t_s^f) time of each slot is related to the start and transition times using constraint (4.8), with the end time of the final slot set equal to the total makespan time T_m.

$$\tau_s = \sum_{i'=1}^{N_P} \sum_{i=1}^{N_P} z_{i',s-1} z_{i,s} \tau_{i',i} \quad \forall s \neq 1 \tag{4.6}$$

$$t_s^s = t_{s-1}^f \quad \forall s \neq 1 \tag{4.7}$$

$$t_s^f \geq t_s^s + \tau_s \quad \forall s \tag{4.8}$$

The total volume of product ω_i is set equal to the demand δ_i, and is related to the timing constraints above using eq 4.9.

$$\omega_i = \delta_i = \sum_{s=1}^{N_s} z_{i,s} q (t_s^f - t_s^s - \tau_s) \quad \forall i \tag{4.9}$$

Finally, a limit of 1 is placed on the number of products made in each slot and the number of slots used for each product using eqs 4.10 and 4.11, respectively.

$$\sum_{i=1}^{N_P} z_{i,s} = 1 \quad \forall s \tag{4.10}$$

$$\sum_{s=1}^{N_s} z_{i,s} = 1 \quad \forall i \tag{4.11}$$

It should be noted here that while modifications can be readily made to the objective function or to the model constraints (e.g. raw material corresponding to each product can be different, products can be manufactured over two separate time slots, sale of off-spec product can be accounted for, etc.), the overall framework is applicable for all scheduling problems, in that it consists of an objective function that maximizes profit subject to constraints that describe the physical limitations and mathematical relationships of the plant [63].

The control system plays the very critical role of executing the production schedule. Several assumptions are made in the solution of the scheduling problem with regards to the control system. First, solving the scheduling problem involves making integer decisions with regard to the operation of the process, assuming constant values for the transition times $\tau_{i',i}$. The example presented in Section 4.2 clearly illustrates that the values of these transition times are closely tied to the process dynamics (e.g. eq 4.1), choice of control structure, and the performance of the control system. Furthermore, it is assumed that all the product made in the production slot s is of the required quality, which may not be the case if disturbances occur. Therefore, successful execution of the schedule by the control system is tied to the ability of the control system to transition between operating points, reject process disturbances, and maintain process stability. It is therefore clear that the monetary value of the control system is directly related to the total profit derived from implementing the optimal production schedule.

4.4 Motivating Example (cont'd): CSTR Production Schedule

In this section, I aim to demonstrate the use of the integrated scheduling and control framework presented in Section 4.3 on the cyclical CSTR problem presented in Section 4.2. First, I solve the scheduling optimization problem, and use the results to identify the role of control on the overall production schedule. Then, I fix a production sequence and makespan, and perform four simulations with different values of transition times, allowing me to make quantitative observations about the effect of transition time, and the nonlinearity of the closed-loop system dynamics on the economic performance of the production schedule.

4.4.1 Optimization of Production Schedule

Production scheduling of the cyclical CSTR problem presented in Section 4.2 was performed using the framework in Section 4.3 and transition times in Table 4.3. For this problem, the number of products (N_P) and slots (N_s) are both 3, with only a single product allowed per slot as enforced by constraint (4.10). The values of the parameters used are shown in Table 4.4.

The MINLP consisting of eqs 4.2 - 4.11 was solved to optimality for both control structures, and the Gantt charts of the optimal schedules for the linear and nonlinear controllers are shown in Figure 4.4. The different controllers result in different production schedules, with the cascaded PI controller resulting in the sequence $P_3 \rightarrow P_2 \rightarrow P_1$ and an hourly profit of \$62.71/h, and

Table 4.4: Product properties.

	$i = 1$	$i = 2$	$i = 3$
Demand, $\delta_i[m^3]$	10	30	10
Sale price, $\pi_i[\$/m^3]$	100	120	200
Storage cost, $c_{\text{storage},i}[\$/m^3h]$	2	2	2
Flow rate, $q[m^3/h]$	1		
Raw material cost, $c_{rm}[\$/m^3]$	20		

the linearizing controller resulting in the sequence $P_3 \rightarrow P_1 \rightarrow P_2$ and an hourly profit of \$65.54/h. The higher total profit generated when using the input/output linearizing controller can be attributed to the lower makespan.

Figure 4.4 shows that transition between products takes more than 15% of the total schedule for both control structures. Furthermore, since the only difference between the two problems was the transition times that were dictated by the specific controllers implemented, it is clear that the major contributor to the change in profit of an integrated scheduling and control problem arises from the difference in the transition times from one product to the next. Figure 4.4 also shows the schedules if a hypothetical, zero-transition time controller were to be implemented for the same process, assuming that the production schedule does not change. It can be seen that for this controller, the makespan of the scheduling cycle is reduced to 50 hours, and will achieve an hourly profit of \$76.30/h. The higher profit can be attributed to the cost savings in raw materials and storage. In addition, this ideal schedule will result in an increase in annual profits because of the availability of more cycles per year.

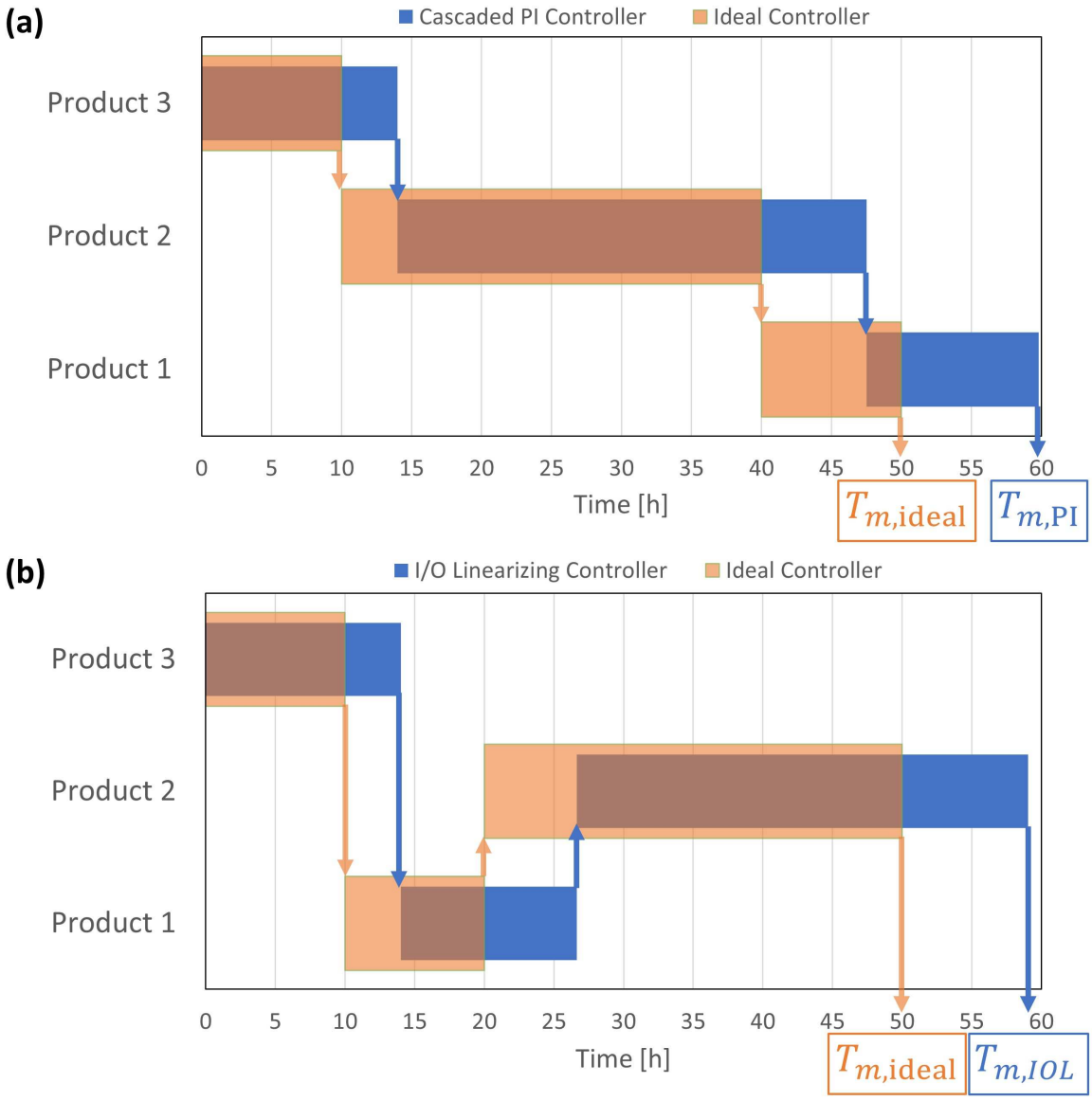

Figure 4.4: Gantt chart of optimal schedule for (a) the cascaded PI controller and (b) the input/output linearizing controller

This simple example illustrates that the control structure has a direct impact on both the sequencing and economics of any proposed schedule. It

is important to note that the implementation of the cascaded PI controller is much simpler than the linearizing controller. The latter requires developing a process model and would therefore be more costly and time consuming. It is therefore essential to be able to quantify the monetary value of improving control in order to make such decisions.

4.4.2 Simulation of Production Schedule

In this section, I aim to delineate the specific effect of transition time that arises from using different control structures, as well as the effect of the nonlinearity of the closed-loop system dynamics on the economic performance. I do not aim to provide a rigorous analysis of the effect of nonlinearity, but instead aim to illustrate numerically that controller nonlinearity does have an effect on production economics. The effect of nonlinearity can only be investigated if an appropriate metric for nonlinearity is first defined. To that end, I first note that for linear controllers, $\tau_{i',i''} = \tau_{i'',i'}$ for all combinations of i', i''. Therefore, for linear system dynamics, the standard deviation of transition times for all possible transitions (σ [hrs]) is zero. Thus, for the purpose of this analysis, a reasonable metric for nonlinearity is the standard deviation of all transition times.

I perform four simulations of a fixed production sequence (namely, $P_3 \rightarrow P_2 \rightarrow P_1 \rightarrow P_3 \rightarrow P_1 \rightarrow P_2 \rightarrow P_3$) that employs all the possible production transitions. The duration of each time slot is 10 hours. Different control structures are considered with their corresponding transition times. As such,

the quantity of each product produced in each simulated campaign using the four control structures, and therefore the total hourly profit, will be different. The transition times of the four simulations are described as follows:

1. The transition times for the cascaded PI control structure, as given in Table 4.3. The average transition time and standard deviation for this control structure are $\overline{\tau}_{i'',i'} = 4.94$ and $\sigma = 2.69$ hours, respectively.

2. The transition times for the input/output control structure, as given in Table 4.3. The average transition time and standard deviation for this control structure are $\overline{\tau}_{i'',i'} = 2.65$ and $\sigma = 0.29$ hours, respectively.

3. All transition times set equal to each other, and equal to the average of all transition times for the cascaded PI control structure ($\tau_{i'',i'} = 4.94$ hours $\forall(i'', i')$). This will have the same average transition time as simulation 1, but will have a standard deviation of $\sigma = 0$, corresponding to a linear closed-loop behavior with closed-loop time constant $\tau_{\mathrm{CL}} = 4.94$ hours.

4. All transition times set equal to each other, and equal to the average of all transition times for the input/output linearizing control structure ($\tau_{i'',i'} = 2.65$ hours $\forall(i'', i')$). This will have the same average transition time as simulation 2, but will have a standard deviation of $\sigma = 0$, corresponding to a linear closed-loop behavior with closed-loop time constant $\tau_{\mathrm{CL}} = 2.65$ hours..

Equations 4.2 - 4.5 were used to calculate the total hourly profit for the four cases with the product properties given in Table 4.4. The results are presented in Table 4.5. The total revenue (ϕ_1) and storage costs (ϕ_3) are different for the four simulations due to the production of different amounts of each product P_i in each slot. The total raw material costs (ϕ_2) are the same for all cases since the CSTR uses a single raw material at all times, and the makespan time for all schedules was fixed.

Table 4.5: Total hourly profit and profit breakdown of four simulations of the fixed production schedule.

Case	$\overline{\tau}_{i'',i'}$ [h]	σ [h]	J [\$/h]	T_m [h]	ϕ_1 [\$]	ϕ_2 [\$]	ϕ_3 [\$]
1	4.94	2.69	10.06	64	3653.40	1280.00	1729.80
2	2.65	0.29	40.88	64	6115.00	1280.00	2215.00
3	4.94	0	22.70	64	4250.40	1280.00	1518.00
4	2.65	0	42.02	64	6174.00	1280.00	2205.00

Comparing the hourly profits J of cases 3 and 4, or cases 1 and 2 reveals that the total profit is inversely proportional to the average transition time. Comparing the total profits of cases 1 and 3, or cases 2 and 4, shows that for a fixed average transition time, decreasing controller nonlinearity has a substantial effect on total profit.

Chapter 5

Economic Value of Process Control: Novel Performance Metrics

In this chapter[1], I present two novel performance metrics that can be used to assess the monetary value of process control from a scheduling perspective.

5.1 Monetary Performance Metrics

In this section, I aim to arrive at explicit expressions that allow the evaluation of the monetary benefits of improving process control from a scheduling perspective. In the previous chapter, I proposed the use of transition time as an appropriate performance metric. However, across a scheduling horizon, there could be one or more transitions, each with a different duration. Therefore, the question arises as to which transition time would provide the best measure. I investigate two possibilities:

1. The use of the total transition time across the scheduling horizon as the

[1]The contents of this chapter are largely based on the following publication: [45] Joseph G Costandy, Thomas F Edgar, and Michael Baldea. A Scheduling Perspective on the Monetary Value of Improving Process Control. *Computers & Chemical Engineering*, 112:121–131, 2018. J. C. is the primary author of the manuscript.

performance metric.

2. The use of individual transition times as the performance metric.

Referring to Eqn. (4.2),

$$J = \frac{1}{T_m}\left[\phi_1 - \phi_2 - \phi_3\right] \tag{4.2}$$

I note that the profit is normalized with respect to the total makespan T_m. This profit objective function can be manipulated to clearly see the effect of transition and production times. Eqns. (5.1) and (5.2) define two variables, T_T and T_P, as the total transition and production times within one scheduling cycle, respectively. In Eqn. (5.2), t_s^P is the total production time of slot s. Also, since we are interested in the absolute monetary benefit (j [$]), we multiply both sides of Eqn. (4.2) by T_m, yielding Eqn. (5.3).

$$T_T \equiv \text{Total Transition Time [h]} = \sum_{s=1}^{N_s} \tau_s = \tau_{s=1} + \sum_{s=2}^{N_s}\sum_{i'=1}^{N_P}\sum_{i''=1}^{N_P} z_{i'',s-1} z_{i',s} \tau_{i'',i'} \tag{5.1}$$

$$T_P \equiv \text{Total Production Time [h]} = \sum_{s=1}^{N_s} t_s^P = \sum_{s=1}^{N_s} (t_s^f - t_s^s - \tau_s) \tag{5.2}$$

$$j = T_m J = \sum_{i=1}^{N_P} \pi_i \omega_i - q c_{rm}(T_T + T_P)$$
$$- \sum_{i=1}^{N_P} c_{\text{storage},i} \omega_i \sum_{s=1}^{N_s} z_{i,s} \left\{ \left(T_T - \tau_{s=1} - \sum_{s'=2}^{s} \sum_{i'=1}^{N_P} \sum_{i''=1}^{N_P} z_{i'',s'-1} z_{i',s'} \tau_{i'',i'} \right) + \left(T_P - \sum_{s'=1}^{s} t_{s'}^P \right) \right\} \tag{5.3}$$

Then, the monetary value can be obtained by evaluating $dj/d\Theta$, where Θ is the chosen performance metric.

5.1.1 Performance Metric 1: Total Transition Time

The first performance metric to examine is the total transition time, T_T, defined in Eqn. (5.1). Since T_T is a function of the product $z_{i',s-1} z_{i,s}$, and as a consequence, the optimal production schedule, the derivative dj/dT_T cannot be obtained unless we assume the production sequence is not modified by minor changes in the individual transition times.

To calculate the profit associated with a production schedule executed with an ideal controller, j^{ideal} [\$/h], all transition times (and therefore T_T) are set to zero in Eqn. (5.3):

$$j^{\text{ideal}} = \left[\sum_{i=1}^{N_P} \pi_i \omega_i - \sum_{i=1}^{N_P} c_{\text{storage},i} \omega_i \sum_{s=1}^{N_s} z_{i,s} \left(T_P - \sum_{s'=1}^{s} t_{s'}^P \right) - q c_{rm} T_P \right] \tag{5.4}$$

Subtracting Eqn. (5.3) from Eqn. (5.4) yields, after simplification:

$$j^{\text{ideal}} - j = \sum_{i=1}^{N_P} c_{\text{storage},i}\omega_i \sum_{s=1}^{N_s} z_{i,s} \left(T_T - \tau_{s=1} - \sum_{s'=2}^{s} \sum_{i'=1}^{N_P} \sum_{i''=1}^{N_P} z_{i'',s'-1} z_{i',s'} \tau_{i'',i'} \right) + q c_{rm} T_T \tag{5.5}$$

which provides the cost incurred by imperfect control. The first term of Eqn. (5.5) corresponds to the reduction in storage costs due to decreasing the makespan, and the second term corresponds to the reduction in raw material costs.

Next, noting that $j = (T_T + T_P)J$, and $dj^{\text{ideal}}/dT_T = 0$, the derivative of Eqn. (5.5) is evaluated with respect to T_T yielding, after simplification:

$$\frac{dj}{dT_T} = -\left(\sum_{i=1}^{N_P} c_{\text{storage},i}\omega_i \sum_{s=1}^{N_s - 1} z_{i,s} + q c_{rm} + J \right) \tag{5.6}$$

which indicates that a reduction of one hour in the total transition time yields savings due to a reduction of one hour of storing each product made before the last time slot (since the model assumes that the product made in the final slot is not sent to storage), a reduction in the cost of raw material equivalent to the price of one hour flow of raw material, and an additional profit J that arises from the reduction of the makespan.

The main advantage of this result is its simplicity. One can immediately evaluate the expression upon solving the scheduling problem to test whether further improvement of the control would result in significant monetary benefits. However, the expression is only applicable for the evaluation of the effects of small changes in transition times that will not affect the optimal schedule.

The result cannot be applied to cases where the production sequence in the optimal schedule is very sensitive to changes in the transition times, since the analysis presented herein assumed the optimal production sequence remains unchanged.

5.1.2 Performance Metric 2: Individual Transition Times

An individual transition time $\tau_{i'',i'}$ between products i'' and i' can be used as the performance metric over which the monetary value of improving process control for the total production schedule is evaluated, assuming that all other transition times remain constant. In order to differentiate the total profit with respect to an individual transition time, the total transition time (Eqn. (5.1)) is first differentiated with respect to a single transition time, as shown in Eqn. (5.7):

$$\frac{dT_T}{d\tau_{i'',i'}} = \sum_{s=2}^{N_s} z_{i'',s-1} z_{i',s} \tag{5.7}$$

This result can then be used to find the derivative of the total profit j (Eqn. (5.5)) with respect to an individual transition time:

$$\frac{dj}{d\tau_{i'',i'}} = -\left[\sum_{i=1}^{N_P} c_{\text{storage},i}\omega_i \sum_{s=1}^{N_s} z_{i,s}\left(\sum_{s'=2}^{N_s} z_{i'',s'-1} z_{i',s'} - \sum_{s'=2}^{s} z_{i'',s'-1} z_{i',s'}\right)\right] - qc_{rm}\sum_{s=2}^{N_s} z_{i'',s-1} z_{i',s} \tag{5.8}$$

Before discussing this expression in more detail, I should note that this derivative is an explicit function of the production schedule, and the value

of the derivative is dependent upon the optimal production sequence, given by $z_{i,s}$. In the following discussion, I will refer to the production transitions that appear in the optimal sequence as "active", and those that do not play a role in this sequence as "inactive". For example, in the optimal sequence obtained with the cascaded PI controller (Fig. (4.4a)), the active transitions are $P_3 \rightarrow P_2$ and $P_2 \rightarrow P_1$, while the remaining transitions are inactive.

In the case of active transitions, the first term in Eqn. (5.8) provides the reduction in storage costs for all the products made prior to, and including, the transition being investigated, while the second term is the reduction in raw material costs due to the reduction in the makespan time by one hour. The resulting savings in storage costs are intuitive: products made prior to the transition will be stored for a shorter period of time until the end of the cycle, while the cost of storage of products made after the transition will not be affected by the reduction in the transition time. This simple result is highly relevant for a production plant that is already in place, and improvements to the profit by improving process control are sought. It provides a clear indication of where the process control engineers should focus their efforts so as to have the largest possible influence on total profit.

In the case of active transitions, the linear dependence of the total profit j on the transition times results in a constant increase in profit with a decreasing transition time, until the point when the transition time reaches zero. However, this is not the case for an inactive transition time. Reducing an inactive transition time will initially have no effect on the total profit, since

the optimal schedule remains unchanged. However, if the inactive transition time becomes sufficiently low to warrant a change in the optimal production sequence to require this transition to occur, the inactive transition will now become active in the optimal schedule. Therefore, the problem of finding the effect of inactive transition times on the total profit made from a production schedule is analogous to performing a sensitivity analysis on the profit objective function to identify the points at which the schedule changes, and what the new optimal production sequence is. The problem would be to find how far one must decrease the transition time for a different optimal production schedule ($z_{i,s}$) to be selected, and what is the new optimal production schedule. Performing such an analysis will allow process engineers to identify whether the improvement of process control would yield significant monetary benefits even if the particular transition in question is currently not implemented on an online plant.

5.2 Motvating Example (cont'd): Value of Control for CSTR Operation

5.2.1 Performance Metric 1: Total Transition Time

First, I use the total transition time as the performance metric to quantify the monetary value of process control, to find the maximum possible value of improving process control for the full production schedule. Evaluating Eqn. (5.6) for the two studied controllers gives savings of \$162.71/hr for the cascaded PI controller and \$125.54/h for the input/output linearizing controller. Based

on this, one can conclude that for this problem, an improvement of process control would result in a larger profit if either controller was upgraded, with higher monetary benefits of improving control if the cascaded PI controller was implemented than if the linearizing controller was implemented. In other words, the linearizing controller in its current design provides better overall control performance for this production schedule such that its improvement will not yield as much benefit for the schedule as if the cascaded PI controller were improved.

In addition, I applied Eqn. (5.6) to calculate the value of control for the four fixed production schedules introduced in Section 4.4.2. In order to account for the fact that each product was made in more than one slot, the equation was modified by summing the total quantity of each product made in each slot:

$$\frac{dj}{dT_T} = -\left(\sum_{i=1}^{N_P} c_{\text{storage},i} \sum_{s=1}^{N_s-1} z_{i,s}\omega_{i,s} + qc_{rm} + J\right) \tag{5.9}$$

The calculated value of control for the four cases is shown in Table 5.1. Comparing case 1 with case 3, or case 2 with case 4, reveals that the nonlinearity of the closed-loop system dynamics (as reflected by transition time standard deviation) is indirectly proportional to the value of control. In other words, improvement of process control is economically attractive if the closed-loop behavior becomes more linear, in the sense defined in section 4.4.2.

Table 5.1: Value of control for the four simulations with a fixed production schedule using total transition time as the performance metric.

Case	$\overline{\tau}_{i'',i'}$ [h]	σ [h]	j [\$]	dj/dT_T [\$/h]
1	4.94	2.69	643.60	87.18
2	2.65	0.29	2616.00	134.88
3	4.94	0	1452.40	93.29
4	2.65	0	2689.00	135.52

5.2.2 Performance Metric 2: Individual Transition Times

Next, I investigate the effect of improving the specific transitions from one product to the other in order to identify where an improvement in process control would yield the highest monetary benefits for the production schedule. As discussed in section 5.1.2, a systematic sensitivity analysis is needed to investigate the effect of modifying individual transition times on the total profit. To this end, I have conducted an investigation wherein I examined the effect of gradually reducing each transition time from its nominal value (given in Table 4.3) by some increment Δt, until it reaches zero, while keeping all other transition times at their nominal values, and solving the scheduling optimization problem given by Eqns. (4.2) - (4.11) to find the new optimal production sequence and hourly profit. The results of one such analysis are shown in Figure 5.1, for the sensitivity of total profit to the (decreasing) value $\tau_{3,1}$ for the cascaded PI controller. The analysis begins at the left of the plot, where $\tau_{3,1}$ is at its nominal value of 4.45 hours ($\Delta\tau_{3,1} = 0$). I then decrease $\tau_{3,1}$ by a small increment and re-solve the optimization problem to find the optimal production sequence with the new value of $\tau_{3,1}$. Any changes in total

profit or production sequence are recorded. I then continue to decrease $\tau_{3,1}$ until it reaches zero (at the right of the plot). The change $\Delta\tau_{3,1}$ is shown on the bottom abscissa.

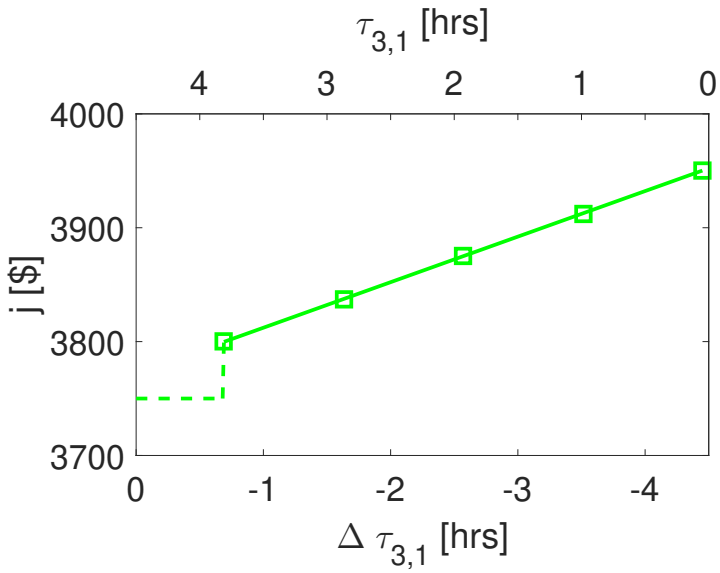

Figure 5.1: Total profit as a function of transition time $\tau_{3,1}$ (top abscissa), or change in transition time $\Delta\tau_{3,1}$ (bottom abscissa) for the cascaded PI controller.

Results of this investigation for all transition times $\tau_{i'',i'}$ are shown in Figures 5.2 and 5.3 for the cascaded PI and the input/output linearizing controllers, respectively. In these figures, each line represents the variation of the total profit, j, as a different transition time, $\tau_{i'',i'}$, is reduced from its nominal value (where $\Delta\tau = 0$) to zero (where $\Delta\tau = -\tau_{i'',i'}$, as given in Table 4.3). Different line colors are used to represent different transitions. Solid lines indicate that the transition is active in the optimal schedule, while dashed lines indicate that the transition is inactive. Finally, different markers

denote the optimal production sequence. In addition, the derivative of the total profit with respect to the transition time, $dj/d\tau_{i'',i'}$, as calculated using Eqn. (5.8), is also plotted as a function of the change in transition time for all the individual transition times.

Figures 5.2 and 5.3 illustrate the difference between active and inactive transitions. For active transitions, any modification in the transition time has no effect on the optimal production sequence but results in an immediate increase in the total profit. The value of control can be assessed directly for active transitions using Eqn. (5.8). For example, we evaluate the expression for the schedule of Fig. (4.4a) with the two active transitions $\tau_{3,2}$ and $\tau_{2,1}$:

$$\frac{dj}{d\tau_{3,2}} = -\left(c_{\text{storage},3}\omega_3 + qc_{rm}\right) = -\$40/hr \tag{5.10}$$

$$\frac{dj}{d\tau_{2,1}} = -\left(c_{\text{storage},3}\omega_3 + c_{\text{storage},2}\omega_2 + qc_{rm}\right) = -\$100/hr \tag{5.11}$$

which can be seen on the bottom plot of Figure 5.2. This result indicates that if the cascaded PI controller was implemented and the plant was designed such that the schedule of Figure 4.4 was followed, then improving the transition between products P_2 and P_1 would yield 2.5 times the monetary benefits as improving the transition between products P_3 and P_2, while improving the control structure to reduce any of the other product transitions would yield no economic benefits for the current production sequence. Similarly, we can

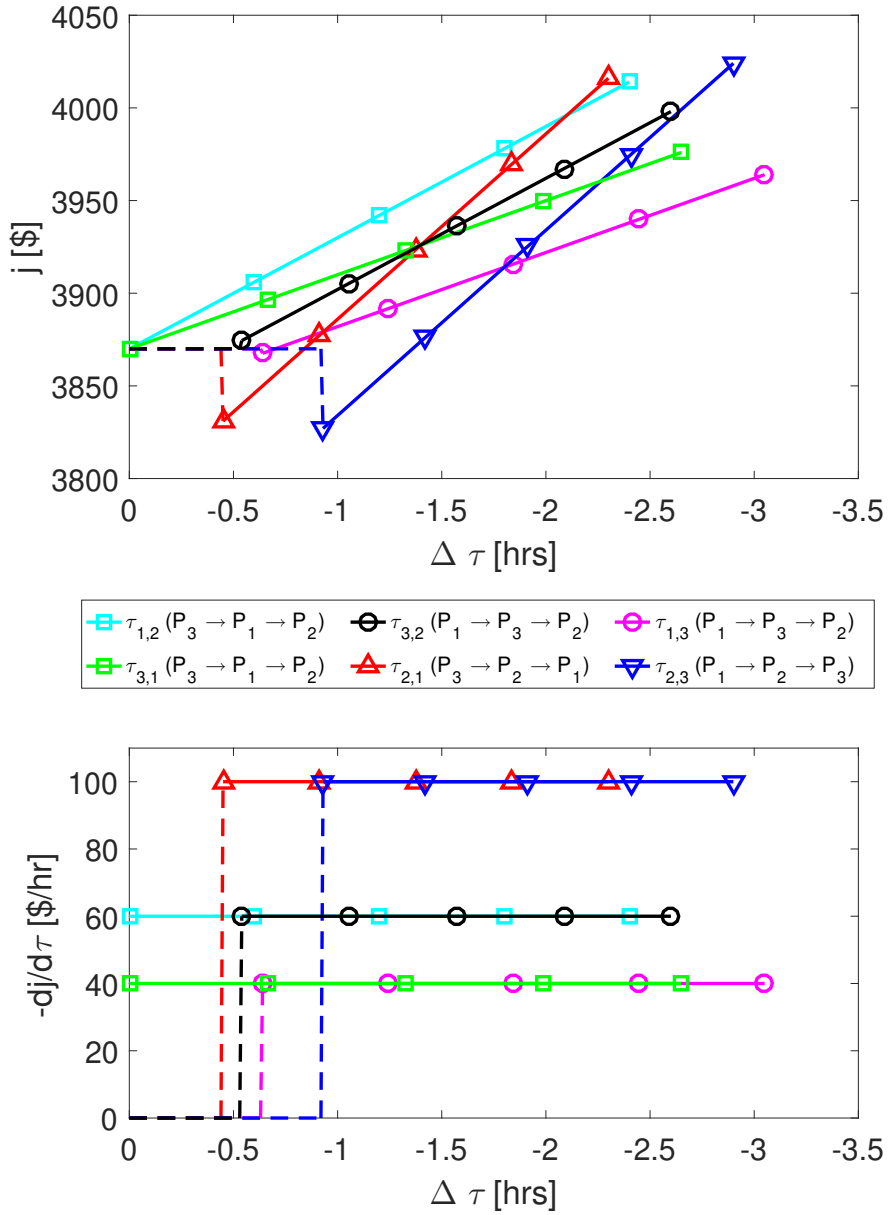

Figure 5.2: Total profit and derivative of profit with respect to transition time as a function of change in individual transition times for the cascaded PI controller. Solid lines indicate that the transition is active in the schedule, while dashed lines indicate the transition is inactive. Line color represents the particular transition. The optimal schedule is indicated by the marker type: $\triangle$ is $P_3 \to P_2 \to P_1$, $\boxdot$ is $P_3 \to P_1 \to P_2$, $\bigcirc$ is $P_1 \to P_3 \to P_2$, $\diamond$ is $P_2 \to P_1 \to P_3$, and $\bigtriangledown$ is $P_1 \to P_2 \to P_3$.

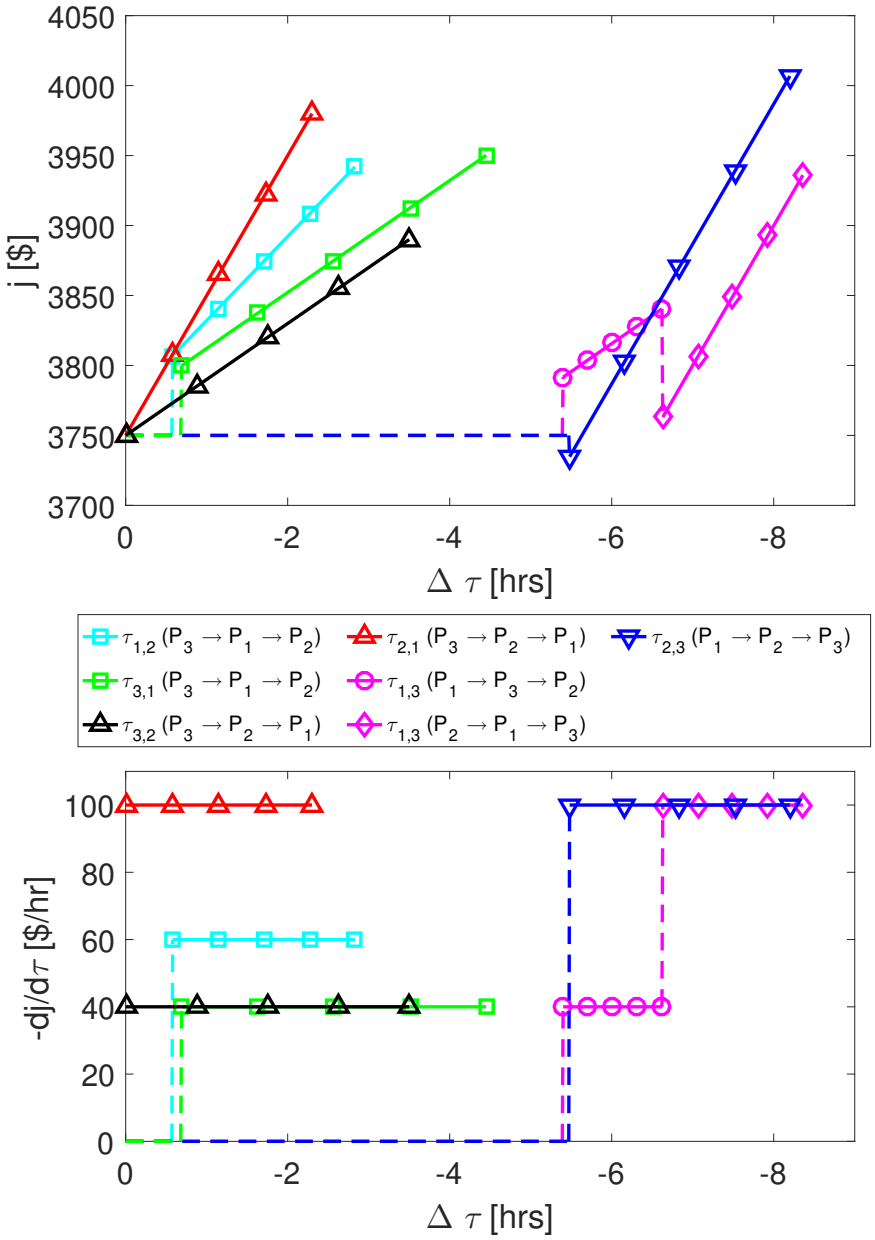

Figure 5.3: Total profit and derivative of profit with respect to transition time as a function of change in individual transition times for the input/output linearizing controller. Visual representations of active vs. inactive transitions, particular transitions, and optimal schedule are the same as Fig. 5.2.

compute the value of $dj/d\tau_{i'','}$ using Eqn. (5.8) for the active transitions if the input/output linearizing controller were implemented, and find that reducing $\tau_{3,1}$ and $\tau_{1,2}$ by one hour results in increases of \$40 and \$60, respectively, as can be seen on the bottom plot of Figure 5.3.

The next question is whether implementing different production sequences with improved control would provide higher monetary benefits than the current production sequence. Different production sequences would become optimal when the currently inactive transitions become active upon significant reduction in their corresponding transition times. For this reason, Figures 5.2 and 5.3 show that for small values of $\Delta\tau$, when the transition is inactive, the total profit j does not change, and the value of improving control, $dj/d\tau_{i'',i'}$ is zero. However, a discontinuity occurs in the plot when the transition time becomes small enough to warrant a change in the optimal production sequence. It should be noted that the optimization problem is solved to maximize the total hourly profit, $J[\$/h]$, and not the total absolute profit, $j[\$]$, which is why some changes in the optimal production sequence result in lower total profits despite having higher hourly profits (e.g. $\tau_{2,3}$ in the top plot of Figure 5.2). Upon selecting another production sequence, the total profit j increases linearly with decreasing transition time, and the derivative of the total profit with respect to transition time can now be calculated using Eqn. (5.8) for the new production sequence.

Figure 5.2 shows that the most economically beneficial improvement of control would be achieved if the duration of the transition between P_2 and

P_1 is reduced, with an improvement of \$100/hr. This is also an active transition in the optimal schedule for the cascaded PI control structure. The same economic benefit could also be achieved by another sequence if the duration of the transitions between products P_2 and P_3 or P_1 and P_3 are drastically reduced by more than 5 hours. Therefore, if this controller was implemented, it would be best to operate with the currently optimal production sequence and improve the particular transition between products P_2 and P_1.

From the inspection of Figure 5.3, it can be seen that the improvement of any of the two active transitions would yield a maximum benefit of \$60/hr. However, if a slight reduction of less than half an hour was made for the transition between products P_2 and P_1 using the input/output linearizing controller, then the optimal production sequence will change to $P_3 \rightarrow P_2 \rightarrow P_1$ (same as the optimal sequence for the cascaded PI controller), and any further reduction of $\tau_{2,1}$ would yield \$100/hr. Similarly, a reduction of $\tau_{2,3}$ by slightly less than an hour would result in the optimal production sequence becoming $P_1 \rightarrow P_2 \rightarrow P_3$, and any further reduction would also yield \$100/hr. Therefore, we have identified two inactive transitions whose improvement can be significantly more economically attractive than the improvement of the currently optimal production sequence.

To conclude this section, I make two observations about the metrics I have developed and demonstrated. First, while the initial investigation using the total transition time as the performance metric revealed that improvement of process control would be more economically beneficial for the case of the

cascaded PI controller, the detailed investigation of individual transition times revealed that the same economic benefits can be achieved if either control structure were implemented provided that we know exactly which transition times play a larger role on the total profit. The use of the individual transition times as the performance metric therefore provided more information about the specific areas where upgrading the implemented controller would yield significant monetary benefits. This, however, does not negate the worth of using the total transition time as a performance metric, since it provided a rapid answer as to whether the improvement of process control would yield significant monetary benefits. Second, the use of individual transition times as the performance metric as I have illustrated in this section is a multivariate assessment of the value of control, in that it accounts for all the variables that affect the objective function.

5.3 Summary and Future Directions

This chapter presented a novel framework for quantifying the monetary value of improving process control in the case of predominantly transient plant operation from a scheduling perspective. I presented two novel performance metrics. The first metric was the total transition time within a single production cycle. The corresponding performance metric was shown to provide an upper bound on the potential gains that can be made by improving process control, but suffered from the assumption that the optimal production sequence is not modified by the changes in transition time. Nevertheless, the

performance metric gives an indication as to whether further investigation into improving process control would yield significant monetary benefits. The second performance metric I examined was the transition time between individual products. I showed that by using this metric, one can identify specific areas of a chemical plant where improving process control would yield the highest economic benefits. Furthermore, this metric can be used without making the assumption that the production sequence remains unchanged upon modification of the transition time, allowing a more in-depth understanding of all the potential benefits that can be gained by improving the setpoint tracking capabilities of the particular control structure that is implemented, assuming that the attained benefits are not affected by decreased disturbance rejection capabilities.

While the proposed framework and expressions herein focused on the monetary value of process control in particular, the methodology employed can be extended to identify other types of dynamic bottlenecks (e.g., equipment-related, value of Research) in a production process by performing similar sensitivity analyses.

Bibliography

[1] Industrial and Laboratory Reactors. In A Kayode Coker, Coker A B T Modeling of Chemical Kinetics Kayode, and Reactor Design, editors, *Modeling of Chemical Kinetics and Reactor Design*, chapter 4, pages 218–259. Gulf Professional Publishing, Woburn, 2001.

[2] Thomas K. Abraham and Martin Feinberg. Kinetic Bounds on Attainability in the Reactor Synthesis Problem. *Industrial and Engineering Chemistry Research*, 43(2):449–457, 2004.

[3] L. K E Achenie and L. T. Biegler. A superstructure based approach to chemical reactor network synthesis. *Computers and Chemical Engineering*, 14(1):23–40, 1990.

[4] Luke E.K. Achenie and Lorenz T. Blegler. Algorithmic Synthesis of Chemical Reactor Networks Using Mathematical Programming. *Industrial and Engineering Chemistry Fundamentals*, 25(4):621–627, 1986.

[5] Luke K.E. Achenie and Lorenz T. Biegler. Developing Targets for the Performance Index of a Chemical Reactor Network: Isothermal Systems. *Industrial and Engineering Chemistry Research*, 27(10):1811–1821, 1988.

[6] Andrea Adamo, Rachel L Beingessner, Mohsen Behnam, Jie Chen, Timothy F Jamison, Klavs Jensen, Jean-Christophe M Monbaliu, Al-

lan S Myerson, Eve M Revalor, David R Snead, Torsten Stelzer, Nopphon Weeranoppanant, Shin Yee Wong, and Ping Zhang. On-demand continuous-flow production of pharmaceuticals in a compact, reconfigurable system. *Science*, 352(6281):61–67, 2016.

[7] Vishal Agarwal, Suman Thotla, and Sanjay M. Mahajani. Attainable regions of reactive distillation-Part I. Single reactant non-azeotropic systems. *Chemical Engineering Science*, 63(11):2946–2965, 2008.

[8] David J. am Ende, editor. *Chemical engineering in the pharmaceutical industry: R&D to manufacturing.* John Wiley & Sons, Inc., 2011.

[9] Rishi Amrit, James B. Rawlings, and David Angeli. Economic optimization using model predictive control with a terminal cost. *Annual Reviews in Control*, 35(2):178–186, 2011.

[10] Neal G Anderson. Using Continuous Processes to Increase Production. *Organic Process Research & Development*, 16:852–869, 2012.

[11] Ann-Marie McIntyre. Dynamic Competition: Research and Development. In *Key Issues in the pharmaceutical industry*, chapter 4, pages 71–103. John Wiley & Sons, Inc., West Sussex, England, 1999.

[12] Thomas Aronsson, Mats A Bergman, and Niklas Rudholm. The Impact of Generic Drug Competition on Brand Name Market Shares – Evidence from Micro Data. *Review of Industrial Organization*, 19:425–435, 2001.

[13] V. M. Ashley and P. Linke. A novel approach for reactor network synthesis using knowledge discovery and optimization techniques. *Chemical Engineering Research and Design*, 82(8):952–960, 2004.

[14] Nana Asiedu, Diane Hildebrandt, and David Glasser. Experimental simulation of a two-dimensional attainable region and its application in the optimization of production rate and process time of an adiabatic batch reactor. *Industrial and Engineering Chemistry Research*, 53(34):13308–13319, 2014.

[15] Deenesh K. Babi, Johannes Holtbruegge, Philip Lutze, Andrzej Gorak, John M. Woodley, and Rafiqul Gani. Sustainable process synthesis–intensification. *Computers and Chemical Engineering*, 81:218–244, 2015.

[16] Deenesh K. Babi, Philip Lutze, John M. Woodley, and Rafiqul Gani. A process synthesis-intensification framework for the development of sustainable membrane-based operations. *Chemical Engineering and Processing: Process Intensification*, 86:173–195, 2014.

[17] Franz D. Bähner and Jakob K. Huusom. A Debottlenecking Study of an Industrial Pharmaceutical Batch Plant. *Industrial and Engineering Chemistry Research*, 58(43):20003–20013, 2019.

[18] Subash Balakrishna and Lorenz T. Biegler. Constructive Targeting Approaches for the Synthesis of Chemical Reactor Networks. *Industrial and Engineering Chemistry Research*, 31(1):300–312, 1992.

[19] Subash Balakrishna and Lorenz T. Biegler. Targeting Strategies for the Synthesis and Energy Integration of Nonisothermal Reactor Networks. *Industrial and Engineering Chemistry Research*, 31(9):2152–2164, 1992.

[20] Michael Baldea, Thomas F Edgar, Bill L Stanley, and Anton A Kiss. Modular Manufacturing Processes: Status, Challenges, and Opportunities. *AIChE Journal*, 63(10):4262–4272, 2017.

[21] Michael Baldea and Iiro Harjunkoski. Integrated production scheduling and process control: A systematic review. *Computers and Chemical Engineering*, 71:377–390, 2014.

[22] Péter Bana, Róbert Örkényi, Klára Lövei, Ágnes Lakó, György István Túrós, János Éles, Ferenc Faigl, and István Greiner. The route from problem to solution in multistep continuous flow synthesis of pharmaceutical compounds. *Bioorganic & Medicinal Chemistry*, 25:6180–6189, 2017.

[23] Margret Bauer and Ian K Craig. Economic assessment of advanced process control - A survey and framework. *Journal of Process Control*, 18(1):2–18, 2008.

[24] Margret Bauer, Ian K Craig, Elsa Tolsma, and Hannes de Beer. A profit index for assessing the benefits of process control. *Industrial & Engineering Chemistry Research*, 46(17):5614–5623, 2007.

[25] Arno Behr, Volker A. Brehme, C. L J Ewers, Heidi Grön, Thorsten Kimmel, Stephan Küppers, and Ingo Symietz. New developments in chemical engineering for the production of drug substances. *Engineering in Life Sciences*, 4(1):15–24, 2004.

[26] Brahim Benyahia, Richard Lakerveld, and Paul I Barton. A Plant-Wide Dynamic Model of a Continuous Pharmaceutical Process. *Industrial & Engineering Chemistry Research*, 51:15393–15412, 2012.

[27] Tarun Bhatia and Lorenz T. Biegler. Dynamic optimization in the design and scheduling of multiproduct batch plants. *Industrial and Engineering Chemistry Research*, 35(7):2234–2246, 1996.

[28] Deepak B. Birewar and Ignacio E. Grossmann. Efficient Optimization Algorithms for Zero-Wait Scheduling of Multiproduct Batch Plants. *Industrial and Engineering Chemistry Research*, 28(9):1333–1345, 1989.

[29] Deepak B. Birewar and Ignacio E. Grossmann. Simultaneous Production Planning and Scheduling in Multiproduct Batch Plants. *Industrial and Engineering Chemistry Research*, 29(4):570–580, 1990.

[30] Andrew R. Bogdan, Sarah L. Poe, Daniel C. Kubis, Steven J. Broadwater, and D. Tyler McQuade. The continuous-flow synthesis of ibuprofen. *Angewandte Chemie*, 121:8699–8702, 2009.

[31] Fani Boukouvala, Anwesha Chaudhury, Maitraye Sen, Ruijie Zhou, Lukasz Mioduszewski, Marianthi G Ierapetritou, and Rohit Ramachan-

dran. Computer-Aided Flowsheet Simulation of a Pharmaceutical Tablet Manufacturing Process Incorporating Wet Granulation. *Journal of Pharmaceutical Innovation*, 8:11–27, 2013.

[32] Fani Boukouvala and Marianthi G Ierapetritou. Surrogate-Based Optimization of Expensive Flowsheet Modeling for Continuous Pharmaceutical Manufacturing. *Journal of Pharmaceutical Innovation*, 8:131–145, 2013.

[33] Fani Boukouvala, Fernando J Muzzio, and Marianthi G Ierapetritou. Predictive Modeling of Pharmaceutical Processes with Missing and Noisy Data. *AIChE Journal*, 56(11):2860–2872, 2010.

[34] Fani Boukouvala, Fernando J Muzzio, and Marianthi G Lerapetritou. Design Space of Pharmaceutical Processes Using Data-Driven-Based Methods. *Journal of Pharmaceutical Innovations*, 5:119–137, 2010.

[35] Fani Boukouvala, Vasilios Niotis, Rohit Ramachandran, Fernando J. Muzzio, and Marianthi G. Ierapetritou. An integrated approach for dynamic flowsheet modeling and sensitivity analysis of a continuous tablet manufacturing process. *Computers and Chemical Engineering*, 42:30–47, 2012.

[36] Katrin Brandt and Gerhard Schembecker. Production Rate-Dependent Key Performance Indicators for a Systematic Design of Biochemical Downstream Processes. *Chemical Engineering & Technology*, 39(2):354–364, 2016.

[37] Baris Burnak and Efstratios N. Pistikopoulos. Integrated process design, scheduling, and model predictive control of batch processes with closed-loop implementation. *AIChE Journal*, 66(10):1–14, 2020.

[38] Gary S Calabrese and Sergio Pissavini. From Batch to Continuous Flow Processing in Chemicals Manufacturing. *AIChE Journal*, 57(4):828–834, 2011.

[39] Elisabet Capón-García, Aarón D. Bojarski, Antonio Espuña, and Luis Puigjaner. Multiobjective Optimization of Multiproduct Batch Plants Scheduling Under Environmental and Economic Concerns. *AIChE Journal*, 57(10):2766–2782, 2011.

[40] Christian C. Carmona-Vargas, Leandro C. De Alves, Timothy J Brocksom, and Kleber T. De Oliveira. Combining batch and continuous flow setups in the end-to-end synthesis of naturally occurring curcuminoids. *Reaction Chemistry and Engineering*, 2(3):366–374, 2017.

[41] Qi Chen and I E Grossmann. Recent Developments and Challenges in Optimization-Based Process Synthesis. *Annual Review of Chemical and Biomolecular Engineering*, 8(1):249–283, jun 2017.

[42] Surya P. Chitra and Rakesh Govind. Yield optimization for complex reactor systems. *Chemical Engineering Science*, 36(7):1219–1225, 1981.

[43] Michael J. Coolbaugh, Chad T. Varner, Tarl A. Vetter, Emily K. Davenport, Brad Bouchard, Marcus Fiadeiro, Nihal Tugcu, Jason Walther,

Rohan Patil, and Kevin Brower. Pilot-scale demonstration of an end-to-end integrated and continuous biomanufacturing process. *Biotechnology and Bioengineering*, (September 2020):1–15, 2021.

[44] J G Costandy, T F Edgar, and M Baldea. Switching from Batch to Continuous Reactors Is a Trajectory Optimization Problem. *Industrial & Engineering Chemistry Research*, 58(30):13718–13736, 2019.

[45] Joseph G Costandy, Thomas F Edgar, and Michael Baldea. A Scheduling Perspective on the Monetary Value of Improving Process Control. *Computers & Chemical Engineering*, 112:121–131, 2018.

[46] Joseph G. Costandy, Thomas F. Edgar, and Michael Baldea. A Unified Reactor Network Synthesis Framework for Simultaneous Consideration of Batch and Continuous-Flow Reactor Alternatives. *Industrial and Engineering Chemistry Research*, 60:7232–7256, 2021.

[47] I K Craig and R G D Henning. Evaluation of advanced industrial control projects: a framework for determining economic benefits. *Control Engineering Practice*, 8(7):769–780, 2000.

[48] J. E. Cuthrell and L. T. Biegler. Simultaneous optimization and solution methods for batch reactor control profiles. *Computers and Chemical Engineering*, 13(1-2):49–62, 1989.

[49] Rolf Dach, Jinhua J Song, Frank Roschangar, Wendelin Samstag, and Chris H Senanayake. The Eight Criteria Defining a Good Chemical Man-

ufacturing Process. *Organic Process Research & Development*, 16:1697–1706, 2012.

[50] Prodromos Daoutidis and Costas Kravaris. Structural evaluation of control configurations for multivariable nonlinear processes. *Chemical Engineering Science*, 47(5):1091–1107, apr 1992.

[51] H Ted Davis and Kendall T Thomson. *Linear algebra and linear operators in engineering: with applications in mathematica*. Academic press, volume 3 edition, 2000.

[52] Ivana Dencic, Denise Ott, Dana Kralisch, Timothy Noel, Jan Meuldijk, Mart de Croon, Volker Hessel, Yosra Laribi, and Philippe Perrichon. Eco-efficiency Analysis for Intensified Production of an Active Pharmaceutical Ingredient: A Case Study. *Organic Process Research & Development*, 18:1326–1338, 2014.

[53] Samir Diab and Dimitrios I. Gerogiorgis. Design space identification and visualization for continuous pharmaceutical manufacturing. *Pharmaceutics*, 12(3):235–258, 2020.

[54] Lisia S Dias and Marianthi G Lerapetritou. Integration of scheduling and control under uncertainties: Review and challenges. *Chemical Engineering Research and Design*, 116:1–16, 2016.

[55] A. Dietz, C. Azzaro-Pantel, L. Pibouleau, and S. Domenech. A framework for multiproduct batch plant design with environmental consider-

ation: Application to protein production. *Industrial and Engineering Chemistry Research*, 44(7):2191–2206, 2005.

[56] Thomas F Edgar. Control of unconventional processes. *Journal of Process Control*, 6(2):99–110, 1996.

[57] Thomas F Edgar. Control and operations: When does controllability equal profitability? *Computers and Chemical Engineering*, 29(1):41–49, 2004.

[58] Victor N. Emenike, René Schenkendorf, and Ulrike Krewer. A systematic reactor design approach for the synthesis of active pharmaceutical ingredients. *European Journal of Pharmaceutics and Biopharmaceutics*, 126:75–88, 2018.

[59] W. R. Esposito and C. A. Floudas. Deterministic global optimization in isothermal reactor network synthesis. *Journal of Global Optimization*, 22(1-4):59–95, 2002.

[60] Liang-tseng Fan, Mahendra M Gharpuray, and Yong-Hyun Lee. *Cellulose Hydrolysis*. Springer-Verlag Berlin Heidelberg, 1987.

[61] Martin Feinberg. Toward a theory of process synthesis. *Industrial and Engineering Chemistry Research*, 41(16):3751–3761, 2002.

[62] Martin Feinberg and Diane Hildebrandt. Optimal reactor design from a geometric viewpoint- I. Universal properties of the attainable region. *Chemical Engineering Science*, 52(10):1637–1665, 1997.

[63] Antonio Flores-Tlacuahuac and Ignacio E Grossmann. Simultaneous cyclic scheduling and control of a multiproduct CSTR. *Industrial and Engineering Chemistry Research*, 45(20):6698–6712, 2006.

[64] Christodoulos A. Floudas, Alexander M. Niziolek, Onur Onel, and Logan R. Matthews. Multi-scale systems engineering for energy and the environment: Challenges and opportunities. *AIChE Journal*, 62(3):602–623, mar 2016.

[65] H. Scott Fogler. *Elements of Chemical Reaction Engineering*. Prentice Hall, United Kingdom, 2016.

[66] Felipe A.S. Fonseca, José A. Vidal-Vieira, and Sergio P. Ravagnani. Transesterification of vegetable oils: Simulating the replacement of batch reactors with continuous reactors. *Bioresource Technology*, 101(21):8151–8157, 2010.

[67] Hannsjörg Freund and Kai Sundmacher. Towards a methodology for the systematic analysis and design of efficient chemical processes. Part 1. From unit operations to elementary process functions. *Chemical Engineering and Processing: Process Intensification*, 47(12):2051–2060, 2008.

[68] Yanina Fumero, Gabriela Corsano, and Jorge M. Montagna. Detailed design of multiproduct batch plants considering production scheduling. *Industrial and Engineering Chemistry Research*, 50(10):6146–6160, 2011.

[69] Masashi Furuta, Kouji Mukai, David Cork, and Kazuhiro Mae. Continuous crystallization using a sonicated tubular system for controlling particle size in an API manufacturing process. *Chemical Engineering & Processing: Process Intensification*, 102:210–218, 2016.

[70] Tanja Gaich and Phil S Baran. Aiming for the Ideal Synthesis. *Journal of Organic Chemistry*, 75:4657–4673, 2010.

[71] David Glasser, Diane Hildebrandt, and Cameron Crowe. A Geometric Approach to Steady Flow Reactors: The Attainable Region and Optimization in Concentration Space. *Industrial and Engineering Chemistry Research*, 26(9):1803–1810, 1987.

[72] A. Goršek and P. Glavič. Design of batch versus continuous processes - Part I: Single-purpose equipment. *Chemical Engineering Research and Design*, 75(7):709–717, oct 1997.

[73] A. Goršek and P. Glavič. Design of batch versus continuous processes Part III: Extended analysis of cost parameters. *Chemical Engineering Research and Design*, 78(2):231–244, mar 2000.

[74] A. Goršek and P. Glavič. Design of batch versus continuous processes Part II: multi-purpose equipment. *Chemical Engineering Research and Design*, 78(2):231–244, oct 2002.

[75] Arun Gupta, Tarun Mathur, Konrad S Stadler, and Eduardo Gallestey. A pragmatic approach for performance assessment of advanced process

control. In *2013 IEEE International Conference on Control Applications (CCA)*, 2013.

[76] J. Haber, M. N. Kashid, A. Renken, and L. Kiwi-Minsker. Heat management in single and multi-injection microstructured reactors: Scaling effects, stability analysis, and role of mixing. *Industrial and Engineering Chemistry Research*, 51(4):1474–1489, 2012.

[77] Daniel M Hallow, Boguslaw M Mudryk, Alan D Braem, Jose E Tabora, Olav K Lyngberg, James S Bergum, Lucius T Rossano, and Srinivas Tummala. An Example of Utilizing Mechanistic and Empirical Modeling in Quality by Design. *Journal of Pharmaceutical Innovation*, 5:193–203, 2010.

[78] Ryan L. Hartman, Jonathan P. McMullen, and Klavs F. Jensen. Deciding whether to go with the flow: Evaluating the merits of flow reactors for synthesis. *Angewandte Chemie - International Edition*, 50(33):7502–7519, 2011.

[79] James B Hendrickson. Systematic Synthesis Design .IV. Numerical Codification of Construction Reactions. *Journal of the American Chemical Society*, 97(October):5784–5800, 1975.

[80] Benjamin Hentschel, Andreas Peschel, Hannsjörg Freund, and Kai Sundmacher. Simultaneous design of the optimal reaction and process concept for multiphase systems. *Chemical Engineering Science*, 115:69–87, 2014.

[81] A Hertrampf, H Müller, J C Menezes, and T Herdling. A PAT-based qualification of pharmaceutical excipients produced by batch or continuous processing. *Journal of Pharmaceutical and Biomedical Analysis*, 114:208–215, 2015.

[82] Volker Hessel. Novel Process Windows – Gate to Maximizing Process Intensification via Flow Chemistry. *Chemical Engineering Technology*, 32(11):1655–1681, 2009.

[83] Volker Hessel, B Cortese, and M H J M De Croon. Novel process windows – Concept, proposition and evaluation methodology, and intensified superheated processing. *Chemical Engineering Science*, 66(7):1426–1448, 2011.

[84] D. Hildebrandt and D. Glasser. The attainable region and optimal reactor structures. *Chemical Engineering Science*, 45(8):2161–2168, 1990.

[85] Diane Hildebrandt, David Glasser, and Cameron M. Crowe. Geometry of the Attainable Region Generated by Reaction and Mixing: With and without Constraints. *Industrial and Engineering Chemistry Research*, 29(1):49–58, 1990.

[86] Magne Hillestad. A systematic generation of reactor designs: I. Isothermal conditions. *Computers and Chemical Engineering*, 28(12):2717–2726, 2004.

[87] Magne Hillestad. A systematic generation of reactor designs: II. Non-isothermal conditions. *Computers and Chemical Engineering*, 29(5):1101–1112, 2005.

[88] Magne Hillestad. Systematic staging in chemical reactor design. *Chemical Engineering Science*, 65(10):3301–3312, 2010.

[89] Marianthi Ierapetritou, Fernando Muzzio, and Gintaras Reklaitis. Perspectives on the continuous manufacturing of powder-based pharmaceutical processes. *AIChE Journal*, 62(6):1846–1862, jun 2016.

[90] Maiju A Järvinen, Marko Paavola, Sami Poutiainen, Päivi Itkonen, Ville Pasanen, Katja Uljas, Kauko Leiviskä, Mikko Juuti, Jarkko Ketolainen, and Kristiina Järvinen. Comparison of a continuous ring layer wet granulation process with batch high shear and fl uidized bed granulation processes. *Powder Technology*, 275:113–120, 2015.

[91] Hikaru G Jolliffe and Dimitrios I Gerogiorgis. Process modelling and simulation for continuous pharmaceutical manufacturing of ibuprofen. *Chemical Engineering Research and Design*, 97:175–191, 2015.

[92] Hikaru G Jolliffe and Dimitrios I Gerogiorgis. Plantwide design and economic evaluation of two Continuous Pharmaceutical Manufacturing (CPM) cases: Ibuprofen and artemisinin. *Computers & Chemical Engineering*, 91:269–288, 2016.

[93] Hikaru G Jolliffe and Dimitrios I Gerogiorgis. Process modelling and simulation for continuous pharmaceutical manufacturing of artemisinin. *Chemical Engineering Research and Design*, 112:310–325, 2016.

[94] Markus Kaiser and Hannsjörg Freund. A multimodular pseudoheterogeneous model framework for optimal design of catalytic reactors exemplified by methanol synthesis. *Chemical Engineering Science*, 206:401–423, 2019.

[95] N M Kaiser, R J Flassig, and K Sundmacher. Reactor-network synthesis via flux profile analysis. *Chemical Engineering Journal*, 335(April 2017):1018–1030, 2018.

[96] Shehzaad Kauchali, William C. Rooney, Lorenz T. Biegler, David Glasser, and Diane Hildebrandt. Linear programming formulations for attainable region analysis. *Chemical Engineering Science*, 57(11):2015–2028, 2002.

[97] Norbert Kockmann. Pressure loss and transfer rates in microstructured devices with chemical reactions. *Chemical Engineering and Technology*, 31(8):1188–1195, 2008.

[98] Norbert Kockmann, Michael Gottsponer, Bertin Zimmermann, and Dominique M. Roberge. Enabling continuous-flow chemistry in microstructured devices for pharmaceutical and fine-chemical production. *Chemistry - A European Journal*, 14(25):7470–7477, 2008.

[99] A. C. Kokossis and C. A. Floudas. Stability in optimal design: Synthesis of complex reactor networks. *AIChE Journal*, 40(5):849–861, 1994.

[100] Antonis C. Kokossis and Floudas Christodoulos A. Optimization of complex reactor networks-I. Isothermal operation. *Chemical Engineering Science*, 45(3):595–614, 1990.

[101] Ajay Lakshmanan and Lorenz T. Biegler. Synthesis of Optimal Chemical Reactor Networks. *Industrial and Engineering Chemistry Research*, 35(4):1344–1353, 1996.

[102] Ajay Lakshmanan and Lorenz T. Biegler. Synthesis of Optimal Chemical Reactor Networks with Simultaneous Mass Integration. *Industrial and Engineering Chemistry Research*, 35(12):4523–4536, 1996.

[103] P R Latour. Process control: CLIFFTENT shows its more profitable than expected. *Hydrocarbon Processing*, 75(12):75–80, 1996.

[104] E W Lemmon, M O McLinden, and D G Friend. Thermophysical properties of fluid systems. In P J Linstrom and W G Mallard, editors, *NIST Chemistry WebBook, NIST Standard Reference Database Number 69*. National Institute of Standards and Technology, Gaithersburg MD, 2014.

[105] H. Leuenberger. New trends in the production of pharmaceutical granules: Batch versus continuous processing. *European Journal of Pharmaceutics and Biopharmaceutics*, 52(3):289–296, 2001.

[106] Xiaoxia Lin, Christodoulos A. Floudas, Sweta Modi, and Nikola M. Juhasz. Continuous-time optimization approach for medium-range production scheduling of a multiproduct batch plant. *Industrial and Engineering Chemistry Research*, 41(16):3884–3906, 2002.

[107] Rasika B Mane and Chandrashekhar V Rode. Continuous Dehydration and Hydrogenolysis of Glycerol over Non-Chromium Copper Catalyst: Laboratory-Scale Process Studies. *Organic Process Research & Development*, 16:1043–1052, 2012.

[108] G D Martin, L E Turpin, and R P Cline. Estimating control function benefits. *Hydrocarbon Processing*, 70:68–73, 1991.

[109] Kensaku Matsunami, Takuya Nagato, Koji Hasegawa, and Hirokazu Sugiyama. A large-scale experimental comparison of batch and continuous technologies in pharmaceutical tablet manufacturing using ethenzamide. *International Journal of Pharmaceutics*, 559(December 2018):210–219, 2019.

[110] Vipul L. Mehta and Antonis Kokossis. Development of novel multiphase reactors using a systematic design framework. *Computers and Chemical Engineering*, 21(SUPPL.1), 1997.

[111] Vipul L. Mehta and Antonis C. Kokossis. Nonisothermal synthesis of homogeneous and multiphase reactor networks. *AIChE Journal*, 46(11):2256–2273, 2000.

[112] Duncan A. Mellichamp. New discounted cash flow method: Estimating plant profitability at the conceptual design level while compensating for business risk/uncertainty. *Computers and Chemical Engineering*, 48:251–263, 2013.

[113] Duncan A. Mellichamp. Internal rate of return: Good and bad features, and a new way of interpreting the historic measure. *Computers and Chemical Engineering*, 106:396–406, 2017.

[114] Andreza D.M. Mendonça, Alline V.B. De Oliveira, and João Cajaiba. A Comparison between Continuous and Batch Processes to Capture Aldehydes and Ketones by Using a Scavenger Resin. *Organic Process Research and Development*, 21(11):1794–1800, 2017.

[115] David Ming, David Glasser, and Diane Hildebrandt. Application of attainable region theory to batch reactors. *Chemical Engineering Science*, 99:203–214, 2013.

[116] D Mukesh, A A Banerji, R Newadkar, and H S Bevinakatti. Lipase catalysed transesterification of vegetable oils - A comparative study in batch and tubular reactors. *Biotechnology Letters*, 15(1):77–82, 1993.

[117] Kenneth R Muske. Estimating the economic benefit from improved process control. *Industrial & Engineering Chemistry Research*, 42(20):4535–4544, 2003.

[118] Kevin D. Nagy, Bo Shen, Timothy F. Jamison, and Klavs F. Jensen. Mixing and dispersion in small-scale flow systems. *Organic Process Research and Development*, 16(5):976–981, 2012.

[119] D. J. Oosthuizen, I. K. Craig, and P. C. Pistorius. Economic evaluation and design of an electric arc furnace controller based on economic objectives. *Control Engineering Practice*, 12(3):253–265, 2004.

[120] Fabio Pammolli, Laura Magazzini, and Massimo Riccaboni. The productivity crisis in pharmaceutical R&D. *Nature Reviews Drug Discovery*, 10:428–438, 2011.

[121] Michael Patrascu and Paul I. Barton. Optimal campaigns in end-to-end continuous pharmaceuticals manufacturing. Part 1: Nonsmooth dynamic modeling. *Chemical Engineering and Processing - Process Intensification*, 125(August 2017):298–310, 2018.

[122] Michael Patrascu and Paul I. Barton. Optimal campaigns in end-to-end continuous pharmaceuticals manufacturing. Part 2: Dynamic optimization. *Chemical Engineering and Processing - Process Intensification*, 125(August 2017):124–132, 2018.

[123] Michael Patrascu and Paul I. Barton. Optimal Dynamic Continuous Manufacturing of Pharmaceuticals with Recycle. *Industrial and Engineering Chemistry Research*, 58(30):13423–13436, 2019.

[124] Andreas Peschel, Hannsjörg Freund, and Kai Sundmacher. Methodology for the design of optimal chemical reactors based on the concept of elementary process functions. *Industrial and Engineering Chemistry Research*, 49(21):10535–10548, 2010.

[125] Andreas Peschel, Benjamin Hentschel, Hannsjörg Freund, and Kai Sundmacher. Design of optimal multiphase reactors exemplified on the hydroformylation of long chain alkenes. *Chemical Engineering Journal*, 188:126–141, 2012.

[126] Andreas Peschel, Andreas Jrke, Kai Sundmacher, and Hannsjrg Freund. Optimal reaction concept and plant wide optimization of the ethylene oxide process. *Chemical Engineering Journal*, 207-208:656–674, 2012.

[127] Andreas Peschel, Florian Karst, Hannsjörg Freund, and Kai Sundmacher. Analysis and optimal design of an ethylene oxide reactor. *Chemical Engineering Science*, 66(24):6453–6469, 2011.

[128] Max S. Peters, Klaus D. Timmerhaus, and Ronald E. West. *Plant Design and Economics for Chemical Engineers*. McGraw-Hill Education, 5 edition, 2003.

[129] Spas B. Petkov and Costas D. Maranas. Multiperiod Planning and Scheduling of Multiproduct Batch Plants under Demand Uncertainty. *Industrial and Engineering Chemistry Research*, 36(11):4864–4881, 1997.

[130] Efstratios N Pistikopoulos and Nikolaos A Diangelakis. Towards the integration of process design, control and scheduling: Are we getting closer? *Computers & Chemical Engineering*, 91:85–92, 2016.

[131] Patrick Plouffe, Arturo Macchi, and Dominique M Roberge. From Batch to Continuous Chemical Synthesis - A Toolbox Approach. *Organic Process Research & Development*, 18:1286–1294, 2014.

[132] Keith Plumb. Continuous processing in the pharmaceutical industry: Changing the mind set. *Chemical Engineering Research and Design*, 83(6 A):730–738, 2005.

[133] Alberto Posada and Vasilios Manousiouthakis. Multi-feed attainable region construction using the Shrink-Wrap algorithm. *Chemical Engineering Science*, 63(23):5571–5592, 2008.

[134] Andrew Prpich, Mary T am Ende, Thomas Katzschner, Veronika Lubczyk, Holger Weyhers, and Georg Bernhard. Drug product modeling predictions for scale-up of tablet film coating — A quality by design approach. *Computers and Chemical Engineering*, 34(7):1092–1097, 2010.

[135] S Joe Qin and Thomas A Badgwell. A survey of industrial model predictive control technology. *Control Engineering Practice*, 11:733–764, 2003.

[136] A. Renken, V. Hessel, P. Löb, R. Miszczuk, M. Uerdingen, and L. Kiwi-Minsker. Ionic liquid synthesis in a microstructured reactor for process

intensification. *Chemical Engineering and Processing: Process Intensification*, 46(9 SPEC. ISS.):840–845, 2007.

[137] D. M. Roberge, Laurent Ducry, Nikolaus Bieler, Philippe Cretton, and Bertin Zimmermann. Microreactor Technology: A Revolution for the Fine Chemical and Pharmaceutical Industries? *Chemical Engineering & Technology*, 28(3):318–323, mar 2005.

[138] Dominique M Roberge. An Integrated Approach Combining Reaction Engineering and Design of Experiments for Optimizing Reactions. *Organic Process Research & Development*, 8(6):1049–1053, 2004.

[139] Dominique M Roberge, Bertin Zimmermann, Fabio Rainone, Michael Gottsponer, Markus Eyholzer, and Norbert Kockmann. Microreactor Technology and Continuous Processes in the Fine Chemical and Pharmaceutical Industry: Is the Revolution Underway? *Ongoing Process Research & Development*, 12(5):905–910, 2008.

[140] C V Rode, A A Ghalwadkar, R B Mane, A M Hengne, S T Jadkar, and N S Biradar. Selective Hydrogenolysis of Glycerol to 1,2-Propanediol: Comparison of Batch and Continuous Process Operations. *Organic Process Research & Development*, 14(2):1385–1392, 2010.

[141] Amanda Rogers and Marianthi Ierapetritou. Challenges and opportunities in modeling pharmaceutical manufacturing processes. *Computers and Chemical Engineering*, 81:32–39, 2015.

[142] Amanda J Rogers, Chaitali Inamdar, and Marianthi G Ierapetritou. An Integrated Approach to Simulation of Pharmaceutical Processes for Solid Drug Manufacture. *Industrial & Engineering Chemistry Research*, 53:5128–5147, 2014.

[143] Joonjae Ryu, Lingxun Kong, Arthur E. Pastore de Lima, and Christos T. Maravelias. A generalized superstructure-based framework for process synthesis. *Computers and Chemical Engineering*, 133:106653, 2020.

[144] Spencer D. Schaber, Dimitrios I. Gerogiorgis, Rohit Ramachandran, James M. B. Evans, Paul I. Barton, and Bernhardt L. Trout. Economic Analysis of Integrated Continuous and Batch Pharmaceutical Manufacturing: A Case Study. *Industrial & Engineering Chemistry Research*, 50(17):10083–10092, 2011.

[145] C A Schweiger and C A Floudas. Optimization framework for the synthesis of chemical reactor networks. *Industrial and Engineering Chemistry Research*, 38(3):744–766, 1999.

[146] Maitraye Sen, Anwesha Chaudhury, Ravendra Singh, Joyce John, and Rohit Ramachandran. Multi-scale flowsheet simulation of an integrated continuous purification – downstream pharmaceutical manufacturing process. *International Journal of Pharmaceutics*, 445(1-2):29–38, 2013.

[147] Maitraye Sen, Amanda Rogers, Ravendra Singh, Anwesha Chaudhury, Joyce John, Marianthi G Ierapetritou, and Rohit Ramachandran. Flowsheet optimization of an integrated continuous purification-processing

pharmaceutical manufacturing operation. *Chemical Engineering Science*, 102:56–66, 2013.

[148] Yan Shen, Azman Maamor, Jehad Abu-Dharieh, Jillian M. Thompson, Bal Kalirai, E. Hugh Stitt, and David W. Rooney. Moving from batch to continuous operation for the liquid phase dehydrogenation of tetrahydrocarbazole. *Organic Process Research and Development*, 18(3):392–401, 2014.

[149] Simo-pekka Simonaho, Jarkko Ketolainen, Tuomas Ervasti, Maunu Toiviainen, and Ossi Korhonen. Continuous manufacturing of tablets with PROMIS-line — Introduction and case studies from continuous feeding, blending and tableting. *European Journal of Pharmaceutical Sciences*, 90:38–46, 2016.

[150] David R Snead and Timothy F Jamison. A Three-Minute Synthesis and Purification of Ibuprofen: Pushing the Limits of Continuous-Flow Processing. *Angewandte Chemie*, 127:997–1001, 2015.

[151] B. Srinivasan, S. Palanki, and D. Bonvin. Dynamic optimization of batch processes. *Computers & Chemical Engineering*, 27(1):1–26, 2003.

[152] E Hugh Stitt and David W Rooney. Switching from Batch to Continuous Processing for Fine and Intermediate-Scale Chemicals Manufacture. In Andrzej Cybulski, Jacob A Moulijn, and Andrzej Stankiewicz, editors,

Novel Concepts in Catalysis and Chemical Reactors: Improving the Efficiency for the Future, chapter 14, pages 309–330. WILEY-VCH Verlag GmbH & Co., 2010.

[153] Prashant L. Suryawanshi, Sarang P. Gumfekar, Bharat A. Bhanvase, Shirish H. Sonawane, and Makarand S. Pimplapure. A review on microreactors: Reactor fabrication, design, and cutting-edge applications. *Chemical Engineering Science*, 189:431–448, 2018.

[154] Soo Khean Teoh, Chetankumar Rathi, and Paul Sharratt. Practical Assessment Methodology for Converting Fine Chemicals Processes from Batch to Continuous. *Organic Process Research & Development*, 20:414–431, 2016.

[155] Yuhe Tian, Salih Emre Demirel, M. M. Faruque Hasan, and Efstratios N. Pistikopoulos. An Overview of Process Systems Engineering Approaches for Process Intensification: State of the Art. *Chemical Engineering and Processing - Process Intensification*, 133(July):160–210, 2018.

[156] Yuhe Tian, Iosif Pappas, Baris Burnak, Justin Katz, and Efstratios N. Pistikopoulos. A Systematic Framework for the synthesis of operable process intensification systems – Reactive separation systems. *Computers and Chemical Engineering*, 134:106675, 2020.

[157] Yuhe Tian and Efstratios N. Pistikopoulos. Synthesis of operable process intensification systems: advances and challenges. *Current Opinion in Chemical Engineering*, 25:101–107, 2019.

[158] Emanuele Tomba, Marialuisa De Martin, Pierantonio Facco, John Robertson, Simeone Zomer, Fabrizio Bezzo, and Massimiliano Barolo. General procedure to aid the development of continuous pharmaceutical processes using multivariate statistical modeling – An industrial case study. *International Journal of Pharmaceutics*, 444(1-2):25–39, 2013.

[159] A Tonkovich, D Kuhlmann, A Rogers, J McDaniel, S Fitzgerald, R Arora, and T Yuschak. Microchannel technology scale-up to commercial capacity. *Chemical Engineering Research and Design*, 83:634–639, 2005.

[160] Gavin Towler and Ray Sinnott. *Chemical Engineering Design: Principles, Practice and Economics of Plant and Process Design*. Butterworth-Heinemann, Boston, 2 edition, 2013.

[161] Calvin Tsay, Richard C. Pattison, Michael Baldea, Ben Weinstein, Steven J. Hodson, and Robert D. Johnson. A superstructure-based design of experiments framework for simultaneous domain-restricted model identification and parameter estimation. *Computers and Chemical Engineering*, 107:408–426, 2017.

[162] Fernando E. Valera, Michela Quaranta, Antonio Moran, John Blacker, Alan Armstrong, João T. Cabral, and Donna G. Blackmond. The flow's the thing... Or is it? Assessing the merits of homogeneous reactions in flask and flow. *Angewandte Chemie - International Edition*, 49(14):2478–2485, 2010.

[163] Koen van Aken, Lucjan Strekowski, and Luc Patiny. EcoScale , a semi-quantitative tool to select an organic preparation based on economical and ecological parameters. *Beilstein Journal of Organic Chemistry*, 2:1–7, 2006.

[164] Geert Van Der Vorst, Wim Aelterman, Bruno De Witte, Bert Heirman, H. Van Langenhove, and Jo Dewulf. Reduced resource consumption through three generations of Galantamine·HBr synthesis. *Green Chemistry*, 15(3):744–748, 2013.

[165] Chris Vervaet and Jean Paul Remon. Continuous granulation in the pharmaceutical industry. *Chemical Engineering Science*, 60:3949–3957, 2005.

[166] Thomas Vetter, Christopher L. Burcham, and Michael F. Doherty. Regions of attainable particle sizes in continuous and batch crystallization processes. *Chemical Engineering Science*, 106:167–180, 2014.

[167] Jeetmanyu P. Vin and Marianthi G. Ierapetritou. A new approach for efficient rescheduling of multiproduct batch plants. *Industrial and Engineering Chemistry Research*, 39(11):4228–4238, 2000.

[168] Thomas Westermann and Leslaw Mleczko. Heat Management in Microreactors for Fast Exothermic Organic Syntheses-First Design Principles. *Organic Process Research and Development*, 20(2):487–494, 2016.

[169] T. Winkelnkemper and G. Schembecker. Purification performance index and separation cost indicator for experimentally based systematic downstream process development. *Separation and Purification Technology*, 72(1):34–39, 2010.

[170] P. M. Witt, S. Somasi, I. Khan, D. W. Blaylock, J. A. Newby, and S. V. Ley. Modeling mesoscale reactors for the production of fine chemicals. *Chemical Engineering Journal*, 278:353–362, 2015.

[171] Loretta L Wong, Run Ling Wong, Gabriel Loh, Phyllis E W Tan, Soo Khean Teoh, Salim M Shaik, Paul N Sharratt, Wee Chew, Suat Teng Tan, and David Wang. Multikilogram Synthesis of 4-D-Erythronolactone via Batch and Continuous Processing. *Organic Process Research & Development*, 16:1003–1012, 2012.

[172] Mingquan Xie and Hannsjörg Freund. Fast synthesis of optimal chemical reactor networks based on a universal system representation. *Chemical Engineering and Processing: Process Intensification*, 123(November 2017):280–290, 2018.

[173] Mingquan Xie and Hannsjörg Freund. Optimal reactor design and operation taking catalyst deactivation into account. *Chemical Engineering Science*, 175:405–415, 2018.

[174] Mingquan Xie and Hannsjörg Freund. Rigorous design of multiphase reactors: Identification of optimal conditions for mass transfer limited

reactions. *Chemical Engineering and Processing - Process Intensification*, 124(April 2017):174–185, 2018.

[175] Ou Yang, Maen Qadan, and Marianthi Ierapetritou. Economic Analysis of Batch and Continuous Biopharmaceutical Antibody Production: a Review. *Journal of Pharmaceutical Innovation*, 15(1):182–200, 2020.

[176] Jun Ichi Yoshida, Yusuke Takahashi, and Aiichiro Nagaki. Flash chemistry: Flow chemistry that cannot be done in batch. *Chemical Communications*, 49(85):9896–9904, 2013.

[177] Lawrence X Yu. Pharmaceutical quality by design: Product and process development, understanding, and control. *Pharmaceutical Research*, 25(4):781–791, 2008.

[178] Haitao Zhang, Richard Lakerveld, Patrick L Heider, Mengying Tao, Min Su, Christopher J Testa, Alyssa N D'Antonio, Paul I Barton, Richard D Braatz, Bernhardt L Trout, Allan S Myerson, Klavs F Jensen, and James M B Evans. Application of Continuous Crystallization in an Integrated Continuous Pharmaceutical Pilot Plant. *Crystal Growth & Design*, 14:2148–2157, 2014.

[179] Jinzhong Zhang and Robin Smith. Design and optimisation of batch and semi-batch reactors. *Chemical Engineering Science*, 59(2):459–478, 2004.

[180] Chao Zhao, Yu Zhao, Hongye Su, and Biao Huang. Economic performance assessment of advanced process control with LQG benchmarking. *Journal of Process Control*, 19(4):557–569, 2009.

[181] Y Zhou and J F Forbes. Determining controller benefits via probabilistic optimization. *International Journal of Adaptive Control and Signal Processing*, 17:553–568, 2003.